Géométrie différentielle des fibrés vectoriels et algèbres de Clifford appliquées au traitement d'images multicanaux

Thomas Batard

Ecole doctorale S2I

THÈSE

Présentée pour obtenir

LE GRADE DE DOCTEUR
DE L'UNIVERSITÉ DE LA ROCHELLE

Spécialité: Mathématiques et applications

par

Thomas BATARD

Géométrie différentielle des fibrés vectoriels et algèbres de Clifford appliquées au traitement d'images multicanaux

Soutenue le 07 Décembre 2009 à La Rochelle devant le Jury composé de:

Pr. Eduardo Bayro-Corrochano	Cinvestav, Unidad Guadalajara	(Rapporteur)
Pr. Michel Berthier	Université de la Rochelle	(Directeur de thèse)
Pr. Mohamed Daoudi	Institut Télécom, Lille 1	(Examinateur)
Dr. Christophe Saint-Jean	Université de La Rochelle	(Examinateur)
Pr. Nir Sochen	University of Tel-Aviv	(Rapporteur)
Pr. Pol Vanhaecke	Université de Poitiers	(Président du jury)

Thèse préparée au
Laboratoire Mathématiques, Image et Applications (EA 3165)
Université de La Rochelle
17 042 La Rochelle CEDEX

Résumé

Le sujet de cette thèse est l'apport d'applications du formalisme des algèbres de Clifford au traitement d'images multicanaux. Nous y introduisons également l'utilisation du cadre des fibrés vectoriels en traitement d'image.
La Partie 1 est consacrée à la segmentation d'images multicanaux. Nous généralisons l'approche de Di Zenzo pour la détection de contours en construisant des tenseurs métriques adaptés au choix de la segmentation. En utilisant le cadre des fibrés en algèbres de Clifford, nous montrons que le choix d'une segmentation d'une image est directement lié au choix d'une métrique, d'une connexion et d'une section sur un tel fibré. La Partie 2 est consacrée à la régularisation. Nous utilisons le cadre des équations de la chaleur associées à des Laplaciens généralisés sur des fibrés vectoriels. Le résultat principal que nous obtenons est qu'en considérant l'équation de la chaleur associée à l'opérateur de Hodge sur le fibré de Clifford d'une variété Riemannienne bien choisie, nous obtenons un cadre global pour régulariser de manière anisotrope des images (vidéos) multicanaux, et des champs s'y rapportant tels des champs de vecteurs ou des champs de repères orthonormés. Enfin, dans la Partie 3, nous nous intéressons à l'analyse spectrale via la définition d'une transformée de Fourier d'une image multicanaux. Cette définition repose sur une théorie abstraite de la transformée de Fourier basée sur la notion de représentation de groupe. De ce point de vue, la transformée de Fourier usuelle pour les images en niveau de gris est basée sur les représentations irréductibles du groupe des translations du plan. Nous l'étendons aux images multicanaux en lui associant les représentations réductibles de ce groupe.

Mots-clefs : Algèbre de Clifford, fibré vectoriel, transformée de Fourier abstraite, image multicanaux, segmentation, régularisation, analyse spectrale.

Abstract

This thesis is devoted to supply applications of Clifford algebras to multichannel image processing. Moreover, we introduce the use of vector bundles framework in image processing.
Part 1 is devoted to multichannel image segmentation. We generalize Di Zenzo's approach to edge detection by constructing metric tensors related to the choice of the segmentation. Using the framewok of Clifford algebras bundles, we show that the choice of a segmentation of an image is related to the choice of a connection and a section on such a bundle. Part 2 is devoted to regularization. We make use of heat equations associated to generalized Laplacians on vector bundles. The main result of this part is the following. Considering the heat equation associated to the Hodge operator on the Clifford bundle of a well-chosen Riemannian manifold, we obtain a common framework for anisotropic regularization of images (videos), and related fields such as vector fields and orthonormal frame fields. At last, in Part 3, we deal with spectral analysis via the definition of a Fourier transform of a multichannel image. This definition is related to an abstract theory of Fourier transform based on the notion of group representation. From this point of view, the usual Fourier transform of grey level images is related with irreducible representations of the translations of the plane. We extend this Fourier transform to multichannel images by considering reducible representations of this group.

Keywords : Clifford algebra, vector bundle, abstract Fourier transform, multichannel image, segmentation, regularization, spectral analysis.

Remerciements

Je suis extrêmement reconnaissant envers Michel Berthier pour m'avoir fait confiance en m'offrant l'opportunité de préparer cette thèse. Je le remercie également pour ses nombreux conseils durant ces trois ans, ainsi que pour toutes ces conversations 'brusselloises' très enrichissantes.

Je remercie beaucoup Christophe Saint-Jean d'avoir accepté d'intervenir dans l'encadrement de cette thèse.

Je tiens à témoigner ma gratitude à Eduardo Bayro-Corrochano et Nir Sochen d'avoir accepté de rapporter cette thèse, ainsi qu'à Mohamed Daoudi et Pol Vanhaecke d'avoir accepté de faire partie du jury de cette thèse.

Je tiens à remercier les membres du laboratoire Mathématique, Image et Applications de l'Université de La Rochelle, avec une attention toute particulière pour les doctorants des bureaux 258 et 260 qui ont partagé mon quotidien ces trois dernières années : Chevreuil attentif, Clara, Delphine, E.T. et Mimosa.

Je remercie enfin ma famille pour m'avoir toujours soutenu durant mes études.

Table des matières

Introduction **9**

Contexte de la thèse 9

Présentation de la thèse 14

I Fibrés en algèbres de Clifford pour la segmentation d'image **38**

1 A metric approach to nD images edge detection with Clifford algebras **39**

1.1 Introduction 39

1.2 Clifford algebras and color-infrared spaces 40

1.3 Edge detection in color-infrared images 45

1.4 Applications 54

Appendix. Tensor product of $\mathcal{CT}(D)$-valued 1-forms 63

2 Clifford algebras bundles to multidimensional image segmentation **65**

2.1 Introduction 65

2.2 Preliminaries 66

2.3 A general method to multidimensional image edge detection 69

2.4 Applications 76

II Equations de la chaleur associées à des Laplaciens généralisés pour la régularisation **91**

3 Heat kernels of generalized Laplacians : application to multichannel images/videos regularization **92**

3.1 Heat kernels of generalized Laplacians : application to color image smoothing 92

3.2 Curved kernel for video regularization 101

4 Clifford bundles : a unifying framework for images(videos), vector fields and orthonormal frame fields regularization **106**

4.1 Introduction 106

4.2 Heat equations on vector bundles 108

4.3 The Clifford-Hodge Laplacian : an extension of the scalar Laplacian for multivector fields smoothing 112
4.4 The case $m = 2$ 118
4.5 The case $m = 3$ 126

III Transformée de Fourier-Clifford pour le traitement d'image 137

5 Clifford-Fourier Transform for Color Image Processing 138
5.1 Introduction 138
5.2 Fourier transform and group actions 138
5.3 Clifford Fourier transform in $L^2(\mathbb{R}^2, (\mathbb{R}^n, Q))$ 140
5.4 Application to color image filtering 146
5.5 Related works 153
Appendix 156

Références 162

Introduction

Contexte de la thèse

L'utilisation de modèles mathématiques pour le traitement d'images (vidéos) et en vision est en plein essor depuis une dizaine d'années [2],[19],[53],[61],[65],[72].

Dans cette thèse, on détermine de nouveaux modèles géométriques des images, avec un intérêt particulier pour les images multicanaux, que nous illustrons par des applications à la segmentation, régularisation, et à l'analyse fréquentielle.

L'idée à l'origine est de définir un cadre mathématique dans lequel plonger l'espace d'acquisition d'une image à n canaux (nD) pour traiter de manière unifiée les composantes de cette image. En effet, les composantes d'une image multicanaux sont généralement traitées de manière marginale, et l'information vectorielle n'est pas prise en compte. Pour cela, on s'inspire des travaux de Sangwine et al. [32],[33],[68],[69],[70] sur la représentation des couleurs dans l'espace RGB par des quaternions

$$(r, g, b) \longleftrightarrow ri + gj + bk$$

La structure d'algèbre de $\mathbb{H}$ permet alors de coder de manière immédiate des opérations géométriques sur les couleurs. Cherchant à étendre cette idée aux composantes d'une image à n canaux, nous proposons de considérer l' **algèbre de Clifford** associée à un espace vectoriel de dimension n. Etant donné un espace vectoriel V de dimension finie n sur $\mathbb{R}$, muni d'une forme quadratique Q et $(e_1, \cdots, e_n)$ une base orthonormale de V pour Q, l' algèbre de Clifford $Cl(V, Q)$ associée à (V, Q) est une algèbre associative unitaire sur $\mathbb{R}$ de dimension 2^n de base

$$\{1, e_1, \cdots, e_n, e_1e_2, \cdots, e_{n-1}e_n, \cdots, e_1 \cdots e_n\}$$

En particulier, $\mathbb{R}$ et V se plongent dans $Cl(V, Q)$, et nous avons les relations

$$e_i^2 = 1 \qquad\qquad e_ie_j = -e_je_i$$

Plus généralement, pour u, v dans le plongement de V dans $Cl(V, Q)$, on a

$$u^2 = Q(u) \qquad\qquad uv + vu = B(u, v)$$

où B est la forme bilinéaire symmétrique associée à Q.

De manière formelle, on a la définition suivante.

Définition 1 *Soit V un espace vectoriel sur $\mathbb{R}$ de dimension finie muni d'une forme quadratique Q. On note $T(V)$ l'algèbre tensorielle de V, i.e.*

$$T(V) := \bigoplus_{i=0}^{\infty} V^{\otimes i} = \mathbb{R} \oplus V \oplus (V \otimes V) \oplus \cdots$$

L'algèbre de Clifford $Cl(V, Q)$ est le quotient

$$Cl(V, Q) = T(V) \Big/ (x \otimes x - Q(x)1)$$

de $T(V)$ par l'idéal bilatère engendré par les éléments de type $x \otimes x - Q(x)1$ pour $x \in V$.

Les propriétés de base des algèbres de Clifford sont données Section 1.2.1.

Etant donnée une image nD donnée par la fonction

$$I\colon (x,y) \longmapsto (I_1(x,y), \cdots, I_n(x,y))$$

nous plongeons son espace d'acquisition dans $(\mathbb{R}^n, Q)$ pour une certaine forme quadratique Q, de telle sorte que

$$I(x,y) = I_1(x,y)e_1 + \cdots + I_n(x,y)e_n$$

où $(e_1, \cdots, e_n)$ est une base non nécessairement orthonormale pour Q.

Ensuite, en utilisant le plongement de $(\mathbb{R}^n, Q)$ dans $Cl(\mathbb{R}^n, Q)$, nous voyons l'image comme une fonction à valeur dans l'algèbre de Clifford $Cl(\mathbb{R}^n, Q)$ de la forme

$$I\colon (x,y) \longmapsto I_1(x,y)e_1 + \cdots + I_n(x,y)e_n$$

avec

$$e_i^2 = Q(e_i) \qquad\qquad e_ie_j + e_je_i = B(e_i, e_j)$$

En particulier, on considère une image couleur

$$I\colon (x,y) \longmapsto (r(x,y), g(x,y), b(x,y))$$

comme une fonction à valeur dans $Cl(\mathbb{R}^3, Q)$ de la forme

$$I\colon (x,y) \longmapsto r(x,y)e_1 + g(x,y)e_2 + b(x,y)e_3$$

On plonge ainsi l'espace d'acquisition RGB d'une image couleur dans l'algèbre de Clifford associée à $(\mathbb{R}^3, Q)$, où Q est une forme quadratique à déterminer, dépendant de l'application envisagée. On peut alors montrer que les opérations sur les couleurs codées par des opérations dans $\mathbb{H}$ dans les travaux de Sangwine et al. [33],[68],[70] peuvent se réecrire en utilisant le cadre de $Cl(\mathbb{R}^3, Q)$. De plus, $Cl(\mathbb{R}^3, Q)$ a une structure plus riche que $\mathbb{H}$ car de dimension 8 alors que $\mathbb{H}$ est de dimension 4. En ce sens-là, $Cl(\mathbb{R}^3, Q)$ fournit un cadre plus riche pour traiter la couleur que $\mathbb{H}$. En atteste la Proposition suivante où l'on montre qu'une teinte peut être assimilée à un élément de $Cl(\mathbb{R}^3, Q)$.

Proposition 1 *Soit T l'ensemble des bivecteurs de la forme*

$$T = \{(e_1 + e_2 + e_3) \wedge \alpha,\ \alpha \in RGB\}$$

et la relation d'équivalence suivante sur T :

$$B \simeq C \iff B = \lambda C \quad \textit{for } \lambda > 0$$

Alors il existe une bijection entre $T/\simeq$ et l'ensemble des teintes.

Le terme $\wedge$ représente le produit extérieur dans $Cl(\mathbb{R}^n, Q)$ (voir Section 1.2.1). L'expression $\alpha \in RGB$ signifie que α est un élément de $Cl(\mathbb{R}^3, Q)$ qui code une couleur, i.e. de la forme $re_1 + ge_2 + be_3$.

Plus généralement, par les travaux de Hestenes [47], les algèbres de Clifford, appelées alors **algèbres géométriques**, fournissent un langage pour implémenter efficacement des opérations géométriques de nature diverses. Le formalisme des algèbres géométriques est ainsi utilisé dans beaucoup de disciplines des mathématiques appliquées telles les sciences de l'ingénieur [9],[10],[28],[75] et la physique théorique [27],[48],[49].

Parallèlement à l'utilisation des algèbres de Clifford pour le traitement d'images multicanaux, on s'intéresse également dans cette thèse à l'application du cadre des **fibrés vectoriels** au traitement d'images. L'idée est la suivante : la géométrie Riemannienne, dont l'utilisation en traitement d'image et en vision est bien établie (voir e.g. [20],[38],[62],[74],[77],[81]), se révèle être un cas particulier de géométrie de fibré vectoriel puisqu'elle traite de la connexion de Levi-Cevita sur le fibré tangent d'une variété Riemannienne. Il est ainsi naturel d'envisager que l'utilisation d'une théorie plus générale ouvre la voie à de nouvelles applications. Les fibrés vectoriels, ou plus généralement les espaces fibrés [51],[54],[79] sont très utilisés en physique théorique [36]. Dans cette thèse, nous utilisons les notions de connexion ou dérivation covariante, et de transport parallèle sur des fibrés vectoriels triviaux.

Dans la suite, nous donnons les définitions des concepts de géométrie différentielle que nous utilisons dans cette thèse.

Quelques notions de Géométrie différentielle :

Définition 2 (fibré vectoriel) *Un fibré vectoriel (réel) de rang n consiste en*
1. des espaces topologiques X (espace de base) et E (espace total)
2. une surjection continue $\pi\colon E \to X$ (projection)
3. pour $x \in X$, une structure d'espace vectoriel de dimension n sur $E_x := \pi^{-1}(\{x\})$ (la fibre au-dessus de x)

*avec une condition de **trivialisation locale**, i.e.*
pour tout $x \in X$, il existe un ouvert $U \subset X$ contenant x et un homéomorphisme

$$\Phi\colon U \times \mathbb{R}^n \longrightarrow \pi^{-1}(U)$$

tel que
- $\pi \circ \Phi(y, f) = y$ pour tout $y \in U$ et $f \in \mathbb{R}^n$
- l'application $\Phi_y\colon f \longmapsto \Phi(y, f)$ est un isomorphisme d'espace vectoriel entre $\mathbb{R}^n$ et $\pi^{-1}(\{y\})$.

On note (E, π, X) ce fibré vectoriel (ou parfois E de manière abusive).

Lorsque la trivialisation est globale, i.e. il existe un homéomorphisme $\Phi\colon X \times \mathbb{R}^n \longrightarrow E$, le fibré vectoriel est dit **trivial**.

Dans la suite, les espaces E et X sont des variétés différentiables et les trivialisations locales Φ sont des difféomorphismes.

Définition 3 (section) *Une section du fibré (E, π, X) est une application différentiable $S\colon X \longrightarrow E$ telle que $\pi \circ S = Id_X$. L'ensemble des sections de (E, π, X) est noté $\Gamma(E)$.*

Soit $(f_1, \cdots, f_k)$ une base de $\mathbb{R}^n$. Dans une trivialisation locale (U, Φ) de E, toute section S prend la forme

$$S(y) = \sum_{i=1}^{n} S_i(y)\Phi(y, f_i)$$

pour certaines fonctions $S_i \in C^k(X), k \geqslant 1$.

Définition 4 (métrique de fibré) *Soit (E, π, X) un fibré vectoriel. Une métrique de fibré h sur (E, π, X) est la donnée en tout point $x \in X$ d'un produit scalaire h_x dans la fibre E_x au-dessus de x, et qui varie de manière différentiable avec le point.*

Dans cette thèse, on est ammené à considérer des fibrés en algèbres de Clifford. Ce sont des fibrés vectoriels dont les fibres ont une structure d'algèbre de Clifford. Un fibré en algèbre de Clifford se construit à partir d'un fibré vectoriel muni d'une métrique de fibré.

Définition 5 (fibré en algèbres de Clifford) *Soit (E, π, X, h) un fibré vectoriel muni d'une métrique de fibré h. Le fibré en algèbres de Clifford $Cl(E, h)$ associé au fibré (E, π, X, h) est le fibré quotient*

$$Cl(E, h) = \mathcal{T}(E) \Big/ I(E)$$

où $\mathcal{T}(E)$ est le fibré sur X dont la fibre en $x \in X$ est l'algèbre tensorielle $T(E_x)$ de E_x et $I(E)$ est le fibré sur X dont la fibre en $x \in X$ est l'idéal bilatère dans $T(E_x)$ engendré par les éléments $v \otimes v - h_x(v, v)1$ pour $v \in E_x$.

La structure d'algèbre de Clifford des fibres $Cl(E, h)_x$ génère une structure d'algèbre sur $C^\infty(X)$ des sections de $Cl(E, h)$. Un repère local orthonormé $(e_1, \cdots, e_n)$ de TX génère un repère local $(1, e_1, \cdots, e_n, e_1e_2, \cdots, e_{n-1}e_n, \cdots, e_1 \cdots e_n)$ de $Cl(E, h)$.

Définition 6 (connexion) *Une connexion sur (E, π, X) est une loi de dérivation sur les sections de E. Plus précisemment, soient $v, v' \in \Gamma(TX)$ deux champs de vecteurs tangents sur X et $f, g \in C^k(X)$, une connexion ∇ est une application $\Gamma(TX) \times \Gamma(E) \longrightarrow \Gamma(E)$ satisfaisant*
-$\nabla_v(S + S') = \nabla_v S + \nabla_v S'$
-$\nabla_{fv+gv'} S = f\nabla_v S + g\nabla_{v'} S$
-$\nabla_v fS = f\nabla_v S + (d_v f)S$
*L'opérateur ∇_v est appelé **dérivée covariante** le long de v.*

Soit (U, Φ) une trivialisation locale de (E, π, X) avec X de dimension m. Soient $(e_1, \cdots, e_m)$ un repère local de TX sur U et $(s_1, \cdots, s_n)$ un repère local de E sur U. Une connexion ∇^E sur E est alors déterminée sur (U, Φ) par $n^2 \times m$ fonctions Υ_{ij}^k définies par

$$\nabla_{e_i} s_j = \sum_{k=1}^{n} \Upsilon_{ij}^k s_k$$

Définition 7 (transport parallèle) *Soit (E, π, X) un fibré vectoriel muni d'une connexion ∇^E, $y \in X$ et $Y_0 \in E_y$. Soit γ une courbe C^1 dans X telle que $\gamma(0) = y$.*

Le transport parallèle de Y_0 le long de γ est la solution $Y(t) \in E_{\gamma(t)}$ de l'équation différentielle

$$\begin{cases} \nabla^E_{\dot\gamma} Y(t) = 0 \\ Y(0) = Y_0 \end{cases}$$

En considérant un fibré vectoriel particulier : le fibré tangent d'une variété Riemannienne, on retrouve les concepts de courbure de Gauss d'une surface et de courbe géodésique en géométrie Riemannienne.

Définition 8 (fibré tangent) *Le fibré tangent d'une variété de dimension m est le fibré vectoriel de rang m dont l'espace total TX est l'union disjointe sur X des espaces tangents, i.e. $TX = \bigcup_{x\in X} T_xX$. Les champs de vecteurs tangents de X sont les sections de TX.*

Définition 9 (fibré de Clifford d'une variété) *Soit (X, g) une variété munie d'une métrique, i.e. g est une métrique de fibré pour le fibré TX. Le fibré de Clifford $Cl(X, g)$ de (X, g) est le fibré en algèbres de Clifford généré par (TX, g).*

Dans le cadre d'une connexion sur le fibré tangent d'une variété de dimension m, on note Γ^k_{ij} les m^3 fonctions qui déterminent la connexion.

Etant donnée une connexion ∇ sur TX, on lui associe deux tenseurs R et T appelés respectivement **tenseur de courbure** et **tenseur de torsion**, définis par

$$R(U,V)W = \left(\nabla_U\nabla_V - \nabla_V\nabla_U - \nabla_{[U,V]}\right) W$$
$$T(U,V) = \nabla_U V - \nabla_V U - [U,V]$$

pour U, V, W trois champs de vecteurs tangents de X.

Définition 10 (connexion de Levi-Cevita) *Soit (X, g) une variété Riemannienne. La connexion de Levi-Cevita ∇ sur TX est l'unique connexion sans torsion dont le transport parallèle préserve le produit scalaire. Elle est définie par les* ***symboles de Christoffel***

$$\Gamma^k_{ij} = \frac{1}{2} g^{kl}(\partial_j g_{li} + \partial_i g_{lj} - \partial_l g_{ij})$$

en utilisant les notations d'Einstein.

La courbure de Gauss d'une surface se déduit du tenseur de courbure de la connexion de Levi-Cevita, et les courbes géodésique sur une variété Riemannienne se définissent à partir au transport parallèle associé à cette connexion.

Soit S une surface plongée dans $\mathbb{R}^3$, et g la première forme fondamentale sur S induite par le produit scalaire euclidien de $\mathbb{R}^3$. Le couple (S, g) est une variété de dimension 2. Soit K la courbure de Gauss de S. On a la formule suivante

$$K(p) = -\frac{g_p(R_p(U,V)U, V)}{\|U \vee V\|^2}$$

quelque soient les vecteurs $U, V \in T_pS$ linéairement indépendants, et où $\|U \vee V\|$ dénote l'aire du parallélogramme engendré par U et V.

Définition 11 (courbe géodésique) *Soit γ une courbe C^1 sur une variété Riemannienne (X, g). γ est appelée courbe géodésique si son champ de vecteurs tangents $\dot{\gamma}$ est transporté parallèlement le long de γ, c'est-à-dire si $\nabla_{\dot{\gamma}}\dot{\gamma} = 0$.*

Dans cette thèse, on utilise le cadre des fibrés vectoriels dans deux applications : la segmentation d'image nD et la régularisation d'image nD et de champs s'y rapportant.

Dans le cadre de la segmentation, on définit une image nD comme une section d'un fibré en algèbres de Clifford trivial de rang 2^n au-dessus de son domaine de définition, de la forme

$$I(x, y) = I_1(x, y)e_1(x, y) + \cdots + I_n(x, y)e_n(x, y)$$

On formalise alors la segmentation d'objets sur une image en associant le choix d'une segmentation avec le choix d'une métrique de fibré, d'une connexion et de sections que l'on dérive par cette connexion.

Dans le cadre de la régularisation d'image, on considère une image nD comme une section d'un fibré vectoriel E de rang n au-dessus de son domaine de définition D muni d'une structure de variété Riemannienne (D, g). On utilise la théorie des équations de la chaleur associées à des Laplaciens généralisés sur des fibrés vectoriels [13]. Le choix d'une connexion sur ce fibré et d'une section F de $\mathrm{End}(E)$, le fibré sur D dont les fibres $\mathrm{End}(E)_x$ sont les endomorphismes de E_x détermine alors la régularisation de l'image. Par cette même théorie, on régularise également des champs de vecteurs et des champs de repères orthonormés associés à une image, en considérant le fibré de Clifford de (D, g) pour g bien choisie.

Présentation de la thèse

Partie 1 : Fibrés en algèbres de Clifford pour la segmentation d'image

Dans cette première Partie, nous étendons l'approche de détection de contours initiée par Di Zenzo [26] en construisant des tenseurs métriques adaptés au choix de la segmentation (voir Section 2.2.1 pour des détails sur cette méthode). En effet, d'un point de vue géométrique, cette méthode consiste à construire des métriques de surfaces. Plus précisemment, étant donnée une image nD

$$I\colon (x, y) \longmapsto (I_1(x, y), \cdots, I_n(x, y))$$

définie sur un domaine $D \subset \mathbb{R}^2$, et la surface S paramétrée par

$$\varphi\colon (x, y) \longmapsto (x, y, I_1(x, y), \cdots, I_n(x, y))$$

on construit la métrique g sur S induite par le plongement de S dans $\mathbb{R}^{n+2}$ muni du produit scalaire euclidien $<, >$. On a

$$g = E\,dx^2 + 2F\,dxdy + G\,dy^2$$

avec

$$E = < \frac{\partial\varphi}{\partial x}, \frac{\partial\varphi}{\partial x} > = 1 + \left(\frac{\partial I_1}{\partial x}\right)^2 + \cdots + \left(\frac{\partial I_n}{\partial x}\right)^2$$

$$F =< \frac{\partial\varphi}{\partial x}, \frac{\partial\varphi}{\partial y} >= \frac{\partial I_1}{\partial x}\frac{\partial I_1}{\partial y} + \cdots + \frac{\partial I_n}{\partial x}\frac{\partial I_n}{\partial y}$$
$$G =< \frac{\partial\varphi}{\partial y}, \frac{\partial\varphi}{\partial y} >= 1 + \Big(\frac{\partial I_1}{\partial y}\Big)^2 + \cdots + \Big(\frac{\partial I_n}{\partial y}\Big)^2$$

ou de manière équivalente

$$g = dx^2 + dy^2 + {dI_1}^2 + \cdots + {dI_n}^2$$

Nous proposons alors de construire plus généralement des tenseurs symétriques de type (0,2) sur S de la forme

$$dx^2 + dy^2 + \lambda_1\,{dI_1}^2 + \cdots + \lambda_n\,{dI_n}^2 \tag{1}$$

où $\lambda_1, \cdots, \lambda_n$ sont des fonctions réelles définies sur D. Les tenseurs de la forme (1) peuvent être vus comme des métriques sur S induites par son plongement dans un espace métrique $(\mathbb{R}^{n+2}, h)$. En effet, si on plonge S dans $\mathbb{R}^{n+2}$ muni de la métrique

$$h = \begin{pmatrix} 1 & 0 \\ 0 & 1 \end{pmatrix} \oplus \begin{pmatrix} \lambda_1 & 0 & 0 & \cdots\cdots & 0 \\ 0 & \lambda_2 & 0 & \cdots\cdots & 0 \\ 0 & 0 & \ddots & & \vdots \\ \vdots & \vdots & & \ddots & \vdots \\ 0 & 0 & \cdots\cdots & 0 & \lambda_n \end{pmatrix}$$

la métrique induite sur S par h est

$$g = E\,dx^2 + 2F\,dxdy + G\,dy^2$$

avec

$$E = h\Big(\frac{\partial\varphi}{\partial x}, \frac{\partial\varphi}{\partial x}\Big) = 1 + \lambda_1\Big(\frac{\partial I_1}{\partial x}\Big)^2 + \cdots + \lambda_n\Big(\frac{\partial I_n}{\partial x}\Big)^2$$
$$F = h\Big(\frac{\partial\varphi}{\partial x}, \frac{\partial\varphi}{\partial y}\Big) = \lambda_1\frac{\partial I_1}{\partial x}\frac{\partial I_1}{\partial y} + \cdots + \lambda_n\frac{\partial I_n}{\partial x}\frac{\partial I_n}{\partial y}$$
$$G = h\Big(\frac{\partial\varphi}{\partial y}, \frac{\partial\varphi}{\partial y}\Big) = 1 + \lambda_1\Big(\frac{\partial I_1}{\partial y}\Big)^2 + \cdots + \lambda_n\Big(\frac{\partial I_n}{\partial y}\Big)^2$$

En développant, on obtient

$$g = dx^2 + dy^2 + \lambda_1\Big[\Big(\frac{\partial I_1}{\partial x}\Big)^2 dx^2 + 2\frac{\partial I_1}{\partial x}\frac{\partial I_1}{\partial y}dxdy + \Big(\frac{\partial I_1}{\partial y}\Big)^2 dy^2\Big] + \cdots$$

$$+\lambda_n\Big[\Big(\frac{\partial I_n}{\partial x}\Big)^2 dx^2 + 2\frac{\partial I_n}{\partial x}\frac{\partial I_n}{\partial y}dxdy + \Big(\frac{\partial I_n}{\partial y}\Big)^2 dy^2\Big]$$
$$= dx^2 + dy^2 + \lambda_1\Big(\frac{\partial I_1}{\partial x}dx + \frac{\partial I_1}{\partial y}dy\Big)\otimes\Big(\frac{\partial I_1}{\partial x}dx + \frac{\partial I_1}{\partial y}dy\Big) + \cdots$$
$$+\lambda_n\Big(\frac{\partial I_n}{\partial x}dx + \frac{\partial I_n}{\partial y}dy\Big)\otimes\Big(\frac{\partial I_n}{\partial x}dx + \frac{\partial I_n}{\partial y}dy\Big)$$
$$= dx^2 + dy^2 + \lambda_1{dI_1}^2 + \cdots + \lambda_n{dI_n}^2$$

où $\otimes$ dénote le produit tensoriel sur le $C^k(D)$-module des 1-formes différentielles sur D.

L'idée de voir les tenseurs (1) comme des tenseurs métriques permet d'appliquer la méthode de détection de contours. Les fonctions λ_i vont alors servir de poids aux composantes I_i dans la mesure des variations de I. Pratiquement, elles déterminent le type de contours à détecter.

L'objectif de cette première Partie est de montrer que les fibrés en algèbres de Clifford fournissent un cadre plus naturel pour construire des tenseurs métriques de la forme (1) que l'approche usuelle surfacique qui consiste à calculer une première forme fondamentale. Nous considérons une image comme une section d'un fibré en algèbre de Clifford trivial $(\mathcal{CT}(D), \pi, D)$ au-dessus de son domaine de définition D. La différentielle de fonctions est alors remplacée par une connection ∇ sur le fibré. De plus, le produit tensoriel $\otimes$ sur le $C^k(D)$-module des 1-formes différentielles sur D est remplacé par le produit tensoriel sur le $\Gamma(\mathcal{CT}(D))$-bimodule des 1-formes différentielles sur D à valeur dans $\mathcal{CT}(D)$. Sur ce dernier point, nous obtenons le résultat suivant.

On note $\mathcal{A}$ l'anneau des fonctions définies sur D à valeur dans $\mathbb{R}$, et $\mathcal{B}$ l'anneau $\Gamma(\mathcal{CT}(D))$ des sections de $\mathcal{CT}(D)$.

Proposition 2 *Le couple*

$$(\Gamma_1, \varphi) := (\Gamma(T^*D \otimes_{\mathcal{A}} T^*D \otimes_{\mathcal{A}} \mathcal{CT}(D)), \varphi)$$

est une solution du problème universel définissant le produit tensoriel du $\mathcal{B}$-bimodule

$$\Gamma_0 := \Gamma(T^*D \otimes_{\mathcal{A}} \mathcal{CT}(D))$$

avec lui-même, où φ est l'application de $\Gamma_0 \times \Gamma_0$ dans Γ_1 définie par

$$((\omega_1 \otimes m_1), (\omega_2 \otimes m_2)) \longmapsto (\omega_1 \otimes \omega_2) \otimes (m_1 m_2)$$

De la Proposition 1, $\Gamma_0 \otimes_{\mathcal{B}} \Gamma_0$ est isomorphe à l'ensemble des tenseurs de rang 2 à valeur dans $\mathcal{CT}(D)$. Si η_1 et η_2 sont dans $\Gamma(T^*D)$, s_1 et s_2 sont dans $\mathcal{B}$, alors $(\eta_1 \otimes s_1) \otimes (\eta_2 \otimes s_2)$ peut s'identifier avec le tenseur de rang 2 à valeur dans $\mathcal{CT}(D)$ qui envoie $(X \otimes Y)$ sur $\eta_1(X)\eta_2(Y)s_1 s_2$.

On note

$$(\eta_1 \otimes s_1)(\eta_2 \otimes s_2) = (\eta_1 \eta_2) \otimes (s_1 s_2)$$

le produit symmétrique de $(\eta_1 \otimes s_1)$ et $(\eta_2 \otimes s_2)$. On l'étend par linéarité. Ce produit symmétrique peut s'identifier avec le tenseur symmétrique de rang 2 à valeur dans $\mathcal{CT}(D)$ défini par

$$(X \otimes Y) \longmapsto \frac{1}{2}(\eta_1(X)\eta_2(Y) + \eta_2(X)\eta_1(Y))s_1 s_2$$

Enfin on note $(\eta_1 \otimes s_1) \underline{\otimes} (\eta_2 \otimes s_2)$ l'élément $(\eta_1 \otimes s_1) \otimes (\eta_2 \otimes s_2)$ de $\Gamma_0 \otimes_{\mathcal{B}} \Gamma_0$ pour préciser que le produit tensoriel est par rapport $\mathcal{B}$.

On construit alors des tenseurs symétriques (0,2) sur D à valeur dans $\mathcal{CT}(D)$ de la forme

$$dx^2 \otimes 1 + dy^2 \otimes 1 + {dI_1}^2 \otimes \lambda_1 + \cdots {dI_n}^2 \otimes \lambda_n$$

ou

$$dx^2 \otimes 1 + dy^2 \otimes 1 + \lambda_1 \, {dI_1}^2 \otimes 1 + \cdots \lambda_n \, {dI_n}^2 \otimes 1 \tag{2}$$

En identifiant $\mathbb{R}$ et son injection dans chaque fibre $\pi^{-1}(q)$, le tenseur (2) s'identifie à

$$dx^2 + dy^2 + \lambda_1 \, {dI_1}^2 + \cdots \lambda_n \, {dI_n}^2$$

qui est un tenseur de la forme (1).

Section 1. A metric approach to nD images edge detection with Clifford algebras. Dans cette Section, on s'intéresse à détecter des contours sur des images couleur ($n = 3$) et couleur/infrarouge ($n = 4$) dans la base $LSHT$ (Luminance, Saturation, Hue, Temperature) en utilisant l'approche métrique de Di Zenzo. On cherche à calculer la première forme fondamentale de la surface paramétrée par

$$\varphi \colon (x, y) \longmapsto (x, y, l(x, y), s(x, y), h(x, y), t(x, y))$$

plongée dans $\mathbb{R}^6$ muni de la métrique

$$\begin{pmatrix} 1 & 0 \\ 0 & 1 \end{pmatrix} \oplus \begin{pmatrix} \lambda & 0 & 0 & 0 \\ 0 & \lambda & 0 & 0 \\ 0 & 0 & \kappa\,\xi & 0 \\ 0 & 0 & 0 & \eta \end{pmatrix} \tag{3}$$

où λ, κ et η sont des fonctions positives servant à déterminer le poids des composantes de luminance, saturation, teinte et température dans la segmentation. Notons que la composante teinte, définie sur $\mathbb{R}/2\pi\mathbb{Z}$, est ici plongée dans $\mathbb{R}$. Le rôle de la fonction ξ est de contrôler la pertinence de la teinte en fonction de la saturation. En effet, un même écart de teinte représente visuellement un plus grand écart de couleur à fortes saturations qu'à faibles saturations.

Le tenseur symmétrique de type (0,2) que l'on cherche à calculer est donc

$$g = dx^2 + dy^2 + \lambda \, dl^2 + \lambda \, ds^2 + \kappa \, \xi \, dh^2 + \eta \, dt^2 \tag{4}$$

Le résultat principal de cette Section est que l'on peut construire (4) sans considérer la différentielle de chacune des composantes l, s, h et t, contrairement à l'approche basée sur les surfaces. D'un point de vue pratique, cela signifie que l'on peut calculer les coefficients g_{ij} de g sans avoir à calculer explicitement les dérivées de chaque composante. De plus, dans le cadre de certaines applications, les informations contenues dans les différentes composantes sont mixées pour ajuster les coefficients de la métrique (3), ce qu'une approche marginale ne permet pas.

Pour cela, nous considérons le fibré en algèbres de Clifford trivial $(\mathcal{CT}(D), \pi, D)$ au-dessus de D où la fibre au-dessus un point q de D est l'algèbre de Clifford générée par $\mathbb{R}^4$ muni de la forme quadratique $Q(q)$ de représentation matricielle

$$\begin{pmatrix} \lambda(q)/3 & 0 & 0 & 0 \\ 0 & \lambda(q)/3 & 0 & 0 \\ 0 & 0 & \lambda(q)/3 & 0 \\ 0 & 0 & 0 & \eta(q) \end{pmatrix}$$

dans la base $(e_1(q), e_2(q), e_3(q), e_4(q))$.

En tant que fibré vectoriel de rang 16, on munit $(\mathcal{CT}(D), \pi, D)$ d'une connection ∇ déterminée par les symboles

$$\Upsilon_{ij}^k = \begin{cases} \dfrac{\partial_i \lambda}{\lambda} & \text{si } k = j \in \{6, 7, 9\} \\ \\ 0 & \text{sinon} \end{cases}$$

dans le repère holonome $(\partial/\partial x, \partial/\partial y)$ du fibré tangent de D et le repère (e_1, e_2, e_3, e_4) de $(\mathcal{CT}(D), \pi, D)$.

Ensuite, on plonge l'espace d'acquisition d'une image couleur-infrarouge *RGBT* (Red, Green, Blue, Temperature) dans $\mathbb{R}^4$. Ainsi, on va considérer une image couleur/infrarouge I comme un section de $(\mathcal{CT}(D), \pi, D)$ de la forme

$$I(q) = r(q)e_1(q) + g(q)e_2(q) + b(q)e_3(q) + t(q)e_4(q)$$

À partir de I, on construit deux sections Ψ et γ données par

$$\Psi = S^\dagger I S$$

où S est la section à valeur dans le groupe des spineurs

$$S = \exp\left[-\frac{h}{2}\left(\frac{e_1e_2 - e_1e_3 + e_2e_3}{\|e_1e_2 - e_1e_3 + e_2e_3\|}\right)\right]$$

et

$$\gamma = \frac{v}{\|v\|}\rho$$

où ρ est le vecteur chrominance unitaire de la couleur rouge et v est la section vecteur chrominance de I. Le symbole $\| \ \|$ signifie que l'on considère la norme en chaque fibre $\pi^{-1}(q)$.

Le résultat principal de cette section est la Proposition suivante.

Proposition 3 *Soient*

i. P_1 (resp. P_2) la section de $\mathrm{End}(\mathcal{CT}(D))$ *telle que $P_1(q)$ (resp. $P_2(q)$) est la projection orthogonale sur le plan engendré par la luminance et la temperature (resp. sur le plan de chrominance) dans la fibre $\pi^{-1}(q)$;*

ii. dx (resp. dy) la 1-forme à valeur dans $\mathcal{CT}(D)$ $dx \otimes 1$ (resp. $dy \otimes 1$) et X (resp. Y) le champ de vecteurs sur D de coordonnées $(1, 0)$ *(resp.* $(0, 1)$*) ;*

iii. E, F, G les coefficients de la première forme fondamentale de $\varphi(D)$ et χ le tenseur de rang 2 à valeur dans $\mathcal{CT}(D)$:

$$\chi = dx \underline{\otimes} dx + dy \underline{\otimes} dy + P_1(\tilde{\nabla}\psi)P_1(\tilde{\nabla}\psi) + \frac{9}{2}P_2(\tilde{\nabla}\psi)\underline{\otimes}P_2(\tilde{\nabla}\psi) - \kappa\xi(\gamma^\dagger\tilde{\nabla}\gamma)\underline{\otimes}(\gamma^\dagger\tilde{\nabla}\gamma)$$

Alors par l'identification de $\mathbb{R}$ et son injection dans une algèbre de Clifford, nous avons

$$E = \chi(X \otimes X) \qquad F = \chi(X \otimes Y) \qquad G = \chi(Y \otimes Y) \tag{5}$$

En d'autres termes, χ peut être vu comme la métrique de la surface $\varphi(D)$.

Remarques sur les notations. Le symbole $\underline{\otimes}$ dénote le produit tensoriel sur l'anneau des sections $\mathcal{CT}(D)$, alors que le symbole $\otimes$ denote le produit tensoriel sur l'anneau des fonctions définies sur D à valeur dans $\mathbb{R}$. $P_1(\widetilde{\nabla}\psi)P_1(\widetilde{\nabla}\psi)$ est le produit symmétrique de $P_1(\widetilde{\nabla}\psi)$ par lui-même.

De (5), on déduit une formulation discrète des coefficients E, F et G. Pour cela, on généralise le filtre dérivatif de Sobel au cadre des fibrés vectoriels en utilisant le transport parallèle associé à la connexion ∇.

Nous appliquons ces formules à de la détection de contours sur des images couleur (vues comme section d'un sous-fibré de rang 3 de $\mathcal{CT}(D)$) et couleur/infrarouge en jouant sur les fonctions λ, η et κ.

Section 2. Clifford algebras bundles to multidimensional image segmentation
La finalité de la Section 2 est la même que celle de la Section 1, c'est-à-dire construire des tenseurs symétriques d'ordre 2 de la forme (1) pour détecter des contours sur des images multicanaux en jouant sur les valeurs des fonctions λ_i. Comme dans la Section 1, nous utilisons le cadre des fibrés en algèbres de Clifford pour construire ces tenseurs. Ici, nous montrons que le choix d'une connexion ∇ sur le fibré en algèbres de Clifford trivial $D \times \mathbb{R}_{n,0}$ et d'une section S que l'on dérive avec cette connexion fournit l'information nécessaire pour construire des tenseurs de la forme (1). En effet, nous montrons que le terme ∇S contient à la fois la différentielle de la fonction image (les différentielles dI_i des composantes I_i) et les informations permettant de construire les fonctions λ_i déterminant la segmentation. En un sens, cette approche se situe en amont des approches basée sur les surfaces et celle en Section 1, puisque l'on a ici un cadre où l'on construit également les fonctions λ_i, c'est-à-dire la métrique de l'espace ambient dans l'approche surfacique et la métrique du fibré dans l'approche de la Section 1.

Nous présentons une méthode générale pour construire des tenseurs de la forme (1). Les applications à la détection de contour sur des images couleur et couleur/infrarouge que l'on présente dans cette Section en sont des cas particuliers.

On utilise en particulier le résultat suivant. Sur un fibré en algèbre de Clifford trivial $E = D \times \mathbb{R}_{n,0}$, toute connexion ∇ peut s'écrire

$$\nabla = d + \omega$$

où d est la différentielle sur $C^k(D)$ et $\omega \in \Gamma(T^*D \otimes \mathrm{End}(E)) = \Gamma(T^*D) \otimes \mathrm{End}(\mathbb{R}_{n,0})$. En d'autres termes, pour $S = \sum S_{i_1 \cdots i_k} e_{i_1 \cdots i_k} \in \Gamma(E)$, on a

$$\nabla S = \sum dS_{i_1 \cdots i_k} \otimes e_{i_1 \cdots i_k} + \omega.S$$

Finalement, une connexion sur E est complètement déterminée par la 1-forme ω.

On considère un fibré vectoriel trivial (E_1, π_1, D) de rang n de repère global $(e_1, \cdots, e_n)$, et un sous-fibré (F_1, π_1, D) de (E_1, π_1, D) de rang m de repère global $(e_{j_1}, \cdots, e_{j_m})$. Le fibré (E_1, π_1, D) génère un fibré en algèbres de Clifford $(\mathcal{CT}_1(D), \widetilde{\pi}_1, D)$ de repère global $(1, e_1, e_2, \cdots, e_n, e_1e_2, \cdots, e_1e_2 \cdots e_n)$. Soient respectivement ∇_1 et S une connexion

et une section sur $(\mathcal{CT}_1(D), \widetilde{\pi}_1, D)$. La 1-forme $\nabla_1 S$ sur D à valeur dans $\mathcal{CT}_1(D)$ se décompose de la manière suivante

$$\nabla_1 S = \langle \nabla_1 S \rangle_0 + \langle \nabla_1 S \rangle_1 + \langle \nabla_1 S \rangle_2 + \cdots + \langle \nabla_1 S \rangle_n$$

où $\langle \nabla_1 S \rangle_k$ est la partie de degré k de $\nabla_1 S$.
En particulier, la partie vectorielle $\eta_1 := \langle \nabla_1 S \rangle_1$ est de la forme

$$\eta_1 = \sum_{i=1}^{n} \eta_{1i} \otimes e_i$$

On suppose que chaque 1-forme η_{1i} est exacte, i.e. η_{1i} peut s'écrire comme la différentielle ds_i d'une fonction s_i sur D, ainsi

$$\eta_1 = \sum_{i=1}^{n} ds_i \otimes e_i \tag{6}$$

On construit un fibré vectoriel trivial (E_2, π_2, D) de rang m de repère global $(f_1, \cdots, f_m)$. À partir de l'information fournie par $\nabla_1 S$, on construit des fonctions $h_i, i = 1 \cdots m$ déterminant les coefficients de la métrique

$$h = \begin{pmatrix} h_1 & 0 & 0 & \cdots\cdots & 0 \\ 0 & h_2 & 0 & \cdots\cdots & 0 \\ 0 & 0 & \ddots & & \vdots \\ \vdots & \vdots & & \ddots & \vdots \\ 0 & 0 & \cdots\cdots & 0 & h_n \end{pmatrix}$$

du fibré (E_2, π_2, D) dans le repère $(f_1, \cdots, f_m)$. On note $(\mathcal{CT}_2(D), \widetilde{\pi}_2, D)$ le fibré en algèbre de Clifford généré par (E_2, π_2, D) muni de la métrique h et on considère le morphisme de fibré vectoriel $\widetilde{\psi}$ de $(\mathcal{CT}_1(D), \widetilde{\pi}_1, D)$ dans $(\mathcal{CT}_2(D), \widetilde{\pi}_2, D)$ défini par

$$\widetilde{\psi}(p)\Big(e_{i_1}(p) e_{i_2}(p) \cdots e_{i_k}(p)\Big) = \begin{cases} f_{\alpha_1}(p) f_{\alpha_2}(p) \cdots f_{\alpha_k}(p) & \text{si} \quad \left| \begin{array}{l} e_{i_1}(p) = e_{j_{\alpha_1}}(p) \\ e_{i_2}(p) = e_{j_{\alpha_2}}(p) \\ \qquad \vdots \\ e_{i_k}(p) = e_{j_{\alpha_k}}(p) \end{array} \right. \\ 0 & \text{sinon} \end{cases}$$

De $\widetilde{\psi}$, on construit un morphisme de fibré vectoriels Ψ de $(T^*D \otimes CT_1(D), p_1, D)$ dans$(T^*D \otimes CT_2(D), p_2, D)$ qui envoie $\eta(p) \otimes e_{i_1}(p) e_{i_2}(p) \cdots e_{i_k}(p)$ sur

$$\begin{cases} \eta(p) \otimes f_{\alpha_1}(p) f_{\alpha_2}(p) \cdots f_{\alpha_k}(p) & \text{si} \quad \left| \begin{array}{l} e_{i_1}(p) = e_{j_{\alpha_1}}(p) \\ e_{i_2}(p) = e_{j_{\alpha_2}}(p) \\ \qquad \vdots \\ e_{i_k}(p) = e_{j_{\alpha_k}}(p) \end{array} \right. \\ 0 & \text{sinon} \end{cases} \tag{7}$$

On applique ce morphisme à $\{\eta_1(p), p \in D\}$ et on obtient la forme $\eta_2 \in \Gamma(T^*D \otimes \mathcal{CT}_2(D))$ donnée par

$$\eta_2 = \sum_{l=1}^{m} ds_{j_l} \otimes f_l$$

En calculant le produit tensoriel symmetrisé de η_2 avec lui-même, on a

$$(\eta_2)^2 = \Big(\sum_{l=1}^{m} ds_{j_l} \otimes f_l\Big)\Big(\sum_{l=1}^{m} ds_{j_l} \otimes f_l\Big) = \sum_{l=1}^{m} (ds_{j_l})^2 \otimes h_l \tag{8}$$

Ainsi, en considérant

$$dx^2 \otimes 1 + dy^2 \otimes +(\eta_2)^2$$

on construit un tenseur symmétrique de type (0,2) à valeur dans $\mathcal{CT}_2(D)$ de la forme (2).

Dans la deuxième partie de cette Section, nous donnons des exemples de choix 1-formes ω, de sections que l'on dérive avec la connexion $\nabla_1 = d + \omega$, et de sous-fibrés (F_1, π_1, D), ainsi que l'illustration des détections de contour qu'ils engendrent.

Partie 2 : Equations de la chaleur associées à des Laplaciens généralisés pour la régularisation.

Dans cette Partie, nous utilisons un nouveau cadre théorique pour la régularisation de champs tels des images (vidéos) multicanaux, champs de vecteurs et champs de repères orthonormés. Plus précisemment, nous utilisons le cadre des équations de la chaleur associées à des Laplaciens généralisés sur des fibrés vectoriels au-dessus de variétés Riemanniennes [13]. Le flot de Beltrami de Sochen et al. (voir e.g.[74],[77]) et l'approche de Tschumperlé et al. [83] basée sur les Laplaciens orientés peuvent être considérés de ce point de vue, ceci fait l'objet de la Section 3. Nous y construisons également une classe de Laplaciens généralisés associés à des repères mobiles, étendant l'approche de Tschumperlé et al. où les Laplaciens orientés sont associés à des repères localement fixes. Dans la Section 4, nous étendons le flot de Beltrami aux champs de vecteurs et champs de repères orthonormés en considérant l'équation de la chaleur associée à l'opérateur de Hodge (ou Clifford-Hodge) sur le fibré de Clifford d'une variété Riemannienne bien choisie.

La plupart des EDP's utilisées dans la régularisation d'images nD sont des EDP's d'ordre 2 de la forme

$$\frac{\partial I^i}{\partial t} = \sum_{j,k=1}^{2} f_{jk} \frac{\partial^2 I^i}{\partial j\, \partial k} + \text{termes d'ordre inférieur} \tag{9}$$

de condition initiale $I\colon (x,y) \longmapsto (I^1(0,x_1,x_2), \cdots, I^n(0,x_1,x_2))$ une image nD où les f_{jk} sont des fonctions réelles. On peut alors remarquer que l'ensemble des termes de droite de l'équation (9), pour $i = 1 \cdots n$, peut être vu comme un opérateur différentiel H d'ordre 2 agissant sur une section I d'un fibré vectoriel E de rang n au dessus d'une variété Riemannienne X de dimension 2, appelé **Laplacien généralisé**.

Définition 12 *Soit E un fibré vectoriel au-dessus d'une variété Riemannienne (X, g). Un **Laplacien généralisé** sur E est un opérateur différentiel $H\colon \Gamma(E) \longrightarrow \Gamma(E)$ d'ordre 2 qui s'écrit*

$$H = -\sum_{ij} g^{ij} \partial_i\, \partial_j + (\textit{termes d'ordre} \leqslant 2)$$

dans un système de coordonnées locales, où g^{ij} est tel que $(g^{ij}(x))$ est l'inverse de la matrice $g(x) = (g_{ij}(x))$.

À tout Laplacien généralisé H, on peut associer un opérateur $e^{-tH}\colon \Gamma(E) \longrightarrow \Gamma(E)$ pour $t > 0$, tel que $I(t,x) = e^{-tH} I(x)$ satisfait **l'équation de la chaleur**

$$\frac{\partial I}{\partial t} + HI = 0$$

L'opérateur e^{-tH} est un opérateur intégral de la forme

$$(e^{-tH} I)(x) = \int_X K_t(x,y,H) I(y)\, dy \tag{10}$$

où $K_t(x,y,H)\colon E_y \longrightarrow E_x$ est une application linéaire. L'application $(t,x,y)\colon \longmapsto K_t(x,y,H)$ est appelée **noyau de la chaleur de** H.

En toute généralité, il n'existe pas d'expression explicite pour le noyau $K_t(x,y,H)$ et par conséquent pour la solution (10). Il existe cependant des noyaux $K_t^N(x,y,H), N \in \mathbb{N}$, ayant des expressions explicites et approximant localement le noyau de la chaleur de H pour t petit. Pour déterminer leurs expressions, il faut tout d'abord associer l'opérateur H à une connexion ∇^E sur le fibré. Cela se fait au moyen du **Laplacien connexion**.

Définition 13 *Soit E un fibré vectoriel au-dessus d'une variété Riemannienne (X,g), muni d'une connexion ∇^E. Comme (X,g) est Riemannienne, elle possède une connexion canonique, la connexion de Levi-Cevita ∇. À toute paire de champs de vecteurs tangents V et W sur X, on associe un opérateur $\nabla^2_{V,W}\colon \Gamma(E) \longrightarrow \Gamma(E)$ en posant*

$$\nabla^2_{V,W}\varphi \equiv \nabla^E_V \nabla^E_W \varphi - \nabla^E_{\nabla_V W}\varphi \tag{11}$$

*Le **Laplacien connexion** $\Delta^E\colon \Gamma(E) \longrightarrow \Gamma(E)$ est défini par*

$$\Delta^E \varphi = -trace(\nabla^2_{\cdot,\cdot}\varphi)$$

où trace dénote la contraction avec la métrique g.

Nous avons le résultat suivant [13] :
Tout Laplacien généralisé est de la forme $\Delta^E + F$, où Δ^E est le Laplacien connexion associé à une certaine connexion ∇^E, et F est une section du fibré End(E). En particulier, un Laplacien connexion Δ^E est un Laplacien généralisé.

Dans le théorème suivant, nous donnons l'expression du noyau $K_t^N(x,y,H)$ et quelques propriétés sous-jacentes [13].

Théoreme 1 *Soit $x \in X$ (de dimension m) et un système de coordonnées normales autour de x, on dénote par $\mathbf{y^i}$ les coordonnées normales d'un point y dans le rayon d'injectivité de X en x, ∂_i les dérivées partielles correspondantes, et par $g_{ij}(\mathbf{y})$ le produit scalaire de ∂_i et ∂_j en $\mathbf{y}$. De plus, on définit*

$$J(x,y) = det(g_{ij}(\mathbf{y}))^{1/2} \qquad pour\ y = exp_x(\mathbf{y})$$

Soit ϵ choisi plus petit que le rayon d'injectivité de X. Soit $\Psi\colon \mathbb{R}_+ \longrightarrow [0,1]$ une fonction lisse telle que $\Psi(s) = 1$ si $s < \epsilon^2/4$ et $\Psi(s) = 0$ si $s > \epsilon^2$.

Soit $\tau(x,y)$: $E_y \longrightarrow E_x$ le transport parallèle le long de l'unique géodésique joignant x et y, et $d(x,y)$ sa longueur.
Soit $K_t^N(x,y,H)$ le noyau défini par

$$\Big(\frac{1}{4\pi t}\Big)^{\frac{m}{2}} e^{-d(x,y)^2/4t}\ \Psi(d(x,y)^2) \sum_{i=0}^{N} t^i \Phi_i(x,y,H) J(x,y)^{-\frac{1}{2}}$$

où les sections Φ_i sont données par $\Phi_0(x,y,H) = \tau(x,y)$ et

$$\tau(x,y)^{-1}\Phi_i(x,y,H) = -\int_0^1 s^{i-1}\tau(x_s,y)^{-1}(B_x.\Phi_{i-1})(x_s,y,H)ds$$

B_x est l'opérateur $J^{1/2} \circ H_x \circ J^{-1/2}$ où H_x est l'opérateur H par rapport à la première variable.

1. Pour tout $N > m/2$, le noyau $K_t^N(x,y,H)$ est asymptotique à $K_t(x,y,H)$:

$$\Big\| \partial_t^k \big[\, K_t(x,y,H) - K_t^N(x,y,H) \,\big] \Big\|_l = O(t^{N-m/2-l/2-k})$$

où $\|\ \|_l$ est une norme sur les sections de classe C^l.

2. On dénote k_t^N l'opérateur défini par

$$(k_t^N I)(x) = \int_X K_t^N(x,y,H) I(y)\, dy \tag{12}$$

Alors pour tout N, $\lim_{t\to 0} \|k_t^N I - I\|_l = 0$.

Dans la pratique, le processus de régularisation que nous utilisons provient de la discrétisation de l'opérateur k_t^N (12), pour un certain N. D'aprés l'expression du noyau $K_t^N(x,y,H)$, cela nécessite de déterminer les courbes géodésiques associées à la connexion de Levi-Cevita sur la variété de base, et l'application transport parallèle associée à la connexion ∇^E sur le fibré. Le calcul de distances géodésiques dans un cadre discret a fait l'objet de nombreux travaux(voir e.g. [76] pour une utilisation de l'algorithme Fast Marching).

Par exemple, l'opérateur k_t^0 est donné par

$$\begin{aligned}(k_t^0 I)(x) &= \int_X K_t^0(x,y,H) I(y) dy \\ &= \Big(\frac{1}{4\pi t}\Big)^{\frac{m}{2}} \int_X e^{-d(x,y)^2/4t}\ \Psi(d(x,y)^2)\, \tau(x,y) I(y)\, J(x,y)^{-\frac{1}{2}}\, dy\end{aligned}$$

Dans le cadre continu, la fonction Ψ détermine les voisinages normaux servant de cadre aux convolutions. Dans le cadre discret, Ψ détermine la taille des masques de convolution. De plus, en nous basant sur la propriété suivante : $J(x,y) = 1 + O(\|\mathbf{y}\|^2)$, nous approximons la fonction J par 1.

Finalement, nous discrétisons $(k_t^0 I)(x)$ par la convolution discrète de $\tau(x,y)I(y)$ avec un masque dont les coefficients sont les distances du point courant au point x (à la normalisation près) si il existe une unique géodésique joignant ce point à x, et 0 sinon.

Section 3. Heat kernels of generalized Laplacians : application to multichannel images/videos regularization. Dans un premier temps, on montre que le flot de Beltrami, dans le contexte de la régularisation d'images, peut être formulé comme une équation de la chaleur sur un fibré vectoriel de rang 1, puis qu'il s'étend de manière naturelle à un fibré vectoriel de rang n dans le cadre de la régularisation d'images nD. Le flot de Beltrami est basé sur la fonctionnelle de Polyakov [66], qui mesure l'énergie du plongement $\varphi : M \longrightarrow N$ d'une variété Riemannienne (M, g) dans une variété Riemannienne (N, h) donnée par

$$E(\varphi) = \int_M g^{\mu\nu} h_{ij} \partial_\mu \varphi^i \partial_\nu \varphi^j \sqrt{g}\, dx$$

où l'on utilise la sommation d'Einstein. Le flot de Beltrami est obtenu par minimisation de cette fonctionnelle. Les équations d'Euler-Lagrange correspondantes mènent au processus de descente de gradient suivant

$$\frac{\partial \varphi^i}{\partial t} = \frac{1}{\sqrt{g}} \partial_\mu (\sqrt{g} g^{\mu\nu} \partial_\nu \varphi^i) + \Gamma^k_{ij} \partial_\mu \varphi^j \partial_\nu \varphi^k g^{\mu\nu}$$

pour $i = 1, \cdots, dim(N)$, où les symboles Γ^k_{ij} sont les symboles de la connexion de Levi-Cevita de (N, h).

Dans ce cadre-là, une image couleur $I\colon (x, y) \longmapsto (r(x, y), g(x, y), b(x, y))$ définie sur $D \subset \mathbb{R}^2$ est considérée comme une variété Riemannienne (D, g) de dimension 2 de métrique

$$g = dx^2 + dy^2 + \lambda dr^2 + \lambda dg^2 + \lambda db^2$$

et le graphe φ de I réalise le plongement de (D, g) dans $(\mathbb{R}^5, h)$ où h est la métrique

$$h = \begin{pmatrix} 1 & 0 \\ 0 & 1 \end{pmatrix} \oplus \begin{pmatrix} \lambda & 0 & 0 \\ 0 & \lambda & 0 \\ 0 & 0 & \lambda \end{pmatrix}$$

Le principe est identique pour une image nD. On retrouve la définition d'une image utilisée dans la Partie 1.

La fonctionnelle de Polyakov de ce plongement est l'aire de D, i.e.

$$E(\varphi) = \int_M \sqrt{g}\, dx$$

La variété $(\mathbb{R}^5, h)$ a pour connexion $\Gamma^k_{ij} \equiv 0$, d'où les équations de la descente de gradient

$$\frac{\partial \varphi^i}{\partial t} = \frac{1}{\sqrt{g}} \partial_\mu (\sqrt{g} g^{\mu\nu} \partial_\nu \varphi^i) \tag{13}$$

pour $i = 3, 4, 5$, avec $\varphi^3 = r$, $\varphi^4 = g$ et $\varphi^5 = b$.

Le terme de droite de l'équation (13) est un opérateur différentiel d'ordre 2 agissant sur la fonction φ^i appelé **opérateur de Laplace-Beltrami** et noté Δ_g.

Le flot de Beltrami (13) peut être reformulé dans le contexte des équations de la chaleur associées à des Laplaciens généralisés à l'aide du **Laplacien scalaire**.

En effet, le Laplacien scalaire sur une variété Riemannienne (X, g) de dimension m est le Laplacien connexion sur le fibré vectoriel $E = C^\infty(X)$. En d'autres termes, c'est le Laplacien connexion sur un fibré vectoriel de rang 1 muni d'une connexion ∇^E définie par les symboles

$$\Upsilon_1 = \cdots = \Upsilon_m$$

i.e. $\nabla^E_X(f) = d_X f$. Dans un système de coordonnées locales, le Laplacien scalaire est défini par

$$\Delta(f) = -\sum_{ij} g^{ij}\Big(\partial_i\partial_j - \sum_k \Gamma^k_{ij}\partial_k\Big)f \tag{14}$$

Il est bien connu que si (X, g) est muni de la connexion de Levi-Cevita, alors l'opérateur de Laplace-Beltrami Δ_g est moins le Laplacien scalaire (14). Ainsi les EDP's $\partial I/\partial t = \Delta_g I$ et $\partial I/\partial t + \Delta I = 0$ sont équivalentes.

Par conséquent, le flot de Beltrami (13) est obtenu par convolution de chaque composante de la condition initiale avec le noyau de la chaleur $K_t(x, y, \Delta)$ du Laplacien scalaire de (D, g). Dans [77], le processus de régularisation est issu de la convolution discrète de chaque composante de l'image initiale avec un noyau discrétisant le noyau $K^0_t(x, y, \Delta)$. En particulier, l'application transport parallèle est l'application Identité.

Dans la Partie 1 nous avons utilisé le cadre des fibrés vectoriels de rang n pour la segmentation d'image nD. Cherchant à réutiliser ce cadre dans le domaine de la régularisation d'image nD, nous montrons que l'on peut définir le flot de Beltrami sur un fibré vectoriel de rang n au dessus de (D, g) en étendant l'équation de la chaleur $\partial I/\partial t + \Delta I = 0$ sur un tel fibré. Par rapport aux applications aux images couleur présentées, nous prenons $n = 3$.

Le Laplacien scalaire peut être étendu en un Laplacien connexion Δ^E sur un fibré vectoriel trivial E de rang 3 de base globale (e_1, e_2, e_3) associé à la connexion ∇^E définie par

$$\Upsilon^k_{ij} = 0 \quad \text{pour} \quad i = 1, 2 \quad \text{et} \quad k, j = 1, 2, 3 \tag{15}$$

i.e. $\nabla^E_{\partial_i} e_j = \sum_k \Upsilon^k_{ij} e_k = 0$.
Ainsi pour $I = I_1 e_1 + I_2 e_2 + I_3 e_3 \in \Gamma(E)$,

$$\Delta^E(I) = \Delta I_1\, e_1 + \Delta I_2\, e_2 + \Delta I_3\, e_3$$

De plus, l'application transport parallèle sur E associée à ∇^E est l'application Identité.

L'article *Vector-Valued Image Regularization with PDEs : A Common Framework for Different Applications* de Tschumperlé et al. [83] traite d'une diffusion anisotrope à l'aide d'une classe d'opérateurs différentiels d'ordre 2 agissant sur les fonctions réelles définies sur $D \subset \mathbb{R}^2$ appelés **Laplaciens orientés**. Ce sont les opérateurs de la forme

$$\Delta(f) = c_1 d^2_{\xi,\xi} f + c_2 d^2_{\eta,\eta} f \tag{16}$$

où c_1, c_2 sont deux fonctions et (ξ, η) un repère localement constants sur D.

Supposons que les fonctions c_1, c_2 et le repère (ξ, η) soient constants sur D. Alors la solution de l'équation de la chaleur

$$\frac{\partial f}{\partial t} = \Delta(f) \tag{17}$$

provient de la convolution de la condition initiale avec un noyau G, appelé **noyau gaussien orienté**, et défini par

$$G_t(x, y, \Delta) = \frac{1}{4\pi t} exp\left(-\frac{(x \quad y)\,\mathbf{T}^{-1}\,(x \quad y)^T}{4t}\right) \tag{18}$$

où $\mathbf{T}$ est la matrice $c_1\xi\xi^T + c_2\eta\eta^T$.

Dans la pratique, les fonctions c_1, c_2 et le repère (ξ, η) sont supposés constants sur le voisinage 5x5 de chaque $x \in D$. Le processus de diffusion provient de la convolution discrète de chaque composante de l'image avec un masque de taille 5x5 discrétisant le noyau $G_t(x, y, \Delta)$.

Dans cette Section, nous généralisons cette diffusion au cas où les fonctions c_1, c_2 et le repère (ξ, η) ne sont plus supposés localement constants. Nous montrons que les Laplaciens (16) peuvent alors être vus, à signe près, comme des Laplaciens généralisés. C'est le sujet de la Proposition suivante.

Proposition 4 *Soit (X, g) une variété Riemannienne de dimension 2 avec*

$$g = \frac{1}{c_1 c_2 (\xi_1\eta_2 - \eta_1\xi_2)^2} \begin{pmatrix} c_1\,{\xi_2}^2 + c_2\,{\eta_2}^2 & -(c_1\xi_1\xi_2 + c_2\eta_1\eta_2) \\ -(c_1\xi_1\xi_2 + c_2\eta_1\eta_2) & c_1\,{\xi_1}^2 + c_2\,{\eta_1}^2 \end{pmatrix}$$

Soit E un fibré vectoriel de rang 1 au-dessus de X de repère global e_1, muni de la connexion ∇^E définie par $\nabla^E_{\partial_x} e_1 = \Upsilon_1\, e_1$ and $\nabla^E_{\partial_y} e_1 = \Upsilon_2\, e_1$ où

$$\Upsilon_1 = \frac{1}{2}(g_{11}a + g_{12}b) \qquad \Upsilon_2 = \frac{1}{2}(g_{12}a + g_{22}b)$$

et

$$a = c_1\frac{\partial\xi_1}{\partial x}\xi_1 + c_1\frac{\partial\xi_1}{\partial y}\xi_2 + c_2\frac{\partial\eta_1}{\partial x}\eta_1 + c_2\frac{\partial\eta_1}{\partial y}\eta_2 + 2g^{12}\,\Gamma^1_{12} + g^{11}\,\Gamma^1_{11} + g^{22}\,\Gamma^1_{22}$$

$$b = c_1\frac{\partial\xi_2}{\partial x}\xi_1 + c_1\frac{\partial\xi_2}{\partial y}\xi_2 + c_2\frac{\partial\eta_2}{\partial x}\eta_1 + c_2\frac{\partial\eta_2}{\partial y}\eta_2 + 2g^{12}\,\Gamma^2_{12} + g^{11}\,\Gamma^2_{11} + g^{22}\,\Gamma^2_{22}$$

Soit $\tilde{f} = f e_1 \in \Gamma(E)$. L'opérateur différentiel H d'ordre 2 défini par

$$H(\tilde{f}) = \Delta(f)\, e_1 \tag{19}$$

est un Laplacien généralisé sur E.

Par conséquent, la solution de l'équation de la chaleur

$$\frac{\partial\tilde{f}}{\partial t} + H\tilde{f} = 0 \tag{20}$$

provient de la convolution de la condition initiale avec le noyau de la chaleur $K_t(x, y, H)$. Dans la pratique, le processus de diffusion est issu de la convolution de la condition initiale avec un noyau $K^N_t(x, y, H)$. Cela nécessite de déterminer le transport parallèle associé à la connexion ∇^E.

Proposition 5 *Soient (X, g), E et ∇^E de la Proposition précédente.*
Soit $\gamma(t) = (\gamma_1(t), \gamma_2(t))$ une courbe C^1 dans X telle que $\gamma(0) = y$, et $Y_0 = Y_0^1 e_1(y) \in E_y$.
Alors, le transport parallèle Y de Y_0 le long de γ est défini par

$$Y(t) \;=\; Y_0^1\, exp\Big(-\int_0^t \dot\gamma_1(s)\Upsilon_1(\gamma(s)) + \dot\gamma_2(s)\Upsilon_2(\gamma(s))\;\; ds\Big)\, e_1(\gamma(t))$$

Le processus de régularisation consiste alors à considérer chaque composante d'une image multicanaux comme une section du fibré E et à la convoluer avec un noyau de type $K_t^N(x, y, H)$. Comme précédemment avec le flot de Beltrami, nous cherchons à réutiliser le formalisme de la Partie 1 en considérant une image nD comme une section d'un fibré vectoriel de rang n et en étendant l'équation de la chaleur (20) sur un tel fibré. Par rapport aux applications aux images couleur présentées, nous prenons $n = 3$. Dans un premier temps, nous montrons que H (19) peut être étendu en un Laplacien généralisé sur un fibré vectoriel de dimension 3 de la manière suivante.

Corollaire 1 *Soit (X, g) une variété Riemannienne de dimension 2 avec*

$$g = \frac{1}{c_1 c_2(\xi_1\eta_2 - \eta_1\xi_2)^2}\begin{pmatrix} c_1\,{\xi_2}^2 + c_2\,{\eta_2}^2 & -(c_1\xi_1\xi_2 + c_2\eta_1\eta_2) \\ -(c_1\xi_1\xi_2 + c_2\eta_1\eta_2) & c_1\,{\xi_1}^2 + c_2\,{\eta_1}^2 \end{pmatrix}$$

Soit E un fibré vectoriel trivial de rang 3 au-dessus de X muni d'une connexion ∇^E donnée par les symboles Υ_{ij}^k pour $k, j \in \{1, 2, 3\}$ et $i \in \{1, 2\}$, définis par $\Upsilon_{ij}^k = 0$ si $k \neq j$ et

$$\Upsilon_{ij}^k = \begin{cases} \dfrac{g^{12}b - g^{22}a}{2g^{11}g^{22} - 2(g^{12})^2} & si \quad i = 1 \quad et \quad k = j \\ \\ \dfrac{g^{12}a - g^{11}b}{2g^{11}g^{22} - 2(g^{12})^2} & si \quad i = 2 \quad et \quad k = j \end{cases}$$

dans le repère global (e_1, e_2, e_3) de E et le repère $\partial_i := \partial/\partial x_i$ de TX, où

$$a = c_1\frac{\partial\xi_1}{\partial x}\xi_1 + c_1\frac{\partial\xi_1}{\partial y}\xi_2 + c_2\frac{\partial\eta_1}{\partial x}\eta_1 + c_2\frac{\partial\eta_1}{\partial y}\eta_2 + 2g^{12}\Gamma_{12}^1 + g^{11}\Gamma_{11}^1 + g^{22}\Gamma_{22}^1$$

$$b = c_1\frac{\partial\xi_2}{\partial x}\xi_1 + c_1\frac{\partial\xi_2}{\partial y}\xi_2 + c_2\frac{\partial\eta_2}{\partial x}\eta_1 + c_2\frac{\partial\eta_2}{\partial y}\eta_2 + 2g^{12}\Gamma_{12}^2 + g^{11}\Gamma_{11}^2 + g^{22}\Gamma_{22}^2$$

Soit $s = s_1e_1 + s_2e_2 + s_3e_3 \in \Gamma(E)$. Alors l'opérateur différentiel H d'ordre 2 défini par

$$H(s) = \Delta(s_1)\, e_1 + \Delta(s_2)\, e_2 + \Delta(s_3)\, e_3 \tag{21}$$

est un Laplacien généralisé sur E.

On en déduit l'application transport parallèle associée à la connexion ∇^E.

Corollaire 2 *Soient (X, g), E et ∇^E du Corollaire précédent, $\gamma(t) = (\gamma_1(t), \gamma_2(t))$ une courbe C^1 dans X telle que $\gamma(0) = y$, et $Y_0 = Y_0^1 e_1(y) + Y_0^2 e_2(y) + Y_0^3 e_3(y) \in E_y$. Le transport parallèle de Y_0 le long de γ est*

$$Y(t) = Y_0^1\, exp\Big(-\int_0^t \frac{\partial\gamma_1}{\partial s}(s)\Upsilon_1(s) + \frac{\partial\gamma_2}{\partial s}(s)\Upsilon_2(s)\;\; ds\Big)\, e_1(\gamma(t))$$

$$+Y_0^2\, exp\Big(-\int_0^t \frac{\partial\gamma_1}{\partial s}(s)\Upsilon_1(s) + \frac{\partial\gamma_2}{\partial s}(s)\Upsilon_2(s)\ ds\Big)e_2(\gamma(t))$$
$$+Y_0^3\, exp\Big(-\int_0^t \frac{\partial\gamma_1}{\partial s}(s)\Upsilon_1(s) + \frac{\partial\gamma_2}{\partial s}(s)\Upsilon_2(s)\ ds\Big)e_3(\gamma(t))$$

En terme d'applications, nous comparons les processus de diffusion générés par les équations de la chaleur associées aux Laplaciens scalaire, orientés et leur généralisation avec une application à la régularisation d'image couleur. Le processus de régularisation généré par les équations de la chaleur associées aux Laplaciens orientés généralisés semble plus adapté à la préservation des textures sur une image.

Dans la perspective d'applications à la régularisation de vidéos, nous étendons à des variétés de dimension 3 la généralisation des Laplaciens orientés proposée précédemment en dimension 2. Nous montrons dans un premier temps que les opérateurs différentiels Δ d'ordre 2 de la forme

$$\Delta(f) = -c_1 d^2_{\xi,\xi} f - c_1 d^2_{\eta,\eta} f - c_3 d^2_{\lambda,\lambda} f$$

agissant sur les fonctions d'une variété X de dimension 3 où (ξ, η, λ) est un repère mobile sur X et c_1, c_2, c_3 sont trois fonctions sur X peuvent être vus comme des Laplaciens généralisés sur des fibrés vectoriels de rang 1 au-dessus de X.

Proposition 6 *Soit (X, g) une variété Riemannienne de dimension 3 avec*

$$\begin{aligned}
g^{11} &= c_1\,{\xi_1}^2 + c_2\,{\eta_1}^2 + c_3\,{\lambda_1}^2\\
g^{12} &= 2\,c_1\,\xi_1\,\xi_2 + 2\,c_2\,\eta_1\,\eta_2 + 2\,c_3\,\lambda_1\,\lambda_2\\
g^{13} &= 2\,c_1\,\xi_1\,\xi_3 + 2\,c_2\,\eta_1\,\eta_3 + 2\,c_3\,\lambda_1\,\lambda_3\\
g^{22} &= c_1\,{\xi_2}^2 + c_2\,{\eta_2}^2 + c_3\,{\lambda_2}^2\\
g^{23} &= 2\,c_1\,\xi_2\,\xi_3 + 2\,c_2\,\eta_2\,\eta_3 + 2\,c_3\,\lambda_2\,\lambda_3\\
g^{33} &= c_1\,{\xi_3}^2 + c_2\,{\eta_3}^2 + c_3\,{\lambda_3}^2
\end{aligned}$$

Soit E un fibré vectoriel trivial de rang 1 au-dessus de X de repère global e_1, muni de la connexion ∇^E définie par $\nabla^E_{\partial_x} e_1 = \Upsilon_1\, e_1$, $\nabla^E_{\partial_y} e_1 = \Upsilon_2\, e_1$ et $\nabla^E_{\partial_z} e_1 = \Upsilon_3\, e_1$, où

$$\Upsilon_1 = \frac{1}{2}(g_{11}a + g_{12}b + g_{13}c) \qquad \Upsilon_2 = \frac{1}{2}(g_{12}a + g_{22}b + g_{23}c) \qquad \Upsilon_3 = \frac{1}{2}(g_{13}a + g_{23}b + g_{33}c)$$

et

$$\begin{aligned}
a = {} & c_1\frac{\partial\xi_1}{\partial x}\xi_1 + c_1\frac{\partial\xi_1}{\partial y}\xi_2 + c_1\frac{\partial\xi_1}{\partial z}\xi_3 + c_2\frac{\partial\eta_1}{\partial x}\eta_1 + c_2\frac{\partial\eta_1}{\partial y}\eta_2 + c_2\frac{\partial\eta_1}{\partial z}\eta_3 + c_3\frac{\partial\lambda_1}{\partial x}\lambda_1 + c_3\frac{\partial\lambda_1}{\partial y}\lambda_2\\
& + c_3\frac{\partial\lambda_1}{\partial z}\lambda_3 + g^{11}\Gamma^1_{11} + 2g^{12}\Gamma^1_{12} + 2g^{13}\Gamma^1_{13} + g^{22}\Gamma^1_{22} + 2g^{23}\Gamma^1_{23} + g^{33}\Gamma^1_{33}
\end{aligned}$$

$$\begin{aligned}
b = {} & c_1\frac{\partial\xi_2}{\partial x}\xi_1 + c_1\frac{\partial\xi_2}{\partial y}\xi_2 + c_1\frac{\partial\xi_2}{\partial z}\xi_3 + c_2\frac{\partial\eta_2}{\partial x}\eta_1 + c_2\frac{\partial\eta_2}{\partial y}\eta_2 + c_2\frac{\partial\eta_2}{\partial z}\eta_3 + c_3\frac{\partial\lambda_2}{\partial x}\lambda_1 + c_3\frac{\partial\lambda_2}{\partial y}\lambda_2\\
& + c_3\frac{\partial\lambda_2}{\partial z}\lambda_3 + g^{11}\Gamma^2_{11} + 2g^{12}\Gamma^2_{12} + 2g^{13}\Gamma^2_{13} + g^{22}\Gamma^2_{22} + 2g^{23}\Gamma^2_{23} + g^{33}\Gamma^2_{33}
\end{aligned}$$

$$c = c_1\frac{\partial\xi_3}{\partial x}\xi_1 + c_1\frac{\partial\xi_3}{\partial y}\xi_2 + c_1\frac{\partial\xi_3}{\partial z}\xi_3 + c_2\frac{\partial\eta_3}{\partial x}\eta_1 + c_2\frac{\partial\eta_3}{\partial y}\eta_2 + c_2\frac{\partial\eta_3}{\partial z}\eta_3 + c_3\frac{\partial\lambda_3}{\partial x}\lambda_1 + c_3\frac{\partial\lambda_3}{\partial y}\lambda_2$$

$$+c_3\frac{\partial\lambda_3}{\partial z}\lambda_3 + g^{11}\Gamma_{11}^3 + 2g^{12}\Gamma_{12}^3 + 2g^{13}\Gamma_{13}^3 + g^{22}\Gamma_{22}^3 + 2g^{23}\Gamma_{23}^3 + g^{33}\Gamma_{33}^3$$

Soit $\tilde{f} = fe_1 \in \Gamma(E)$. Alors l'opérateur différentiel H d'ordre 2 défini par

$$H(\tilde{f}) = \Delta(f)e_1 \tag{22}$$

est un Laplacien généralisé sur E.

Puis, nous déterminons l'application transport parallèle associée à la connexion ∇^E.

Proposition 7 *Soient (X, g), E et ∇^E de la Proposition précédente.*
Soit $\gamma(t) = (\gamma_1(t), \gamma_2(t), \gamma_3(t))$ une courbe C^1 dans X telle que $\gamma(0) = y$, et $Y_0 = Y_0^1 e_1(y)$.
Alors le transport parallèle Y de Y_0 le long de γ est défini par

$$Y(t) = Y_0^1\, exp\left(-\int_0^t \dot{\gamma_1}(s)\Upsilon_1(\gamma(s)) + \dot{\gamma_2}(s)\Upsilon_2(\gamma(s)) + \dot{\gamma_3}(s)\Upsilon_3(\gamma(s))\ ds\right) e_1(\gamma(t))$$

Section 4. Clifford bundles : a unifying framework for images(videos), vector fields and orthonormal frame fields regularization. Dans cette Section, nous étendons le flot de Beltrami aux champs de vecteurs et champs de repères orthonormés en considérant l'équation de la chaleur associée à **l'opérateur de Clifford-Hodge** sur un fibré de Clifford. On l'appelle le **flot de Clifford-Hodge**.

Sous l'identification du fibré de Clifford $Cl(X, g)$ d'une variété Riemannienne (X, g) et du fibré des formes différentielles $\bigwedge^* TX$, l'opérateur de Clifford-Hodge s'identifie avec **l'opérateur de Laplace-Hodge**

$$\Delta = d\delta + \delta d$$

où d est la dérivée extérieure et δ son adjoint [24]. En particulier, sur les 0-formes c'est-à-dire sur les fonctions, Δ correspond au Laplacien scalaire.

Soit $(e_1, \cdots, e_m)$ un repère orthonormé du fibré tangent de (X, g). L'opérateur de Clifford-Hodge est le carré d'un opérateur différentiel d'ordre 1, **l'opérateur de Dirac** noté D, et défini par

$$D = \sum e_i \nabla_{e_i}^C$$

où ∇^C est la connexion sur $Cl(X, g)$ induite par la Levi-Cevita sur (TX, g) [14].

L'opérateur D^2 est un Laplacien généralisé sur $Cl(X, g)$ pour la connexion ∇^C, c'est l' **identité de Bochner** [55]

$$D^2 = \Delta^C + \sum_{i<j} e_i e_j R_{e_i e_j}$$

où Δ^C est le Laplacien connexion associé à la connexion ∇^C et $R_{e_i e_j}$ est un opérateur d'ordre 0 appelé **transformation de courbure** associée à e_i et e_j.

On peut ainsi considérer l'équation de la chaleur sur le fibré de Clifford

$$\frac{\partial I}{\partial t} + D^2 I = 0 \tag{23}$$

de condition initiale $I : x \longmapsto I(0,x)$, et dont la solution $e^{-tD^2} I$ est donnée par

$$(e^{-tD^2} I)(x) = \int_X K_t(x, y, D^2) I(y)\, dy$$

En particulier, en identifiant les fonctions sur (X, g) avec les sections de $Cl(X, g)$ de degré 0 : $\Gamma(\bigwedge^0 TX)$, l'équation de la chaleur (23) sur $\Gamma(\bigwedge^0 TX)$ s'identifie avec l'EDP (13). Finalement, le flot de Clifford-Hodge sur les sections de degré 0 correspond au flot de Beltrami dans le contexte de la régularisation d'image.

Plus généralement, l'opérateur de Clifford-Hodge a la propriété de préserver la graduation, i.e. $D^2(\Gamma(\bigwedge^k TX)) \subset \Gamma(\bigwedge^k TX)$ pour $k \in \{0, \cdots, n\}$. Par conséquent, le flot de Clifford-Hodge préserve également la graduation.

Par le plongement de $T_x X$ dans $Cl(T_x X, g(x))$ pour $x \in X$, les champs de vecteurs tangents d'une variété Riemannienne s'identifient avec les sections du fibré de Clifford de degré 1. On en déduit que le flot de Clifford-Hodge préserve la structure de champ de vecteurs tangents, et fournit ainsi un moyen de régulariser des champs de vecteurs sur une image.

Pour la régularisation de champs de repères orientés orthonormés $\Gamma(\mathrm{P\,SO}(X))$, nous procédons de la manière suivante. Etant donnée une trivialisation locale (U, Φ) de $Cl(X, g)$, nous avons les identifications

$$\Gamma(P\,\mathrm{SO}(U)) \simeq C^\infty(U, \mathrm{SO}(m)) \qquad \Gamma(\textstyle\bigwedge^2 TU) \simeq C^\infty(U, \mathfrak{so}(m))$$

la seconde venant de l'isomorphisme d'algèbre de Lie $\mathfrak{spin}(m) \simeq \mathfrak{so}(m)$ (Section 1.2.2). On appelle les champs $\Gamma(\bigwedge^2 TX)$ les **générateurs de champs de repères orthonormés**. Ce sont les sections locales de degré 2 du fibré de Clifford. Le flot de Clifford-Hodge préserve ainsi la structure de générateur de champ de repères orthonormés.

L'idée est qu'à travers la régularisation des générateurs, on peut régulariser les champs de repères orientés orthonormés. Etant donnée une application f de U dans $\mathrm{SO}(m)$, on contruit $\tilde{f} \in \Gamma(\bigwedge^2 TU)$ telle que $f = \rho \circ exp \circ \tilde{f}$ où ρ est la projection du revêtement $\mathrm{Spin}(m) \longrightarrow \mathrm{SO}(m)$ et exp l'application exponentielle de $\mathfrak{spin}(m)$ dans $\mathrm{Spin}(m)$. La régularisation de $\tilde{f}$, à travers le flot de Clifford-Hodge, nous donne des sections $\tilde{f}_{t,t\geqslant 0}$. Puis en calculant $\rho \circ exp \circ \tilde{f}_{t,t\geqslant 0}$, on obtient des fonctions $f_{t,t\geqslant 0} \in C^\infty(U, \mathrm{SO}(m))$. C'est en ce sens-là que le flot de Clifford-Hodge permet de régulariser des champs de repères.

Notons qu'il n'y a pas unicité de $\tilde{f}$, due à la non unicité du générateur infinitésimal d'un élément de $\mathrm{SO}(m)$. Cela soulève le problème de la convolution de $\tilde{f}$ avec le noyau $K_t(x, y, D^2)$. Par exemple, pour $m = 2$, on a $\mathrm{Spin}(2) \simeq \mathrm{SO}(2)$ et l'on retrouve le problème de la régularisation d'orientation (voir e.g. [52],[63],[80]). En effet, étant donnée

$f \in C^\infty(U, \mathrm{SO}(2))$ champ de rotations d'angles θ, on construit $\tilde{f} = \tilde{\theta} e_1 e_2$ telle que $exp(\tilde{\theta} e_1 e_2) = cos(\theta) + sin(\theta) e_1 e_2$. On a donc une 2π périodicité dans le choix de $\tilde{f}$, que l'on peut résoudre en définissant $\tilde{f}$ localement sur les voisinages normaux déterminés par la fonction Ψ. Soient $x_0 \in U$ et la fonction θ définie au-dessus. Soit $\Omega_{x_0} \subset U$ un tel voisinage de x_0. On pose $\widetilde{\theta}(x) = \theta(x) - 2\pi$ si $\theta(x) - \theta(x_0) \geqslant \pi$, $\widetilde{\theta}(x) = \theta(x) + 2\pi$ si $\theta(x) - \theta(x_0) < -\pi$, et $\widetilde{\theta}(x) = \theta(x)$ sinon. Ainsi la fonction $\widetilde{\theta}$ est à valeur dans $[\theta(x_0) - \pi, \theta(x_0) + \pi[$ sur Ω_{x_0}. On définit alors $\tilde{f} = \widetilde{\theta} e_1 e_2$ sur Ω_{x_0}. En étendant cette construction pour chaque $x_0 \in U$, on construit $\tilde{f}$ que l'on peut convoluer avec le noyau $K_t(x, y, D^2)$.

Dans la pratique, la régularisation provient de la convolution de la condition initiale avec un noyau de type $K_t^N(x, y, D^2)$. Cela nécessite de déterminer l'application transport parallèle sur $Cl(X, g)$ associée à la connexion ∇^C. Pour les applications traitées dans cette Section, nous nous restreignons à des variétés de dimensions 2 (Proposition 8) et 3 (Proposition 9 et Corollaire 3).

Proposition 8 *Soit (X, g) une variété Riemannienne de dimension 2. Soit (e_1, e_2) un champ de repères orthonormaux de TX, et $Y_0 = Y_0^1 1(y) + Y_0^2 e_1(y) + Y_0^3 e_2(y) + Y_0^4 e_1 e_2(y) \in Cl(X, g)_y$. Soit γ une courbe C^1 dans X telle que $\gamma(0) = y$. Le transport parallèle Y de Y_0 le long de γ est*

$$Y(t) = Y_0^1\, 1(\gamma(t)) + \Big[f_1 \cdot \Big((Y_0^2 f_1 + Y_0^3 f_2) S(t) \Big) \Big] e_1(\gamma(t))$$
$$+ \Big[f_2 \cdot \Big((Y_0^2 f_1 + Y_0^3 f_2) S(t) \Big) \Big] e_2(\gamma(t)) + Y_0^4\, e_1 e_2(\gamma(t))$$

où (f_1, f_2) est une base orthonormale de $(\mathbb{R}^2, \| \ \|_2)$ générant $Cl(\mathbb{R}^2, \| \ \|_2)$ et $S(t) \in$ Spin(2) $\subset Cl(\mathbb{R}^2, \| \ \|_2)$ définie par

$$S(t) = exp\Big(f_1 f_2 \int_0^t \dot{\gamma}_1(s)\, \Gamma_{11}^{2'}(s) + \dot{\gamma}_2(s)\, \Gamma_{21}^{2'}(s)\, ds \Big)$$

Proposition 9 *Soit (X, g) une variété Riemannienne de dimension 3. Soit (e_1, e_2, e_3) un champ de repères orthonormaux de TX, et $Y_0 = Y_0^1 1(y) + Y_0^2 e_1(y) + Y_0^3 e_2(y) + Y_0^4 e_3(y) + Y_0^5 e_1 e_2(y) + Y_0^6 e_1 e_3(y) + Y_0^7 e_2 e_3(y) + Y_0^8 e_1 e_2 e_3(y) \in Cl(X, g)_y$. Soit γ une courbe C^1 dans X telle que $\gamma(0) = y$. Le transport parallèle Y de Y_0 le long de γ s'obtient de la solution de l'équation différentielle suivante sur $\mathbb{R}^8$.*

$$dY_1/dt = 0, \begin{pmatrix} dY_2/dt \\ dY_3/dt \\ dY_4/dt \end{pmatrix} = A \begin{pmatrix} Y_2 \\ Y_3 \\ Y_4 \end{pmatrix}, \begin{pmatrix} dY_5/dt \\ dY_6/dt \\ dY_7/dt \end{pmatrix} = B \begin{pmatrix} Y_5 \\ Y_6 \\ Y_7 \end{pmatrix}, dY_8/dt = 0 \qquad (24)$$

où $A =$

$$\begin{pmatrix} 0 & \dot{\gamma}_1 \Gamma_{11}^{2'} + \dot{\gamma}_2 \Gamma_{21}^{2'} + \dot{\gamma}_3 \Gamma_{31}^{2'} & \dot{\gamma}_1 \Gamma_{11}^{3'} + \dot{\gamma}_2 \Gamma_{21}^{3'} + \dot{\gamma}_3 \Gamma_{31}^{2'} \\ -\dot{\gamma}_1 \Gamma_{11}^{2'} - \dot{\gamma}_2 \Gamma_{21}^{2'} - \dot{\gamma}_3 \Gamma_{31}^{2'} & 0 & \dot{\gamma}_1 \Gamma_{12}^{3'} + \dot{\gamma}_2 \Gamma_{22}^{3'} + \dot{\gamma}_3 \Gamma_{32}^{3'} \\ -\dot{\gamma}_1 \Gamma_{11}^{3'} - \dot{\gamma}_2 \Gamma_{21}^{3'} - \dot{\gamma}_3 \Gamma_{31}^{2'} & -\dot{\gamma}_1 \Gamma_{12}^{3'} - \dot{\gamma}_2 \Gamma_{22}^{3'} - \dot{\gamma}_3 \Gamma_{32}^{3'} & 0 \end{pmatrix}$$

et $B =$

$$\begin{pmatrix} 0 & \dot\gamma_1\Gamma_{12}^{3'} + \dot\gamma_2\Gamma_{22}^{3'} + \dot\gamma_3\Gamma_{32}^{3'} & -\dot\gamma_1\Gamma_{11}^{3'} - \dot\gamma_2\Gamma_{21}^{3'} - \dot\gamma_3\Gamma_{31}^{2'} \\ -\dot\gamma_1\Gamma_{12}^{3'} - \dot\gamma_2\Gamma_{22}^{3'} - \dot\gamma_3\Gamma_{32}^{3'} & 0 & \dot\gamma_1\Gamma_{11}^{2'} + \dot\gamma_2\Gamma_{21}^{2'} + \dot\gamma_3\Gamma_{31}^{2'} \\ \dot\gamma_1\Gamma_{11}^{3'} + \dot\gamma_2\Gamma_{21}^{3'} + \dot\gamma_3\Gamma_{31}^{2'} & -\dot\gamma_1\Gamma_{11}^{2'} - \dot\gamma_2\Gamma_{21}^{2'} - \dot\gamma_3\Gamma_{31}^{2'} & 0 \end{pmatrix}$$

de condition initiale $Y_i(0) = Y_0^i$*, pour* $i \in \{1, \cdots, 8\}$.

Les solutions $Y_1(t)$ et $Y_8(t)$ sont données par $Y_1(t) = Y_0^1$ et $Y_8(t) = Y_0^8$. À notre connaissance, il n'existe pas de formule explicite pour $(Y_2(t), Y_3(t), Y_4(t))$ et $(Y_5(t), Y_6(t), Y_7(t))$. En pratique, on suppose que les matrices A et B sont localement constantes. On obtient alors les solutions explicites de (24), données dans le Corollaire suivant.

Corollaire 3 *Supposons que les symboles de Christoffel* $\Gamma_{ij}^{k'}$ *et les coordonnées* $\dot\gamma_i$ *de* $\dot\gamma$ *sont constants sur un ouvert* $\Omega_y \supset y$*. Soit* (f_1, f_2, f_3) *une base orthonormale de* $(\mathbb{R}^3, \| \, \|_2)$ *générant l'algèbre de Clifford* $Cl(\mathbb{R}^3, \| \, \|_2)$ *et* $S_1(t), S_2(t) \in$ *Spin(3)* $\subset Cl(\mathbb{R}^3, \| \, \|_2)$ *définis par*

$$S_1(t) = exp\left[\frac{t\sqrt{\alpha^2+\beta^2+\delta^2}}{2}\left(\frac{\alpha f_1f_2 + \beta f_1f_3 + \delta f_2f_3}{\sqrt{\alpha^2+\beta^2+\delta^2}}\right)\right]$$

et

$$S_2(t) = exp\left[\frac{t\sqrt{\alpha^2+\beta^2+\delta^2}}{2}\left(\frac{\delta f_1f_2 - \beta f_1f_3 + \alpha f_2f_3}{\sqrt{\alpha^2+\beta^2+\delta^2}}\right)\right]$$

où $\alpha = \dot\gamma_1\Gamma_{11}^{2'} + \dot\gamma_2\Gamma_{21}^{2'} + \dot\gamma_3\Gamma_{31}^{2'}$, $\beta = \dot\gamma_1\Gamma_{11}^{3'} + \dot\gamma_2\Gamma_{21}^{3'} + \dot\gamma_3\Gamma_{31}^{2'}$ *et* $\delta = \dot\gamma_1\Gamma_{12}^{3'} + \dot\gamma_2\Gamma_{22}^{3'} + \dot\gamma_3\Gamma_{32}^{3'}$.

La solution $Y(t)$ *de (24) est donnée sur* Ω_y *par* $Y(t)=$

$$\begin{aligned}
&Y_0^1 1(\gamma(t)) + \Big[f_1 \cdot \Big(S_1(t)^\dagger(Y_0^2 f_1 + Y_0^3 f_2 + Y_0^4 f_3)S_1(t)\Big)\Big]e_1(\gamma(t)) \\
&+ \Big[f_2 \cdot \Big(S_1(t)^\dagger(Y_0^2 f_1 + Y_0^3 f_2 + Y_0^4 f_3)S_1(t)\Big)\Big]e_2(\gamma(t)) \\
&+ \Big[f_3 \cdot \Big(S_1(t)^\dagger(Y_0^2 f_1 + Y_0^3 f_2 + Y_0^4 f_3)S_1(t)\Big)\Big]e_3(\gamma(t)) \\
&+ \Big[f_1 \cdot \Big(S_2(t)^\dagger(Y_0^5 f_1 + Y_0^6 f_2 + Y_0^7 f_3)S_2(t)\Big)\Big]e_1e_2(\gamma(t)) \\
&+ \Big[f_2 \cdot \Big(S_2(t)^\dagger(Y_0^5 f_1 + Y_0^6 f_2 + Y_0^7 f_3)S_2(t)\Big)\Big]e_1e_3(\gamma(t)) \\
&+ \Big[f_3 \cdot \Big(S_2(t)^\dagger(Y_0^5 f_1 + Y_0^6 f_2 + Y_0^7 f_3)S_2(t)\Big)\Big]e_2e_3(\gamma(t)) + Y_0^8 e_1e_2e_3(\gamma(t))
\end{aligned}$$

Pour une variété de dimension 2, nous illustrons le flot de Clifford-Hodge sur les fonctions par la régularisation d'une image couleur, puis nous illustrons le flot de Clifford-Hodge sur les champs de vecteurs (resp. sur les champs de repères orthonormés) par la régularisation d'un champ de vecteurs (resp. champ d'orientation) associé à cette image. Pour une variété de dimension 3, nous illustrons le flot de Clifford-Hodge sur les fonctions par la régularisation d'une vidéo couleur.

Il semble que le processus de diffusion induit par le flot de Clifford-Hodge possède les mêmes propriétés que le processus de diffusion induit par le flot de Beltrami qu'il

étend. En d'autres termes, la diffusion est gaussienne sur les zones homogènes et tend à diffuser seulement dans la direction du contour sur les zones à fort contour. Le flot de Clifford-Hodge sur les champs de vecteurs en dimension 3 semble alors particulièrement adapté à la régularisation de flot optique. Ce dernier point fait l'objet d'un travail en cours.

Partie 3 : Une Transformée de Fourier-Clifford pour le traitement d'images

L'idée développée dans cette Partie est d'étendre la notion de transformée de Fourier d'une fonction scalaire définie sur un groupe localement compact unimodulaire aux fonctions vectorielles. On cherche alors à étendre les applications de la transformée de Fourier usuelle sur $\mathbb{R}^2$ sur une image en niveau de gris aux images multicanaux.

La transformée de Fourier usuelle d'une fonction scalaire définie sur $\mathbb{R}^m$ s'étend plus généralement aux fonctions scalaires définies sur un groupe localement compact unimodulaire par la théorie des représentations de groupe (voir Appendice de la Section 6, et [50],[60],[85] pour des détails sur la théorie des représentations de groupe).

Définition 14 *Soit G un groupe localement compact unimodulaire muni d'une mesure de Haar ν. La transformée de Fourier de $f \in L^2(G;\mathbb{C})$ est l'application $\hat{f}$ définie sur $\widehat{G}$, le dual de G, par*

$$\hat{f}(\varphi) = \int_G f(g)\varphi(g^{-1})\, d\nu(g).$$

Théoreme 2 *$\hat{f}(\varphi)$ est un opérateur de Hilbert-Schmidt sur l'espace de la représentation φ. Il existe une mesure sur $\widehat{G}$ notée $\hat{\nu}$ telle que $\hat{f} \in L^2(\widehat{G};\mathbb{C})$ et $f \longmapsto \hat{f}$ est une isométrie. De plus, il existe une formule d'inversion*

$$f(g) = \int_{\hat{G}} Trace(\hat{f}(\varphi)\varphi(g))\, d\hat{\nu}(\varphi).$$

Les représentations irréductibles d'un groupe abélien sont de degré 1, i.e. ce sont les morphismes de groupe de G dans $\mathbb{U}(1) \simeq S^1$. Par exemple, pour les groupes abéliens $\mathbb{R}^m, \mathbb{Z}/N\mathbb{Z}$ et S^1 utilisés en traitement d'images, nous avons :

• Les morphismes de groupe de $\mathbb{R}^m$ dans $\mathbb{U}(1)$ sont de la forme

$$\varphi_\xi : x \longmapsto e^{i(\xi_1 x_1 + \cdots + \xi_m x_m)}$$

avec $\xi = (\xi_1, \cdots, \xi_m) \in \mathbb{R}^m$. Ainsi, les représentations irréductibles de $\mathbb{R}^m$ sont paramétrées par $\mathbb{R}^m$ lui-même, et nous avons $\widehat{\mathbb{R}^m} = \mathbb{R}^m$. On retrouve alors les formules usuelles de la transformée de Fourier sur $\mathbb{R}^m$ et de son inversion.

$$\hat{f}(\xi) = \int_{\mathbb{R}^m} f(x) e^{-i(\xi_1 x_1 + \cdots + \xi_m x_m)}\, dx \qquad f(x) = \int_{\mathbb{R}^m} \hat{f}(\xi) e^{i(\xi_1 x_1 + \cdots + \xi_m x_m)}\, d\xi$$

• Les morphismes de groupe de $\mathbb{Z}/N\mathbb{Z}$ dans $\mathbb{U}(1)$ sont de la forme

$$\varphi_u : k \longmapsto e^{2\pi i \frac{ku}{N}}$$

avec $u \in \mathbb{Z}/N\mathbb{Z}$. Ainsi, les représentations irréductibles de $\mathbb{Z}/N\mathbb{Z}$ sont paramétrées par $\mathbb{Z}/N\mathbb{Z}$ lui-même, et nous avons $\widehat{\mathbb{Z}/N\mathbb{Z}} = \mathbb{Z}/N\mathbb{Z}$. On retrouve alors les formules de transformée de Fourier discrète sur $\mathbb{Z}/N\mathbb{Z}$ et de son inversion.

$$\hat{f}(u) = \sum_{k=0}^{N-1} f(k) e^{-2\pi i \frac{ku}{N}} \qquad f(k) = \sum_{u=0}^{N-1} \hat{f}(u) e^{2\pi i \frac{ku}{N}}$$

• Les morphismes de groupe de S^1 dans $\mathbb{U}(1)$ sont de la forme

$$\varphi_k : \theta \longmapsto e^{ik\theta}$$

avec $k \in \mathbb{Z}$. Ainsi, les représentations irréductibles de S^1 sont paramétrées par $\mathbb{Z}$, et nous avons $\widehat{S^1} = \mathbb{Z}$. On retrouve alors les formules de transformée de Fourier sur S^1 et de son inversion, connue sous le nom de **série de Fourier**

$$\hat{f}(k) = \frac{1}{2\pi} \int_{S^1} f(\theta) e^{-ik\theta}\, d\theta \qquad f(\theta) = \sum_{k \in \mathbb{Z}} \hat{f}(k) e^{ik\theta}$$

Le groupe M_2 des déplacements du plan trouve également des applications en traitement d'image. Dans Gauthier et al. [39],[42],[73], la transformée de Fourier sur M_2 est utilisée dans le contexte de la reconnaissance de formes. On trouve également une utilisation de représentation réductible du groupe M_2 dans le contexte d'une transformée en ondelettes [30].

Une question légitime est comment étendre cette notion abstraite de transformée de Fourier aux fonctions à valeur dans $\mathbb{C}^k$?

Section 5. Clifford-Fourier Transform for Color Image processing Dans cette Section, on étend la transformée de Fourier d'une fonction scalaire définie sur $\mathbb{R}^m$ (identifié avec le groupe de ses translations) aux fonctions à valeur vectorielle. En particulier, pour $m = 2$, nous étendons le filtrage fréquentiel des images en niveau de gris aux images couleur.

La transformée de Fourier d'une fonction $f \in L^2(\mathbb{R}^m; \mathbb{C})$ est associée aux représentations unitaires de $\mathbb{R}^m$ dans $\mathbb{C}$, i.e. de degré 1. L'idée est alors d'associer plus généralement la transformée de Fourier d'une fonction $f \in L^2(\mathbb{R}^m; \mathbb{C}^k)$ avec les représentations unitaires de $\mathbb{R}^m$ dans $\mathbb{C}^k$, i.e. de degré k.

Pour cela, on part du constat que dans le cas de la transformée de Fourier d'une fonction scalaire sur $\mathbb{R}^m$, le terme $f(x)\varphi(x^{-1})$ est de la forme $f(x)e^{-i(\xi_1 x_1 + \cdots + \xi_m x_m)}$ pour un certain $\xi = (\xi_1, \cdots, \xi_m) \in \mathbb{R}^m$, et peut être vu comme l'action de l'endomorphisme unitaire $e^{-i(\xi_1 x_1 + \cdots + \xi_m x_m)}$ sur le nombre complexe $f(x)$. Ainsi, le terme

$$\hat{f}(\xi) = \int_{\mathbb{R}^m} f(x) e^{-i(\xi_1 x_1 + \cdots + \xi_m x_m)}\, dx$$

peut être vu comme l'intégration de l'action de la représentation unitaire de $\mathbb{R}^m$ dans $\mathbb{C}$ paramétrée par ξ sur les valeurs de f.

Ce principe se généralise de manière directe aux fonctions $f \in L^2(\mathbb{R}^m, \mathbb{C}^k)$ où $\mathbb{C}^k$ est munie d'une forme hermitienne Q, par

$$\widehat{f}(\varphi) = \int_{\mathbb{R}^m} f(x) \perp \varphi(x^{-1})\, dx \tag{25}$$

où φ est une représentation unitaire de $\mathbb{R}^m$ dans $\mathbb{C}^k$ pour Q et $\perp$ dénote l'action de $\mathbb{U}(k)$ sur $\mathbb{C}^k$.

Dans cette Section, on s'intéresse aux fonctions dans $L^2(\mathbb{R}^m, (\mathbb{R}^n, Q))$, où Q est une forme quadratique définie positive sur $\mathbb{R}^n$. On va alors remplacer les morphismes de $\mathbb{R}^m$ dans $\mathbb{U}(k)$ par les morphismes de $\mathbb{R}^m$ dans $\mathrm{SO}(Q)$.

Selon la parité de n, on distingue deux définitions de la **transformée de Fourier d'une fonction** $f \in L^2(\mathbb{R}^m, (\mathbb{R}^n, Q))$.

• Si n est pair, on pose

$$\widehat{f}(\varphi) = \int_{\mathbb{R}^m} f(x) \perp \varphi(x^{-1})\, dx$$

où φ est un morphisme de groupe de $\mathbb{R}^m$ dans $\mathrm{SO}(Q)$.

• Si n est impair, on plonge $(\mathbb{R}^n, Q)$ dans $(\mathbb{R}^{n+1}, Q \oplus 1)$ et on pose

$$\widehat{f}(\varphi) = \int_{\mathbb{R}^m} \tilde{f}(x) \perp \varphi(x^{-1})\, dx$$

où $\tilde{f} = (f_1, \cdots, f_n, 0)$ dans $(\mathbb{R}^{n+1}, Q \oplus 1)$ et φ est un morphisme de groupe de $\mathbb{R}^m$ dans $\mathrm{SO}(Q \oplus 1)$.

Pour déterminer les morphismes de groupes de $\mathbb{R}^m$ dans $\mathrm{SO}(Q)$ (resp. $\mathrm{SO}(Q \oplus 1)$), il apparaît plus simple d'utiliser la représentation spinorielle de $\mathrm{SO}(Q)$ (resp. $\mathrm{SO}(Q \oplus 1)$) plutôt que sa représentation matricielle. Concrètement, on détermine les morphismes de groupe de $\mathbb{R}^m$ dans son revêtement universel $\mathrm{Spin}(Q)$ (resp. $\mathrm{Spin}(Q \oplus 1)$), que l'on fait ensuite descendre en morphismes de groupe de $\mathbb{R}^m$ dans $\mathrm{SO}(Q)$ (resp. $\mathrm{SO}(Q \oplus 1)$). On utilise pour cela le contexte des algèbres de Clifford, on parlera alors de **transformée de Fourier-Clifford**.

• Si n est pair, alors par le plongement de $(\mathbb{R}^n, Q)$ dans $Cl(\mathbb{R}^n, Q)$, f peut être vue comme une fonction à valeur dans $Cl(\mathbb{R}^n, Q)$ de la forme $f = f_1 e_1 + f_2 e_2 + \cdots + f_n e_n$, avec $e_i^2 = 1$ et $e_i e_j = -e_j e_i$. Soit φ un morphisme de groupe de $\mathbb{R}^m$ dans $\mathrm{Spin}(Q)$, on définit la transformée de Fourier-Clifford de f par

$$\widehat{f}(\varphi) = \int_{\mathbb{R}^m} \varphi(x_1, \cdots, x_m) f(x_1, \cdots, x_m) \varphi(-x_1, \cdots, -x_m)\, dx_1 \cdots dx_m$$

• si n est impair, on plonge dans un premier temps $(\mathbb{R}^n, Q)$ dans $(\mathbb{R}^{n+1}, Q \oplus 1)$. Ensuite, à partir du plongement de $(\mathbb{R}^{n+1}, Q \oplus 1)$ dans $Cl(\mathbb{R}^{n+1}, Q \oplus 1)$, f peut être vue comme une fonction $\tilde{f}$ à valeur dans $Cl(\mathbb{R}^{n+1}, Q \oplus 1)$ de la forme $\tilde{f} = f_1 e_1 + f_2 e_2 + \cdots + f_n e_n + 0\, e_{n+1}$ avec $e_i^2 = 1$ et $e_i e_j = -e_j e_i$. Soit φ un morphisme de groupe de $\mathbb{R}^m$ dans $\mathrm{Spin}(Q \oplus 1)$, on définit la transformée de Fourier-Clifford de f par

$$\widehat{f}(\varphi) = \int_{\mathbb{R}^m} \varphi(x_1, \cdots, x_m) \tilde{f}(x_1, \cdots, x_m) \varphi(-x_1, \cdots, -x_m)\, dx_1 \cdots dx_m$$

Par rapport aux applications aux images couleur traitées dans cette Section, on s'intéresse au cas $m = 2$ et $n = 3$. On cherche donc à déterminer les morphismes de groupe de $\mathbb{R}^2$ dans $\mathrm{Spin}(Q \oplus 1)$, puis à les faire descendre en morphisme de groupe de $\mathbb{R}^2$ dans $\mathrm{SO}(Q \oplus 1)$ pour Q une forme quadratique définie positive sur $\mathbb{R}^3$. Plus généralement, étant donnée une forme quadratique définie positive Q sur $\mathbb{R}^4$, on note $\mathrm{Spin}(4)$ la représentation de $\mathrm{Spin}(Q)$ dans l'algèbre de Clifford $Cl(\mathbb{R}^4, Q)$. On obtient alors le résultat suivant.

Proposition 10 *Les morphismes de groupe de $\mathbb{R}^2$ dans Spin(4) sont paramétrés par quatre nombres réels u, v, w, z et un bivecteur unitaire D dans $Cl(\mathbb{R}^4, Q)$, et sont de la forme*

$$\widetilde{\Phi}_{u,v,w,z,D}(x, y) = e^{\frac{1}{2}[(x(u+w)+y(v+z))D]}\, e^{\frac{1}{2}[(x(u-w)+y(v-z))ID]} \tag{26}$$

Remarque. On peut également paramétrer les morphismes (26) par quatre nombres réels a, b, c, d et un bivecteur unitaire D pour lesquels ils ont la forme

$$\widetilde{\Phi}_{a,b,c,d,D}(x, y) = e^{\frac{1}{2}[(xa+yb)D]}\, e^{\frac{1}{2}[(xc+yd)ID]}$$

La Proposition 10 nous amène à une formulation explicite de la transformée de Fourier-Clifford dans $L^2((\mathbb{R}^3, Q))$ ou $L^2((\mathbb{R}^4, Q))$.

Définition 15 *Soit $f \in L^2(\mathbb{R}^2, (\mathbb{R}^3, Q))$, resp. $L^2(\mathbb{R}^2, (\mathbb{R}^4, Q))$ et dénotons par f le plongement de f dans l'algèbre de Clifford $Cl(\mathbb{R}^4, Q \oplus 1)$, resp. $Cl(\mathbb{R}^4, Q)$. La transformée de Fourier-Clifford de f est donnée par*

$$\begin{aligned}
\widehat{f}(u, v, w, z, D) &= \int_{\mathbb{R}^2} f(x, y) \perp \widetilde{\Phi}_{u,v,w,z,D}(-x, -y) dx\, dy \\
&= \int_{\mathbb{R}^2} e^{\frac{1}{2}[(x(u+w)+y(v+z))D]} e^{\frac{1}{2}[(x(u-w)+y(v-z))ID]} f(x, y) \\
&\qquad e^{-\frac{1}{2}[(x(u+w)+y(v+z))D]} e^{-\frac{1}{2}[(x(u-w)+y(v-z))ID]} dx\, dy
\end{aligned}$$

On obtient une formule d'inversion à gauche pour l'application $\widehat{\ }$ en intégrant sur l'ensemble des représentations unitaires de $\mathbb{R}^m$ dans $(\mathbb{R}^4, Q)$.

Proposition 11 *La transformée de Fourier-Clifford est inversible à gauche. Son inverse est l'application $\check{}$ donnée par*

$$\check{g}(a, b) = \int_{\mathbb{R}^4 \times \mathbb{S}^2_{4,0}} g(u, v, w, z, D) \perp \widetilde{\Phi}_{u,v,w,z,D}(a, b)\, du\, dv\, dw\, dz\, d\nu$$

où ν est une mesure unitaire sur $\mathbb{S}^2_{4,0}$, l'ensemble des bivecteurs unitaires de l'algèbre de Clifford $Cl(\mathbb{R}^4, Q)$.

Pour l'application au filtrage de fréquences dans une image couleur présentée dans cette Section, on utilise une transformée de Fourier partielle, i.e. on considère un sous-ensemble de l'ensemble des représentations unitaires de $\mathbb{R}^2$ dans $(\mathbb{R}^4, Q)$. Plus précisemment, on considère les représentations $\widetilde{\Phi}_{u,v,0,0,D}$, où le bivecteur unitaire D est fixé. Le choix du

bivecteur D dépend des couleurs que l'on cherche à filtrer.
De plus, étant donnée une image couleur $I\colon D \subset \mathbb{R}^2 \longrightarrow \mathbb{R}^3$, il existe une liberté dans le choix de la forme quadratique Q sur $\mathbb{R}^3$, à partir de laquelle on détermine les représentations unitaires. On définit alors la transformée de Fourier d'une image couleur.

Définition 16 *Soit I une image couleur à laquelle on associe une fonction $f \in L^2(\mathbb{R}^2, \mathbb{R}^4)$ définie par*

$$f(x,y) = r(x,y)e_1 + g(x,y)e_2 + b(x,y)e_3 + 0e_4$$

dans une base (e_1, e_2, e_3, e_4), où r, g and b correspondent respectivement aux niveaux de rouge, vert et bleu. Soit Q une forme quadratique définie positive sur $\mathbb{R}^3$.
La transformée de Fourier-Clifford de I par rapport à Q et D est la fonction $\widehat{I}_{Q,D}$ à valeur dans $Cl(\mathbb{R}^4, Q \oplus 1)$ définie par

$$\widehat{I}_{Q,D}(u,v) = \int_{\mathbb{R}^2} f(x,y) \perp \widetilde{\Phi}_{u,v,0,0,D}(-x,-y)dxdy$$

$$= \int_{\mathbb{R}^2} e^{\frac{1}{2}(xu+yv)ID} e^{\frac{1}{2}(xu+yv)D} f(x,y) e^{-\frac{1}{2}(xu+yv)D} e^{-\frac{1}{2}(xu+yv)ID} dxdy$$

En décomposant f en $f = f_{||} + f_{\perp}$ par rapport au plan généré par D, on obtient

$$\widehat{I}_{Q,D}(u,v) = \int_{\mathbb{R}^2} f_{||}\, e^{-(xu+yv)D}\, dxdy + \int_{\mathbb{R}^2} f_{\perp}\, e^{-(xu+yv)ID}\, dxdy$$

En identifiant les plans générés par D et ID avec le plan complexe $\mathbb{C}$, chaque intégrale peut alors s'identifier à la transformée de Fourier usuelle d'une fonction complexe.

On a une formule d'inversion pour cette transformée de Fourier-Clifford partielle

$$\breve{g}(x,y) = \int_{\mathbb{R}^2} g(u,v) \perp \widetilde{\Phi}_{u,v,0,0,D}(x,y)dudv$$

$$= \int_{\mathbb{R}^2} g_{||}\, e^{(xu+yv)D}\, dudv + \int_{\mathbb{R}^2} g_{\perp}\, e^{(xu+yv)ID}\, dudv$$

On voit que la formule d'inversion consiste à appliquer une transformée de Fourier inverse complexe sur chaque composante $g_{||}$ et $g_{\perp}$ par rapport à D.

Finalement, cette transformée de Fourier-Clifford d'une image couleur consiste à décomposer de manière orthogonale la fonction f par rapport au plan engendré par D et la forme quadratique Q, puis à considérer la transformée de Fourier complexe sur chaque composante. En prenant la forme quadratique Q qui a pour représentation matricielle I_4 dans la base (e_1, e_2, e_3, e_4), on retrouve la transformée de Fourier hypercomplexe de Sangwine et al [32].

Dans les applications présentées, nous annulons des fréquences en jouant sur les paramètres D et Q et illustrons le résultat par tranformation de Fourier inverse.

Première partie

Fibrés en algèbres de Clifford pour la segmentation d'image

Sommaire

1 A metric approach to nD images edge detection with Clifford algebras 39
1.1 Introduction . . . 39
1.2 Clifford algebras and color-infrared spaces . . . 40
1.2.1 Clifford algebras . . . 40
1.2.2 The spinor group Spin(n) . . . 42
1.2.3 Color-infrared spaces . . . 44
1.3 Edge detection in color-infrared images . . . 45
1.3.1 First fundamental form of a surface and edge detectors . . . 45
1.3.2 Clifford bundle and color-infrared image . . . 46
1.3.3 Computing E, F, G with $\widetilde{\nabla}$ . . . 49
1.3.4 Discretization and parallel transport . . . 51
1.4 Applications . . . 54
1.4.1 Comparison with the Di Zenzo gradient . . . 54
1.4.2 Color edge detection with respect to hue intervals and saturation levels . . . 57
1.4.3 Color/infrared images edge detection . . . 58
1.4.4 One more example of possible applications : color edge analysis 61
Appendix. Tensor product of $\mathcal{CT}(D)$-valued 1-forms . . . 63

2 Clifford algebras bundles to multidimensional image segmentation 65
2.1 Introduction . . . 65
2.2 Preliminaries . . . 66
2.2.1 Multidimensional image edge detection using metrics of surfaces 66
2.2.2 Color and color/infrared spaces as subsets of Clifford algebras 67
2.3 A general method to multidimensional image edge detection . . . 69
2.3.1 A family $\mathcal{G} = \{\mathcal{G}_n, n \in \mathbb{N}\}$ of Clifford bundles . . . 69
2.3.2 Algebra connection on $(CT(D), \widetilde{\pi}, D)$ . . . 71
2.3.3 Computing first fundamental forms from connections on Clifford bundles . . . 73
2.4 Applications . . . 76
2.4.1 The usual color edge detection : n=3 . . . 76
2.4.2 Color edge detection with respect to a given hue : n=3, m=3 77
2.4.3 Color edge classification : n=3, $\mathbf{m_i = 3}$ . . . 81
2.4.4 Edge detection in the color domain with constraints on the temperature : n=4, m=3 . . . 86
2.4.5 Color/infrared edge detection with constraints on color and temperature : n=4, $\mathbf{m}_\nu = \mathbf{4}$ . . . 88

1 A metric approach to nD images edge detection with Clifford algebras

Cette Section a fait l'objet d'une publication en collaboration avec Michel Berthier et Christophe Saint-Jean [3].

1.1 Introduction

Clifford algebras appear to be a powerful tool in a wide range of applications to computer sciences, see [75] for examples. In particular, the approach of Sangwine & al. of color images segmentation with quaternions [33],[68] can be considered from this viewpoint since $\mathbb{H}$ (the algebra of quaternions) is the Clifford algebra $\mathbb{R}_{0,2}$ and $\mathbb{H}^1$ (the group of unit quaternions) is the spinor group Spin(3). Sangwine's idea is to associate a pure imaginary quaternion to each color of the RGB cube and then make geometric transformations on colors using the product of $\mathbb{H}$ to compute some kind of gradient.

Working in the framework of Clifford algebras has several advantages :
- If we consider a color as a vector of the algebra $\mathbb{R}_{3,0}$ we can use the richness of the structure of this latter. In fact $\mathbb{R}_{3,0}$ is of dimension 8 over $\mathbb{R}$ and contains elements of different degrees (scalars, vectors, bivectors and a pseudoscalar) that carry different information.
- We can benefit from the efficiency of the calculus based on the geometric product when dealing with general images with values in $\mathbb{R}^n$. As it is well known, geometric transformations can be encoded without coordinates by algebraic formula using for example spinors. We will consider in the sequel the example of color-infrared images where $n = 4$.
- A Clifford algebra is defined with respect to a chosen metric of a vector space. Conjointly with the two preceding points, it's an asset when dealing with metric approach of edge detection. In particular, when the metric of the ambient space varies with the point, the Clifford algebras bundle setting arises quite naturally.

The metric approach we adopt in this paper was introduced by Di Zenzo [26], who considered implicitely a n-channels image as an embedded two-dimensional surface in the Euclidean space $\mathbb{R}^{n+2}$. A measure of the "edge strength" and the direction wherein it is highest at each point are defined. This is done by computing respectively the highest eigenvalue of the first fundamental form of the surface and the corresponding eigenvector. Using this method, Cumani [23] gives an explicit definition of an edge point, that is a point where the first directional derivative of the highest eigenvalue in the direction given by the highest eigenvector has a transversal zero-crossing. However, when $n > 1$, the smallest eigenvalue is no more constant ; that's why Sapiro [71] suggests as a measure of the "edge strength" the square root of the difference of the two eigenvalues.

The idea of embedding the surface representing an image in a space endowed with a non-Euclidean metric is proposed in [74], and is applied for color edge detection in [56]. In this latter, the author describes colors with hyperbolic coordinates and endows $\mathbb{R}^5$ with a corresponding metric.

It is our purpose to start from this general definition of a nD image and to develop a general approach of edge detection in color-infrared images based on metric information.

Indeed, we define an image as a section of a fiber bundle. The fibers are Clifford algebras related to the acquisition space $RGBT$ of the color-infrared image endowed with a metric that may vary with the base point. We show that it is possible, staying in the acquisition space, to recover the metric data of the image

$$\varphi : (x, y) \longmapsto (x, y, l, s, h, t)$$

embedded in a $LSHT$-space (l, s, h, t, denotes respectively the luminance, the saturation, the hue and the temperature) equipped with a metric tensor. This is done in both continuous and discrete cases by considering two sections of the Clifford bundle and their covariant derivatives with respect to a well chosen connection.

We may emphasize the following facts :
- We never compute explicitely the derivatives of luminance, saturation, hue and temperature whereas the approach based on surfaces does.
- The information contained in the various channels (for example color and temperature in Section 1.4.3) is mixed to adjust the coefficients of the metric of the embedding space. That is why the process we propose can't be achieved with marginal approaches.

This paper is organized as follows. Section 1.2 is mainly devoted to basic notions and results on Clifford algebras and spinor groups. We show also how to derive the transition formulas from $RGBT$ to $LSHT$ with geometric calculus. In Section 1.3, we first compute the coefficients of the first fundamental form of a color-infrared image defined as a two-dimensional surface embedded in a $LSHT$-space equipped with a metric tensor. Then, we show how to interpret such an image as a section of a Clifford algebras bundle. The rest of the section is devoted to the continuous and discrete computations of the coefficients of the first fundamental form as explained above. In Section 1.4, we propose three applications : a comparison with the Di Zenzo's method, a detection of transitions between colors of a given hue interval with respect to their saturation levels and an edge detection in a color-infrared image with constraints on color and temperature of objects. We discuss also other applications, related to different choices of connections and sections, to show the genericity of the proposed method. In particular, segmentations of shadows and highlights are briefly investigated.

1.2 Clifford algebras and color-infrared spaces

1.2.1 Clifford algebras

The aim of this section is to give basic definitions and results concerning Clifford algebras and spinor groups. We refer the reader to [9],[21],[22],[47],[48],[49],[57],[67] for further details on history, definitions, results and applications.

Let V be a vector space of finite dimension n over $\mathbb{R}$ equipped with a quadratic form Q. We are looking for an algebra $Cl(V, Q)$ that contains V and in which the following relation holds for all v in V :

$$v^2 = Q(v).1$$

This implies in particular that for all u and v in V :

$$uv + vu = 2B(u, v).1$$

where B denotes the symmetric bilinear form corresponding to Q. We can decompose the product uv into

$$uv = B(u,v).1 + u \wedge v$$

by defining

$$u \wedge v = \frac{1}{2}(uv - vu).$$

This shows that $Cl(V,Q)$ contains with scalars and vectors other elements called bivectors and generally multivectors which appear to generalize the notion of vector. It is possible to add and multiply all the elements, the multiplication being not commutative.

As an example, let us mention that the Clifford algebra of $\mathbb{R}^2$ with the quadratic form

$$Q(u_1,u_2) = -u_1^2 - u_2^2$$

is isomorphic to the algebra of quaternions : An isomorphism is given by sending respectively 1, e_1, e_2 and e_1e_2 to 1, i, j and k).

Formally speaking, the Clifford algebra $Cl(V,Q)$ is the solution of the following universal problem. We search a couple $(Cl(V,Q), i_Q)$ where $Cl(V,Q)$ is an $\mathbb{R}$-algebra and $i_Q : V \longrightarrow Cl(V,Q)$ is $\mathbb{R}$-linear satisfying :

$$(i_Q(v))^2 = Q(v).1$$

for all v in V (1 denotes the unit of $Cl(V,Q)$) such that for each $\mathbb{R}$-algebra A and each $\mathbb{R}$-linear map $f : V \longrightarrow A$ with

$$(f(v))^2 = Q(v).1$$

for all v in V (1 denotes the unit of A), then there exists a unique morphism

$$g : Cl(V,Q) \longrightarrow A$$

of $\mathbb{R}$-algebras such that $f = g \circ i_Q$.

The solution is unique up to isomorphisms and is given as the (non commutative) quotient

$$T(V)/(v \otimes v - Q(v).1)$$

of the tensor algebra of V by the ideal generated by $v \otimes v - Q(v).1$, where v belongs to V (see [67] for a proof).

It is well known that there exists a unique anti-automorphism t on $Cl(V,Q)$ such that

$$t(i_Q(v)) = i_Q(v)$$

for all v in V. It is called reversion and usually denoted by $x \longmapsto x^\dagger$, x in $Cl(V,Q)$. In the same way there exists a unique automorphism α on $Cl(V,Q)$ such that

$$\alpha(i_Q(v)) = -i_Q(v)$$

for all v in V. In the rest of this paper we write v for $i_Q(v)$ (according to the fact that i_Q embeds V in $Cl(V,Q)$).

As a vector space $Cl(V,Q)$ is of dimension 2^n on $\mathbb{R}$ and a basis is given by the set

$$\{e_{i_1}e_{i_2}\cdots e_{i_k},\quad i_1<i_2<\cdots<i_k,\quad k\in\{1,\ldots,n\}\}$$

and the unit 1. An element of degree k

$$\sum_{i_1<\cdots<i_k}\alpha_{i_1\ldots i_k}e_{i_1}e_{i_2}\cdots e_{i_k}$$

is called a k-vector. A 0-vector is a scalar and $e_1e_2\cdots e_n$ is called the pseudoscalar. We will denote $\langle x\rangle_k$ the component of degree k of an element x of $Cl(V,Q)$.

The inner product of x_r of degree r and y_s of degree s is defined by

$$x_r\cdot y_s=\langle x_ry_s\rangle_{|r-s|}$$

if r and s are positive and by

$$x_r\cdot y_s=0$$

otherwise.

The outer product of x_r of degree r and y_s of degree s is defined by

$$x_r\wedge y_s=\langle x_ry_s\rangle_{r+s}$$

These products extend by linearity on $Cl(V,Q)$. Clearly, if a and b are vectors of V, then the inner product of a and b coincides with the scalar product defined by Q. When it is defined (for example when x is a versor and Q is positive) we denote

$$\|x\|=\sqrt{xx^\dagger}$$

and say that x is a unit if $xx^\dagger=\pm1$.

In the following, we deal in particular with the Clifford algebra of the Euclidean $\mathbb{R}^n$ denoted by $\mathbb{R}_{n,0}$. $\mathbb{R}^k_{n,0}$ is the subspace of elements of degree k and $\mathbb{R}^*_{n,0}$ is the group of elements that admit an inverse in $\mathbb{R}_{n,0}$.

Let a be a vector in $\mathbb{R}_{n,0}$ and B be the k-vector $a_1\wedge a_2\wedge\cdots\wedge a_k$, then the orthogonal projection of a on the k-plane generated by the a_i's is the vector

$$P_B(a)=(a\cdot B)B^{-1}$$

The vector

$$a-(a\cdot B)B^{-1}=(a\wedge B)B^{-1}$$

is called the rejection of a on B.

1.2.2 The spinor group Spin(n)

It is defined by

$$\mathrm{Spin}(n)=\left\{\prod_{i=1}^{2k}a_i,\ a_i\in\mathbb{R}^1_{n,0},\ \|a_i\|=1\right\}$$

or equivalently

$$\mathrm{Spin}(n) = \{x \in \mathbb{R}_{n,0},\ \alpha(x) = x,\ xx^\dagger = 1, xvx^{-1} \in \mathbb{R}^1_{n,0}\ \forall v \in \mathbb{R}^1_{n,0}\}$$

It is well known that $\mathrm{Spin}(n)$ is a connected compact Lie group that universally covers $\mathrm{SO}(n)$ ($n \geqslant 3$). One can verify that $\mathrm{Spin}(3)$ is the group

$$\{a1 + be_1e_2 + ce_2e_3 + de_3e_1,\ a^2 + b^2 + c^2 + d^2 = 1\}$$

and is isomorphic to the group $\mathbb{H}^1$ of unit quaternions. It is also a classical result that $\mathrm{Spin}(4)$ is isomorphic to $\mathrm{Spin}(3)\times\mathrm{Spin}(3)$ (see [57] for more information on spinors in $\mathbb{R}^3$ and $\mathbb{R}^4$).

The Lie algebra of $\mathrm{Spin}(n)$ is $\mathbb{R}^2_{n,0}$ with Lie bracket

$$A \times B = AB - BA$$

As the exponential map from its Lie algebra to $\mathrm{Spin}(n)$ is onto (see [46] for a proof), every spinor can be written as

$$S = \sum_{i=0}^{\infty} \frac{1}{i!} A^i$$

for some bivector A.

From Hestenes and Sobczyk [47], we know that every A in $\mathbb{R}^2_{n,0}$ can be written as

$$A = A_1 + A_2 + \cdots + A_m$$

where $m \leqslant n/2$ and

$$A_j = \|A_j\| a_j b_j, \quad j \in \{1, \ldots, m\}$$

with

$$\{a_1, \ldots, a_m, b_1, \ldots, b_m\}$$

a set of orthonormal vectors. Thus

$$A_j A_k = A_k A_j = A_k \wedge A_j$$

whenever $j \neq k$ and

$$A_k^2 = -\|A_k\|^2 < 0$$

This means that the planes encoded by A_k and A_j are orthogonal and implies that

$$e^{A_1 + A_2 + \cdots + A_m} = e^{A_{\sigma(1)}} e^{A_{\sigma(2)}} \ldots e^{A_{\sigma(m)}}$$

for all σ in the permutation group $\mathfrak{S}(m)$. Actually, as A_k^2 is negative we have

$$e^{A_i} = \cos(\|A_i\|) + \sin(\|A_i\|) \frac{A_i}{\|A_i\|}$$

The corresponding rotation

$$R_i : x \longmapsto e^{-A_i} x e^{A_i}$$

acts in the oriented plane defined by A_i as a plane rotation of angle $2\|A_i\|$. The vectors orthogonal to A_i are invariant under R_i.
It then appears that any element R of $\mathrm{SO}(n)$ is a composition of commuting simple rotations, in the sense that they have only one invariant plane. The vectors left invariant by R are those of the orthogonal subspace to A. If $m = n/2$ this latter is trivial. The previous decomposition is not unique if $\|A_k\| = \|A_j\|$ for some j and k with $j \neq k$. In this case infinitely many planes are left invariant by R.

1.2.3 Color-infrared spaces

As mentioned before, Sangwine's approach of edge detection in color images relies on the fact that $\mathbb{H}_0$ (the set of pure imaginary quaternions) is isomorphic to $\mathbb{R}^3$ equipped with an action of $\mathbb{H}^1$. In the same way, a color image can be treated as an application from $\mathbb{R}^2$ to $\mathbb{R}^3$, this latter being embedded in $\mathbb{R}_{3,0}$ and equipped with an action of Spin(3). It is natural to extend this approach to nD images replacing $\mathbb{R}^3$ by $\mathbb{R}^n$ and $\mathbb{R}_{3,0}$ by $\mathbb{R}_{n,0}$. We focus here on color-infrared images.

Beside RGB color space we consider HSL color space defined as follows. We set first

$$\begin{pmatrix} Y \\ C_1 \\ C_2 \end{pmatrix} = \begin{pmatrix} 1/3 & 1/3 & 1/3 \\ 1 & -1/2 & -1/2 \\ 0 & -\sqrt{3}/2 & \sqrt{3}/2 \end{pmatrix} \begin{pmatrix} r \\ g \\ b \end{pmatrix}$$

Then the luminance l, the saturation s and the hue h are respectively given by

$$l = Y$$

$$s = \sqrt{C_1^2 + C_2^2}$$

$$h = \begin{cases} \arccos(C_2/s) & \text{if } C_2 > 0 \\ 2\pi - \arccos(C_2/s) & \text{otherwise} \end{cases}$$

As it is well known, color spaces based on luminance (value), saturation and hue are more suitable to perception [34].

Let us denote $\mathcal{CT}$ the Clifford algebra of $(\mathbb{R}^4, Q)$ with Q the positive definite quadratic form given by

$$\begin{pmatrix} \beta/3 & 0 & 0 & 0 \\ 0 & \beta/3 & 0 & 0 \\ 0 & 0 & \beta/3 & 0 \\ 0 & 0 & 0 & \delta \end{pmatrix}$$

Thus $e_1^2 = e_2^2 = e_3^2 = \beta/3$ and $e_4^2 = \delta$. Given a color-infrared vector $a = r(a)e_1 + g(a)e_2 + b(a)e_3 + t(a)e_4$, its color component is given by

$$\begin{aligned} c(a) &= r(a)e_1 + g(a)e_2 + b(a)e_3 \\ &= a \cdot (e_1e_2e_3)(e_1e_2e_3)^{-1} \end{aligned}$$

Let us denote

$$\mu = \frac{e_1 + e_2 + e_3}{\sqrt{\beta}}$$

the unit vector generating the achromatic axis, and $v(a)$ the rejection of $c(a)$ on μ, called the chrominance vector of a. Simple computations show that the luminance $l(a)$, the saturation $s(a)$ and the hue $h(a)$ of a can be written

$$\begin{aligned} l(a) &= \frac{1}{\sqrt{\beta}} \|(a \cdot \mu)\mu^{-1}\| \\ &= \frac{1}{\sqrt{\beta}} \sqrt{\left((a \cdot \mu)\mu^{-1}\right)^2} \end{aligned}$$

$$\begin{aligned} s(a) &= \frac{3}{\sqrt{2\beta}}\|(c(a)\wedge\mu)\mu^{-1}\| \\ &= \frac{3}{\sqrt{2\beta}}\sqrt{((c(a)\wedge\mu)\mu^{-1})^2} \end{aligned}$$

$$h(a) = 2\pi + \operatorname{sign}(g(a)-b(a))\arccos\left(\frac{v(a)}{\|v(a)\|}\cdot\rho\right)$$

with ρ the unit chrominance vector of the red color and $h(a)$ defined modulo 2π. In other words, $h(a)$ is the oriented angle from ρ to $v(a)$.

Moreover, the dual of the achromatic axis in the vector space generated by (e_1, e_2, e_3) is a plane, called the chrominance plane, generated by the bivector $e_1e_2 - e_1e_3 + e_2e_3$. Hence we have

$$v(a) = a\cdot(e_1e_2 - e_1e_3 + e_2e_3)\,(e_1e_2 - e_1e_3 + e_2e_3)^{-1}$$

The chrominance vector of a is therefore the orthogonal projection of a on the chrominance plane.

1.3 Edge detection in color-infrared images

1.3.1 First fundamental form of a surface and edge detectors

We recall in this subsection how to define an edge detector using metric information given by the first fundamental form (see [23],[26], [71] and [74], [86] for related works on edge-preserving denoising). For this we consider a color-infrared image as a C^k map, $k \geqslant 1$,

$$\varphi : (x,y) \longmapsto (x, y, l(x,y), s(x,y), h(x,y), t(x,y))$$

from a rectangle D to $\mathbb{R}^6$. In the following q denotes a point in D with image $p = \varphi(q)$ under the map φ. Note that we consider the hue h with values in the universal cover $\mathbb{R}$ of $\mathbb{R}/2\pi\mathbb{Z}$. For a coherent definition of φ, we take $h = 0$ when $s = 0$. As we will see below, this has no consequences on the edge detection.

To take into account the fact that the hue is irrelevant for small values of the saturation, we introduce following Carron [18] the function

$$f(s) = \frac{1}{\pi}\left(\frac{\pi}{2} + \arctan(\beta(s - S_0))\right).$$

f measures the relevance of hue with respect to saturation level. The shape of f is controlled by two parameters S_0 and β. S_0 is the saturation level corresponding to the medium relevance of hue : $f(S_0) = 0.5$. The parameter β is the slope of the function around S_0. In the sequel we choose $S_0 = 50$ and $\beta = 0.07$. The reader may find in [17] similar constructions. We consider also the domain

$$\Omega(p) = \{(x,y),\ \|(x,y) - \varphi^{-1}(p)\|_\infty \leqslant 1\}$$

and set

$$\xi(p) = \exp\left(\frac{1}{4}\int_{\Omega(p)} \ln(f \circ s(x,y))dxdy\right)$$

if $s(u,v) \neq 0$ for all (u,v) in $\Omega(p)$ and $\xi(p) = 0$ otherwise.

Next, we endow $\mathbb{R}^6$ with the following metric

$$\begin{pmatrix} 1 & 0 \\ 0 & 1 \end{pmatrix} \oplus \begin{pmatrix} \lambda(p) & 0 & 0 & 0 \\ 0 & \lambda(p) & 0 & 0 \\ 0 & 0 & \kappa(p)\xi(p) & 0 \\ 0 & 0 & 0 & \eta(p) \end{pmatrix}$$

where λ, κ and η are positive functions. Strictly speaking, as ξ can vanish, this metric is not Riemannian. However the metric induced on the surface $\varphi(D)$ is Riemannian : It is the first fundamental form of $\varphi(D)$, usually denoted by

$$\mathrm{I}(p) = \begin{pmatrix} E(p) & F(p) \\ F(p) & G(p) \end{pmatrix}$$

The coefficients E, F and G are given by

$$E(p) = 1 + \lambda(p)l_x^2(p) + \lambda(p)s_x^2(p) + \kappa(p)\xi(p)h_x^2(p) + \eta(p)t_x^2(p)$$

$$F(p) = \lambda(p)l_x(p)l_y(p) + \lambda(p)s_x(p)s_y(p) + \kappa(p)\xi(p)h_x(p)h_y(p) + \eta(p)t_x(p)t_y(p)$$

$$G(p) = 1 + \lambda(p)l_y^2(p) + \lambda(p)s_y^2(p) + \kappa(p)\xi(p)h_y^2(p) + \eta(p)t_y^2(p)$$

We denote $\theta_+(p)$ and $\theta_-(p)$, $\theta_+(p) \geqslant \theta_-(p)$, the two eigenvalues of $\mathrm{I}(p)$ and $\Theta_+(p)$, $\Theta_-(p)$ the corresponding eigenvectors. The edge detector is then given by

$$\varpi(p) = \sqrt{\theta_+(p) - \theta_-(p)}$$

More precisely, we say that q in D is an edge point if one of the following conditions holds :

1. The function ϖ has a local maximum at $\varphi(q)$ in the direction given by $\Theta_+(\varphi(q))$;
2. $\Theta_+(\varphi(q)) > 1$ and q is an endpoint of a curve of points satisfying 1.

1.3.2 Clifford bundle and color-infrared image

We explain how to consider a color/infrared image as a section of a Clifford bundle. First of all, let us recall some definitions.

A vector bundle of rank n over a surface S (or more generally over a manifold) consists of a family $\{E_p\}_{p\in S}$ of n-dimensional vector spaces parametrized by S together with a differentiable manifold structure on

$$E = \bigcup_{p\in S} E_p$$

that satisfy the following conditions.
- The projection map $\pi : E \longrightarrow S$ taking E_p to p is differentiable (E_p is called the fiber above p).
- For every p in S, there exists an open set U in S containing p and a diffeomorphism

$$\varphi_U : \pi^{-1}(U) \longrightarrow U \times \mathbb{R}^n$$

taking the vector space E_p isomorphically onto $\{p\} \times \mathbb{R}^n$. The diffeomorphism φ_U is called of trivialization of E over U, and $\mathbb{R}^n$ the typical fiber. If moreover there exists a trivialization over S, we say that E is a trivial vector bundle. Two examples of major importance are the tangent and cotangent bundles, TS and T^*S, corresponding respectively to $E_p = T_pS$ (the tangent space to S at p) and $E_p = T_p^*S$ (the cotangent space to S at p). We denote $\Gamma(S, E)$ the module of sections of E over S.

Vector bundles are particular cases of fiber bundles, where we only require the fibers to be topological spaces. In the sequel, we will sometimes use the term fiber bundle when talking about the Clifford bundle we consider.

A section σ of the vector bundle E over S is a differentiable map

$$\sigma : S \longrightarrow E$$

such that $\sigma(p)$ belongs to E_p for all p in S. It is well known that sections of TS, resp. T^*S, correspond to vector fields, resp. 1-forms, on S.

One more ingredient that is used in the sequel is the notion of connection (see [36]). A connection ∇ on a fiber bundle E is an operator taking sections σ of E into E-valued 1-forms $\nabla\sigma$ such that the Leibniz rule holds; if f is a function, then

$$\nabla(f\sigma) = f\nabla\sigma + \sigma \otimes df.$$

A connection is essentially a way of differentiating sections. To any connection we associate covariant derivatives that generalize to vector bundles the notion of directional derivatives on vector-valued functions.

Lots of computations we make in the next subsection necessitate to deal with tensor products, the definition and properties of which can be found in [1] and [67].

Let $\| \ \|_2$ be the Euclidean norm on $\mathbb{R}^n$. Keeping the notations of 1.3.1, we associate to each point q of D the Clifford algebra $\mathcal{CT}(q)$ of the four-dimensional vector space containing the $RGBT$-space endowed with the metric $Q(q)$

$$\begin{pmatrix} \lambda(q)/3 & 0 & 0 & 0 \\ 0 & \lambda(q)/3 & 0 & 0 \\ 0 & 0 & \lambda(q)/3 & 0 \\ 0 & 0 & 0 & \eta(q) \end{pmatrix}$$

(compare with Section 1.2.3 : β is replaced by $\lambda(q)$ and δ is replaced by $\eta(q)$). Let $\mathcal{CT}(D)$ be the disjoint union of $\mathcal{CT}(q)$ for q in D.

Proposition 1.1 *$\mathcal{CT}(D)$ with the projection $\pi : \mathcal{CT}(D) \longrightarrow D$ that maps $\zeta \in \mathcal{CT}(q)$ to q is a trivial vector bundle $(\mathcal{CT}(D), D, \pi)$ with typical fiber $Cl(\mathbb{R}^4, \| \ \|_2)$.*

Proof. We have to show that there exists a diffeomorphism Φ from $\pi^{-1}(D)$ onto $D \times Cl(\mathbb{R}^4, \| \ \|_2)$ such that $\Phi \circ p_1 = \pi$ where p_1 denotes the projection on the first factor. As $\mathcal{CT}(q)$ is isomorphic to $Cl(\mathbb{R}^4, \| \ \|_2)$ by some Φ_q for all q in D, we can define Φ by

$$\Phi : (v \in \mathcal{CT}(q)) \longmapsto (q, \Phi_q(v))$$

It is clearly a diffeomorphism. □

In the sequel, we will call such a vector bundle a Clifford algebras bundle or Clifford bundle, since the fibers (those above D and the typical fiber) are endowed with a Clifford algebra structure. In the literature, when talking about Clifford bundles, we often mean fiber bundles where the fibers are Clifford algebras and the isomorphisms respect the Clifford algebra structure. The situation is different in our case since the isomorphisms are vector space isomorphisms.

A color-infrared image I is now considered as a section

$q \in D \longmapsto r(q)e_1(q) + g(q)e_2(q) + b(q)e_3(q) + t(q)e_4(q)$ of $\mathcal{CT}(D)$.

From the fact that $(\mathcal{CT}(D), D, \pi)$ is trivial we know that any connection on it can be written as

$$\nabla = d + \omega$$

for some ω in $\Gamma(D, T^*D \otimes \mathrm{End}(\mathcal{CT}(D))$, d being the exterior differential [44].

If $X = (X_1, X_2)$ is a vector field on D and $Y = Y_0 1 + Y_1 e_1 + \cdots + Y_{15} e_1 e_2 e_3 e_4$ is a section of $\mathcal{CT}(D)$ then

$$(\omega(X)Y)_j = \sum_{k=0}^{15} (\Upsilon_{1k}^j X_1 + \Upsilon_{2k}^j X_2) Y_k$$

so that the connection is entirely determined by the symbols Υ_{ij}^k, $i = 1, 2$ and $j, k = 0, \ldots, 15$.

In the next paragraph we deal with the following three objects :
i. The connection $\widetilde{\nabla}$ defined by

$$\Upsilon_{ij}^k = \begin{cases} \dfrac{\partial_i \lambda}{\lambda} & \text{if } k = j \in \{6, 7, 9\} \\ \\ 0 & \text{otherwise} \end{cases}$$

ii. The section ψ of $(\mathcal{CT}(D), D, \pi)$ given by $\psi = S^\dagger I S$ with

$$S = \exp\left[-\frac{h}{2} \left(\frac{e_1 e_2 - e_1 e_3 + e_2 e_3}{\| e_1 e_2 - e_1 e_3 + e_2 e_3 \|} \right) \right]$$

iii. The section γ of $(\mathcal{CT}(D), D, \pi)$ given by $\gamma = \dfrac{v}{\|v\|} \rho$ where ρ is the unit chrominance vector of the red color, v is the chrominance vector, h is the hue (see Sect. 1.2.3) and $\| \ \|$ means that we take the norm of each fiber $\pi^{-1}(q)$.

1.3.3 Computing E, F, G with $\tilde{\nabla}$

The main result of this part is that the preceding coefficients E, F and G can be computed using covariant derivatives with respect to $\tilde{\nabla}$.

Proposition 1.2 *Let*

i. P_1 *(resp.* P_2*) be the section of* $\mathrm{End}(\mathcal{CT}(D))$ *such that* $P_1(q)$ *(resp.* $P_2(q)$*) is the orthogonal projection on the plane generated by the luminance and the temperature (resp. on the chrominance plane) in the fiber* $\pi^{-1}(q)$ *;*

ii. dx *(resp.* dy*) be the canonical* $\mathcal{CT}(D)$*-valued 1-form* $dx \otimes 1$ *(resp.* $dy \otimes 1$*) and* X *(resp.* Y*) be the vector field on* D *of coordinates* $(1,0)$ *(resp.* $(0,1)$*) ;*

iii. E*,* F*,* G *be the coefficients of the first fundamental form of* $\varphi(D)$ *(see Section 1.3.1) and* χ *be the* $\mathcal{CT}(D)$*-valued symmetric tensor of rank 2 :*

$$\chi = dx \underline{\otimes} dx + dy \underline{\otimes} dy + P_1(\tilde{\nabla}\psi)P_1(\tilde{\nabla}\psi) + \frac{9}{2}P_2(\tilde{\nabla}\psi)\underline{\otimes}P_2(\tilde{\nabla}\psi) - \kappa\xi(\gamma^\dagger\tilde{\nabla}\gamma)\underline{\otimes}(\gamma^\dagger\tilde{\nabla}\gamma)$$

then, under the identification of $\mathbb{R}$ *and its injection into a Clifford algebra, we have*

$$E = \chi(X \otimes X) \qquad F = \chi(X \otimes Y) \qquad G = \chi(Y \otimes Y)$$

(see Section 1.3.1 for the definitions of κ *and* ξ*). In other words,* χ *may be viewed as the metric on the surface* $\varphi(D)$*.*

Remarks on the notations. As it is mentioned at the end of the Appendix, the symbol $\underline{\otimes}$ *denotes the tensor product over the ring of sections of* $\mathcal{CT}(D)$*, whereas the symbol* $\otimes$ *denotes the tensor product over the ring of* $\mathbb{R}$*-valued functions on* D*.* $P_1(\tilde{\nabla}\psi)P_1(\tilde{\nabla}\psi)$ *is the symmetric product we define in the Appendix of* $P_1(\tilde{\nabla}\psi)$ *by itself.*

Proof. From Section 1.3.2 we know that S is a Spin(4)-valued section whose action on I for each $q \in D$, namely $S(q)^\dagger I(q)S(q)$, is a rotation (see Section 1.2.3). We explicit this rotation.
The 4-dimensional vector subspace of $\mathcal{CT}(q)$ isomorphic to $\mathbb{R}^1_{4,0}$ by trivialization can be decomposed into two orthogonal planes :
i. The plane generated by the luminance and the temperature components, represented by the bivector $e_1(q)e_4(q) + e_2(q)e_4(q) + e_3(q)e_4(q)$.
ii. The chrominance plane represented by the bivector $e_1(q)e_2(q) - e_1(q)e_3(q) + e_2(q)e_3(q)$.

From this we deduce that the rotation lets the luminance and temperature parts of $I(q)$ invariant and acts on the chrominance plane as a rotation of angle $-h(q)$. That is, it sends the chrominance vector $v(q)$ on the vector $\|v(q)\|\rho(q)$.

Since P_1 and P_2 are linear maps, we have

$$d(P_i(\psi)) = P_i d(\psi) \quad i = 1, 2$$

From the definition of $\tilde{\nabla}$, it leads to $P_i(\tilde{\nabla}\psi) = \tilde{\nabla}P_i(\psi)$. Then

$$\begin{aligned} P_1(\tilde{\nabla}\psi) &= \tilde{\nabla}P_1(\psi) \\ &= \tilde{\nabla}(\, l(e_1 + e_2 + e_3) + te_4) \\ &= dl \otimes (e_1 + e_2 + e_3) + dt \otimes e_4 \end{aligned}$$

hence

$$P_1(\tilde{\nabla}\psi)P_1(\tilde{\nabla}\psi) = dl\otimes dl\otimes(e_1+e_2+e_3)^2+\frac{1}{2}(dl\otimes dt+dt\otimes dl)\otimes(e_1+e_2+e_3)e_4$$

$$+\frac{1}{2}(dt\otimes dl + dl\otimes dt)\otimes e_4(e_1+e_2+e_3) + dt\otimes dt\otimes (e_4)^2$$

So, we have

$$P_1(\tilde{\nabla}\psi)P_1(\tilde{\nabla}\psi) = dl\otimes dl\otimes\lambda + dt\otimes dt\otimes\eta$$

Simple computations show that $\rho = \sigma/\sqrt{\lambda}$ with $\sigma = \sqrt{2}e_1 - \frac{\sqrt{2}}{2}e_2 - \frac{\sqrt{2}}{2}e_3$, then

$$\begin{aligned} P_2(\tilde{\nabla}\psi) &= \tilde{\nabla}\left(\frac{\|v\|\sigma}{\sqrt{\lambda}}\right) \\ &= \left(d\frac{\|v\|}{\sqrt{\lambda}}\right)\otimes\sigma + \frac{\|v\|}{\sqrt{\lambda}}\tilde{\nabla}\sigma \\ &= \left(d\frac{\|v\|}{\sqrt{\lambda}}\right)\otimes\sigma \end{aligned}$$

Recall that $\|v\| = \frac{\sqrt{2}}{3}\sqrt{\lambda}s$ to obtain $P_2(\tilde{\nabla}\psi) = \frac{\sqrt{2}}{3}ds\otimes\sigma$ which leads to

$$\begin{aligned} P_2(\tilde{\nabla}\psi)\underline{\otimes}P_2(\tilde{\nabla}\psi) &= \frac{2}{9}ds\otimes ds\otimes\sigma^2 \\ &= \frac{2}{9}ds\otimes ds\otimes\lambda \end{aligned}$$

The section γ can be decomposed as

$$\gamma = \frac{v}{\|v\|}\cdot\rho + \frac{v}{\|v\|}\wedge\rho$$

Since $\frac{v}{\|v\|}\cdot\rho = \cos(h)$ and $\frac{v}{\|v\|}\wedge\rho = \sin(h)\left(\frac{e_1e_2 - e_1e_3 + e_2e_3}{\|e_1e_2 - e_1e_3 + e_2e_3\|}\right)$, we have then

$$\gamma = \cos(h) + \sin(h)\left(\frac{e_1e_2 - e_1e_3 + e_2e_3}{\|e_1e_2 - e_1e_3 + e_2e_3\|}\right)$$

The expression of $\tilde{\nabla}\gamma$ is therefore

$$\tilde{\nabla}\gamma = -dh\otimes\sin(h) + \cos(h)\tilde{\nabla}1 + dh\otimes\cos(h)\left(\frac{e_1e_2 - e_1e_3 + e_2e_3}{\|e_1e_2 - e_1e_3 + e_2e_3\|}\right)$$

$$+\sqrt{3}\sin(h)\tilde{\nabla}\left(\frac{e_1e_2}{\lambda} - \frac{e_1e_3}{\lambda} + \frac{e_2e_3}{\lambda}\right)$$

However by definition of $\tilde{\nabla}$

$$\tilde{\nabla}1 = \tilde{\nabla}\left(\frac{e_1e_2}{\lambda}\right) = \tilde{\nabla}\left(\frac{e_1e_3}{\lambda}\right) = \tilde{\nabla}\left(\frac{e_2e_3}{\lambda}\right) = 0$$

and so

$$\tilde{\nabla}\gamma = -dh\otimes\sin(h) + dh\otimes\cos(h)\left(\frac{e_1e_2 - e_1e_3 + e_2e_3}{\|e_1e_2 - e_1e_3 + e_2e_3\|}\right)$$

This implies that

$$\gamma^\dagger\widetilde{\nabla}\gamma = \left[\cos(h) - \sin(h)\left(\frac{e_1e_2 - e_1e_3 + e_2e_3}{\|e_1e_2 - e_1e_3 + e_2e_3\|}\right)\right] \times \left[(-dh\otimes\sin(h) + dh\otimes\cos(h)\left(\frac{e_1e_2 - e_1e_3 + e_2e_3}{\|e_1e_2 - e_1e_3 + e_2e_3\|}\right)\right]$$

and

$$\gamma^\dagger\widetilde{\nabla}\gamma = dh\otimes\left(\frac{e_1e_2 - e_1e_3 + e_2e_3}{\|e_1e_2 - e_1e_3 + e_2e_3\|}\right)$$

Consequently

$$(\gamma^\dagger\widetilde{\nabla}\gamma)\underline{\otimes}(\gamma^\dagger\widetilde{\nabla}\gamma) = -dh\otimes dh\otimes 1$$

Let $Z_1 = (Z_{11}, Z_{12})$ and $Z_2 = (Z_{21}, Z_{22})$ be two vector fields on D, then by definition of χ :

$$\chi(Z_1\otimes Z_2) = dx\underline{\otimes}dx(Z_1\otimes Z_2) + dy\underline{\otimes}dy(Z_1\otimes Z_2) + P_1(\widetilde{\nabla}\psi)P_1(\widetilde{\nabla}\psi)\,(Z_1\otimes Z_2)$$

$$+\frac{9}{2}P_2(\widetilde{\nabla}\psi)\underline{\otimes}P_2(\widetilde{\nabla}\psi)\,(Z_1\otimes Z_2) - \kappa\xi(\gamma^\dagger\widetilde{\nabla}\gamma)\underline{\otimes}(\gamma^\dagger\widetilde{\nabla}\gamma)\,(Z_1\otimes Z_2)$$

From what we have shown above, we have

$$\chi(Z_1\otimes Z_2) = dx\underline{\otimes}dx(Z_1\otimes Z_2) + dy\underline{\otimes}dy(Z_1\otimes Z_2) + dl\otimes dl\otimes\lambda\,(Z_1\otimes Z_2) + dt\otimes dt\otimes\eta\,(Z_1\otimes Z_2)$$

$$+ds\otimes ds\otimes\lambda\,(Z_1\otimes Z_2) + \kappa\xi\,dh\otimes dh\otimes 1\,(Z_1\otimes Z_2)$$

Hence $\chi(Z_1\otimes Z_2)=$

$$Z_{11}Z_{21} + Z_{12}Z_{22} + dl(Z_1)dl(Z_2)\lambda + dt(Z_1)dt(Z_2)\eta + ds(Z_1)ds(Z_2)\lambda + \kappa\xi dh(Z_1)dh(Z_2)$$

Taking $Z_1 = Z_2 = X$, we get the expression of E. Similarly, taking $Z_1 = Z_2 = Y$, we get the expression of G, and from $Z_1 = X, Z_2 = Y$ or $Z_1 = Y, Z_2 = X$, we get the expression of F. □

1.3.4 Discretization and parallel transport

In practice, if an image is represented as a two-dimensional surface S parametrized by a function φ on a domain D, only the points of S corresponding to integer coordinates points of D are to be taken into account. This implies that derivatives of φ must be discretized. For 1D images (i.e. grey level images) Prewitt, Sobel or Canny-Deriche filters can be used to make the approximation. This also may be applied more generally to nD images by computing the discrete derivatives of each component of φ.

However, in the vector bundles setting we consider in this paper, such methods are irrelevant since they necessitate to do operations (additions) between objets (multivectors) which don't belong to the same space (they live in different fibers). To solve this problem, we move these objects using the so-called parallel transport so that they can be considered as living in the same fiber.

Let us remind the definition of parallel transport. Let (E, π, M) be a vector bundle endowed with a connection ∇, $\gamma : J \subset \mathbb{R} \to M$ a curve in M and v a vector of $\pi^{-1}(\gamma(0))$. The parallel transport of v along γ is the solution $\tau_\gamma(t, v)$ of the following ordinary differential equation :

$$\begin{cases} \nabla_{\dot\gamma(t)} \tau_\gamma = 0 \quad \forall t \in J \\ \\ \tau_\gamma(0, v) = v \end{cases}$$

The parallel transport appears classically when dealing with geodesics on manifolds. More precisely, consider the tangent bundle $(TM, \tilde\pi, M)$ of a manifold M (not necessarily equipped with a metric) endowed with a connection ∇. A geodesic is defined as a curve $\gamma : J \to M$ whose tangent vector field $\dot\gamma : J \to TM$ is parallel along γ :

$$\nabla_{\dot\gamma(t)} \dot\gamma = 0 \quad \forall t \in J$$

The usual notion of geodesic over surfaces arises from the Levi-Cevita connection [29] induced by the first fundamental form of the surface.

Let us now explain how to compute the coefficients E, F, and G of Section 1.3.3 when dealing with the integer coordinates points of D. In what follows, we use the matricial coordinates system.

We denote

$$\gamma_{(1,0)}^{(i,j)}, \quad \gamma_{(0,1)}^{(i,j)}, \quad \gamma_{(1,1)}^{(i,j)}, \quad \gamma_{(1,-1)}^{(i,j)}$$

the classes of curves on D from the point (i, j) that satisfy :

$$\dot\gamma_{(1,0)}^{(i,j)}(t) = (1, 0), \quad \dot\gamma_{(1,0)}^{(i,j)}(t) = (0, 1), \quad \dot\gamma_{(1,1)}^{(i,j)}(t) = (1, 1), \quad \dot\gamma_{(1,-1)}^{(i,j)}(t) = (1, -1)$$

for all t. The corresponding parallel transports (with respect to $\widetilde{\nabla}$)

$$\tau_{(1,0)}^{(i,j)}(t, .), \quad \tau_{(0,1)}^{(i,j)}(t, .), \quad \tau_{(1,1)}^{(i,j)}(t, .), \quad \tau_{(1,-1)}^{(i,j)}(t, .)$$

are linear maps from $\pi^{-1}(i, j)$ to $\pi^{-1}(\gamma_{(1,0)}^{(i,j)}(t))$ resp. $\pi^{-1}(\gamma_{(0,1)}^{(i,j)}(t))$, $\pi^{-1}(\gamma_{(1,1)}^{(i,j)}(t))$ and $\pi^{-1}(\gamma_{(1,-1)}^{(i,j)}(t))$.

By definition of $\widetilde{\nabla}$, if γ is one of the preceding classes of curves and w is a vector of $\pi^{-1}(\gamma(0))$, i.e $w = w_1 e_1(\gamma(0)) + w_2 e_2(\gamma(0)) + w_3 e_3(\gamma(0)) + w_4 e_4(\gamma(0))$, then the parallel transport of w at $\pi^{-1}(\gamma(t))$ is the vector

$$w_1 e_1(\gamma(t)) + w_2 e_2(\gamma(t)) + w_3 e_3(\gamma(t)) + w_4 e_4(\gamma(t))$$

Let us consider the vector

$$\tau_1(i, j) = \frac{1}{8} \Big\{ \tau_{(1,-1)}^{(i+1,j-1)}(-1, \psi) + 2\tau_{(1,0)}^{(i+1,j)}(-1, \psi) + \tau_{(1,1)}^{(i+1,j+1)}(-1, \psi) - \tau_{(1,1)}^{(i-1,j-1)}(1, \psi)$$

$$-2\tau_{(1,0)}^{(i-1,j)}(1, \psi) - \tau_{(1,-1)}^{(i-1,j+1)}(1, \psi) \Big\}$$

and the scalar

$$\tau_2(i,j) = \frac{1}{8}\left\{\arccos(a\cdot b) + 2\arccos(c\cdot d) + \arccos(e\cdot f)\right\}$$

where

$$a = \frac{\tau_{(1,1)}^{(i-1,j-1)}(1,v)}{\|\tau_{(1,1)}^{(i-1,j-1)}(1,v)\|} \quad b = \frac{\tau_{(1,-1)}^{(i+1,j-1)}(-1,v)}{\|\tau_{(1,-1)}^{(i+1,j-1)}(-1,v)\|} \quad c = \frac{\tau_{(1,0)}^{(i-1,j)}(1,v)}{\|\tau_{(1,0)}^{(i-1,j)}(1,v)\|}$$

$$d = \frac{\tau_{(1,0)}^{(i+1,j)}(-1,v)}{\|\tau_{(1,0)}^{(i+1,j)}(-1,v)\|} \quad e = \frac{\tau_{(1,-1)}^{(i-1,j+1)}(1,v)}{\|\tau_{(1,-1)}^{(i-1,j+1)}(1,v)\|} \quad f = \frac{\tau_{(1,1)}^{(i+1,j+1)}(-1,v)}{\|\tau_{(1,1)}^{(i+1,j+1)}(-1,v)\|}$$

These are elements of $\pi^{-1}(i,j)$.

The vector $\tau_1(i,j)$ (resp. the scalar $\tau_2(i,j)$) is a discrete approximation of $\widetilde{\nabla}\psi$ (resp. $dh\otimes 1$) in the direction given by the tangent vector of coordinates $(1,0)$ at (i,j). We obtain thus a discrete version of the coefficient G of the fundamental form I, namely

$$G_d = 1 + (P_1(\tau_1))^2 + \frac{9}{2}(P_2(\tau_1))^2 + \kappa\xi\tau_2^2$$

Detailing the computation of G_d, Clifford algebras reveal all their assets (at least, the three mentionned in the Introduction). First, we exploit the efficiency of the geometric calculus to compute τ_1 and τ_2 in a concise way. Indeed, we don't need matrix representation to compute the rotations $S^\dagger IS$ but only algebraic operations using spinors. The computation is trivial when remark that, as

$$\left(\frac{e_1e_2 - e_1e_3 + e_2e_3}{\|e_1e_2 - e_1e_3 + e_2e_3\|}\right)^2 = -1,$$

we have

$$S = \cos\left(\frac{h}{2}\right) - \sin\left(\frac{h}{2}\right)\frac{e_1e_2 - e_1e_3 + e_2e_3}{\|e_1e_2 - e_1e_3 + e_2e_3\|}$$

From a generalized directional Sobel filter applied to $S^\dagger IS$ using parallel transport, we obtain τ_1 that is a discrete approximation of the vector-valued section

$$l_y(e_1+e_2+e_3) + t_y e_4 + \frac{\sqrt{2}}{3}s_y\,\sigma$$

Let us remark that the angle between two chrominance vectors represents the hue difference between the two corresponding colors. This allows us to compute hue discrete derivatives efficiently. Let $(i,j)\in D$, we first compute chrominance vectors of the 3x3 neighborhood of (i,j) using the rejection operator of geometric calculus (Section 1.2.1), and we map them into the fiber $\pi^{-1}(i,j)$ by parallel transport. Then, computing some angles from the inner product of the normalized vectors, we derive a kind of Sobel mask and we obtain $\tau_2(i,j)$, that is a dicrete approximation of h_y at (i,j). The way we get this approximation avoids to compute discrete derivatives of the function (that is the problem of measuring distances on S^1).

As a second asset, we see that all the information we need to compute G_d may be

included into a single multivector-valued section $\tau := \tau_1 + \tau_2$ which contains a scalar and a vector part. Inversely, from the multivector τ, we get

$$\tau_1 = \frac{t(\tau) - \alpha(\tau)}{2}$$

and

$$\tau_2 = \frac{t(\tau) + \alpha(\tau)}{2}$$

where t and α are the extensions of the two morphisms defined in Section 1.2.1 to $\mathcal{CT}(D)$.

At last, we use the computability of the orthogonal projection operator (Section 1.2.1), and the property of Clifford algebras that a squared vector gives its squared norm in the associated quadratic vector space. Indeed we may compute directly G_d from τ and the functions ξ and κ, where ξ is fixed (Section 1.2.3) and κ has to be determined (depends on the chosen edge detection) by the following formula. We have

$$G_d = 1 + P_1 \left(\frac{t(\tau) - \alpha(\tau)}{2} \right)^2 + \frac{9}{2} P_2 \left(\frac{t(\tau) - \alpha(\tau)}{2} \right)^2 + \kappa\xi \left(\frac{t(\tau) + \alpha(\tau)}{2} \right)^2$$

In other words, we compute a discrete approximation of $1 + \lambda l_y^2 + \lambda s_y^2 + \kappa\xi h_y^2 + \eta t_y^2$. In the same way, we get a discrete version of the coefficients E and F.

1.4 Applications

We propose three applications of the computation of χ of Section 1.3.3 : First we compare our approach with the method developed by Di Zenzo, then we focus on detecting edges in color images with respect to a given hue interval and saturation levels of colors. The third application is devoted to detect edges in color-infrared images with constraints on color and temperature. Finally we describe briefly further work on color edges analysis, related to the classification of edges in function of they are due to shadows, highlights, or transitions between objects.

1.4.1 Comparison with the Di Zenzo gradient

In this part, we first show that we obtain the metric of the Di Zenzo's approach by derivating the section representing a color image with the connection $\widetilde{\nabla}$ and taking a well-chosen metric on the fiber bundle. Then, we explicit the difference between the metric of Di Zenzo and the one given by Proposition 1.2.

Di Zenzo's approach of edge detection is to consider a color image as a 2-dimensional surface parametrized by

$$\varphi : (x, y) \longmapsto (x, y, r(x, y), g(x, y), b(x, y))$$

embedded in $(\mathbb{R}^5, \| \ \|_2)$.

Coefficients of the first fundamental form are therefore given by :

$$E_{DZ} = 1 + (r_x)^2 + (g_x)^2 + (b_x)^2$$
$$F_{DZ} = r_x r_y + g_x g_y + b_x b_y$$
$$G_{DZ} = 1 + (r_y)^2 + (g_y)^2 + (b_y)^2$$

Let us consider the Clifford bundle $(\mathcal{CT}(D), \pi, D)$ constructed from the metric

$$\begin{pmatrix} 1/3 & 0 & 0 & 0 \\ 0 & 1/3 & 0 & 0 \\ 0 & 0 & 1/3 & 0 \\ 0 & 0 & 0 & \eta \end{pmatrix}$$

where η is any strictly positive function, so that the fiber bundle is well-defined.

Remark. As we deal with color images, the values of η will not affect the result of the edge detection. Note that we could have constructed a Clifford bundle from a vector bundle of rank 3. In this paper, we have chosen to consider a color image as the color part of a color/infrared image so that to make our method relevant to deal more generally with nD images edge detection. Let $I(q) = r(q)e_1(q) + g(q)e_2(q) + b(q)e_3(q) + t(q)e_4(q)$ be a color/infrared image, seen as a section of $\mathcal{CT}(D)$, and let us denote $I_{col}(q) = r(q)e_1(q) + g(q)e_2(q) + b(q)e_3(q)$ its color part, that is

$$I_{col} = I \cdot (e_1e_2e_3)(e_1e_2e_3)^{-1}$$

Then, we have

$$\widetilde{\nabla} I_{col} = dr \otimes e_1 + dg \otimes e_2 + db \otimes e_3$$

and the symmetric product of $\widetilde{\nabla}$ by itself (see Appendix) is therefore :

$$\widetilde{\nabla} I_{col} \widetilde{\nabla} I_{col} = dr \otimes dr \otimes \frac{1}{3} + dg \otimes dg \otimes \frac{1}{3} + db \otimes db \otimes \frac{1}{3}$$

So, using the same notations as in Proposition 1.2, and considering the symmetric tensor of rank 2 χ_{DZ} defined by

$$\chi_{DZ} = dx \underline{\otimes} dx + dy \underline{\otimes} dy + 3\widetilde{\nabla} I_{col} \widetilde{\nabla} I_{col}$$

we get

$$E_{DZ} = \chi_{DZ}(X \otimes X) \quad F_{DZ} = \chi_{DZ}(X \otimes Y) \quad G_{DZ} = \chi_{DZ}(Y \otimes Y)$$

Furthermore we can split I_{col} into

$$(I_{col} \cdot \mu)\mu^{-1} + (I_{col} \wedge \mu)\mu^{-1} = l(e_1 + e_2 + e_3) + v$$

Since

$$\widetilde{\nabla} I_{col} = dl \otimes (e_1 + e_2 + e_3) + \widetilde{\nabla} v$$

we see that the method of Di Zenzo deals with the derivative $\widetilde{\nabla} v$ of the chrominance vector which, by definition of $\widetilde{\nabla}$, corresponds to the usual derivative of the vector-valued function v. Moreover, since $(e_1 + e_2 + e_3)$ and v are orthogonal, then

$$\widetilde{\nabla} I_{col} \widetilde{\nabla} I_{col} = dl \otimes dl \otimes 1 + \widetilde{\nabla} v \widetilde{\nabla} v$$

and

$$\chi_{DZ} = dx \underline{\otimes} dx + dy \underline{\otimes} dy + dl \otimes dl \otimes 3 + 3\widetilde{\nabla} v \widetilde{\nabla} v$$

From simple computations, we have

$$\begin{aligned} E_{DZ} &= 1 + 3(l_x)^2 + v_x^2 \\ F_{DZ} &= 3(l_x l_y) + v_x \cdot v_y \\ G_{DZ} &= 1 + 3(l_y)^2 + v_y^2 \end{aligned}$$

If we apply now Proposition 1.2 for $\psi = S^\dagger I_{col} S$ in the context of this fiber bundle, the corresponding coefficients are given by

$$\begin{aligned} E &= 1 + (l_x)^2 + (s_x)^2 + \kappa\xi(h_x)^2 \\ F &= l_x l_y + s_x s_y + \kappa\xi h_x h_y \\ G &= 1 + (l_y)^2 + (s_y)^2 + \kappa\xi(h_y)^2 \end{aligned}$$

and variations of the chrominance part are given by **both** variations of saturation and hue components.

We conclude that these two methods differ first by the weight of the luminance part, then by the metric of the chrominance part, which is Euclidean for the Di Zenzo's method, and Riemannian for the method we propose (the coefficient ξ of the metric associated to the hue component varies with the saturation).

Let us consider as an example the case where the hue is locally constant, i.e. $dh = 0$, then

$$\widetilde{\nabla} v = d(\|v\|) \otimes \frac{v}{\|v\|}$$

and

$$\widetilde{\nabla} v \widetilde{\nabla} v = d(\|v\|) \otimes d(\|v\|) \otimes 1 = ds \otimes ds \otimes \frac{2}{9}$$

The coefficients for the Di Zenzo gradient are therefore

$$\begin{aligned} E_{DZ} &= 1 + 3(l_x)^2 + \frac{2}{3} s_x^2 \\ F_{DZ} &= 3(l_x l_y) + \frac{2}{3} s_x s_y \\ G_{DZ} &= 1 + 3(l_y)^2 + \frac{2}{3}(s_y)^2 \end{aligned}$$

while those we have defined are

$$\begin{aligned} E &= 1 + (l_x)^2 + (s_x)^2 \\ F &= l_x l_y + s_x s_y \\ G &= 1 + (l_y)^2 + (s_y)^2 \end{aligned}$$

We can see in this very particular case that the two methods differ from the ratio

$$\text{weight of luminance/weight of saturation}$$

in the measure of the variations of a color image.

FIGURE 1.1 – left : original image - right : edge detection in the hue interval Red-Yellow

However, let us mention the problem of determining which one of the two metrics is the most perceptual. A solution to solve this problem could be to compare these two metrics with the perceptual metric of *Lab* pull-backed on RGB.

1.4.2 Color edge detection with respect to hue intervals and saturation levels

The aim of this application is to detect edges characterizing transitions between highly saturated colors of a given hue interval.

Let $I_{col}(q) = r(q)e_1(q) + g(q)e_2(q) + b(q)e_3(q)$ be a section of $\mathcal{CT}(D)$ corresponding to the color part of a color/infrared image, where the coefficients of the metric generating $\mathcal{CT}(D)$ are defined as follows. As for this application, we don't deal with temperature variations, η can be taken as any strictly positive function again. Moreover, since we only consider hue variations, the choice of κ influences the result, and λ doesn't. Therefore let us take λ be any strictly positive function, high enough so that the norm of a vector at each fiber is numerically computable. Indeed, we only have to compute the part which contains the information about hue variations. It is given by $1 + \kappa\xi\tau_2^2$ (see Section 1.3.4). By definition of τ_2, we compute norms of vectors, which depend on the value of λ.

In the continuous setting, this information is given by

$$dx\underline{\otimes}dx + dy\underline{\otimes}dy - \kappa\xi(\gamma^\dagger\widetilde{\nabla}\gamma)\underline{\otimes}(\gamma^\dagger\widetilde{\nabla}\gamma)$$

This latter can be viewed as the first fundamental form of the surface parametrized by

$$\varphi : (x, y) \mapsto (x, y, h)$$

embedded in $\mathbb{R}^3$ equipped with the metric

$$\begin{pmatrix} 1 & 0 & 0 \\ 0 & 1 & 0 \\ 0 & 0 & \kappa\,\xi \end{pmatrix}$$

Let us now detail the construction of the function κ.

In the sequel, for $q \in D$, we consider the domain

$$\Omega(q) = \{(x, y),\ \|(x, y) - q\|_\infty \leqslant 1\}$$

Let θ in $[0, 2\pi]$. The unit chrominance vector v_θ of hue θ is

$$v_\theta = \cos(\theta)\rho + \sin(\theta)\rho B$$

where B is the unit bivector coding the chrominance plane. The angular distance δ between two hues h_3 and h_4 may be computed using the corresponding unit chrominance vectors

$$\delta(h_3, h_4) = \arccos(v_{h_3} \cdot v_{h_4})$$

Let us note h_1 and h_2 the two hues representing boundaries of the given hue interval. We set $\kappa(q) = 1$ if

$$\max_{z \in \Omega(q)} (\max(\delta(h(z), h_1), \delta(h(z), h_2))) \leqslant \delta(h_1, h_2)$$

and extend κ into a derivable function on $[0, \pi]$ that is strictly decreasing on $[\delta(h_1, h_2), \pi]$.

In the illustration of this application, $h_1 = 0$ is the red hue, $h_2 = \pi/3$ is the yellow hue, and κ equals 0 for any value greater than $\pi/3$.
As we can see Fig. 1.1 (right), we principally detect edges of Fig. 1.1 (left) inside petals. Let us explain this result. First, due to the definition of κ, as soon as there is a pixel in the neighborhood of a point q in D whose hue is not in the interval red-yellow, color variations at q are not detected. That's why edges involving green color, as on stems, are not detected. Then, one may find inside petals variations between yellow and red hues, which implies that $\kappa\, dh$ is maximal. Moreover, these colors have almost a full saturation, so ξ almost equals 1. In the same way, variations where one of the colors has low saturation are not detected, since ξ decreases strongly when the surrounding saturation declines. This explains why transitions between colors of yellow or red hue and colors which look white are not detected.

1.4.3 Color/infrared images edge detection

We present here an edge detection combining information given by both color and temperature variations of a scene. It seems to be particulary suitable to detect humans. Indeed, humans may be characterized by their temperature and the color of their skin. Then, variations of temperature provide transitions between humans and their environment. Conjointly, color variations allow us to have a better description of humans, by detecting edges inside the regions they determine.
Let us consider the following situation : a man is standing in front of a wall and is handing a cup of hot coffee (see Fig. 1.2). We want to detect edges corresponding to regions of temperature similar to the temperature of the human body and of color similar to the color of the skin, that is his face and his arm (see Fig. 1.2).

FIGURE 1.2 – left and center : color and temperature information of the scene - right : regions where $g_1 = 1$ in white

First, let us consider this color-infrared image as a function $D \longrightarrow \mathbb{R}_{4,0}$

$$I(q) = r(q)e_1 + g(q)e_2 + b(q)e_3 + t(q)e_4$$

and let I_{col} be its color part.
Let $\zeta = \zeta_1 e_1 + \zeta_2 e_2 + \zeta_3 e_3 = I_{col}(x, y)$ for (x, y) located on the face or on the arm and chosen arbitrarily. Therefore ζ is a relevant representant of the color of the skin.

Then, we proceed as follows :

We compute the function ζI, which may be decomposed as the sum of a scalar and a bivector function :

$$\zeta I = \zeta \cdot I + \zeta \wedge I$$

From the information given by $\zeta \cdot I$ and $\zeta \wedge I$, we construct the metric generating a Clifford bundle $\mathcal{CT}(D)$, and the function κ. Then, we consider the color/infrared image as a section of this fiber bundle

$$I(q) = r(q)e_1(q) + g(q)e_2(q) + b(q)e_3(q) + t(q)e_4(q)$$

and compute the tensor χ in this setting. We get then the coefficients of the first fundamental form of the surface parametrized by

$$\varphi : (x, y) \longmapsto (x, y, l(x, y), s(x, y), h(x, y), t(x, y))$$

embedded in $\mathbb{R}^6$ equipped with metric

$$\begin{pmatrix} 1 & 0 \\ 0 & 1 \end{pmatrix} \oplus \begin{pmatrix} \lambda(p) & 0 & 0 & 0 \\ 0 & \lambda(p) & 0 & 0 \\ 0 & 0 & \kappa(p)\xi(p) & 0 \\ 0 & 0 & 0 & \eta(p) \end{pmatrix}$$

Let us detail how we proceed to construct the metric generating $\mathcal{CT}(\mathcal{D})$.

If we denote by α the function which gives for each $q \in D$ the angle between ζ and $I_{col}(q)$, we have $|\tan(\alpha)| =$

$$\frac{\|\zeta\|\|I_{col}\||\sin(\alpha)|}{\|\zeta\|\|I_{col}\||\cos(\alpha)|} = \frac{\|\langle \zeta I \rangle_2 \cdot (e_1e_2e_3)\,(e_1e_2e_3)^{-1}\|}{|\langle \zeta I \rangle_0|}$$

From $|\tan(\alpha)|$, we get $|\alpha|$ since $-\pi/2 \leqslant \alpha \leqslant \pi/2$ (ζ and $I_{col}(q)$ are vectors in the RGB cube).

Note that $|\alpha|$ appears to be a suitable measure of similarity to skin color. Indeed, we can see on Fig. 1.2 that the skin color is darker on the parts corresponding to the beard and shadow on the arm ; luminance and saturation are decreased, hue is almost unchanged. Moreover, in RGB space, decrease or increase of luminance and saturation with the same scale parameter combined with unchanged hue is represented by an homothety of the corresponding color vector. More precisely, simple computations show that

$$l(ka) = kl(a), \quad s(ka) = ks(a), \quad h(ka) = h(a)$$

for $k \in \mathbb{R}$ and $a \in RGB$ such that $ka \in RGB$.

To summarize, we say that color variations located on the face and the arm may be, roughly speaking, assimilated to homotheties. Then, the choice of $|\alpha|$ to characterize them arises from the invariance of α with respect to homotheties.

Then, we determine thresholds on $|\alpha|$ and t respectively α_0 and t_0 that define regions of interest using the following map (see Fig. 1.2).

We set $g_1(q) = 1$ if

$$\min_{z \in \Omega(q)} |\alpha(z)| \leqslant \alpha_0 \quad \text{and} \quad \max_{z \in \Omega(q)} t(z) \geqslant t_0$$

and extend g_1 into a derivable function on $[0, \pi/2] \times [0, 255]$ that is strictly decreasing with respect to the first variable on $[\alpha_0, \pi/2]$, and with respect to the second variable on $[0, t_0]$. Moreover we ask g_1 to be strictly positive since the metric g we take to generate $\mathcal{CT}(D)$ is

$$g := \begin{pmatrix} g_1 & 0 & 0 & 0 \\ 0 & g_1 & 0 & 0 \\ 0 & 0 & g_1 & 0 \\ 0 & 0 & 0 & \nu g_1 \end{pmatrix}$$

The role of ν is to control the weight of temperature variations in the image.
Moreover, we choose $\kappa = 255 g_1/\pi$ so that the hue component has the same weight in the measure of variations of I as the two other color components, that are luminance and saturation.

Fig. 1.3 shows the results of edge detections for different values of ν, increasing from the left to the right. On the left, ν is taken small so that the edge detection is similar to a color edge detection with constraints on color and temperature. We see that transitions between the man and his environment are not well detected on some parts (the region around the nose and the transition between the hand and the cup of coffee). For the two pictures at the center, both color and temperature variations are taken into account. In the case of $\nu = 10$, we still detect color details as the eye, the beard and shadow on the arm. Moreover, we see that transitions between the man and his environment are better localized. Increasing again the weight of temperature variations ($\nu = 30$), we don't detect anymore color details, but only edges characterizing the frontiers of the regions of interest (see Fig. 1.2). The last picture shows an edge detection for ν taken high, that is an edge detection which can be assimilated to a temperature edge detection

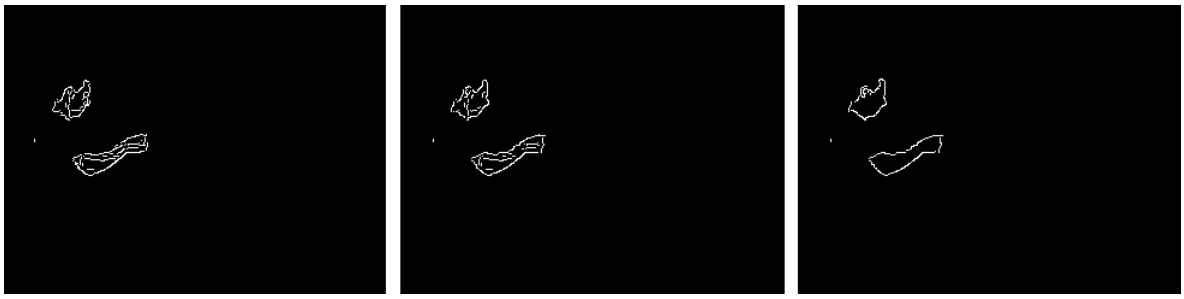

FIGURE 1.3 – Color/temperature edge detections for different values of ν. From left to right : $\nu = 0.001, 10, 30, 100$

with respect to color and temperature constraints. We remark that the frontier between face and hair is not well detected. This comes from the fact that this region represents small temperature variations, as we can see on the temperature information of the scene (Fig. 1.2).

1.4.4 One more example of possible applications : color edge analysis

As mentioned in the Introduction, many other applications can be considered from the general setting we have described before. To conclude this section we discuss one of them. Since the approach is slightly different and necessitates more mathematical developments, we only sketch the main steps of the process. Details will appear elsewhere [4].
The problem is the following one. In [40] Gevers & al. classify edges of a color image depending on whether they are due to the presence of different objects, shadows, or highlights, under the assumptions of white illumination and neutral interface reflection. Their method is based on color models they introduced in [41] for the purpose of color objects recognition.
We propose here to show how to obtain similar results (under the same assumptions) using the mathematical formalism of Section. 1.3. Unlike other edge detections we have presented in this paper, the metrics we construct don't depend on the values of the image, but of the values of its derivatives.

We proceed in several steps :

First, we consider a nD image as a section of a Clifford bundle $(\mathcal{CT}_1(D), \pi_1, D)$ generated by a metric

$$g = \begin{pmatrix} g_1 & & & \\ & g_2 & & \\ & & \ddots & \\ & & & g_n \end{pmatrix}$$

The main difference with the framework developed in Sec. 1.3 is that a nD image takes now the following form

$$I(q) = I_1(q)\frac{e_1(q)}{\sqrt{g_1(q)}} + I_2(q)\frac{e_2(q)}{\sqrt{g_2(q)}} + \ldots + I_n(q)\frac{e_n(q)}{\sqrt{g_n(q)}}$$

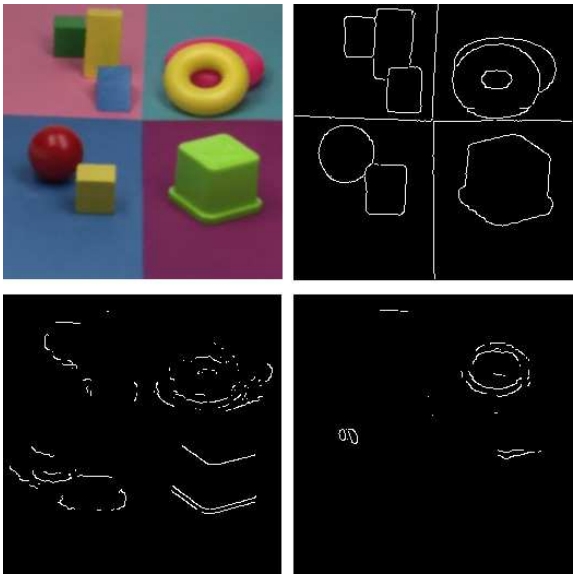

FIGURE 1.4 – Clockwise from upper left : original image, objects, highlights, shadows

In other words, we choose a trivialization that makes the fibers isomorphic (as algebras) to the typical fiber. Therefore we can define a covariant derivative $\widetilde{\nabla}$ which is compatible with the Clifford product, i.e.

$$\widetilde{\nabla}(MN) = \widetilde{\nabla}(M)N + M\widetilde{\nabla}(N) \quad \forall M, N \in \Gamma(\mathcal{CT}(D))$$

For the purpose of this application, we deal with $n = 3$ for color images.

From I, we derive the section S defined by

$$S = I + \left[\left(\frac{e_1}{\sqrt{g_1}} + \frac{e_2}{\sqrt{g_2}} + \frac{e_3}{\sqrt{g_3}} \right) \wedge I \right] B$$

where B is a bivector-valued section coding the current hue.

Then, differentiating S with $\widetilde{\nabla}$ leads to a 1-form with values in the Clifford bundle, i.e $\widetilde{\nabla}(S) \in \Gamma(T^*D \otimes \mathcal{CT}_1(D))$. It may be written as

$$\widetilde{\nabla}(S) = \widetilde{\nabla}(S)_0 + \widetilde{\nabla}(S)_1 + \widetilde{\nabla}(S)_2$$

where $\widetilde{\nabla}(S)_j$ is an element of $\Gamma(T^*D \otimes \mathcal{CT}_1(D))$ of degree j. Each of them codes a particular information. From the scalar and bivector parts, we construct metrics h_i generating Clifford bundles $(\mathcal{CT}_i(D), \pi_i, D)$ over D.
At last, by mapping the vector part into each one of the bundles $(T^*D \otimes \mathcal{CT}_i(D), p_i, D)$ where p_i denotes the projection maps, we can measure the variations of I with respect to the metrics h_i. In this way we obtain edge detections of Fig. 1.4.

Appendix. Tensor product of $\mathcal{CT}(D)$-valued 1-forms

We state more precisely in this Appendix how the tensor product of $\mathcal{C}T(D)$-valued 1-forms and the symmetric product used in particular in Proposition 1.2 are defined. Let $(\mathcal{C}T(D), D, \pi)$ be the fiber bundle introduced in Section 1.3.2. We denote $\mathcal{A}$ the ring of $\mathbb{R}$-valued functions defined on D and $\mathcal{B}$ the ring $\Gamma(\mathcal{CT}(D))$ of sections of $\mathcal{CT}(D)$.

Proposition 1.3 *The couple*

$$(\Gamma_1, \varphi) := (\Gamma(T^*D \otimes_{\mathcal{A}} T^*D \otimes_{\mathcal{A}} \mathcal{CT}(D)), \varphi)$$

is a solution of the universal problem defining the tensor product of the $\mathcal{B}$-bimodule

$$\Gamma_0 := \Gamma(T^*D \otimes_{\mathcal{A}} \mathcal{CT}(D))$$

with itself, where φ is the application from $\Gamma_0 \times \Gamma_0$ to Γ_1 defined by

$$((\omega_1 \otimes m_1), (\omega_2 \otimes m_2)) \longmapsto (\omega_1 \otimes \omega_2) \otimes (m_1 m_2)$$

Proof. Since $\mathcal{B}$ a $\mathcal{A}$-algebra, there exists a $\mathcal{B}$-bimodule structure on Γ_0

$$\begin{array}{cc} \mathcal{B} \times \Gamma_0 \longrightarrow \Gamma_0 & \Gamma_0 \times \mathcal{B} \longrightarrow \Gamma_0 \\ (b, X \otimes c) \longmapsto X \otimes bc & (X \otimes c, b) \longmapsto X \otimes cb \end{array}$$

We consider the following universel problem :

We search a couple

$$(\Gamma_0 \otimes_{\mathcal{B}} \Gamma_0, \phi)$$

where $\Gamma_0 \otimes_{\mathcal{B}} \Gamma_0$ is a $\mathcal{B}$-bimodule and

$$\phi : \Gamma_0 \times \Gamma_0 \longrightarrow \Gamma_0 \otimes_{\mathcal{B}} \Gamma_0$$

is left $\mathcal{B}$-linear in the first variable and right $\mathcal{B}$-linear in the second variable with

$$\phi(xf, y) = \phi(x, fy)$$

for all x and y in Γ_0 and f in $\mathcal{B}$ such that :

For each $\mathcal{B}$-bimodule N and each map

$$\eta : \Gamma_0 \times \Gamma_0 \longrightarrow N$$

which is left $\mathcal{B}$-linear in the first variable and right $\mathcal{B}$-linear in the second variable and satisfies

$$\eta(xf, y) = \eta(x, fy)$$

for all x and y in Γ_0 and f in $\mathcal{B}$, there exists a unique homomorphism

$$\gamma : \Gamma_0 \otimes_{\mathcal{B}} \Gamma_0 \longrightarrow N$$

of $\mathcal{B}$-bimodule such that :

$$\eta = \gamma \circ \phi$$

The solution is unique up to isomorphisms. A construction may be found in [11].

As above we can show that Γ_1 has a $\mathcal{B}$-bimodule structure. It is a fact that φ is bilinear with respect to the left-module structure in the first variable and the right-module structure in the second variable and satisfies

$$\varphi(xf, y) = \varphi(x, fy)$$

for all x and y in Γ_0 and f in $\mathcal{B}$. So there exists a unique $\mathcal{B}$-bimodule homomorphism γ from $\Gamma_0 \otimes_{\mathcal{B}} \Gamma_0$ to Γ_1 such that

$$\varphi = \gamma \circ \phi$$

Now γ is defined by

$$\gamma : (\omega_1 \otimes m_1) \otimes (\omega_2 \otimes m_2) \longmapsto (\omega_1 \otimes \omega_2) \otimes m_1 m_2$$

The map δ from Γ_1 to $\Gamma_0 \otimes_{\mathcal{B}} \Gamma_0$ that sends $(\omega_1 \otimes \omega_2 \otimes m)$ to $(\omega_1 \otimes m) \otimes (\omega_2 \otimes 1)$ is a $\mathcal{B}$-bimodule homomorphism and is the inverse of γ.

Finally (Γ_1, φ) is a solution to our universal problem. □

From the preceding proposition, $\Gamma_0 \otimes_{\mathcal{B}} \Gamma_0$ is isomorphic to the space of $\mathcal{CT}(D)$-valued rank 2 tensors. If η_1 and η_2 belong to $\Gamma(T^*D)$ and s_1 and s_2 belong to $\mathcal{B}$ then $(\eta_1 \otimes s_1) \otimes (\eta_2 \otimes s_2)$ may be identified with the $\mathcal{CT}(D)$-valued rank 2 tensor that maps $(X \otimes Y)$ to $\eta_1(X)\eta_2(Y)s_1s_2$.

We denote

$$(\eta_1 \otimes s_1)(\eta_2 \otimes s_2) = (\eta_1\eta_2) \otimes (s_1s_2)$$

the symmetric product of $(\eta_1 \otimes s_1)$ and $(\eta_2 \otimes s_2)$. We extend it by linearity. This symmetric product can be identified with the $\mathcal{CT}(D)$-valued symmetric tensor of rank 2 defined by

$$(X \otimes Y) \longmapsto \frac{1}{2}(\eta_1(X)\eta_2(Y) + \eta_2(X)\eta_1(Y))s_1s_2$$

Finally we denote $(\eta_1 \otimes s_1) \underline{\otimes} (\eta_2 \otimes s_2)$ the element $(\eta_1 \otimes s_1) \otimes (\eta_2 \otimes s_2)$ of $\Gamma_0 \otimes_{\mathcal{B}} \Gamma_0$ to emphasize the fact that the tensor product is relative to $\mathcal{B}$.

2 Clifford algebras bundles to multidimensional image segmentation

Cette Section a fait l'objet d'une publication en collaboration avec Michel Berthier [4].

2.1 Introduction

Clifford (Kähler-Atiyah [43]) algebras are widely used in computer sciences for several reasons (see [75] for examples of applications). In this paper, we will take advantage of the following two facts :

1. As it is well known, Clifford algebras provide a particulary efficient framework to make computations without coordinates [47]. We use in the sequel inner, wedge and geometric products as well as the related geometric interpretations of these operations. More precisely, the acquisition space of the image, i.e. the space where the image gets its values, is embedded into a Clifford algebra. We measure the local variations of the values of the pixels, seen as integer coordinates points of the domain D of the image, using geometric information and transformations. We get in this way the metric data of the image surface needed for the edge detection. It appears to be an asset that we can take into account variations of the metric by introducing Clifford bundles.
2. A Clifford algebra contains elements of different degrees (scalar, vectors, bivectors, ..., pseudoscalar). This allows to combine information of different nature in a single multivector to have a global and concise treatment of the used data. For example, when computing the covariant derivative $\nabla_1(S)$, for S a section of a Clifford bundle over D, we obtain a 1-form on D that may be decomposed as a sum of 1-forms with values in the parts of degree k, for $k = 1, \cdots, n$, of the total space of the bundle, each part coding a particular information.

The aim of the paper is to generalize a method of edge detection based on the definition of an image as 2-dimensional surface, in the Clifford bundles framework. As we will see in Section 2.2.1, edges detected by such a method depend completely on the first fundamental form of the surface, i.e the metric induced by the metric of the ambient space. Let us cite some works where images are defined as surfaces with the metric of the ambient space varying with the point. [3] and [56] both propose application to color edge detection. The first deals with hyperbolic coordinates and a corresponding metric, whereas we deal in the second with luminance, saturation and hue components (see Section 2.2.2). In [56], edge detection arises from a diffusion process whereas in [3], edge detection arises from a local definition of edges [71]. Note that in [3], we already proposed to detect only specific edges, and to construct first fundamental forms using Clifford bundles formalism with applications to color and color/infrared images. We also mentioned extensions to nD images, but did not propose there explicit methods.

All the applications we present in this paper follow the same schema : First, we consider appropriate connection ∇_1 and section S relative to a trivial Clifford bundle over D. A metric generating a new Clifford bundle over D is constructed using the parts of degree $\neq 1$ of $\nabla_1(S)$. Roughly speaking, this metric corresponds to the metric of the ambient

space of the surface. Then, a 1-form with values in this new bundle is built from the part of degree 1 of $\nabla_1(S)$. At last, by a tensor product over a well-chosen ring, we associate to this 1-form a symmetric tensor of rank 2 with values in the scalar part of the bundle. It measures variations of S with respect to the metric of the new bundle. Identifying the ring $\mathbb{R}$ and its injection into Clifford algebras, this tensor can be assimilated as the first fundamental form of a surface.

The paper is organized as follows. Section 2.2 is devoted to first, remind the method of edge detection on color images we propose to extend, then to give some basic results on color and color/infrared spaces when embedded into Clifford algebras. In Section 2.3, we detail the global framework we propose for nD image edge detection. It contains the construction of the trivial Clifford bundle wherein a multidimensional image is represented as a section and the construction of a connection compatible with the Clifford product. Moreover, we develop a general method to construct first fundamental forms of 2-dimensional surfaces from the information given by $\nabla_1(S)$. In Section 2.4, we apply the method of Section 2.3 to color and color/infrared images. We present several illustrations due to particular choices of the connection ∇_1 and the section S.

2.2 Preliminaries

2.2.1 Multidimensional image edge detection using metrics of surfaces

A usual method of edge detection on color images is to consider a color image, of components (r, g, b) (see Section 2.2.2) defined on a subset D of $\mathbb{R}^2$ as a 2-dimensional surface S parametrized by

$$\varphi : (x, y) \longmapsto (x, y, r(x, y), g(x, y), b(x, y))$$

embedded into $(\mathbb{R}^5, \| \ \|_2)$. The euclidean metric of the embedding space $\mathbb{R}^5$ induces a metric on S called the first fundamental form of S, which takes the following form

$$dS^2 := dx^2 + dy^2 + dr^2 + dg^2 + db^2 \tag{2.1}$$

Then, color variations on the image are assimilated to tangent vectors of S and a measure of these variations is given by dS^2. The rest of the method is devoted to select the strongest local variations, called edges.
More precisely, let $I(q)$ be the matrix representation of the metric dS^2 at $q = \varphi(p)$ in the coordinates system given by $(d_p\varphi(1, 0), d_p\varphi(0, 1))$. Let $\theta_+(q)$ and $\theta_-(q)$, $\theta_+(q) \geqslant \theta_-(q)$, be the two eigenvalues of $I(q)$ and $\Theta_+(q)$, $\Theta_-(q)$ the corresponding eigenvectors. The edge measure is then given by

$$\varpi(q) = \sqrt{\theta_+(q) - \theta_-(q)} \tag{2.2}$$

and we say that $p \in D$ is an edge point if the function ϖ has a local maximum at $\varphi(p)$ in the direction given by $\Theta_+(\varphi(p))$.

We propose to generalize this method in two-folds. First, by considering images of higher dimension, that are represented in this context by 2-dimensional surfaces embedded in higher dimensional spaces. For example, a color/infrared image is represented by a

2-dimensional surface embedded into $\mathbb{R}^6$. Secondly, by considering embedding spaces equipped with metrics varying with the point, so that to detect only specific edges on the image.

2.2.2 Color and color/infrared spaces as subsets of Clifford algebras

There are many ways to represent the set of colors i.e. there are many color spaces. The standard color space, based on the physical properties of the human vision is RGB (red, green, blue). Each color is identified by its red, green and blue levels, which are generally encoded by integers from 0 to 255. The RGB space is geometrically represented by a cube.

In the seminal papers [33] and [68], Sangwine & al. propose to embed RGB into the space of imaginary quaternions $\mathbb{H}_0$ by

$$(r, g, b) \longmapsto ri + gj + bk$$

so that to compute geometric transformations on colors, as rotations, using only the addition and product laws of the algebra of quaternions $\mathbb{H}$. As a consequence, applying such transformations on some pixels of a color image, seen as a $\mathbb{H}$-valued function

$$\begin{array}{rccc} & D & \longrightarrow & \mathbb{H} \\ f: & (x,y) & \longmapsto & r(x,y)i + g(x,y)j + b(x,y)k \end{array}$$

the authors define new kinds of color image segmentation, as chrominance (see later) edge detection.

Such results may be recovered by embedding RGB into the vector part of the Clifford algebra $Cl(\mathbb{R}^3, Q)$ associated to $\mathbb{R}^3$ equipped with an euclidean quadratic form Q.

$$(r, g, b) \longmapsto re_1 + ge_2 + be_3$$

Using this last framework presents two assets comparing to quaternions. First, as $Cl(\mathbb{R}^3, Q)$ is of dimension 8 and $\mathbb{H}$ is of dimension 4, the former may carry more information about colors. Moreover, as one can associate a Clifford algebra to a vector space of any dimension, it is possible to deal with nD images : The acquisition space of a nD image is embedded, as before, into the vector part of $Cl(\mathbb{R}^n, Q)$ where Q is an euclidean quadratic form. In particular, for color/infrared images, we embed $RGBT$ into $Cl(\mathbb{R}^4, Q)$, where T stands for temperature, by the following map

$$(r, g, b, t) \longmapsto re_1 + ge_2 + be_3 + te_4$$

There exist other color spaces based on the perceptual properties of the human vision and parametrized by luminance (or intensity), saturation and hue. Let us mention the HSL color spaces represented by a double cone. Such color spaces are called perceptual since effects of variations of each one of the components can be interpreted. In particular, the hue corresponds to the usual notion of color, i.e. we distinguish red, yellow, green, blue, purple...hues. We refer to [34] for more details.

Beside RGB color space we consider the HSL color space defined as follows. We set first

$$\begin{pmatrix} Y \\ C_1 \\ C_2 \end{pmatrix} = \begin{pmatrix} 1/3 & 1/3 & 1/3 \\ 1 & -1/2 & -1/2 \\ 0 & -\sqrt{3}/2 & \sqrt{3}/2 \end{pmatrix} \begin{pmatrix} r \\ g \\ b \end{pmatrix}$$

Then the luminance l, the saturation s and the hue h are respectively given by

$$l = Y$$

$$s = \sqrt{C_1^2 + C_2^2}$$

$$h = \begin{cases} \arccos(C_2/s) & \text{if } C_2 > 0 \\ 2\pi - \arccos(C_2/s) & \text{otherwise} \end{cases}$$

Note that the hue is an angular information. At the end of this part, we will see another representation of hues.

We can compute h from r, g and b in the setting of the Clifford algebra $\mathbb{R}_{3,0}$ as follows. Let $a = r(a)e_1 + g(a)e_2 + b(a)e_3 \in \mathbb{R}_{3,0}$ be a color, and let $h(a)$ denote its hue. The vector a may be decomposed into its projection on the achromatic axis, generated by the unit vector $(e_1 + e_2 + e_3)/3$ and its rejection $v(a)$, which corresponds obviously to the projection on the plane generated by the dual of $(e_1 + e_2 + e_3)/3$, called the chrominance plane. The vector $v(a)$ is called the chrominance vector of the color a. Simple computations show that

$$h(a) = 2\pi + \operatorname{sign}(g(a) - b(a)) \arccos\left(\frac{v(a)}{\|v(a)\|} \cdot \rho(a)\right)$$

with $\rho(a)$ the unit chrominance vector corresponding to colors colinear to e_1 and $h(a)$ defined modulo 2π. In other words, $h(a)$ is the oriented angle from $\rho(a)$ to $v(a)$. To conclude this part, let us explain how to define the hue using bivectors.

Proposition 2.1 *Let T be the set of bivectors*

$$T = \{(e_1 + e_2 + e_3) \wedge \alpha,\ \alpha \in RGB\}$$

with the following equivalence relation :

$$B \simeq C \iff B = \lambda C \quad \text{for } \lambda > 0$$

Then, there is a bijection between $T/\simeq$ and the set of hues.

Proof. We have

$$(e_1 + e_2 + e_3) \wedge \alpha = (e_1 + e_2 + e_3)v_\alpha$$

where v_α is the projection of α on the chrominance. Then, there is a bijection between $T/\simeq$ and the set $(e_1 + e_2 + e_3)\, v$ for v a unit vector in the chrominance plane. This latter being in bijection with the set of different hues, we conclude that there exists a bijection between $T/\simeq$ and the set of hues. □

As complementary hues are given by opposite chrominance axis, they generate opposite bivectors.

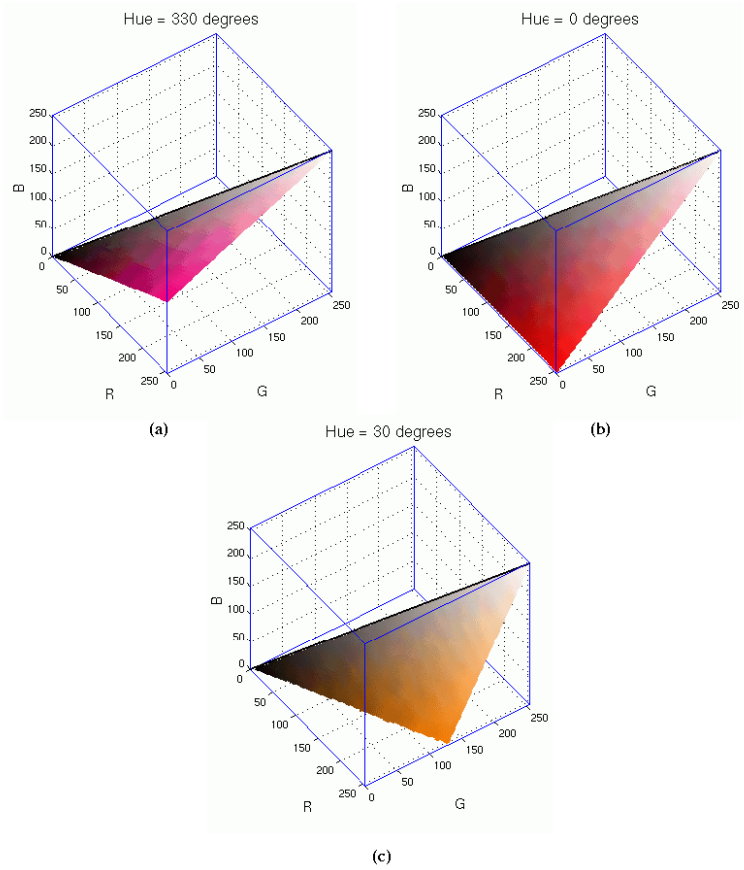

FIGURE 2.1 – (a) colors of hue 330°- (b) colors of hue 0° - (c) colors of hue 30°

Fig. 2.1 [1] shows the representation of the set of colors having the same hue in RGB color space, for $h = 330°, 0°, 30°$.

2.3 A general method to multidimensional image edge detection

2.3.1 A family $\mathcal{G} = \{\mathcal{G}_n, n \in \mathbb{N}\}$ of Clifford bundles

The aim of this subsection is to describe the family of Clifford bundles we consider to perform the edge detection. As before D denotes the domain of the image. To each point $p \in D$, we associate a vector space E_p of dimension n endowed with a definite positive quadratic form $g(p)$ such that in the basis $(e_1(p), e_2(p), \ldots, e_n(p))$ of E_p, $g(p)$

1. This picture was found at the address `http://www.linuxtopia.org/online_books/graphics_tools/gimp_advanced_guide/`

takes the following form

$$g(p) = \begin{pmatrix} g_1(p) & 0 & 0 & \cdots\cdots & 0 \\ 0 & g_2(p) & 0 & \cdots\cdots & 0 \\ 0 & 0 & \ddots & & \vdots \\ \vdots & \vdots & & \ddots & \vdots \\ 0 & 0 & \cdots\cdots & 0 & g_n(p) \end{pmatrix}$$

Let E be the disjoint union of E_p for p in D, and $\pi : E \to D$ that maps $v \in E_p$ to p. We construct a trivial Riemannian vector bundle of rank n (E, π, D) as follows. Let φ be the bijection

$$\begin{array}{lcl} D \times (\mathbb{R}^n, \| \, \|_2) & \longrightarrow & E \\ \Big(p \ , (u_1, u_2, \cdots, u_n)\Big) & \longmapsto & u_1 \dfrac{e_1(p)}{\sqrt{g_1(p)}} + u_2 \dfrac{e_2(p)}{\sqrt{g_2(p)}} + \ldots + u_n \dfrac{e_n(p)}{\sqrt{g_n(p)}} \end{array}$$

where for a fixed p, $\varphi : (\mathbb{R}^n, \| \, \|_2) \to E_p$ is an isometry from the euclidean space $\mathbb{R}^n$ to E_p. We define a topology on E by stating that $U \in E$ is open iff $\varphi^{-1}(U)$ is open in $D \times (\mathbb{R}^n, \| \, \|_2)$. This topology makes φ an homeomorphism and E a manifold with φ^{-1} as global chart. Consequently, φ is a diffeomorphism and therefore (E, π, D) is a trivial Riemannian vector bundle of rank n having φ as global trivialization. We denote $\mathcal{F}_n$ the family of bundles (E, π, D) of rank n obtained in this way.

In the trivialization φ, any section S can be written :

$$S(p) = s_1(p) \frac{e_1(p)}{\sqrt{g_1(p)}} + s_2(p) \frac{e_2(p)}{\sqrt{g_2(p)}} + \ldots + s_n(p) \frac{e_n(p)}{\sqrt{g_n(p)}}$$

Each fiber E_p endowed with the quadratic form $g(p)$ generates a Clifford algebra $Cl(E_p, g(p))$. In particular, the basis $(e_1(p), e_2(p), \ldots, e_n(p))$ of E_p generates a basis of $Cl(E_p, g(p))$:

$$\Big\{1(p), e_1(p), e_2(p), \ldots, e_n(p), e_1(p)e_2(p), \ldots, e_1(p)e_2(p) \ldots e_n(p)\Big\}$$

Let us denote $CT(D)$ the disjoint union of $Cl(E_p, g(p))$ for $p \in D$, and $\widetilde{\pi}$ that maps $v \in Cl(E_p, g(p))$ to p. Then, from (E, π, D), we construct a trivial Clifford bundle $(CT(D), \widetilde{\pi}, D)$ as follows. Let $\widetilde{\varphi}$ be the bijection

$$\begin{array}{lcl} D \times Cl(\mathbb{R}^n, \| \, \|_2) & \longrightarrow & CT(D) \\ \Big(p \ , (u_0, u_1, \cdots, u_{2^n-1})\Big) & \longmapsto & u_0 \, 1(p) + u_1 \dfrac{e_1(p)}{\sqrt{g_1(p)}} + \cdots + u_{2^n-1} \dfrac{e_1(p) \ldots e_n(p)}{\sqrt{g_1(p) \ldots g_n(p)}} \end{array}$$

where for a fixed p, $\widetilde{\varphi} : Cl(\mathbb{R}^n, \| \, \|_2) \to Cl(E_p, g_p)$ is an algebra isomorphism. As previously done, we endow $CT(D)$ with a topology by stating that $U \in CT(D)$ is open iff $\widetilde{\varphi}^{-1}(U)$ is open in $D \times Cl(\mathbb{R}^n, \| \, \|_2)$. Then, the bijection $\widetilde{\varphi}$ is an homeomorphism, and $CT(D)$ is a manifold having $\widetilde{\varphi}^{-1}$ as global chart. Consequently, $\widetilde{\varphi}$ is a diffeomorphism.

We conclude that $(CT(D), \widetilde{\pi}, D)$ is a trivial Clifford bundle having $\widetilde{\varphi}$ as global trivialization. We denote $\mathcal{G}_n$ the family of those bundles $(CT(D), \widetilde{\pi}, D)$.

In the trivialization $\widetilde{\varphi}$, any section S may be written :

$$S(p) = s_0(p)\,1(p) + s_1(p)\frac{e_1(p)}{\sqrt{g_1(p)}} + \cdots + s_{2^n-1}(p)\frac{e_1(p)e_2(p)\ldots e_n(p)}{\sqrt{g_1(p)g_2(p)\ldots g_n(p)}}$$

Let us mention that $(CT(D), \widetilde{\pi}, D)$ is, in particular, a trivial vector bundle.

2.3.2 Algebra connection on $(CT(D), \widetilde{\pi}, D)$

In what follows, $\Gamma(H)$ denotes the space of C^k sections, $k \geqslant 1$, of a vector bundle of total space H. Let us recall that any connection ∇ on a trivial vector bundle (H, π_1, M) of rank n takes the form

$$\nabla = d + \omega \tag{2.3}$$

for some $\omega \in \Gamma(T^*M \otimes \mathrm{End}(H)) = \Gamma(T^*M) \otimes \mathrm{End}(\mathbb{R}^n)$ and d being the usual differentiation of functions. More precisely, let $f_1, f_2, \cdots, f_n$ be a basis of the fiber of (H, π_1, M), and Φ be a global trivialization. Then $(\Phi(., f_1), \Phi(., f_2), \cdots, \Phi(., f_n))$ defines a global frame, i.e. for each $p \in M$, $(\Phi(p, f_1), \Phi(p, f_2), \cdots, \Phi(p, f_n))$ is a basis of H_p.
Then, any section $u \in \Gamma(H)$ may be written

$$u = \sum_{i=1}^{n} u_i \Phi(., f_i)$$

and

$$\nabla u = \sum_{i=1}^{n} du_i\, \Phi(., f_i) + u_i\, \omega(\Phi(., f_i))$$

On a vector bundle $(E, \pi, D) \in \mathcal{F}_n$ of metric g, we denote ∇_0 the connection where $\omega \equiv 0$ in the trivialization φ. For $s \in \Gamma(E)$, we have therefore

$$\nabla_0(s) = \sum_{i=1}^{n} ds_i\, \frac{e_i}{\sqrt{g_i}}$$

Proposition 2.2 *Let $(CT(D), \widetilde{\pi}, D) \in \mathcal{G}_n$ generated by $(E, \pi, D) \in \mathcal{F}_n$. The connection ∇_0 induces an algebra connection on $(CT(D), \widetilde{\pi}, D)$, i.e. a connection $\widetilde{\nabla}_0$ satisfying*

$$\widetilde{\nabla}_0(MN) = \widetilde{\nabla}_0(M)N + M\widetilde{\nabla}_0(N)$$

for all M and N in $\Gamma(CT(D))$.

Proof. First, let us remark that ∇_0 is compatible with the fiber metric, i.e

$$d_X g(s, s') = g(\nabla_{0_X} s, s') + g(s, \nabla_{0_X} s')$$

for $s, s' \in \Gamma(E)$ and $X \in \Gamma(TD)$.

Indeed, in the global frame $\left(\frac{e_1}{\sqrt{g_1}}, \frac{e_2}{\sqrt{g_2}}, \ldots, \frac{e_n}{\sqrt{g_n}}\right)$ induced by φ, the metric g takes the form

$$g = \begin{pmatrix} 1 & 0 & 0 & \cdots\cdots & 0 \\ 0 & 1 & 0 & \cdots\cdots & 0 \\ 0 & 0 & \ddots & & \vdots \\ \vdots & \vdots & & \ddots & \vdots \\ 0 & 0 & \cdots\cdots & 0 & 1 \end{pmatrix}$$

Then, if $s = \sum_{i=1}^{n} s_i \frac{e_i}{\sqrt{g_i}}$ and $s' = \sum_{i=1}^{n} s'_i \frac{e_i}{\sqrt{g_i}}$, we have

$$d_X g(s, s') = \sum_{i=1}^{n} d_X s_i \, s'_i + s_i \, d_X s'_i$$

and

$$g(\nabla_{0_X} s, s') = \sum_{i=1}^{n} d_X s_i \, s'_i \qquad g(s, \nabla_{0_X} s') = \sum_{i=1}^{n} s_i \, d_X s'_i$$

Secondly, the condition for a connection ∇ on a vector bundle equipped with a metric to be compatible with the fiber metric is in fact a sufficient condition to construct an algebra connection on the induced Clifford bundle. Indeed, ∇ can be extended in a unique way to the corresponding tensor algebra bundle by linearity and Leibniz's rule, and stating that $\nabla(f) = df$ for $f \in C^k(M)$ where M is the base manifold. Then, the compatibility with the fiber metric ensures that ∇ preserves the ideal genenerated by $\Big(x \otimes x - g(x, x)\Big)$ [14]. Consequently, ∇ defines a connection on the quotient that preserves the product in the quotient algebra bundle which is a Clifford bundle. In our case, this means that ∇_0 induces a connection $\widetilde{\nabla}_0$ on $(CT(D), \widetilde{\pi}, D)$ that satisfies

$$\widetilde{\nabla}_{0_X}(MN) = \widetilde{\nabla}_{0_X}(M)N + M\widetilde{\nabla}_{0_X}(N)$$

for all M, N in $\Gamma(CT(D))$ and $X \in \Gamma(TD)$.

At last, from the fact that $\Gamma(T^*D \otimes CT(D))$ may be endowed with a $\Gamma(CT(D))$-bimodule structure by the two following maps

$$\begin{array}{ccc} \Gamma(CT_2(D)) \times \Gamma(T^*D \otimes CT_2(D)) & \longrightarrow & \Gamma(T^*D \otimes CT_2(D)) \\ (b \ , \xi \otimes c) & \longmapsto & \xi \otimes bc \end{array} \tag{2.4}$$

$$\begin{array}{ccc} \Gamma(T^*D \otimes CT_2(D)) \times \Gamma(CT_2(D)) & \longrightarrow & \Gamma(T^*D \otimes CT_2(D)) \\ (\xi \otimes c \ , b) & \longmapsto & \xi \otimes cb \end{array} \tag{2.5}$$

we have

$$\widetilde{\nabla}_0(MN) = \widetilde{\nabla}_0(M)N + M\widetilde{\nabla}_0(N) \qquad \square$$

Let us verify that the algebra connection $\widetilde{\nabla}_0$ we have defined on $(CT(D), \widetilde{\pi}, D)$ corresponds to the connection on $(CT(D), \widetilde{\pi}, D)$ with $\omega \equiv 0$. For this, we just need to verify

that

$$\widetilde{\nabla}_0\left(s_{i_1i_2\cdots i_k}\frac{e_{i_1}}{\sqrt{g_{i_1}}}\frac{e_{i_2}}{\sqrt{g_{i_2}}}\cdots\frac{e_{i_k}}{\sqrt{g_{i_k}}}\right)=d(s_{i_1i_2\cdots i_k})\left(\frac{e_{i_1}}{\sqrt{g_{i_1}}}\frac{e_{i_2}}{\sqrt{g_{i_2}}}\cdots\frac{e_{i_k}}{\sqrt{g_{i_k}}}\right)$$

By compatibility of $\widetilde{\nabla}_0$ with the Clifford product, the expression

$$\widetilde{\nabla}_0\left(s_{i_1i_2\cdots i_k}\frac{e_{i_1}}{\sqrt{g_{i_1}}}\frac{e_{i_2}}{\sqrt{g_{i_2}}}\cdots\frac{e_{i_k}}{\sqrt{g_{i_k}}}\right)$$

can be decomposed into

$$\widetilde{\nabla}_0\left(s_{i_1i_2\cdots i_k}\frac{e_{i_1}}{\sqrt{g_{i_1}}}\right)\left(\frac{e_{i_2}}{\sqrt{g_{i_2}}}\cdots\frac{e_{i_k}}{\sqrt{g_{i_k}}}\right)+\left(s_{i_1i_2\cdots i_k}\frac{e_{i_1}}{\sqrt{g_{i_1}}}\right)\widetilde{\nabla}_0\left(\frac{e_{i_2}}{\sqrt{g_{i_2}}}\cdots\frac{e_{i_k}}{\sqrt{g_{i_k}}}\right)$$

$$=\left(d(s_{i_1i_2\cdots i_k})\frac{e_{i_1}}{\sqrt{g_{i_1}}}+s_{i_1i_2\cdots i_k}\widetilde{\nabla}_0(\frac{e_{i_1}}{\sqrt{g_{i_1}}})\right)\left(\frac{e_{i_2}}{\sqrt{g_{i_2}}}\cdots\frac{e_{i_k}}{\sqrt{g_{i_k}}}\right)$$

$$=\left(d(s_{i_1i_2\cdots i_k})\frac{e_{i_1}}{\sqrt{g_{i_1}}}\right)\left(\frac{e_{i_2}}{\sqrt{g_{i_2}}}\cdots\frac{e_{i_k}}{\sqrt{g_{i_k}}}\right)$$

$$=d(s_{i_1i_2\cdots i_k})\left(\frac{e_{i_1}}{\sqrt{g_{i_1}}}\frac{e_{i_2}}{\sqrt{g_{i_2}}}\cdots\frac{e_{i_k}}{\sqrt{g_{i_k}}}\right)$$

Therefore, any connection ∇_1 on $(CT(D),\widetilde{\pi},D)$ may be written

$$\nabla_1=\widetilde{\nabla}_0+\omega \tag{2.6}$$

for some $\omega\in\Gamma(T^*D\otimes\mathrm{End}(CT(D)))=\Gamma(T^*D)\otimes\mathrm{End}(\mathbb{R}_{n,0})$.

As it is written in the Introduction, an image I is considered as a section of a bundle $(CT(D),\widetilde{\pi},D)\in\mathcal{G}_n$, where $n=3$ for color images, and $n=4$ for color/infrared images. Let I be a color/infrared image. Then, in the global frame induced by the global trivialization φ, we have

$$I(p)=r(p)\frac{e_1(p)}{\sqrt{g_1(p)}}+g(p)\frac{e_2(p)}{\sqrt{g_2(p)}}+b(p)\frac{e_3(p)}{\sqrt{g_3(p)}}+t(p)\frac{e_4(p)}{\sqrt{g_4(p)}}$$

where r,g,b,t are respectively red, green, blue and temperature components in the $RGBT$ color/infrared space.

2.3.3 Computing first fundamental forms from connections on Clifford bundles

This is the main part of the paper. We propose a general method to construct first fundamental forms of 2-dimensional surfaces representing nD images in the setting of Clifford algebras bundles. This is done in such a way that all the applications we present in this paper appear as particular cases, the embedding spaces being $\mathbb{R}^6$ for color/infrared images and $\mathbb{R}^5$ for color images.

Let $(E_1,\pi_1,D)\in\mathcal{F}_n$ of metric g, and (F_1,π_1,D) a subbundle[2] of rank m with global frame $(e_{j_1},e_{j_2},\ldots,e_{j_m})$. Following the construction of the previous part, (E_1,π_1,D)

2. The reason why to consider such subbundles will be clarified in Section 2.4 devoted to applications

generates a Clifford bundle $(CT_1(D), \widetilde{\pi}_1, D) \in \mathcal{G}_n$. Let ∇_1 and S be respectively a connection and a section of $(CT_1(D), \widetilde{\pi}_1, D)$. The 1-form $\nabla_1(S)$ defined on D with values in $CT_1(D)$ may be written

$$\nabla_1(S) = \langle \nabla_1(S) \rangle_0 + \langle \nabla_1(S) \rangle_1 + \langle \nabla_1(S) \rangle_2 + \cdots + \langle \nabla_1(S) \rangle_n$$

where $\langle \nabla_1(S) \rangle_k$ denotes the part of $\nabla_1(S)$ of degree k. Strictly speaking, $\langle \nabla_1(S) \rangle_k$ is a 1-form on D with values in the part of $CT_1(D)$ of degree k.

Next we construct a vector bundle $(E_2, \pi_2, D) \in \mathcal{F}_m$ (m is the rank of the subbundle F_1) whose metric h arises from the information given by all the parts of $\nabla_1(S)$ except the one of degree 1. Roughly speaking, this metric corresponds to the metric of the ambient space of the surface. Then using a vector bundle morphism and a tensor product over a well-chosen ring, the vector part of $\nabla_1(S)$ provides a way to measure variations of S with respect to the metric h, which corresponds to the metric of the surface induced by the metric of its ambient space, i.e. its first fundamental form.

We now detail the last part of the construction. Let us denote $(CT_2(D), \widetilde{\pi}_2, D)$ the Clifford bundle of $\mathcal{G}_m$ generated by (E_2, π_2, D). We define a vector bundle morphism ψ from (E_1, π_1, D) to (E_2, π_2, D) by

$$\psi(p)\left(\frac{e_i(p)}{\sqrt{g_i(p)}}\right) = \begin{cases} \dfrac{e_l(p)}{\sqrt{h_l(p)}} & \text{if} \quad e_i(p) = e_{j_l}(p) \in F_1(p) \\ \\ 0 & \text{otherwise} \end{cases}$$

This morphism induces a vector bundle morphism $\widetilde{\psi}$ from $(CT_1(D), \widetilde{\pi}_1, D)$ to $(CT_2(D), \widetilde{\pi}_2, D)$ defined by

$$\widetilde{\psi}(p)\left(\frac{e_{i_1}(p)e_{i_2}(p)\cdots e_{i_k}(p)}{\sqrt{g_{i_1}(p)g_{i_2}(p)\cdots g_{i_k}(p)}}\right) = \begin{cases} \dfrac{e_{\alpha_1}(p)e_{\alpha_2}(p)\cdots e_{\alpha_k}(p)}{\sqrt{h_{\alpha_1}(p)h_{\alpha_2}(p)\cdots h_{\alpha_k}(p)}} & \text{if} \quad \left| \begin{array}{l} e_{i_1}(p) = e_{j_{\alpha_1}}(p) \\ e_{i_2}(p) = e_{j_{\alpha_2}}(p) \\ \quad \vdots \\ e_{i_k}(p) = e_{j_{\alpha_k}}(p) \end{array} \right. \\ \\ 0 & \text{otherwise} \end{cases}$$

From $\widetilde{\psi}$, we construct a vector bundle morphism Ψ from $(T^*D \otimes CT_1(D), p_1, D)$ to $(T^*D \otimes CT_2(D), p_2, D)$ that maps

$$\eta(p) \otimes \frac{e_{i_1}(p)e_{i_2}(p)\cdots e_{i_k}(p)}{\sqrt{g_{i_1}(p)g_{i_2}(p)\cdots g_{i_k}(p)}}$$

to

$$\begin{cases} \eta(p) \otimes \dfrac{e_{\alpha_1}(p)e_{\alpha_2}(p)\cdots e_{\alpha_k}(p)}{\sqrt{h_{\alpha_1}(p)h_{\alpha_2}(p)\cdots h_{\alpha_k}(p)}} & \text{if} \quad \left| \begin{array}{l} e_{i_1}(p) = e_{j_{\alpha_1}}(p) \\ e_{i_2}(p) = e_{j_{\alpha_2}}(p) \\ \quad \vdots \\ e_{i_k}(p) = e_{j_{\alpha_k}}(p) \end{array} \right. \\ \\ 0 & \text{otherwise} \end{cases} \tag{2.7}$$

Let η_1 be the vector part of $\nabla_1(S)$. It is important to notice that for all the applications to be treated in Section 2.4, we may suppose that

$$\eta_1 = \sum_{i=1}^{n} \eta_{1i} \otimes \frac{e_i}{\sqrt{g_i}}$$

where for each i, the 1-form η_{1i} is exact, i.e. may be written as the differential df_i of $f_i \in C^k(D)$. We have therefore

$$\Psi(p)(\eta_1(p)) = \sum_{i=1}^{n} df_i(p) \otimes \psi(p) \left(\frac{e_i(p)}{\sqrt{g_i(p)}} \right) = \sum_{l=1}^{m} df_{j_l}(p) \otimes \left(\frac{e_l(p)}{\sqrt{h_l(p)}} \right)$$

Let η_2 be the section of $(T^*D \otimes CT_2(D), p_2, D)$ given by the set $\Psi(p)(\eta_1(p))$, for $p \in D$:

$$\eta_2 = \sum_{l=1}^{m} df_{j_l} \otimes \left(\frac{e_l}{\sqrt{h_l}} \right)$$

From η_2, we aim at constructing a symmetric tensor of rank 2 with values in $CT_2(D)$ that could be interpreted as the first fundamental form of a 2-dimensional surface embedded into $\mathbb{R}^{m+2}$ equipped with a Riemannian metric.

From the bimodule structure of $\Gamma(T^*D \otimes CT_2(D))$ over $\Gamma(CT_2(D))$ given by isomorphisms (2.4) and (2.5), we have

$$\sum_{l=1}^{m} \frac{1}{2} \left(\frac{e_l}{\sqrt{h_l}} \eta_2 + \eta_2 \frac{e_l}{\sqrt{h_l}} \right) e_l = \sum_{l=1}^{m} df_{j_l} \otimes e_l \tag{2.8}$$

If we denote $\mathcal{B}$ the ring $\Gamma(CT_2(D))$, then we may show that

$$\Gamma(T^*D \otimes CT_2(D)) \otimes_{\mathcal{B}} \Gamma(T^*D \otimes CT_2(D)) \simeq \Gamma(T^*D \otimes T^*D \otimes CT_2(D))$$

the isomorphism being given by the two following morphisms

$$\gamma \colon (\omega_1 \otimes s_1) \otimes (\omega_2 \otimes s_2) \longmapsto (\omega_1 \otimes \omega_2) \otimes s_1 s_2$$

$$\delta \colon (\omega_1 \otimes \omega_2 \otimes s) \longmapsto (\omega_1 \otimes s) \otimes (\omega_2 \otimes 1)$$

From this tensor product, we define a symmetrized tensor product by

$$(\omega_1 \otimes s_1)(\omega_2 \otimes s_2) := \frac{1}{2} \Big[(\omega_1 \otimes s_1) \otimes (\omega_2 \otimes s_2) + (\omega_2 \otimes s_1) \otimes (\omega_1 \otimes s_2) \Big]$$

Applying this latter to (2.8) with itself gives

$$\left(\sum_{l=1}^{m} df_{j_l} \otimes e_l \right) \left(\sum_{l=1}^{m} df_{j_l} \otimes e_l \right) = \sum_{l=1}^{m} (df_{j_l})^2 \otimes h_l \tag{2.9}$$

Then we can consider the following $CT_2(D)$-valued symmetric tensor of rank 2

$$dx^2 \otimes 1 + dy^2 \otimes 1 + (df_{j_1})^2 \otimes h_1 + (df_{j_2})^2 \otimes h_2 + \cdots + (df_{j_m})^2 \otimes h_m$$

Identifying $\mathbb{R}$ and its injection into each fiber, this $CT_2(D)$-valued tensor may be viewed as the first fundamental form of the surface S parametrized by

$$\varphi\colon (x,y) \longmapsto (x, y, f_{j_1}(x,y), f_{j_2}(x,y), \cdots, f_{j_m}(x,y))$$

embedded into $\mathbb{R}^{m+2}$ equipped with the metric

$$\begin{pmatrix} 1 & 0 \\ 0 & 1 \end{pmatrix} \oplus \begin{pmatrix} h_1 & 0 & 0 & \cdots\cdots & 0 \\ 0 & h_2 & 0 & \cdots\cdots & 0 \\ 0 & 0 & \ddots & & \vdots \\ \vdots & \vdots & & \ddots & \vdots \\ 0 & 0 & \cdots\cdots & 0 & h_m \end{pmatrix}$$

Indeed, the first fundamental form of S is the symmetric tensor of rank 2

$$dS^2 = dx^2 + dy^2 + h_1(df_{j_1})^2 + h_2(df_{j_2})^2 + \cdots + h_m(df_{j_m})^2$$

2.4 Applications

The aim of this part is to show that by the choices of the vector subspaces $F_1(p)$ (of dimension m), the 1-form ω and the section we derive with the connection $\nabla_1 = \widetilde{\nabla}_0 + \omega$, we may perform several kinds of edge detection.

Let us remark that the vector spaces $E_1(p)$ (of dimension n) are fixed in the sense that they are acquisition spaces of the images. Moreover, we have seen that the first fundamental form we construct is independant of the metric g of (E_1, π_1, D).

In what follows, we denote by $\|\ \|$ the function mapping a blade x to $\sqrt{x\,t(x)}$, where t is the main anti-automorphism of the corresponding Clifford algebra.

2.4.1 The usual color edge detection : n=3

In this part, we show that we may obtain the metric (2.1) of the usual method of color edge detection following the Clifford bundles framework described above. However, in this very particular case, the general method of the previous section may be simplified to compute (2.1) since this one does not depend on any information on the image that needs to be computed.

Let $(E_1, \pi_1, D) \in \mathcal{F}_3$ of metric

$$g := \begin{pmatrix} 1 & 0 & 0 \\ 0 & 1 & 0 \\ 0 & 0 & 1 \end{pmatrix}$$

Let I be the considered color image, seen as a section of the Clifford bundle $(CT_1(D), \widetilde{\pi}_1, D)$ generated by (E_1, π_1, D), i.e.

$$I(p) = r(p)\, e_1(p) + g(p)\, e_2(p) + b(p)\, e_3(p)$$

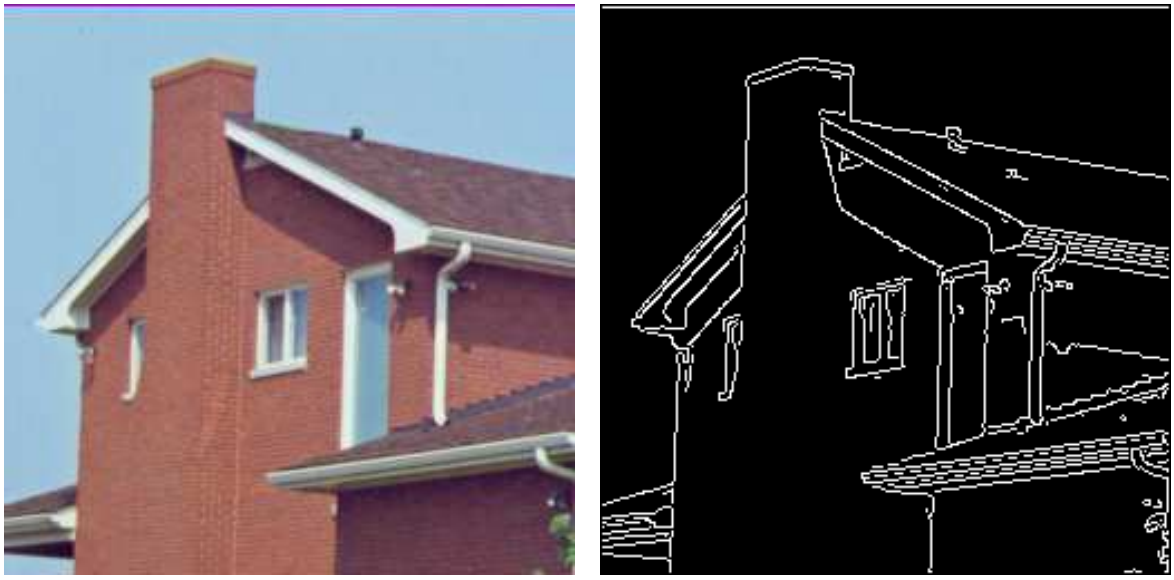

(a) (b)

FIGURE 2.2 – a. original image b. Color edge detection

where $e_1(p)^2 = e_2(p)^2 = e_3(p)^2 = 1$.

Let ∇_1 be the connection on $(CT_1(D), \widetilde{\pi}_1, D)$ defined by $\nabla_1 = \widetilde{\nabla}_0$. In other words, we choose $\omega \equiv 0$. Then,

$$\nabla_1(I) = dr \otimes e_1 + dg \otimes e_2 + db \otimes e_3$$

We apply (2.9) to $\nabla_1(I)$ to get the following $CT_1(D)$-valued symmetric tensor of rank 2

$$dr^2 \otimes 1 + dg^2 \otimes 1 + db^2 \otimes 1$$

At last, we have only to remark that

$$dx^2 \otimes 1 + dy^2 \otimes 1 + dr^2 \otimes 1 + dg^2 \otimes 1 + db^2 \otimes 1$$

may indeed be viewed as the first fundamental form of the surface parametrized by

$$\varphi\colon (x, y) \longmapsto (x, y, r(x, y), g(x, y), b(x, y))$$

embedded into $(\mathbb{R}^5, \| \|_2)$.

Fig. 2.2 shows the result of such an edge detection. We see that it consists in detecting the strongest color variations of the image.

2.4.2 Color edge detection with respect to a given hue : n=3, m=3

The aim of this application is to detect edges on a color image without taking into account those located in a region of hue similar to a given hue h_0.

Let us first mention how to proceed with the method based on a surfacic approach. We consider a color image as a 2-dimensional surface S parametrized by

$$\varphi\colon (x,y) \longmapsto (x,y,r(x,y),g(x,y),b(x,y))$$

embedded into $\mathbb{R}^5$ equipped with the metric

$$g := \begin{pmatrix} 1 & 0 \\ 0 & 1 \end{pmatrix} \oplus \begin{pmatrix} \lambda & 0 & 0 \\ 0 & \lambda & 0 \\ 0 & 0 & \lambda \end{pmatrix}$$

where we define λ as follows. We consider the domain

$$\Omega(p) = \{(x,y),\ \|(x,y)-p\|_\infty \leqslant 1\}$$

We set

$$\lambda(p) = 1 \qquad \text{if} \quad \max_{(x,y)\in\Omega(p)} d\Big(h_0, h[r(x,y),g(x,y),b(x,y)]\Big) > d_0 \tag{2.10}$$

where d_0 is a threshold that determines if there is similarity or not, and d is the angular distance on S^1. Then, we extend λ into a derivable strictly positive function on $[0,\pi]$ such that λ is negligible on $[0, d_0-\epsilon]$, where $\epsilon << 1$ is fixed, the aim being to not take into account color variations in the domain of similarity $\overline{B}(h_0,d_0)$ of the hue h_0. Then, from the first fundamental form of S :

$$dS^2 = dx^2 + dy^2 + \lambda dr^2 + \lambda dg^2 + \lambda db^2$$

we derive the "edge detector" of Section 2.2.1.

Let us now explain how to construct such a metric in the Clifford bundles framework. We take $(F_1,\pi_1,D) = (E_1,\pi_1,D) \in \mathcal{F}_3$ as subbundle of (E_1,π_1,D). Let I be the section of $(CT_1(D),\widetilde{\pi}_1,D)$ representing the considered color image, i.e.

$$I(p) = r(p)\frac{e_1(p)}{\sqrt{g_1(p)}} + g(p)\frac{e_2(p)}{\sqrt{g_2(p)}} + b(p)\frac{e_3(p)}{\sqrt{g_3(p)}}$$

For each $p \in D$, we denote $A(p)$ the endomorphism

$$A(p)(x) = \begin{cases} \left[\left(\dfrac{e_1(p)}{\sqrt{g_1(p)}} + \dfrac{e_2(p)}{\sqrt{g_2(p)}} + \dfrac{e_3(p)}{\sqrt{g_3(p)}}\right) \wedge x\right] B(p) & \text{if } x \text{ is a vector} \\ 0 & \text{otherwise} \end{cases}$$

where $B(p)$ is the bivector

$$B(p) = \left(\frac{e_1(p)}{\sqrt{g_1(p)}} + \frac{e_2(p)}{\sqrt{g_2(p)}} + \frac{e_3(p)}{\sqrt{g_3(p)}}\right) \wedge \mu(p)$$

and

$$\mu(p) = \mu_1\frac{e_1(p)}{\sqrt{g_1(p)}} + \mu_2\frac{e_2(p)}{\sqrt{g_2(p)}} + \mu_3\frac{e_3(p)}{\sqrt{g_3(p)}}$$

is a vector of hue h_0. Remark that $A(p)$ makes the geometric product between a representant of the current hue and a representant of the hue h_0.

Let ∇_1 be the connection on $(CT_1(D), \widetilde{\pi}_1, D)$ defined by

$$\nabla_1 = \widetilde{\nabla}_0 + (dx + dy) \otimes A$$

Then,

$$\nabla_1(I) = \widetilde{\nabla}_0(I) + (dx + dy) \otimes \left[\left(\frac{e_1}{\sqrt{g_1}} + \frac{e_2}{\sqrt{g_2}} + \frac{e_3}{\sqrt{g_3}} \right) \wedge I \right] B$$

We see that the vector part, the scalar part and the bivector part of $\nabla_1(I)$ are respectively given by

$$\widetilde{\nabla}_0(I)$$

$$(dx + dy) \otimes \left[\left(\frac{e_1}{\sqrt{g_1}} + \frac{e_2}{\sqrt{g_2}} + \frac{e_3}{\sqrt{g_3}} \right) \wedge I \right] \cdot B$$

$$(dx + dy) \otimes \left[\left(\frac{e_1}{\sqrt{g_1}} + \frac{e_2}{\sqrt{g_2}} + \frac{e_3}{\sqrt{g_3}} \right) \wedge I \right] \times B$$

Denoting by $\Delta(h)$ the function measuring for each p the hue difference between $I(p)$ and μ, we have the following result :

Proposition 2.3 *Let X be the constant vector field on D of coordinates $(1, 0)$, then*

$$|tan(\Delta(h))| = \frac{\left\| \langle \nabla_{1_X}(I) \rangle_2 \right\|}{\left| \langle \nabla_{1_X}(I) \rangle_0 \right|}$$

Proof. We have

$$\langle \nabla_{1_X}(I) \rangle_2 = \left[\left(\frac{e_1}{\sqrt{g_1}} + \frac{e_2}{\sqrt{g_2}} + \frac{e_3}{\sqrt{g_3}} \right) \wedge I \right] \times B$$

and

$$\langle \nabla_{1_X}(I) \rangle_0 = \left[\left(\frac{e_1}{\sqrt{g_1}} + \frac{e_2}{\sqrt{g_2}} + \frac{e_3}{\sqrt{g_3}} \right) \wedge I \right] \cdot B$$

The proof is trivial once the expression of

$$\left[\left(\frac{e_1}{\sqrt{g_1}} + \frac{e_2}{\sqrt{g_2}} + \frac{e_3}{\sqrt{g_3}} \right) \wedge I \right] B$$

is simplified.
For this, we orthogonalize each one of the two bivectors (strictly speaking, they are bivector-valued sections). Let us treat the example of B. We have

$$B = \left(\frac{e_1}{\sqrt{g_1}} + \frac{e_2}{\sqrt{g_2}} + \frac{e_3}{\sqrt{g_3}} \right) \wedge \left[\mu - k \left(\frac{e_1}{\sqrt{g_1}} + \frac{e_2}{\sqrt{g_2}} + \frac{e_3}{\sqrt{g_3}} \right) \right]$$

for any $k \in \mathbb{R}$. Then, we search k_0 such that

$$\left[\left(\mu_1 \frac{e_1}{\sqrt{g_1}} + \mu_2 \frac{e_2}{\sqrt{g_2}} + \mu_3 \frac{e_3}{\sqrt{g_3}} \right) - k_0 \left(\frac{e_1}{\sqrt{g_1}} + \frac{e_2}{\sqrt{g_2}} + \frac{e_3}{\sqrt{g_3}} \right) \right] \cdot \left(\frac{e_1}{\sqrt{g_1}} + \frac{e_2}{\sqrt{g_2}} + \frac{e_3}{\sqrt{g_3}} \right) = 0$$

A simple computation leads to

$$k_0 = \frac{\mu_1 + \mu_2 + \mu_3}{3}$$

Therefore, B may be written

$$\left(\frac{e_1}{\sqrt{g_1}} + \frac{e_2}{\sqrt{g_2}} + \frac{e_3}{\sqrt{g_3}}\right)\tilde{\mu}$$

where $\tilde{\mu} =$

$$\left[\left(\mu_1 - \frac{\mu_1+\mu_2+\mu_3}{3}\right)\frac{e_1}{\sqrt{g_1}} + \left(\mu_2 - \frac{\mu_1+\mu_2+\mu_3}{3}\right)\frac{e_2}{\sqrt{g_2}} + \left(\mu_3 - \frac{\mu_1+\mu_2+\mu_3}{3}\right)\frac{e_3}{\sqrt{g_3}}\right]$$

We see that $\tilde{\mu}$ is in fact the chrominance vector v_μ of μ.
In the same way, we show that

$$\left(\frac{e_1}{\sqrt{g_1}} + \frac{e_2}{\sqrt{g_2}} + \frac{e_3}{\sqrt{g_3}}\right) \wedge I = \left(\frac{e_1}{\sqrt{g_1}} + \frac{e_2}{\sqrt{g_2}} + \frac{e_3}{\sqrt{g_3}}\right) P_{Ch}(I)$$

where P_{Ch} denotes the orthogonal projection on the chrominance plane.

Consequently,

$$\begin{aligned}\left[\left(\frac{e_1}{\sqrt{g_1}} + \frac{e_2}{\sqrt{g_2}} + \frac{e_3}{\sqrt{g_3}}\right) \wedge I\right] B &= \left(\frac{e_1}{\sqrt{g_1}} + \frac{e_2}{\sqrt{g_2}} + \frac{e_3}{\sqrt{g_3}}\right) P_{Ch}(I) \left(\frac{e_1}{\sqrt{g_1}} + \frac{e_2}{\sqrt{g_2}} + \frac{e_3}{\sqrt{g_3}}\right) v_\mu \\ &= -3\, P_{Ch}(I)\, v_\mu \end{aligned} \tag{2.11}$$

At last, let us remark that the (non-oriented) angle between $P_{Ch}(I)$ and v_μ is in fact Δh. Then we have

$$\frac{\|\langle \nabla_{1_X} I\rangle_2\|}{|\langle \nabla_{1_X} I\rangle_0|} = \frac{\|\langle P_{Ch}(I)\, v_\mu\rangle_2\|}{|\langle P_{Ch}(I)\, v_\mu\rangle_0|} = \frac{\|P_{Ch}(I)\|\|v_\mu\||sin(\pm\Delta h)|}{\|P_{Ch}(I)\|\|v_\mu\||cos(\pm\Delta h)|} = |tan(\pm\Delta h)|$$

□

From the sign of the scalar part $-3\,[P_{Ch}(I)\cdot v_\mu]$ of $\nabla_{1_X} I$, we know if $\pm\Delta h$ is in $[-\pi/2, \pi/2]$ or not. Moreover, as the tangent map is odd, we have $|tan(\pm\Delta h)| = |tan(\Delta h)|$. Therefore, if the scalar part is negativ, we obtain

$$\Delta h = arctan(|tan(\pm\Delta h)|)$$

In a similar way, we may obtain Δh when the sign of the scalar part is positiv.

We construct the function λ mentioned above from Δh, just replacing (2.10) by

$$\lambda(p) = 1 \qquad \text{if} \quad \max_{(x,y)\in\Omega(p)} \Delta h(x,y) > d_0$$

Then, we apply the rest of the method described in Section 2.3.3, i.e. (F_1, π_1, D) generates a vector bundle (E_2, π_2, D) of rank 3 equipped with a metric h given by

$$h := \begin{pmatrix} \lambda & 0 & 0 \\ 0 & \lambda & 0 \\ 0 & 0 & \lambda \end{pmatrix}$$

(a) (b) (c)

FIGURE 2.3 – a. original image b. usual color edge detection c. color edge detection with respect to the magenta hue

and a Clifford bundle $(CT_2(D), \widetilde{\pi}_2, D)$. Then, we construct a 1-form η_2 with values in $CT_2(D)$

$$\eta_2 = dr \otimes \frac{e_1}{\sqrt{h_1}} + dg \otimes \frac{e_2}{\sqrt{h_2}} + db \otimes \frac{e_3}{\sqrt{h_3}}$$

from the 1-form

$$\nabla_1(I) = dr \otimes \frac{e_1}{\sqrt{g_1}} + dg \otimes \frac{e_2}{\sqrt{g_2}} + db \otimes \frac{e_3}{\sqrt{g_3}}$$

Applying formulas (2.8) and (2.9) to η_2, we get the symmetric tensor of rank 2

$$dx^2 \otimes 1 + dy^2 \otimes 1 + dr^2 \otimes \lambda + dg^2 \otimes \lambda + db^2 \otimes \lambda$$

which can be assimilated to the metric of S.

Fig. 2.3 shows an example of such an application. We aim at not detecting edges corresponding to the ornaments of the hat. The picture (c) is the result of the computations detailled above for $h_0 = \frac{5\pi}{3}$(the magenta hue) and $d_0 = 0.43$. We observe that almost all the color variations inside this region are not detected, and the frontier of the region is globally well-detected (in particular transitions with the background and with the hat). It is more difficult to detect transitions with the hair since their hue is close to the magenta hue.

2.4.3 Color edge classification : n=3, $\mathbf{m_i = 3}$

Let I be the section of $(CT_1(D), \widetilde{\pi}_1, D) \in \mathcal{G}_3$ representing a color image

$$I = r\frac{e_1}{\sqrt{g_1}} + g\frac{e_2}{\sqrt{g_2}} + b\frac{e_3}{\sqrt{g_3}}$$

Measure of variations with respect to a hue. We say that I is varying at a given point in the direction X with respect to the hue h_0 if its usual derivative in the direction X, $\widetilde{\nabla}_{0_X}(I)$, or in the direction $-X$, $-\widetilde{\nabla}_{0_X}(I)$ belongs to RGB and if the corresponding

hue is h_0. We aim at characterizing such vectors in the Clifford algebras (bundles) framework. Let B be a bivector-valued section coding the hue h_0.

First, we suppose that

$$[\widetilde{\nabla}_{0_X}(I)(p) \wedge B(p)]B(p)^{-1} = 0$$

i.e. $\widetilde{\nabla}_{0_X}(I)(p)$ belongs to the plane generated by $B(p)$. We distinguish four cases :

(a) Neither $\widetilde{\nabla}_{0_X}(I)(p)$ nor $-\widetilde{\nabla}_{0_X}(I)(p)$ belongs to RGB.
(b) $\widetilde{\nabla}_{0_X}(I)(p)$ or $-\widetilde{\nabla}_{0_X}(I)(p)$ is along the grey axis.
(c) $\widetilde{\nabla}_{0_X}(I)(p)$ or $-\widetilde{\nabla}_{0_X}(I)(p)$ belongs to RGB and the corresponding hue is the complementary of h_0.
(d) $\widetilde{\nabla}_{0_X}(I)(p)$ or $-\widetilde{\nabla}_{0_X}(I)(p)$ belongs to RGB and the corresponding hue is h_0.

The following result gives a necessary and sufficient condition for the case (d) to occur. We set by convention $\text{sign}(0) = \pm$. Let us denote

$$\Sigma_i = \left(\widetilde{\nabla}_{0_X}(I) \cdot \frac{e_i}{\sqrt{g_i}}\right)$$

for $i = 1, 2, 3$, and

$$\Sigma = \left[\left(\left(\frac{e_1}{\sqrt{g_1}} + \frac{e_2}{\sqrt{g_2}} + \frac{e_3}{\sqrt{g_3}}\right) \wedge \widetilde{\nabla}_{0_X}(I)\right) \cdot B\right]$$

Let also σ_i, for $i = 1, 2, 3$, and σ be defined by $\sigma_i = \text{sign}(\Sigma_i)$ and $\sigma = \text{sign}(\Sigma)$.

Proposition 2.4 *With the previous notations, I is varying at p in the direction X with respect to the hue h_0 if and only if the following conditions are fullfilled :*
(i) The derivative $\widetilde{\nabla}_{0_X}(I)(p)$ is not zero ;
(ii) $\sigma_1 = \sigma_2 = \sigma_3$;
(iii) Σ is not null and $-\sigma$ is equal to the sign of one of the non zero Σ_i.

Proof. Let us first remark that (i) ensures that one of the Σ_i is not zero. The second assertion means that one of two vectors $\widetilde{\nabla}_{0_X}(I)(p)$ or $-\widetilde{\nabla}_{0_X}(I)(p)$ belongs to RGB. As $\Sigma \neq 0$, the case (b) does not occur.
If $\widetilde{\nabla}_{0_X}(I)(p) \in RGB$, then the sign of one of the non zero Σ_i is $+$, and we know from (2.11) that σ is negative if and only if $h\left[\widetilde{\nabla}_{0_X}(I)(p)\right] = h_0$.
If $-\widetilde{\nabla}_{0_X}(I)(p) \in RGB$, then the sign of one of the non zero Σ_i is $-$, and the orthogonal projection of $\widetilde{\nabla}_{0_X}(I)(p)$ onto the chrominance plane (see (2.11)) belongs to the axis generated by the chrominance vector of the complementary hue of the hue of $-\widetilde{\nabla}_{0_X}(I)(p)$. Therefore σ is positive if and only if the hue of $-\widetilde{\nabla}_{0_X}(I)(p)$ is h_0. □

From this proposition we deduce the following corollary : I is varying at p in the direction X with respect to the *complementary* hue of h_0 if and only if the three conditions (i), (ii) and (iv) are fullfilled, where the condition (iv) is obtained by replacing $-\sigma$ by σ

in (iii).

We now suppose that $\widetilde{\nabla}_{0_X}(I)(p)$ does not necessary belong to the plane generated by $B(p)$. The derivative $\widetilde{\nabla}_{0_X}(I)(p)$ is said to be measurable with respect to h_0 if the conditions (i), (ii) and (iii) of the preceding propsition hold. Such a definition makes sense since we deduce from these relations that $\widetilde{\nabla}_{0_X}(I)(p)$ is varying with respect to a hue that is closer of h_0 than of its complementary. In the same way, we can say if $\widetilde{\nabla}_{0_X}(I)(p)$ is measurable with respect to the complementary of h_0 or not. We then measure this variation by the expression

$$\left\| \widetilde{\nabla}_{0_X}(I)(p) \cdot B(p)\, B(p)^{-1} \right\|$$

Application to shadows and highlights detection. The aim of this application is to analyse the nature of the edges of a color image in case of variation of the light. We refer to [40] and [41] for the corresponding classification in shadows, highlights and material edges. The segmentation we deduce from the general framework described before requires the hypothesis of white illumination and neutral interface reflection (see [40],[41]).

Let φ be the parametrization of the surface S representing a color image embedded into $(\mathbb{R}^5, \| \ \|_2)$. The analysis of edges we propose relies on the study of the derivative $\widetilde{\nabla}_{0_X}(I)$ where X is such that $d\varphi(X)$ is an eigenvector associated to the highest eigenvalue of the first fundamental form of S.

Before detailling the parameters of Section 2.3.3 we use for such an application, let us make the following crucial remark. Due to the nature of the objects we use to deal with an image (surfaces or fiber bundles), we only have to consider, in practice, points of D with integer coordinates. Therefore, there exists a certain freedom in the way to compute derivatives of functions defined on D. In particular, derivatives of the components red, green, blue and temperature at such points are given by discrete approximations (Sobel, Canny-Deriche, etc).

Let

$$B = \left(\frac{e_1}{\sqrt{g_1}} + \frac{e_2}{\sqrt{g_2}} + \frac{e_3}{\sqrt{g_3}} \right) \wedge \left(u_1 \frac{e_1}{\sqrt{g_1}} + u_2 \frac{e_2}{\sqrt{g_2}} + u_3 \frac{e_3}{\sqrt{g_3}} \right)$$

be a bivector-valued section of $(CT_1(D), \widetilde{\pi}_1, D)$ such that $h(u_1(p), u_2(p), u_3(p)) = h(I(p))$ and $d_p u_1 = d_p u_2 = d_p u_3 = 0$ for p with integer coordinates. In other words, B is a section coding the current hue and satisfying

$$\begin{aligned}
\widetilde{\nabla}_0(B) = {} & \widetilde{\nabla}_0 \left(\frac{e_1}{\sqrt{g_1}} + \frac{e_2}{\sqrt{g_2}} + \frac{e_3}{\sqrt{g_3}} \right) \left(u_1 \frac{e_1}{\sqrt{g_1}} + u_2 \frac{e_2}{\sqrt{g_2}} + u_3 \frac{e_3}{\sqrt{g_3}} \right) \\
& - \left(\frac{e_1}{\sqrt{g_1}} + \frac{e_2}{\sqrt{g_2}} + \frac{e_3}{\sqrt{g_3}} \right) \widetilde{\nabla}_0 \left(u_1 \frac{e_1}{\sqrt{g_1}} + u_2 \frac{e_2}{\sqrt{g_2}} + u_3 \frac{e_3}{\sqrt{g_3}} \right) \\
= {} & 0
\end{aligned}$$

on integer coordinates points.

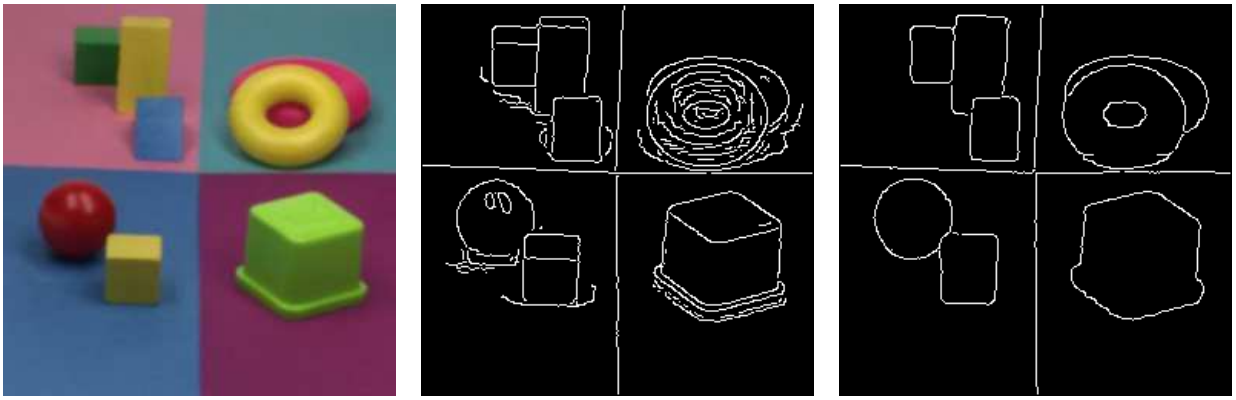

(a) (b) (c)

FIGURE 2.4 – a. original image b. global segmentation c. material edges

Let ∇_1 be the connection with $\omega \equiv 0$, i.e. $\nabla_1 = \widetilde{\nabla}_0$. We have at such points

$$\nabla_1 \left[I + \left(\left(\frac{e_1}{\sqrt{g_1}} + \frac{e_2}{\sqrt{g_2}} + \frac{e_3}{\sqrt{g_3}} \right) \wedge I \right) \cdot B \right] = \nabla_1(I) + \left[\left(\frac{e_1}{\sqrt{g_1}} + \frac{e_2}{\sqrt{g_2}} + \frac{e_3}{\sqrt{g_3}} \right) \wedge \nabla_1(I) \right] \cdot B$$

We obtain a $CT_1(D)$-valued 1-form on D, which may be decomposed into a scalar and a vector part.

From this 1-form, we may perform 6 edge detections : usual edge detection (see Section 2.4.1), material edge detection, non material edge detection, this latter being divided into shadows detection, highlights detection, and others. Therefore, we need to construct 6 vector bundles of rank 3 (E_{2_i}, π_{2_i}, D) equipped with metrics h_i, $i = 1 \dots 6$. The metrics h_i, $i = 2 \dots 6$ are given by the geometry of $\nabla_{1_X}(I)$ for $d\varphi(X)$ be an eigenvector associated to the highest eigenvalue of the first fundamental form of S.

Let us first compute the metric of S by considering the vector bundle (E_{2_1}, π_{2_1}, D) of metric $h_1 = I_3$. This allows us to perform the edge detection of Fig. 2.4.(b) and to obtain for each p the vector $\nabla_{1_Y}(I)$ that maximizes the norm of $\nabla_{1_X}(I)$ for $\|X\| = 1$ in T_pD. Following the arguments of [40], material edge detection arises from rejections of directional derivatives of the image on the planes generated by the light source direction (achromatic axis) and the current colors, which are the planes of the current hues. We now detail how to perform material and non material edge detection using the method of Section 2.3.3.

We can decompose $\nabla_1(I)$ into

$$\nabla_1(I) = \nabla_1(I \wedge B\, B^{-1}) + \nabla_1(I \cdot B\, B^{-1})$$

This leads in particular for p with integer coordinates to

$$\nabla_1(I)(p) = \nabla_1(I)(p) \wedge B(p)\, B(p)^{-1} + \nabla_1(I)(p) \cdot B(p)\, B(p)^{-1}$$

Let λ_2 defined as follows. We set $\lambda_2(p) = 1$ if $\|\nabla_{1_Y}(I)(p) \wedge B(p)\,B(p)^{-1}\| \geqslant N$ for N a threshold to be determined, and we extend λ_2 into a derivable strictly positive function such that λ_2 is negligible on $[0, N-\epsilon]$, where $\epsilon << 1$ is fixed. We also define a function λ_3 by stating that $\lambda_3(p)$ is negligible if $\|\nabla_{1_Y}(I)(p) \wedge B(p)\,B(p)^{-1}\| \geqslant N$, and extending λ_3 into a derivable strictly positive function such that $\lambda_3 \equiv 1$ on $[0, N-\epsilon]$.

From λ_2, we consider the metric $h_2 = \lambda_2 I_3$ generating a vector bundle (E_{2_2}, π_{2_2}, D) and a Clifford bundle $(CT_{2_2}, \widetilde{\pi}_{2_2}, D)$. From the vector-valued 1-form $\nabla_1(I \wedge B\,B^{-1})$, we construct a vector-valued 1-form in $(CT_{2_2}, \widetilde{\pi}_{2_2}, D)$ by (2.7). Following the process gives rise to a symmetric tensor of rank 2 that can be assimilated to the metric of a surface S_2 embedded into $\mathbb{R}^5$ equipped with the metric

$$\begin{pmatrix} 1 & 0 \\ 0 & 1 \end{pmatrix} \oplus \begin{pmatrix} \lambda_2 & 0 & 0 \\ 0 & \lambda_2 & 0 \\ 0 & 0 & \lambda_2 \end{pmatrix}$$

In particular, for p with interger coordinates and $\lambda_2(p) = 1$, we have

$$(dS_2)^2(Z_1, Z_2)(p) = dx \otimes dx\,(Z_1, Z_2)(p) + dy \otimes dy\,(Z_1, Z_2)(p)$$
$$+ \Big(\nabla_{1_{Z_1}}(I)(p) \wedge B(p)\,B(p)^{-1}\Big) \cdot \Big(\nabla_{1_{Z_2}}(I)(p) \wedge B(p)\,B(p)^{-1}\Big)$$

by the identification of $\mathbb{R}$ with its injection into each fiber.

Replacing λ_2 by λ_3 and $\nabla_1(I \wedge B\,B^{-1})$ by $\nabla_1(I \cdot B\,B^{-1})$, the edge detection of Fig. 2.4(c) is replaced by the edge detection of Fig. 2.5(a).

Then, we aim at characterizing shadows and highlights. We say that variations of an image at p are measurable with respect to a hue h_0 if $\nabla_{1_Y}(I)(p)$ is measurable with respect to h_0 for Y be the tangent vector field mentioned above. We then distinguish variations measurable with respect to the current hue and variations measurable with respect to its complementary, the information being given by

$$\left[\left(\left(\frac{e_1}{\sqrt{g_1}} + \frac{e_2}{\sqrt{g_2}} + \frac{e_3}{\sqrt{g_3}}\right) \wedge \nabla_{1_Y}(I)\right) \cdot B\right]$$

or equivalently

$$\nabla_{1_Y}\left[\left(\left(\frac{e_1}{\sqrt{g_1}} + \frac{e_2}{\sqrt{g_2}} + \frac{e_3}{\sqrt{g_3}}\right) \wedge I\right) \cdot B\right]$$

This is precisely the scalar part of the 1-form applied to the tangent vector field Y.

We construct three functions $\lambda_i, i = 4 \ldots 6$, each one of them generating a Clifford bundle $(CT_{2_i}(D), \widetilde{\pi}_{2_i}, D)$ associated to the metric $h_i = \lambda_i I_3$. Then, mapping the 1-form $\nabla_1(I \cdot B\,B^{-1})$ into each one of these Clifford bundles allows to perform different edge detections. Let us now explicit these functions.

We set $\lambda_4(p)$ equals 1 if $\|\nabla_{1_Y}(I)(p) \wedge B(p)\,B(p)^{-1}\| \leqslant N$ and variations of I at p with respect to the hue given by $B(p)$, i.e. the current hue, are measurable. We set $\lambda_5(p)$ equals 1 if $\|\nabla_{1_Y}(I)(p) \wedge B(p)\,B(p)^{-1}\| \leqslant N$ and variations of I at p with respect

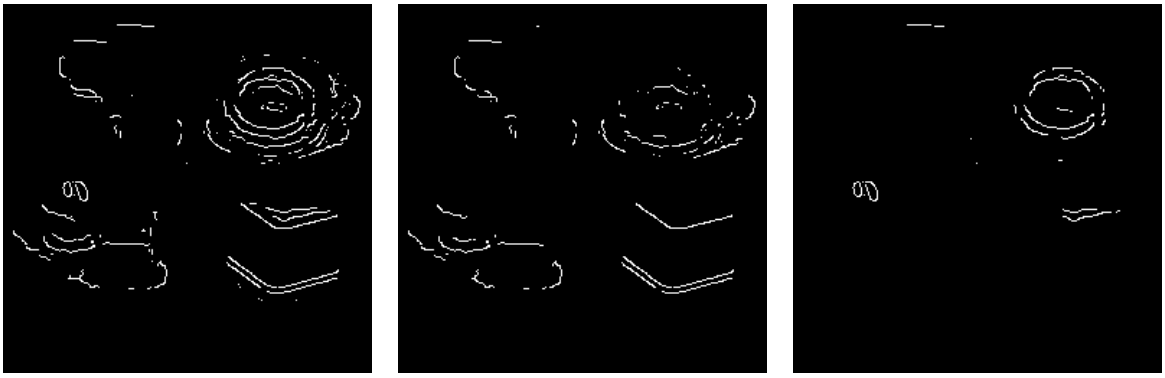

(a) (b) (c)

FIGURE 2.5 – a. non material edges . b. edges arising from the measure of variations with respect to the current hue . c. edges arising from the measure of variations with respect to the complementary of the current hue

to the complementary hue of $B(p)$ are measurable. At last, we set $\lambda_6(p)$ equals 1 if $\|\nabla_{1_Y}(I)(p) \wedge B(p)\, B(p)^{-1}\| \leqslant N$ and variations of I at p are neither measurable with respect to the current hue nor to its complementary. As usual, we extend these functions to strictly positive derivable functions that are negligible where the conditions are not respected.

Fig. 2.5(a) shows edges of the image of Fig. 2.4(a) which are non material edges (see Fig. 2.4(c)). These edges are decomposed in function of the position of $\nabla_{1_Y}(I)$ in the cube RGB. We can see on Fig. 2.5(b) the edges due to shadows. They correspond to high variations with respect to the current hue under the constraint $\|\nabla_{1_Y}(I)(p) \wedge B(p)\, B(p)^{-1}\| \leqslant N$. Highlights are given by Fig. 2.5(c), they correspond to high variations with respect to the complementary of the current hue under the previous constraint. We do not represent edges corresponding to the metric h_6, since they do not represent significative edges.

2.4.4 Edge detection in the color domain with constraints on the temperature : n=4, m=3

The aim of this application is to detect hot objects in a room. We need both color and temperature information (see Fig. 2.6(a) and Fig. 2.6(b)). Therefore we consider the color/infrared image associated to the scene.

Let λ be the function defined as follows. We set $\lambda(p)$ equals 1 if $t(p) \geqslant t_0$ for t_0 a given temperature, and we extend it to a derivable strictly positive function such that λ is negligible on $[0, t_0 - \epsilon]$, for $\epsilon << 1$ fixed. The role of λ is to not take into account color variations where $t < t_0$.

To perform the edge detection, we can either deal with the surface representing the color/infrared image or with the surface representing the color image. In the first case,

we consider the surface parametrized by

$$\varphi\colon (x,y) \longmapsto (x,y,r(x,y),g(x,y),b(x,y),t(x,y))$$

embedded into $\mathbb{R}^6$ equipped with the metric

$$\begin{pmatrix} 1 & 0 \\ 0 & 1 \end{pmatrix} \oplus \begin{pmatrix} \lambda & 0 & 0 & 0 \\ 0 & \lambda & 0 & 0 \\ 0 & 0 & \lambda & 0 \\ 0 & 0 & 0 & 0 \end{pmatrix}$$

In the second case, we consider the surface parametrized by

$$\varphi\colon (x,y) \longmapsto (x,y,r(x,y),g(x,y),b(x,y))$$

embedded into $\mathbb{R}^5$ equipped with the metric

$$\begin{pmatrix} 1 & 0 \\ 0 & 1 \end{pmatrix} \oplus \begin{pmatrix} \lambda & 0 & 0 \\ 0 & \lambda & 0 \\ 0 & 0 & \lambda \end{pmatrix}$$

In both cases, the first fundamental form of the surface is

$$dx^2 + dy^2 + \lambda dr^2 + \lambda dg^2 + \lambda db^2$$

We detail now how to proceed to compute the metric corresponding to the second case. Let $(E_1, \pi_1, D) \in \mathcal{F}_4$ of metric g and let (F_1, π_1, D) be the subbundle of global frame

$$\left(\frac{e_1}{\sqrt{g_1}}, \frac{e_2}{\sqrt{g_2}}, \frac{e_3}{\sqrt{g_3}}\right)$$

We consider the section I of $(CT_1(D), \widetilde{\pi}_1, D) \in \mathcal{G}_4$ generated by (E_1, π_1, D) representing the considered color/infrared image, i.e.

$$I(p) = r(p)\,\frac{e_1(p)}{\sqrt{g_1(p)}} + g(p)\,\frac{e_2(p)}{\sqrt{g_2(p)}} + b(p)\,\frac{e_3(p)}{\sqrt{g_3(p)}} + t(p)\,\frac{e_4(p)}{\sqrt{g_4(p)}}$$

The chosen connection ∇_1 on $(CT_1(D), \widetilde{\pi}_1, D)$ is

$$\nabla_1 = \widetilde{\nabla}_0 + (dx + dy) \otimes A$$

where for $p \in D$, $A(p)$ is the endomorphism

$$A(p)(x) = x \cdot \frac{e_4(p)}{\sqrt{g_4(p)}}$$

Then, we have

$$\nabla_1(I) = dr \otimes \frac{e_1}{\sqrt{g_1}} + dg \otimes \frac{e_2}{\sqrt{g_2}} + db \otimes \frac{e_3}{\sqrt{g_3}} + dt \otimes \frac{e_4}{\sqrt{g_4}} + (dx + dy) \otimes t$$

Here, $\nabla_1(I)$ contains only a scalar and a vector part. From the scalar part, we get the temperature component of the image and thus the function λ defined above. This one

(a) (b) (c)

FIGURE 2.6 – a. color information of the scene b. temperature information of the scene c. color edge detection with respect to temperature constraint.

generates a metric $h = \lambda I_3$ of a vector bundle $(E_2, \pi_2, D) \in \mathcal{F}_3$.

From (2.7), we construct the following element of $\Gamma(CT_2(D))$

$$\eta_2 = dr \otimes \frac{e_1}{\sqrt{h_1}} + dg \otimes \frac{e_2}{\sqrt{h_2}} + db \otimes \frac{e_3}{\sqrt{h_3}}$$

As before we obtain from η_2 a $CT_2(D)$-valued symmetric tensor of rank 2, namely

$$dx^2 \otimes 1 + dy^2 \otimes 1 + dr^2 \otimes \lambda + dg^2 \otimes \lambda + db^2 \otimes \lambda$$

This tensor corresponds to the first fundamental form we aimed at computing.

Fig. 2.6(c) shows the result of such an edge detection on a scene representing a man standing in front of a wall and holding a cup of hot coffee. By a well-chosen t_0, we may detect only the man and the cup.

2.4.5 Color/infrared edge detection with constraints on color and temperature : n=4, $\mathbf{m}_\nu = 4$

The main goal of this application is to rewrite the color/infrared edge detection of [3] with the method described in Section 2.3.3. Note that they are not completely similar since in this paper we measure color variations in the RGB space, whereas we deal with the HSL color space defined in Section 2.2.2 in [3].

Let μ represent the skin color of the man (see Fig. 2.7(a)) with (μ_1, μ_2, μ_3) as RGB coordinates. From μ we construct a section

$$\mu(p) = \mu_1 \frac{e_1(p)}{\sqrt{g_1(p)}} + \mu_2 \frac{e_2(p)}{\sqrt{g_2(p)}} + \mu_3 \frac{e_3(p)}{\sqrt{g_3(p)}}$$

of $(CT_1(D), \widetilde{\pi}_1, D) \in \mathcal{G}_4$ generated by $(E_1, \pi_1, D) \in \mathcal{F}_4$ of metric g. For this application, we choose (E_1, π_1, D) itself as the subbundle (F_1, π_1, D). We consider the color/infrared image I representing the scene as a section of this fiber bundle

$$I(p) = r(p) \frac{e_1(p)}{\sqrt{g_1(p)}} + g(p) \frac{e_2(p)}{\sqrt{g_2(p)}} + b(p) \frac{e_3(p)}{\sqrt{g_3(p)}} + t(p) \frac{e_4(p)}{\sqrt{g_4(p)}}$$

Then, we consider also the following connection

$$\nabla_1 = \widetilde{\nabla}_0 + (dx + dy) \otimes A$$

where $A \in \Gamma(\mathrm{End}(CT_1(D)))$ is defined for each p by

$$A(p)(x) = \mu(p)x$$

Therefore, we have

$$\nabla_1(I) = \widetilde{\nabla}_0(I) + (dx + dy) \otimes \mu\, I$$

Let α denote the function measuring for each p the oriented angle between $\mu(p)$ and the color part of $I(p)$. We have the following result.

Lemma 2.1 *Let X be the constant vector field on D of coordinates $(1, 0)$, then*

$$|tan(\alpha)| = \frac{\left\| \langle \nabla_{1_X}(I) \rangle_2 \cdot (e_1e_2e_3)\,(e_1e_2e_3)^{-1} \right\|}{\left| \langle \nabla_{1_X}(I) \rangle_0 \right|}$$

and

$$t = \frac{\left\| \langle \nabla_{1_X}(I) \rangle_2 - \langle \nabla_{1_X}(I) \rangle_2 \cdot (e_1e_2e_3)\,(e_1e_2e_3)^{-1} \right\|}{\|\mu\|}$$

Proof. We have

$$\langle \nabla_{1_X}(I) \rangle_2 = \mu \wedge I = (\mu \wedge I) \cdot (e_1e_2e_3)(e_1e_2e_3)^{-1} + \mu \wedge t\frac{e_4}{\sqrt{g_4}}$$

$$= \mu \wedge [I \cdot (e_1e_2e_3)(e_1e_2e_3)^{-1}] + \mu \wedge t\frac{e_4}{\sqrt{g_4}}$$

and

$$\langle \nabla_{1_X}(I) \rangle_0 = \mu \cdot I = \mu \cdot [I \cdot (e_1e_2e_3)(e_1e_2e_3)^{-1}]$$

Therefore,

$$\frac{\left\| \langle \nabla_{1_X}(I) \rangle_2 \cdot (e_1e_2e_3)\,(e_1e_2e_3)^{-1} \right\|}{\left| \langle \nabla_{1_X}(I) \rangle_0 \right|} = \frac{\|\mu\| \| I \cdot (e_1e_2e_3)(e_1e_2e_3)^{-1} \| |sin(\alpha)|}{\|\mu\| \| I \cdot (e_1e_2e_3)(e_1e_2e_3)^{-1} \| |cos(\alpha)|}$$

and

$$\frac{\left\| \langle \nabla_{1_X}(I) \rangle_2 - \langle \nabla_{1_X}(I) \rangle_2 \cdot (e_1e_2e_3)\,(e_1e_2e_3)^{-1} \right\|}{\|\mu\|} = \frac{\|\mu\| \| t\frac{e_4}{\sqrt{g_4}} \|}{\|\mu\|}$$

□

From $|tan(\alpha)|$ we may directly determine $|\alpha|$ since $-\frac{\pi}{2} \leqslant \alpha \leqslant \frac{\pi}{2}$ (μ and the color part of I are vectors in the cube RGB).

We set $\lambda(p) = 1$ if

$$\min_{(x,y)\in\Omega(p)} |\alpha(x, y)| \leqslant \alpha_0 \quad \text{and} \quad \max_{(x,y)\in\Omega(p)} t(x, y) \geqslant t_0$$

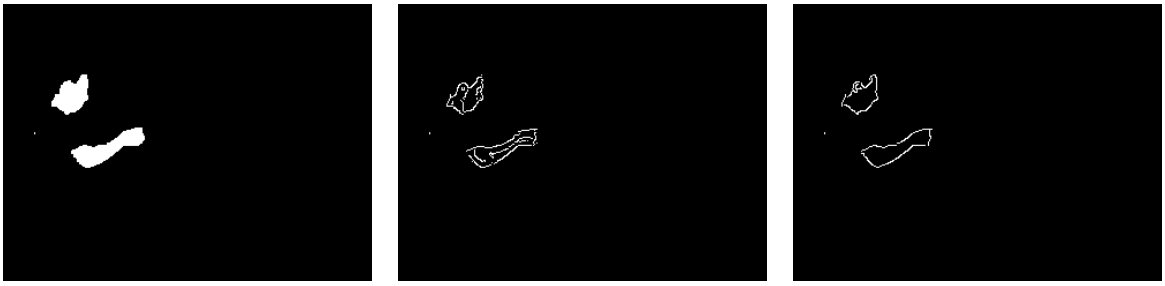

(a) (b) (c)

FIGURE 2.7 – a. regions of interest b. edge detection for $k = 1$ c. edge detection for $k = 25$

where α_0 and t_0 are two thresholds that determine regions of interest. Then, we extend λ into a derivable strictly positive function on $[0, \pi/2] \times [0, 255]$ such that λ is negligible on $[\alpha_0 + \epsilon, \pi/2] \times [0, 255] \bigcup [0, \pi/2] \times [0, t_0 - \epsilon]$ where $\epsilon << 1$ is fixed.
From λ, we derive a family of vector bundles $(E_2, \pi_2, D) \in \mathcal{F}_4$ indexed by $\nu \in \mathbb{N}$ and equipped with the metric

$$h_\nu = \begin{pmatrix} \lambda & 0 & 0 & 0 \\ 0 & \lambda & 0 & 0 \\ 0 & 0 & \lambda & 0 \\ 0 & 0 & 0 & \nu\lambda \end{pmatrix}$$

The role of ν is to control the weight of temperature variations in the image. Each one of these vector bundles generates a Clifford bundle $(CT_2(D), \pi_2, D) \in \mathcal{G}_4$. Following Section 2.3.3, for a given ν we construct

$$\eta_2 = dr \frac{e_1}{\sqrt{h_1}} + dg \frac{e_2}{\sqrt{h_2}} + db \frac{e_3}{\sqrt{h_3}} + dt \frac{e_4}{\sqrt{h_4}}$$

from which we derive a $CT_2(D)$-valued symmetric tensor of rank 2 :

$$dx^2 \otimes 1 + dy^2 \otimes 1 + dr^2 \otimes \lambda + dg^2 \otimes \lambda + db^2 \otimes \lambda + dt^2 \otimes \nu\lambda$$

This tensor can be assimilated to the first fundamental form of the 2-dimensional surface parametrized by

$$\varphi \colon (x, y) \longmapsto (x, y, r(x, y), g(x, y), b(x, y), t(x, y))$$

embedded into $\mathbb{R}^6$ equipped with the metric

$$\begin{pmatrix} 1 & 0 \\ 0 & 1 \end{pmatrix} \oplus \begin{pmatrix} \lambda & 0 & 0 & 0 \\ 0 & \lambda & 0 & 0 \\ 0 & 0 & \lambda & 0 \\ 0 & 0 & 0 & \nu\,\lambda \end{pmatrix}$$

Fig. 2.7 shows results of edge detections for different values of ν. We refer to ([3]) for detailled comments.

Deuxième partie

Equations de la chaleur associées à des Laplaciens généralisés pour la régularisation

Sommaire

3 Heat kernels of generalized Laplacians : application to multichannel images/videos regularization 92

3.1 Heat kernels of generalized Laplacians : application to color image smoothing . . . 92
3.1.1 Introduction . . . 92
3.1.2 Heat kernels of generalized laplacians . . . 93
3.1.3 Related works . . . 94
3.1.4 Applications . . . 100
3.2 Curved kernel for video regularization . . . 101

4 Clifford bundles : a unifying framework for images(videos), vector fields and orthonormal frame fields regularization 106

4.1 Introduction . . . 106
4.2 Heat equations on vector bundles . . . 108
4.2.1 Generalized Laplacians on vector bundles . . . 108
4.2.2 The heat kernel of a generalized Laplacian . . . 109
4.2.3 Discrete approximations of heat equations solutions . . . 110
4.2.4 An example : the scalar/Beltrami Laplacian . . . 111
4.3 The Clifford-Hodge Laplacian : an extension of the scalar Laplacian for multivector fields smoothing . . . 112
4.3.1 The Clifford-Hodge Laplacian : a generalized Laplacian on the Clifford bundle of a Riemannian manifold . . . 112
4.3.2 Application to functions, vector fields and oriented orthonormal frame fields smoothing . . . 116
4.4 The case $m = 2$ . . . 118
4.4.1 The operator D^2 and parallel transport map on $Cl(X, g)$ . . . 118
4.4.2 The particular context of images . . . 121
4.4.3 Experiments . . . 124
4.5 The case $m = 3$ . . . 126
4.5.1 The operator D^2 and parallel transport map on $Cl(X, g)$ . . . 126
4.5.2 The particular context of videos . . . 132
4.5.3 Experiments . . . 135

3 Heat kernels of generalized Laplacians : application to multichannel images/videos regularization

Cette Section fait l'objet d'un travail en cours sur l'utilisation des noyaux de la chaleur associés à des Laplaciens généralisés pour la régularisation d'images et vidéos multicanaux. Ce travail a été initié dans la publication [6] avec une application aux images couleur. La section 3.1 reprend cette publication en y ajoutant les preuves des propositions. La section 3.2 est consacrée à étendre aux vidéos la diffusion associée au noyau "courbé" introduite dans [6] dans le cas de la régularisation d'images.

3.1 Heat kernels of generalized Laplacians : application to color image smoothing

3.1.1 Introduction

Most multivalued image smoothing process are based on PDE's of the form

$$\frac{\partial I^i}{\partial t} = \sum_{j,k=1}^{2} f_{jk} \frac{\partial^2 I^i}{\partial j\, \partial k} + \text{first-order part}$$

of initial condition $I{:}(x,y) \longmapsto (I^1(x,y,0), \cdots, I^n(x,y,0))$ a n-channels image, where f_{jk} are real functions. We refer to [83] for an overview on related works. From a geometric point of view, the set of right terms, for $i = 1 \cdots n$, may be viewed as a second-order differential operator acting on sections of a vector bundle over a Riemannian manifold, namely a **generalized Laplacian** H [13]. As a consequence, it ensures existence and unicity of a kernel $K_t(x,y,H)$ generating the solution of the corresponding heat equation. For arbitrary Riemannian manifold X and vector bundle E, it is usually impossible to find a closed form for solutions of such equations. However, for the problem we consider in this paper, the use of an approximate solution appears to be sufficient. We use existing estimates formula of the kernel $K_t(x,y,H)$ to compute an approximation, for small t, of the solution of the **heat equation** :

$$\frac{\partial I}{\partial t} + HI = 0 \tag{3.1}$$

of initial condition $I = I(x,y,0)$ a given multivalued image, seen as a section of a vector bundle.
Section 2 is devoted to introduce the kernel we use for the smoothing, derived from the heat kernel of a generalized Laplacian. In section 3, we deal in particular with scalar Laplacians and Laplacians associated to frames. This allows us to etablish links with some related works on color image smoothing that involve kernels : Beltrami flow [77], oriented and curvature-preserving diffusions [83],[84]. For a well-chosen frame, we construct a kernel generalizing the oriented kernel. It takes both into account geometries of the base manifold and of the vector bundle, since it involves geodesic distances on the base manifold and parallel transport on the vector bundle. We compare the subsequent diffusion process with other methods mentioned above through a color image smoothing.

3.1.2 Heat kernels of generalized laplacians

We refer to [78] for an introduction to differential geometry. For a smooth vector bundle E over a manifold X, the symbol $\Gamma(E)$ denotes the space of smooth sections of E. For $x \in X$, E_x denotes the fiber over x.

Definition 1. Connection Laplacian
Let E be a vector bundle over a Riemannian manifold X, with a connection ∇^E. Since X is Riemannian, it possesses a canonical connection, the Levi-Cevita connection ∇. To any pair of tangent vector fields V and W on X, we associate an invariant second derivative $\nabla^2_{V,W} : \Gamma(E) \to \Gamma(E)$ by setting

$$\nabla^2_{V,W}\varphi \equiv \nabla^E_V \nabla^E_W \varphi - \nabla^E_{\nabla_V W}\varphi$$

Then the **connection Laplacian** $\Delta^E : \Gamma(E) \to \Gamma(E)$ is defined by

$$\Delta^E \varphi = -trace(\nabla^2_{\cdot,\cdot}\,\varphi)$$

where *trace* denotes the contraction with the metric g.

In particular, with respect to the framing $\partial_i := \partial/\partial x_i$ defined by a coordinate system in X, the operator Δ^E equals

$$\Delta^E = -\sum_{ij} g^{ij}\left(\nabla^E_{\partial_i}\nabla^E_{\partial_j} - \sum_k \Gamma^k_{ij}\nabla^E_{\partial_k}\right)$$

where Γ^k_{ij} are the symbols of the Levi-Cevita connection of X, defined by $\nabla_{\partial_i}\partial_j = \sum_k \Gamma^k_{ij}\partial_k$.

For shortness, we refer to [13] for the definition of a generalized Laplacian. In this paper, we make use of the following result : **Any generalized Laplacian is of the form $\Delta^E + F$, where Δ^E is the connection Laplacian associated to some connection ∇^E, and F is a section of the bundle End(E). In particular, any connection Laplacian Δ^E is a generalized Laplacian.**

To any generalized Laplacian H, one may associate an operator $e^{-tH} : \Gamma(E) \to \Gamma(E)$ for $t > 0$, with the property that if $I_t = e^{-tH} I$ for some $I \in \Gamma(E)$, then I_t satisfies the heat equation (3.1).
We shall define e^{-tH} as an integral operator of the form

$$(e^{-tH} I)(x) = \int_X K_t(x, y, H) I(y) dy$$

where $K_t(x, y, H) : E_y \to E_x$ is a linear map depending smoothly on x, y and t. This kernel is called the **heat kernel of** H [55].

In the following theorem, we give some results on approximations of the heat kernel and solutions of the heat equation. See [13] for details.

Theorem 3.1 *Let $n = dim(X)$. Let ϵ chosen smaller than the injectivity radius of X. Let $\Psi : \mathbb{R}_+ \to [0, 1]$ be a smooth function such that $\Psi(s) = 1$ if $s < \epsilon^2/4$ and $\Psi(s) = 0$ if*

$s > \epsilon^2$.
Let $\tau(x,y)$: $E_y \to E_x$ be the parallel transport along the unique geodesic curve joining y and x, and $d(x,y)$ its length.
There exist functions J and sections Φ_i such that the kernel $K_t^N(x,y,H)$ defined by

$$\Big(\frac{1}{4\pi t}\Big)^{\frac{n}{2}} e^{-d(x,y)^2/4t}\ \Psi(d(x,y)^2) \sum_{i=0}^{N} t^i \Phi_i(x,y,H) J(x,y)^{-\frac{1}{2}}$$

is asymptotic to the heat kernel of H for $N > n/2$.

Moreover, denoting by k_t^N the operator defined by

$$(k_t^N I)(x) = \int_X K_t^N(x,y,H) I(y) dy \tag{3.2}$$

we have $\lim_{t\to 0} \|k_t^N I - I\|_l = 0$ for every N, where $\|\ \|_l$ is a norm on C^l sections .

In what follows, we need the following properties :

1. $J(x,y) = 1 + O(\|\mathbf{y}\|^2)$ where $\mathbf{y}$ are the normal coordinates of y around x.
2. $\Phi_0(x,y) = \tau(x,y)$.

In this paper, for the sake of simplicity, we consider the smoothing process generated by the operator k_t^0 (3.2), as it is done for the short time Beltrami kernel [77]. It is given by $(k_t^0 I)(x) =$

$$\Big(\frac{1}{4\pi t}\Big)^{\frac{n}{2}} \int_X e^{-d(x,y)^2/4t}\ \Psi(d(x,y)^2) \tau(x,y) I(y) dy \tag{3.3}$$

if we approximate $J(x,y)$ by 1. As a consequence, to perform the smoothing process, we need to determine geodesic curves and their lengths on the base manifold, and the parallel transport map on the vector bundle.

3.1.3 Related works

The scalar Laplacian for the Beltrami flow The scalar Laplacian on X is the connection Laplacian on the vector bundle $E = C^\infty(X)$. In other words, it is the connection Laplacian on a vector bundle of rank one with connection ∇^E defined by the symbols

$$\Upsilon_1 = \cdots = \Upsilon_n = 0$$

i.e. $\nabla^E_{\partial_i} 1 = \Upsilon_i = 0$ for $i = 1 \cdots n$.

In local coordinates, it is defined by

$$\Delta(f) = -\sum_{ij} g^{ij} \Big(\partial_i \partial_j - \sum_k \Gamma_{ij}^k \partial_k\Big) f \tag{3.4}$$

It can be extended to the connection Laplacian Δ^E on a trivial vector bundle E of rank 3 of global basis (e_1, e_2, e_3) taking the connection defined by

$$\Upsilon_{ij}^k = 0 \quad \text{for} \quad i = 1,2 \quad \text{and} \quad k,j = 1,2,3 \tag{3.5}$$

i.e. $\nabla^E_{\partial_i} e_j = \sum_k \Upsilon^k_{ij} e_k = 0$.
Hence for $I = I_1 e_1 + I_2 e_2 + I_3 e_3 \in \Gamma(E)$,

$$\Delta^E(I) = \Delta I_1\, e_1 + \Delta I_2\, e_2 + \Delta I_3\, e_3$$

Let γ be a C^1 curve in X such that $\gamma(0) = y$. The parallel transport along γ of the vector $Y_0 = Y_0^1 e_1(y) + Y_0^2 e_2(y) + Y_0^3 e_3(y) \in E_y$ is $Y(t) = Y_0^1 e_1(\gamma(t)) + Y_0^2 e_2(\gamma(t)) + Y_0^3 e_3(\gamma(t))$. This results from the values of the symbols Υ^k_{ij}. We deduce that $\tau(x,y)(I_0^1 e_1(y) + I_0^2 e_2(y) + I_0^3 e_3(y)) = I_0^1 e_1(x) + I_0^2 e_2(x) + I_0^3 e_3(x)$.

In Sochen et al. framework [74],[77], the image regularization is made through the so-called Beltrami flow

$$\frac{\partial I^i}{\partial t} = \Delta_g I^i \qquad i = 1,2,3 \tag{3.6}$$

The operator Δ_g is the Laplace-Beltrami operator defined

$$\Delta_g(f) = \frac{1}{\sqrt{g}} \sum_{j,k=1}^{n} \partial_j(\sqrt{g} g^{jk} \partial_k f)$$

It is well-known that if a Riemannian manifold (X, g) is equipped with the Levi-Cevita connection, then Δ_g is minus the scalar Laplacian (3.4). As a consequence, the system (3.6) may equivalently be solved in the vector bundle framework, defining a color image as a section I of the vector bundle E (3.5) over a manifold (X, g) of dimension 2.
The kernel $(1/4\pi t)\, e^{-d(x,y)^2/4t}\ \Psi(d(x,y)^2)\tau(x,y)$ we consider (3.3) is, in this case, the vector counterpart of the kernel in [77]. This makes the two diffusion process be equivalent.

Oriented and curved kernels Let X be a manifold of dimension 2. Let f be a smooth function defined on X. We consider the differential operator of order 2

$$\Delta(f) = -c_1\, d^2_{\xi,\xi} f - c_2\, d^2_{\eta,\eta} f \tag{3.7}$$

where (ξ, η) is a moving frame, and c_1, c_2 are two smooth functions on X.

In the following proposition, we show that Δ may be viewed as a generalized Laplacian on a vector bundle of rank 1 over X, for a well-chosen metric on X.

Proposition 3.1 *Let (X, g) be a Riemannian manifold of dimension 2 with*

$$g = \frac{1}{c_1 c_2 (\xi_1 \eta_2 - \eta_1 \xi_2)^2} \begin{pmatrix} c_1\, {\xi_2}^2 + c_2\, {\eta_2}^2 & -(c_1 \xi_1 \xi_2 + c_2 \eta_1 \eta_2) \\ -(c_1 \xi_1 \xi_2 + c_2 \eta_1 \eta_2) & c_1\, {\xi_1}^2 + c_2\, {\eta_1}^2 \end{pmatrix}$$

Let E be a trivial vector bundle of rank 1 over X of global basis e_1, endowed with the connection ∇^E defined by $\nabla^E_{\partial_x} e_1 = \Upsilon_1\, e_1$ and $\nabla^E_{\partial_y} e_1 = \Upsilon_2\, e_1$ where

$$\Upsilon_1 = \frac{1}{2}(g_{11} a + g_{12} b) \qquad \Upsilon_2 = \frac{1}{2}(g_{12} a + g_{22} b)$$

and

$$a = c_1\frac{\partial\xi_1}{\partial x}\xi_1 + c_1\frac{\partial\xi_1}{\partial y}\xi_2 + c_2\frac{\partial\eta_1}{\partial x}\eta_1 + c_2\frac{\partial\eta_1}{\partial y}\eta_2 + 2g^{12}\,\Gamma^1_{12} + g^{11}\,\Gamma^1_{11} + g^{22}\,\Gamma^1_{22}$$

$$b = c_1\frac{\partial\xi_2}{\partial x}\xi_1 + c_1\frac{\partial\xi_2}{\partial y}\xi_2 + c_2\frac{\partial\eta_2}{\partial x}\eta_1 + c_2\frac{\partial\eta_2}{\partial y}\eta_2 + 2g^{12}\,\Gamma^2_{12} + g^{11}\,\Gamma^2_{11} + g^{22}\,\Gamma^2_{22}$$

Let $\tilde{f} = fe_1 \in \Gamma(E)$. The differential operator H of order 2 defined by

$$H(\tilde{f}) = \Delta(f)\,e_1 \tag{3.8}$$

is a generalized Laplacian on E.

Proof. Developping (3.7) we obtain

$$\begin{aligned}\Delta(f) = &-\Big(c_1{\xi_1}^2 + c_2{\eta_1}^2\Big)\frac{\partial^2 f}{\partial x^2} - \Big(2c_1\xi_1\xi_2 + 2c_2\eta_1\eta_2\Big)\frac{\partial^2 f}{\partial x\partial y} - \Big(c_1{\xi_2}^2 + c_2{\eta_2}^2\Big)\frac{\partial^2 f}{\partial y^2}\\ &+ \frac{\partial f}{\partial x}\Big(-c_1\xi_1\frac{\partial\xi_1}{\partial x} - c_1\xi_2\frac{\partial\xi_1}{\partial y} - c_2\eta_1\frac{\partial\eta_1}{\partial x} - c_2\eta_2\frac{\partial\eta_1}{\partial y}\Big)\\ &+ \frac{\partial f}{\partial y}\Big(-c_1\xi_1\frac{\partial\xi_2}{\partial x} - c_1\xi_2\frac{\partial\xi_2}{\partial y} - c_2\eta_1\frac{\partial\eta_2}{\partial x} - c_2\eta_2\frac{\partial\eta_2}{\partial y}\Big)\end{aligned}$$

Then we search (g, ∇^E, F) such that $H = \Delta^E + F$ over the Riemannian manifold (X, g). By definition of the connection Laplacian (4.3), we have

$$\begin{aligned}\Delta^E(f) = &-g^{11}\Big(\nabla^E_{\partial_x}\nabla^E_{\partial_x}f - \Gamma^1_{11}\nabla^E_{\partial_x}f - \Gamma^2_{11}\nabla^E_{\partial_y}f\Big) - g^{12}\Big(\nabla^E_{\partial_x}\nabla^E_{\partial_y}f - \Gamma^1_{12}\nabla^E_{\partial_x}f - \Gamma^2_{12}\nabla^E_{\partial_y}f\Big)\\ &- g^{21}\Big(\nabla^E_{\partial_y}\nabla^E_{\partial_x}f - \Gamma^1_{21}\nabla^E_{\partial_x}f - \Gamma^2_{21}\nabla^E_{\partial_y}f\Big) - g^{22}\Big(\nabla^E_{\partial_y}\nabla^E_{\partial_y}f - \Gamma^1_{22}\nabla^E_{\partial_x}f - \Gamma^2_{22}\nabla^E_{\partial_y}f\Big)\end{aligned}$$

The connection ∇^E being defined by $\nabla^E_{\partial_x}e_1 = \Upsilon_1\,e_1$ and $\nabla^E_{\partial_y}e_1 = \Upsilon_2\,e_1$ for some functions Υ_1 and Υ_2, we obtain

$$\begin{aligned}\Delta^E(\tilde{f}) = &-g^{11}\frac{\partial^2 f}{\partial x^2}\,e_1 - g^{12}\frac{\partial^2 f}{\partial x\partial y}e_1 - g^{21}\frac{\partial^2 f}{\partial x\partial y}e_1 - g^{22}\frac{\partial^2 f}{\partial y^2}e_1\\ &+ \frac{\partial f}{\partial x}\Big(-g^{12}\Upsilon_2 + g^{12}\Gamma^1_{12} - g^{21}\Upsilon_2 + g^{21}\Gamma^1_{21} - 2g^{11}\Upsilon_1 + g^{11}\Gamma^1_{11} + g^{22}\Gamma^1_{22}\Big)e_1\\ &+ \frac{\partial f}{\partial y}\Big(-g^{12}\Upsilon_1 + g^{12}\Gamma^2_{12} - g^{21}\Upsilon_1 + g^{21}\Gamma^2_{21} + g^{11}\Gamma^2_{11} - 2g^{22}\Upsilon_2 + g^{22}\Gamma^2_{22}\Big)e_1\\ &+ f\Big(-g^{11}\frac{\partial\Upsilon_1}{\partial x} - g^{11}(\Upsilon_1)^2 + g^{11}\Gamma^1_{11}\Upsilon_1 + g^{11}\Gamma^2_{11}\Upsilon_2 - g^{12}\frac{\partial\Upsilon_2}{\partial x} - g^{12}\Upsilon_1\Upsilon_2\\ &+ g^{12}\Gamma^1_{12}\Upsilon_1 + g^{12}\Gamma^2_{12}\Upsilon_2 - g^{21}\frac{\partial\Upsilon_1}{\partial y} - g^{21}\Upsilon_1\Upsilon_2 + g^{21}\Gamma^1_{21}\Upsilon_1 + g^{21}\Gamma^2_{21}\Upsilon_2\\ &- g^{22}\frac{\partial\Upsilon_2}{\partial y} - g^{22}(\Upsilon_2)^2 + g^{22}\Gamma^1_{22}\Upsilon_1 + g^{22}\Gamma^2_{22}\Upsilon_2\Big)e_1\end{aligned}$$

We see that the second-order part determines the metric g, the first-order part determines the connection ∇^E and the zero-order part determines $F \in \mathrm{End}(E)$.

By identification, we have

$$g^{-1} = \begin{pmatrix} c_1{\xi_1}^2 + c_2{\eta_1}^2 & c_1\xi_1\xi_2 + c_2\eta_1\eta_2 \\ \\ c_1\xi_1\xi_2 + c_2\eta_1\eta_2 & c_1{\xi_2}^2 + c_2{\eta_2}^2 \end{pmatrix}$$

from which follows

$$g = \frac{1}{c_1c_2(\xi_1\eta_2 - \eta_1\xi_2)^2} \begin{pmatrix} c_1{\xi_2}^2 + c_2{\eta_2}^2 & -(c_1\xi_1\xi_2 + c_2\eta_1\eta_2) \\ \\ -(c_1\xi_1\xi_2 + c_2\eta_1\eta_2) & c_1{\xi_1}^2 + c_2{\eta_1}^2 \end{pmatrix}$$

Identifying first order parts we obtain two equalities, where left terms have been simplified using symmetries of coefficients g_{ij} and Γ_{ij}^k symbols

$$-2g^{11}\Upsilon_1 - 2g^{12}\Upsilon_2 + 2g^{12}\Gamma_{12}^1 + g^{11}\Gamma_{11}^1 + g^{22}\Gamma_{22}^1 = -c_1\xi_1\frac{\partial\xi_1}{\partial x} - c_1\xi_2\frac{\partial\xi_1}{\partial y} - c_2\eta_1\frac{\partial\eta_1}{\partial x} - c_2\eta_2\frac{\partial\eta_1}{\partial y}$$

$$-2g^{12}\Upsilon_1 - 2g^{22}\Upsilon_2 + 2g^{12}\Gamma_{12}^2 + g^{11}\Gamma_{11}^2 + g^{22}\Gamma_{22}^2 = -c_1\xi_1\frac{\partial\xi_2}{\partial x} - c_1\xi_2\frac{\partial\xi_2}{\partial y} - c_2\eta_1\frac{\partial\eta_2}{\partial x} - c_2\eta_2\frac{\partial\eta_2}{\partial y}$$

Let us put

$$a = c_1\frac{\partial\xi_1}{\partial x}\xi_1 + c_1\frac{\partial\xi_1}{\partial y}\xi_2 + c_2\frac{\partial\eta_1}{\partial x}\eta_1 + c_2\frac{\partial\eta_1}{\partial y}\eta_2 + 2g^{12}\Gamma_{12}^1 + g^{11}\Gamma_{11}^1 + g^{22}\Gamma_{22}^1$$

$$b = c_1\frac{\partial\xi_2}{\partial x}\xi_1 + c_1\frac{\partial\xi_2}{\partial y}\xi_2 + c_2\frac{\partial\eta_2}{\partial x}\eta_1 + c_2\frac{\partial\eta_2}{\partial y}\eta_2 + 2g^{12}\Gamma_{12}^2 + g^{11}\Gamma_{11}^2 + g^{22}\Gamma_{22}^2$$

Then we obtain the system

$$\begin{cases} -2g^{11}\Upsilon_1 - 2g^{12}\Upsilon_2 &= -a \\ \\ -2g^{12}\Upsilon_1 - 2g^{22}\Upsilon_2 &= -b \end{cases}$$

whose solution is

$$\begin{pmatrix} \Upsilon_1 \\ \\ \Upsilon_2 \end{pmatrix} = \frac{1}{2}\begin{pmatrix} g_{11} & g_{12} \\ \\ g_{12} & g_{22} \end{pmatrix}\begin{pmatrix} a \\ \\ b \end{pmatrix}$$

At last, it is immediat that

$$F = g^{11}\frac{\partial\Upsilon_1}{\partial x} + g^{11}(\Upsilon_1)^2 - g^{11}\Gamma_{11}^1\Upsilon_1 - g^{11}\Gamma_{11}^2\Upsilon_2 + g^{12}\frac{\partial\Upsilon_2}{\partial x} + g^{12}\frac{\partial\Upsilon_1}{\partial y} + 2g^{12}\Upsilon_1\Upsilon_2 - 2g^{12}\Gamma_{12}^1\Upsilon_1$$
$$- 2g^{12}\Gamma_{12}^2\Upsilon_2 + g^{22}\frac{\partial\Upsilon_2}{\partial y} + g^{22}(\Upsilon_2)^2 - g^{22}\Gamma_{22}^1\Upsilon_1 - g^{22}\Gamma_{22}^2\Upsilon_2 \qquad \square$$

Proposition 3.2 *Let (X, g), E and ∇^E of the previous Proposition.*
Let $\gamma(t) = (\gamma_1(t), \gamma_2(t))$ a C^1 curve in X such that $\gamma(0) = y$, and $Y_0 = Y_0^1 e_1(y) \in E_y$. Then, the parallel transport Y of Y_0 along γ is defined by

$$Y(t) \;=\; Y_0^1\, exp\left(-\int_0^t \dot\gamma_1(s)\Upsilon_1(\gamma(s)) + \dot\gamma_2(s)\Upsilon_2(\gamma(s))\;\; ds\right) e_1(\gamma(t))$$

Proof. The parallel transport of Y_0 along γ is the solution $Y(t) = Y^1(t)e_1(\gamma(t))$ of the differential equation

$$\begin{cases} \nabla^E_{\dot\gamma} Y(t) = 0 \\ \\ Y(0) = Y_0 \end{cases} \tag{3.9}$$

$$\begin{aligned} \nabla^E_{\dot\gamma} Y(t) &= \nabla^E_{\dot\gamma}(Y^1\, e_1)(t) \\ &= \frac{\partial Y^1}{\partial t}(t)\, e_1(\gamma(t)) + Y^1(t)\Big(\dot\gamma_1(t)\nabla^E_{\partial_x} e_1(\gamma(t)) + \dot\gamma_2(t)\nabla^E_{\partial_y} e_1(\gamma(t))\Big) \\ &= \frac{\partial Y^1}{\partial t}(t)\, e_1(\gamma(t)) + Y^1(t)\Big(\dot\gamma_1(t)\Upsilon_1(t)\, e_1(\gamma(t)) + \dot\gamma_2(t)\Upsilon_2(t)\, e_1(\gamma(t))\Big) \end{aligned}$$

Finally, we obtain an ordinary differential equation

$$\begin{cases} \dfrac{\partial Y^1}{\partial t}(t) &= -\Big(\dot\gamma_1(t)\Upsilon_1(t) + \dot\gamma_2(t)\Upsilon_2(t)\Big)Y^1(t) \\ \\ Y^1(0) &= Y^1_0 \end{cases}$$

from which we deduce the solution of (3.9). □

H may be extended to a generalized Laplacian on a vector bundle of rank 3 over X as follows.

Corollary 3.1 *Let (X, g) be a Riemannian manifold of dimension 2 with*

$$g = \frac{1}{c_1c_2(\xi_1\eta_2 - \eta_1\xi_2)^2}\begin{pmatrix} c_1\,{\xi_2}^2 + c_2\,{\eta_2}^2 & -(c_1\xi_1\xi_2 + c_2\eta_1\eta_2) \\ -(c_1\xi_1\xi_2 + c_2\eta_1\eta_2) & c_1\,{\xi_1}^2 + c_2\,{\eta_1}^2 \end{pmatrix}$$

Let E be a trivial vector bundle of rank 3 over X with connection ∇^E given by the symbols Υ^k_{ij} for $k, j \in \{1, 2, 3\}$ and $i \in \{1, 2\}$, defined by $\Upsilon^k_{ij} = 0$ if $k \neq j$ and

$$\Upsilon^k_{ij} = \begin{cases} \dfrac{g^{12}b - g^{22}a}{2g^{11}g^{22} - 2(g^{12})^2} & \text{if} \quad i = 1 \quad \text{and} \quad k = j \\ \\ \dfrac{g^{12}a - g^{11}b}{2g^{11}g^{22} - 2(g^{12})^2} & \text{if} \quad i = 2 \quad \text{and} \quad k = j \end{cases}$$

in the global basis (e_1, e_2, e_3) and frame $\partial_i := \partial/\partial x_i$, where

$$a = c_1\frac{\partial\xi_1}{\partial x}\xi_1 + c_1\frac{\partial\xi_1}{\partial y}\xi_2 + c_2\frac{\partial\eta_1}{\partial x}\eta_1 + c_2\frac{\partial\eta_1}{\partial y}\eta_2 + 2g^{12}\Gamma^1_{12} + g^{11}\Gamma^1_{11} + g^{22}\Gamma^1_{22}$$

$$b = c_1\frac{\partial\xi_2}{\partial x}\xi_1 + c_1\frac{\partial\xi_2}{\partial y}\xi_2 + c_2\frac{\partial\eta_2}{\partial x}\eta_1 + c_2\frac{\partial\eta_2}{\partial y}\eta_2 + 2g^{12}\Gamma^2_{12} + g^{11}\Gamma^2_{11} + g^{22}\Gamma^2_{22}$$

Let $s = s_1e_1 + s_2e_2 + s_3e_3 \in \Gamma(E)$. Then the differential operator H of order 2 defined by

$$H(s) = \Delta(s_1)\, e_1 + \Delta(s_2)\, e_2 + \Delta(s_3)\, e_3 \tag{3.10}$$

is a generalized Laplacian on E.

Proof. We first observe that $\Upsilon^k_{1k} = \Upsilon_1$ and $\Upsilon^k_{2k} = \Upsilon_2$. Then $H = \Delta^E + F$ where F is the zero order operator $\Gamma(E) \longrightarrow \Gamma(E)$ defined by

$$\Big(g^{11}\frac{\partial \Upsilon_1}{\partial x} + g^{11}(\Upsilon_1)^2 - g^{11}\Gamma^1_{11}\Upsilon_1 - g^{11}\Gamma^2_{11}\Upsilon_2 + g^{12}\frac{\partial \Upsilon_2}{\partial x} + g^{12}\frac{\partial \Upsilon_1}{\partial y} + 2g^{12}\Upsilon_1\Upsilon_2 - 2g^{12}\Gamma^1_{12}\Upsilon_1\Big)Id$$

in the basis (e_1, e_2, e_3). □

Corollary 3.2 *Let (X, g), E and ∇^E of Corollary 3.1, $\gamma(t) = (\gamma_1(t), \gamma_2(t))$ a C^1 curve in X such that $\gamma(0) = y$, and $Y_0 = Y_0^1 e_1(y) + Y_0^2 e_2(y) + Y_0^3 e_3(y) \in E_y$. The parallel transport of Y_0 along γ is*

$$\begin{aligned} Y(t) = Y_0^1\, exp\Big(-\int_0^t \frac{\partial \gamma_1}{\partial s}(s)\Upsilon_1(s) + \frac{\partial \gamma_2}{\partial s}(s)\Upsilon_2(s)\ ds\Big)\, e_1(\gamma(t)) \\ + Y_0^2\, exp\Big(-\int_0^t \frac{\partial \gamma_1}{\partial s}(s)\Upsilon_1(s) + \frac{\partial \gamma_2}{\partial s}(s)\Upsilon_2(s)\ ds\Big) e_2(\gamma(t)) \\ + Y_0^3\, exp\Big(-\int_0^t \frac{\partial \gamma_1}{\partial s}(s)\Upsilon_1(s) + \frac{\partial \gamma_2}{\partial s}(s)\Upsilon_2(s)\ ds\Big) e_3(\gamma(t)) \end{aligned}$$

Proof. The parallel transport of Y_0 along γ is the solution $Y(t) = Y^1(t)e_1(\gamma(t)) + Y^2(t)e_2(\gamma(t)) + Y^3(t)e_3(\gamma(t))$ of the differential equation

$$\begin{cases} \nabla^E_{\dot\gamma} Y(t) = 0 \\ \\ Y(0) = Y_0 \end{cases} \tag{3.11}$$

$$\begin{aligned} \nabla^E_{\dot\gamma} Y(t) &= \nabla^E_{\dot\gamma}(Y^1 e_1 + Y^2 e_2 + Y^3 e_3)(t) \\ &= \frac{\partial Y^1}{\partial t}(t)\, e_1(\gamma(t)) + Y^1(t)\Big(\dot\gamma_1(t)\nabla^E_{\partial_x} e_1(\gamma(t)) + \dot\gamma_2(t)\nabla^E_{\partial_y} e_1(\gamma(t))\Big) \\ &= +\frac{\partial Y^2}{\partial t}(t)\, e_2(\gamma(t)) + Y^2(t)\Big(\dot\gamma_1(t)\nabla^E_{\partial_x} e_2(\gamma(t)) + \dot\gamma_2(t)\nabla^E_{\partial_y} e_2(\gamma(t))\Big) \\ &= +\frac{\partial Y^3}{\partial t}(t)\, e_3(\gamma(t)) + Y^3(t)\Big(\dot\gamma_1(t)\nabla^E_{\partial_x} e_3(\gamma(t)) + \dot\gamma_2(t)\nabla^E_{\partial_y} e_3(\gamma(t))\Big) \\ &= \frac{\partial Y^1}{\partial t}(t)\, e_1(\gamma(t)) + Y^1(t)\Big(\dot\gamma_1(t)\Upsilon^1_{11}(t)\, e_1(\gamma(t)) + \dot\gamma_2(t)\Upsilon^1_{21}(t)\, e_1(\gamma(t))\Big) \\ &= +\frac{\partial Y^2}{\partial t}(t)\, e_2(\gamma(t)) + Y^2(t)\Big(\dot\gamma_1(t)\Upsilon^2_{12}(t)\, e_2(\gamma(t)) + \dot\gamma_2(t)\Upsilon^2_{22}(t)\, e_2(\gamma(t))\Big) \\ &= +\frac{\partial Y^3}{\partial t}(t)\, e_3(\gamma(t)) + Y^3(t)\Big(\dot\gamma_1(t)\Upsilon^3_{13}(t)\, e_3(\gamma(t)) + \dot\gamma_2(t)\Upsilon^3_{23}(t)\, e_3(\gamma(t))\Big) \end{aligned}$$

Finally, we obtain three ordinary differential equations

$$\begin{cases} \dfrac{\partial Y^1}{\partial t}(t) &= -\Big(\dot\gamma_1(t)\Upsilon_1(t) + \dot\gamma_2(t)\Upsilon_2(t)\Big)Y^1(t) \\ \\ Y^1(0) &= Y_0^1 \end{cases}$$

$$\begin{cases} \dfrac{\partial Y^2}{\partial t}(t) &= -\Big(\dot\gamma_1(t)\Upsilon_1(t) + \dot\gamma_2(t)\Upsilon_2(t)\Big)Y^2(t) \\ \\ Y^2(0) &= Y_0^2 \end{cases}$$

$$\begin{cases} \dfrac{\partial Y^3}{\partial t}(t) &= -\Big(\dot{\gamma_1}(t)\Upsilon_1(t) + \dot{\gamma_2}(t)\Upsilon_2(t)\Big)Y^3(t) \\ Y^3(0) &= Y_0^3 \end{cases}$$

from which we deduce the solution of (4.10). □

Let us study the case where the functions c_1, c_2 and the components $\xi_1, \xi_2, \eta_1, \eta_2$ of the moving frame (ξ, η) are constant on some normal neighborhood D of $x \in X$. Then $\Delta(f)(x) = Trace(T(x)\, H_i(x))$, where $T(x)$ is the matrix $c_1(x)\xi(x)\xi(x)^T + c_2(x)\eta(x)\eta(x)^T$ and H_i is the hessian matrix of f at x in the standard coordinates system.
Moreover symbols Γ_{ij}^k and Υ_{ij}^k vanish on D. It follows that the kernel $(1/4\pi t)\, e^{-d(x,y)^2/4t}\ \Psi(d(x,y)^2)\tau(x,y)$ is given on $D \times D$ by

$$(1/4\pi t)\, e^{-g((x_1-y_1,x_2-y_2),(x_1-y_1,x_2-y_2))/4t} Id(x,y) \tag{3.12}$$

and corresponds to the vector counterpart of the **oriented kernel** of Tschumperlé et al [83]. Indeed the parallel transport of $Y_0 = Y_0^1 e_1(y) + Y_0^2 e_2(y) + Y_0^3 e_3(y)$ along any curve γ in D is $Y(t) = Y_0^1 e_1(\gamma(t)) + Y_0^2 e_2(\gamma(t)) + Y_0^3 e_3(\gamma(t))$. It gives the map $\tau \equiv Id$ on D. A simple computation leads to

$$exp_{(x_1,x_2)}(\mathbf{y_1}, \mathbf{y_2}) = (x_1 + \mathbf{y_1}, x_2 + \mathbf{y_2})$$

On a Riemannian manifold (X, g), $d(x, exp_x \mathbf{y}) = \sqrt{g_x(\mathbf{y}, \mathbf{y})}$. Hence $d(x,y) = \sqrt{g_x(y_1 - x_1, y_2 - x_2), (y_1 - x_1, y_2 - x_2)}$.

At last, let us mention that an extension of the oriented kernel based diffusion is also proposed in [84] from 1D diffusion along line integrals.

3.1.4 Applications

We compare color image smoothing process provided by Beltrami, oriented and curved kernels. The base manifold (X, g) taken for the Beltrami flow is the domain $X \subset \mathbb{R}^2$ of the color image equipped with the metric g induced by the embedding of its graph in $(\mathbb{R}^5, \| \ \|_2)$. For curved and oriented kernel based diffusions, the base manifold is $(X, \tilde{g})$ for $c_1 = 1/(\lambda^+ + \lambda^- - 1)^{0.3}$, $c_2 = 1/(\lambda^+ + \lambda^- - 1)^{0.5}$ where λ^+ (resp. λ^-) is the field of highest (resp. lowest) eigenvalues of g and (ξ, η) is the frame given the respective corresponding unit eigenvectors. Convolutions (3.3) are discretized as discrete convolutions of the maps $\tau(x,y)I(y)$ with 5x5-sized normalized masks whose inputs are geodesic distances. Note that the size of the masks is related with the map Ψ. Fig. 3.1 shows results after 10 iterations for t=0.2, the metrics g and $\tilde{g}$ being updated at each iteration. [3]

We see that the diffusions associated to the Beltrami and oriented kernel resp. on Fig. 3.1(b) and Fig. 3.1(c) have similar results. Indeed, the diffusions tend to behave as gaussian diffusions on regions of low color variations and to diffuse in the direction of edges on regions of high color variations. Whereas it is a well-known behaviour of the Beltrami flow, it comes from the choices of functions c_1, c_2 and moving frame (ξ, η) for

3. The original image Fig. 1(a) is a part of an image taken in the texture image databasis `http://www.cgtextures.com/`.

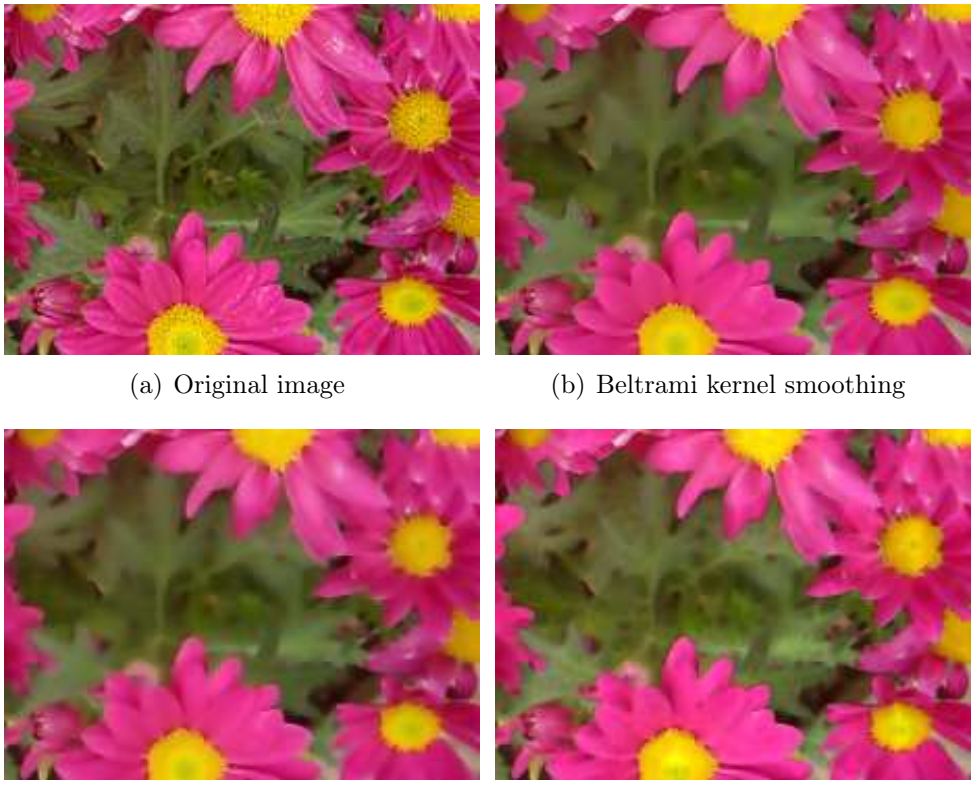

(a) Original image (b) Beltrami kernel smoothing

(c) Oriented kernel smoothing (d) Curved kernel smoothing

FIGURE 3.1 – Comparison of three different anisotropic smoothing

the oriented kernel based diffusion.
Compared to the oriented kernel based diffusion, the one based on the curved kernel takes more into account the local geometry of images. Indeed, we have shown that oriented kernels correspond to curved kernels under the assumption that the components of the moving frame (ξ, η) are locally constant. This means that oriented kernels (3.12) only depend on the directions given by the moving frame , whereas curved kernels also take into account curvatures of their integral curves. Fig. 3.1(d) illustrates a diffusion process induced by the curved kernel. We see that it better preserves fine structures of the image than the two others methods. This is particulary visible on green leaves.

3.2 Curved kernel for video regularization

Let X be a manifold of dimension 3. Let f be a smooth function defined on X. We consider the differential operator of order 2

$$\Delta(f) = -c_1\, d^2_{\xi,\xi} f - c_2\, d^2_{\eta,\eta} f - c_3\, d^2_{\lambda,\lambda} f \tag{3.13}$$

where (ξ, η, λ) is a moving frame, and c_1, c_2, c_3 are three smooth functions on X.

In the following proposition, we show that Δ may be viewed as a generalized Laplacian on a vector bundle of rank 1 over X, for a well-chosen metric.

Proposition 3.3 *Let (X, g) be a Riemannian manifold of dimension 3 with*

$$
\begin{aligned}
g^{11} &= c_1\,{\xi_1}^2 + c_2\,{\eta_1}^2 + c_3\,{\lambda_1}^2\\
g^{12} &= 2\,c_1\,\xi_1\,\xi_2 + 2\,c_2\,\eta_1\,\eta_2 + 2\,c_3\,\lambda_1\,\lambda_2\\
g^{13} &= 2\,c_1\,\xi_1\,\xi_3 + 2\,c_2\,\eta_1\,\eta_3 + 2\,c_3\,\lambda_1\,\lambda_3\\
g^{22} &= c_1\,{\xi_2}^2 + c_2\,{\eta_2}^2 + c_3\,{\lambda_2}^2\\
g^{23} &= 2\,c_1\,\xi_2\,\xi_3 + 2\,c_2\,\eta_2\,\eta_3 + 2\,c_3\,\lambda_2\,\lambda_3\\
g^{33} &= c_1\,{\xi_3}^2 + c_2\,{\eta_3}^2 + c_3\,{\lambda_3}^2
\end{aligned}
$$

Let E be a trivial vector bundle of rank 1 over X of global basis e_1, endowed with the connection ∇^E defined by $\nabla^E_{\partial_x} e_1 = \Upsilon_1\, e_1$, $\nabla^E_{\partial_y} e_1 = \Upsilon_2\, e_1$ and $\nabla^E_{\partial_z} e_1 = \Upsilon_3\, e_1$, where

$$\Upsilon_1 = \frac{1}{2}(g_{11}a + g_{12}b + g_{13}c) \qquad \Upsilon_2 = \frac{1}{2}(g_{12}a + g_{22}b + g_{23}c) \qquad \Upsilon_3 = \frac{1}{2}(g_{13}a + g_{23}b + g_{33}c)$$

and

$$
\begin{aligned}
a = {} & c_1\frac{\partial\xi_1}{\partial x}\xi_1 + c_1\frac{\partial\xi_1}{\partial y}\xi_2 + c_1\frac{\partial\xi_1}{\partial z}\xi_3 + c_2\frac{\partial\eta_1}{\partial x}\eta_1 + c_2\frac{\partial\eta_1}{\partial y}\eta_2 + c_2\frac{\partial\eta_1}{\partial z}\eta_3 + c_3\frac{\partial\lambda_1}{\partial x}\lambda_1 + c_3\frac{\partial\lambda_1}{\partial y}\lambda_2\\
& + c_3\frac{\partial\lambda_1}{\partial z}\lambda_3 + g^{11}\Gamma^1_{11} + 2g^{12}\Gamma^1_{12} + 2g^{13}\Gamma^1_{13} + g^{22}\Gamma^1_{22} + 2g^{23}\Gamma^1_{23} + g^{33}\Gamma^1_{33}
\end{aligned}
$$

$$
\begin{aligned}
b = {} & c_1\frac{\partial\xi_2}{\partial x}\xi_1 + c_1\frac{\partial\xi_2}{\partial y}\xi_2 + c_1\frac{\partial\xi_2}{\partial z}\xi_3 + c_2\frac{\partial\eta_2}{\partial x}\eta_1 + c_2\frac{\partial\eta_2}{\partial y}\eta_2 + c_2\frac{\partial\eta_2}{\partial z}\eta_3 + c_3\frac{\partial\lambda_2}{\partial x}\lambda_1 + c_3\frac{\partial\lambda_2}{\partial y}\lambda_2\\
& + c_3\frac{\partial\lambda_2}{\partial z}\lambda_3 + g^{11}\Gamma^2_{11} + 2g^{12}\Gamma^2_{12} + 2g^{13}\Gamma^2_{13} + g^{22}\Gamma^2_{22} + 2g^{23}\Gamma^2_{23} + g^{33}\Gamma^2_{33}
\end{aligned}
$$

$$
\begin{aligned}
c = {} & c_1\frac{\partial\xi_3}{\partial x}\xi_1 + c_1\frac{\partial\xi_3}{\partial y}\xi_2 + c_1\frac{\partial\xi_3}{\partial z}\xi_3 + c_2\frac{\partial\eta_3}{\partial x}\eta_1 + c_2\frac{\partial\eta_3}{\partial y}\eta_2 + c_2\frac{\partial\eta_3}{\partial z}\eta_3 + c_3\frac{\partial\lambda_3}{\partial x}\lambda_1 + c_3\frac{\partial\lambda_3}{\partial y}\lambda_2\\
& + c_3\frac{\partial\lambda_3}{\partial z}\lambda_3 + g^{11}\Gamma^3_{11} + 2g^{12}\Gamma^3_{12} + 2g^{13}\Gamma^3_{13} + g^{22}\Gamma^3_{22} + 2g^{23}\Gamma^3_{23} + g^{33}\Gamma^3_{33}
\end{aligned}
$$

Let $\tilde{f} = f e_1 \in \Gamma(E)$. Then, the differential operator H of order 2 defined by

$$H(\tilde{f}) = \Delta(f)e_1 \tag{3.14}$$

is a generalized Laplacian on E.

Proof. We use the same scheme as in the case $m = 2$.
We first developp (3.13) to obtain

$$
\begin{aligned}
\Delta(f) = {} & -\Big(c_1{\xi_1}^2 + c_2{\eta_1}^2 + c_3{\lambda_1}^2\Big)\frac{\partial^2 f}{\partial x^2} - \Big(c_1{\xi_2}^2 + c_2{\eta_2}^2 + c_3{\lambda_2}^2\Big)\frac{\partial^2 f}{\partial y^2} - \Big(c_1{\xi_3}^2 + c_2{\eta_3}^2\\
& + c_3{\lambda_3}^2\Big)\frac{\partial^2 f}{\partial z^2} - \Big(2c_1\xi_1\xi_2 + 2c_2\,\eta_1\eta_2 + 2c_3\lambda_1\lambda_2\Big)\frac{\partial^2 f}{\partial x\partial y} - \Big(2c_1\xi_1\xi_3 + 2c_2\,\eta_1\eta_3
\end{aligned}
$$

$$
\begin{aligned}
&+ 2c_3\lambda_1\lambda_3\Big)\frac{\partial^2 f}{\partial x\partial z} + \Big(2c_1\xi_2\xi_3 + 2\,c_2\eta_2\eta_3 + 2c_3\lambda_2\lambda_3\Big)\frac{\partial^2 f}{\partial y\partial z}\\
&- \frac{\partial f}{\partial x}\Big(c_1\frac{\partial \xi_1}{\partial x}\xi_1 + c_1\frac{\partial \xi_1}{\partial y}\xi_2 + c_1\frac{\partial \xi_1}{\partial z}\xi_3 + c_2\frac{\partial \eta_1}{\partial x}\eta_1 + c_2\frac{\partial \eta_1}{\partial y}\eta_2 + c_2\frac{\partial \eta_1}{\partial z}\eta_3 + c_3\frac{\partial \lambda_1}{\partial x}\lambda_1\\
&+ c_3\frac{\partial \lambda_1}{\partial y}\lambda_2 + c_3\frac{\partial \lambda_1}{\partial z}\lambda_3\Big)\\
&- \frac{\partial f}{\partial y}\Big(c_1\frac{\partial \xi_2}{\partial x}\xi_1 + c_1\frac{\partial \xi_2}{\partial y}\xi_2 + c_1\frac{\partial \xi_2}{\partial z}\xi_3 + c_2\frac{\partial \eta_2}{\partial x}\eta_1 + c_2\frac{\partial \eta_2}{\partial y}\eta_2 + c_2\frac{\partial \eta_2}{\partial z}\eta_3 + c_3\frac{\partial \lambda_2}{\partial x}\lambda_1\\
&+ c_3\frac{\partial \lambda_2}{\partial y}\lambda_2 + c_3\frac{\partial \lambda_2}{\partial z}\lambda_3\Big)\\
&- \frac{\partial f}{\partial z}\Big(c_1\frac{\partial \xi_3}{\partial x}\xi_1 + c_1\frac{\partial \xi_3}{\partial y}\xi_2 + c_1\frac{\partial \xi_3}{\partial z}\xi_3 + c_2\frac{\partial \eta_3}{\partial x}\eta_1 + c_2\frac{\partial \eta_3}{\partial y}\eta_2 + c_2\frac{\partial \eta_3}{\partial z}\eta_3 + c_3\frac{\partial \lambda_3}{\partial x}\lambda_1\\
&+ c_3\frac{\partial \lambda_3}{\partial y}\lambda_2 + c_3\frac{\partial \lambda_3}{\partial z}\lambda_3\Big)
\end{aligned}
$$

Then we search (g, ∇^E, F) such that $H = \Delta^E + F$ over the Riemannian manifold (X, g). The connection ∇^E being defined by $\nabla^E_{\partial_x} e_1 = \Upsilon_1\, e_1$, $\nabla^E_{\partial_y} e_1 = \Upsilon_2\, e_1$ and $\nabla^E_{\partial_z} e_1 = \Upsilon_3\, e_1$ for some functions Υ_1, Υ_2 and Υ_3, we obtain

$$
\begin{aligned}
\Delta^E(\tilde{f}) = &-g^{11}\frac{\partial^2 f}{\partial x^2}e_1 - g^{22}\frac{\partial^2 f}{\partial y^2}e_1 - g^{33}\frac{\partial^2 f}{\partial z^2}e_1 - 2g^{12}\frac{\partial^2 f}{\partial x\partial y}e_1 - 2g^{13}\frac{\partial^2 f}{\partial x\partial z}e_1 - 2g^{23}\frac{\partial^2 f}{\partial y\partial z}e_1\\
&+ \frac{\partial f}{\partial x}\Big(- 2g^{11}\Upsilon_1 + g^{11}\Gamma^1_{11} - 2g^{12}\Upsilon_2 + 2g^{12}\Gamma^1_{12} - 2g^{13}\Upsilon_3 + 2g^{13}\Gamma^1_{13} + g^{22}\Gamma^1_{22}\\
&+ 2g^{23}\Gamma^1_{23} + g^{33}\Gamma^1_{33}\Big)e_1\\
&+ \frac{\partial f}{\partial y}\Big(g^{11}\Gamma^2_{11} - 2g^{12}\Upsilon_1 + 2g^{12}\Gamma^2_{12} + 2g^{13}\Gamma^2_{13} - 2g^{22}\Upsilon_2 + g^{22}\Gamma^2_{22} - 2g^{23}\Upsilon_3\\
&+ 2g^{23}\Gamma^2_{23} + g^{33}\Gamma^2_{33}\Big)e_1\\
&+ \frac{\partial f}{\partial z}\Big(g^{11}\Gamma^3_{11} + 2g^{12}\Gamma^3_{12} - 2g^{13}\Upsilon_1 + 2g^{13}\Gamma^3_{13} + g^{22}\Gamma^3_{22} - 2g^{23}\Upsilon_2 + 2g^{23}\Gamma^3_{23}\\
&- 2g^{33}\Upsilon_3 + g^{33}\Gamma^3_{33}\Big)e_1\\
&+ f\Big(- g^{11}\frac{\partial \Upsilon_1}{\partial x} - g^{11}(\Upsilon_1)^2 + g^{11}\Gamma^1_{11}\Upsilon_1 + g^{11}\Gamma^2_{11}\Upsilon_2 + g^{11}\Gamma^3_{11}\Upsilon_3 - g^{12}\frac{\partial \Upsilon_2}{\partial x} - g^{12}\frac{\partial \Upsilon_1}{\partial y}\\
&- 2g^{12}\Upsilon_1\Upsilon_2 + 2g^{12}\Gamma^1_{12}\Upsilon_1 + 2g^{12}\Gamma^2_{12}\Upsilon_2 + 2g^{12}\Gamma^3_{12}\Upsilon_3 - g^{13}\frac{\partial \Upsilon_3}{\partial x} - g^{13}\frac{\partial \Upsilon_1}{\partial z} - 2g^{13}\Upsilon_1\Upsilon_3\\
&+ 2g^{13}\Gamma^1_{13}\Upsilon_1 + 2g^{13}\Gamma^2_{13}\Upsilon_2 + 2g^{13}\Gamma^3_{13}\Upsilon_3 - g^{22}\frac{\partial \Upsilon_2}{\partial y} - g^{22}(\Upsilon_2)^2 + g^{22}\Gamma^1_{22}\Upsilon_1 + g^{22}\Gamma^2_{22}\Upsilon_2\\
&+ g^{22}\Gamma^3_{22}\Upsilon_3 - g^{23}\frac{\partial \Upsilon_3}{\partial y} - g^{23}\frac{\partial \Upsilon_2}{\partial z} - 2g^{23}\Upsilon_2\Upsilon_3 + 2g^{23}\Gamma^1_{23}\Upsilon_1 + 2g^{23}\Gamma^2_{23}\Upsilon_2 + 2g^{23}\Gamma^3_{23}\Upsilon_3\\
&- g^{33}\frac{\partial \Upsilon_3}{\partial z} - g^{33}(\Upsilon_3)^2 + g^{33}\Gamma^1_{33}\Upsilon_1 + g^{33}\Gamma^2_{33}\Upsilon_2 + g^{33}\Gamma^3_{33}\Upsilon_3\Big)e_1
\end{aligned}
$$

Identifying second order parts, we obtain the coefficients g^{ij}. Identifying first-order parts,

we have three equalities

$$\begin{aligned} 2g^{11}\Upsilon_1 + 2g^{12}\Upsilon_2 + 2g^{13}\Upsilon_3 &= c_1\frac{\partial\xi_1}{\partial x}\xi_1 + c_1\frac{\partial\xi_1}{\partial y}\xi_2 + c_1\frac{\partial\xi_1}{\partial z}\xi_3 + c_2\frac{\partial\eta_1}{\partial x}\eta_1 + c_2\frac{\partial\eta_1}{\partial y}\eta_2 \\ &+c_2\frac{\partial\eta_1}{\partial z}\eta_3 + c_3\frac{\partial\lambda_1}{\partial x}\lambda_1 + c_3\frac{\partial\lambda_1}{\partial y}\lambda_2 + c_3\frac{\partial\lambda_1}{\partial z}\lambda_3 + g^{11}\Gamma_{11}^1 \\ &+2g^{12}\Gamma_{12}^1 + 2g^{13}\Gamma_{13}^1 + g^{22}\Gamma_{22}^1 + 2g^{23}\Gamma_{23}^1 + g^{33}\Gamma_{33}^1 \end{aligned} \tag{3.15}$$

$$\begin{aligned} 2g^{12}\Upsilon_1 + 2g^{22}\Upsilon_2 + 2g^{23}\Upsilon_3 &= c_1\frac{\partial\xi_2}{\partial x}\xi_1 + c_1\frac{\partial\xi_2}{\partial y}\xi_2 + c_1\frac{\partial\xi_2}{\partial z}\xi_3 + c_2\frac{\partial\eta_2}{\partial x}\eta_1 + c_2\frac{\partial\eta_2}{\partial y}\eta_2 \\ &+c_2\frac{\partial\eta_2}{\partial z}\eta_3 + c_3\frac{\partial\lambda_2}{\partial x}\lambda_1 + c_3\frac{\partial\lambda_2}{\partial y}\lambda_2 + c_3\frac{\partial\lambda_2}{\partial z}\lambda_3 + g^{11}\Gamma_{11}^2 \\ &+2g^{12}\Gamma_{12}^2 + 2g^{13}\Gamma_{13}^2 + g^{22}\Gamma_{22}^2 + 2g^{23}\Gamma_{23}^2 + g^{33}\Gamma_{33}^2 \end{aligned} \tag{3.16}$$

$$\begin{aligned} 2g^{13}\Upsilon_1 + 2g^{23}\Upsilon_2 + 2g^{33}\Upsilon_3 &= c_1\frac{\partial\xi_3}{\partial x}\xi_1 + c_1\frac{\partial\xi_3}{\partial y}\xi_2 + c_1\frac{\partial\xi_3}{\partial z}\xi_3 + c_2\frac{\partial\eta_3}{\partial x}\eta_1 + c_2\frac{\partial\eta_3}{\partial y}\eta_2 \\ &+c_2\frac{\partial\eta_3}{\partial z}\eta_3 + c_3\frac{\partial\lambda_3}{\partial x}\lambda_1 + c_3\frac{\partial\lambda_3}{\partial y}\lambda_2 + c_3\frac{\partial\lambda_3}{\partial z}\lambda_3 + g^{11}\Gamma_{11}^3 \\ &+2g^{12}\Gamma_{12}^3 + 2g^{13}\Gamma_{13}^3 + g^{22}\Gamma_{22}^3 + 2g^{23}\Gamma_{23}^3 + g^{33}\Gamma_{33}^3 \end{aligned} \tag{3.17}$$

Denoting by a resp. b resp. c the right term of (3.15) resp. (3.16) resp. (3.17), we obtain the system

$$2\begin{pmatrix} g^{11} & g^{12} & g^{13} \\ g^{12} & g^{22} & g^{23} \\ g^{13} & g^{23} & g^{33} \end{pmatrix}\begin{pmatrix} \Upsilon_1 \\ \Upsilon_2 \\ \Upsilon_3 \end{pmatrix} = \begin{pmatrix} a \\ b \\ c \end{pmatrix}$$

whose solution is

$$\begin{pmatrix} \Upsilon_1 \\ \Upsilon_2 \\ \Upsilon_3 \end{pmatrix} = \frac{1}{2}\begin{pmatrix} g_{11} & g_{12} & g_{13} \\ g_{12} & g_{22} & g_{23} \\ g_{13} & g_{23} & g_{33} \end{pmatrix}\begin{pmatrix} a \\ b \\ c \end{pmatrix}$$

At last, the section $F \in \Gamma(\mathrm{End}(E))$ corresponds to the zero order part in the expression of Δ^E. □

Proposition 3.4 *Let (X, g), E and ∇^E of the previous Proposition.*
Let $\gamma(t) = (\gamma_1(t), \gamma_2(t), \gamma_3(t))$ a C^1 curve in X such that $\gamma(0) = y$, and $Y_0 = Y_0^1 e_1(y)$. Then, the parallel transport Y of Y_0 along γ is defined by

$$Y(t) = Y_0^1\, exp\left(-\int_0^t \dot\gamma_1(s)\Upsilon_1(\gamma(s)) + \dot\gamma_2(s)\Upsilon_2(\gamma(s)) + \dot\gamma_3(s)\Upsilon_3(\gamma(s))\ ds\right) e_1(\gamma(t))$$

Proof. The parallel transport of Y_0 along γ is the solution $Y(t) = Y^1(t)\, e_1(\gamma(t))$ of the differential equation

$$\begin{cases} \nabla^E_{\dot\gamma} Y(t) = 0 \\ \\ Y(0) = Y_0 \end{cases} \tag{3.18}$$

$$\nabla^E_{\dot\gamma} Y(t) = \nabla^E_{\dot\gamma}(Y^1\, e_1)(t)$$

$$= \frac{\partial Y^1}{\partial t}(t) e_1(\gamma(t)) + Y^1(t)\Big(\dot\gamma_1(t)\nabla^E_{\partial_x} e_1(\gamma(t)) + \dot\gamma_2(t)\nabla^E_{\partial_y} e_1(\gamma(t)) + \dot\gamma_3(t)\nabla^E_{\partial_z} e_1(\gamma(t))\Big)$$

$$= \frac{\partial Y^1}{\partial t}(t) e_1(\gamma(t)) + Y^1(t)\Big(\dot\gamma_1(t)\Upsilon_1(t) e_1(\gamma(t)) + \dot\gamma_2(t)\Upsilon_2(t) e_1(\gamma(t)) + \dot\gamma_3(t)\Upsilon_3(t) e_1(\gamma(t))\Big)$$

Finally, we obtain an ordinary differential equation

$$\begin{cases} \dfrac{\partial Y^1}{\partial t}(t) &= -\Big(\dot\gamma_1(t)\Upsilon_1(t) + \dot\gamma_2(t)\Upsilon_2(t) + \dot\gamma_3(t)\Upsilon_3(t)\Big) Y^1(t) \\ Y^1(0) &= Y^1_0 \end{cases}$$

from which we deduce the solution of (3.18). □

4 Clifford bundles : a unifying framework for images(videos), vector fields and orthonormal frame fields regularization

Cette Section correspond à la soumission [8]. Une version préliminaire a fait l'objet de la publication [7].

Remarque. Dans cette Section, nous suivons les définitions de [55]. Les fibrés que nous considérons sont alors supposés lisses. De plus, une algèbre de Clifford est définie de la manière suivante.

Définition 17 *Soit V un espace vectoriel sur $\mathbb{R}$ de dimension finie muni d'une forme quadratique Q. On note $T(V)$ l'algèbre tensorielle de V, i.e.*

$$T(V) := \bigoplus_{i=0}^{\infty} V^{\otimes i} = \mathbb{R} \oplus V \oplus (V \otimes V) \oplus \cdots$$

L'algèbre de Clifford $Cl(V,Q)$ est le quotient

$$Cl(V,Q) = T(V) \Big/ (x \otimes x + Q(x)1)$$

de $T(V)$ par l'idéal bilatère engendré par les éléments de type $x \otimes x + Q(x)1$ pour $x \in V$.

Une algèbre de Clifford ainsi définie possède les mêmes propriétés que celles de la Définition 1, à l'exception que les vecteurs de base e_i satisfont la relation $e_i^2 = -Q(e_i)$.

4.1 Introduction

Most multivalued image smoothing process are based on PDE's of the form

$$\frac{\partial I^i}{\partial t} = \sum_{j,k=1}^{2} f_{jk} \frac{\partial^2 I^i}{\partial j \, \partial k} + \text{first-order part}$$

of initial condition $I\colon (x,y) \longmapsto (I^1(0,x,y), \cdots, I^n(0,x,y))$ a nD image, where f_{jk} are real functions. We refer to [83] for an overview on related works. From a geometric viewpoint, the set of right terms, for $i = 1 \cdots n$, may be viewed as a second-order differential operator acting on sections of a vector bundle over a Riemannian manifold called a **generalized Laplacian** H [13]. As a consequence, it ensures existence and unicity of a kernel $K_t(x,y,H)$, called the **heat kernel of** H, generating the solution of the heat equation

$$\frac{\partial I}{\partial t} + HI = 0 \tag{4.1}$$

from a 'convolution' with the initial condition. For arbitrary Riemannian manifold and vector bundle, it is usually impossible to find a closed form for this kernel, and consequently a closed form of the solution. However, for the problem we consider in this paper,

the use of an approximate solution appears to be sufficient. A generalized Laplacian H on a vector bundle E over a Riemannian manifold X is determined by three pieces of data : the metric g of the base manifold X that determines the second order part, a connection on E that determines the first order part, and a section $F \in \Gamma(\mathrm{End}(E))$ that determines the zero order part. It follows that the anisotropy of a regularization is determined by these data. For example, the so-called oriented Laplacians may be viewed as generalized Laplacians [6]. Similarly, on the vector bundle $C^\infty(X)$ of smooth functions on X, there is a canonical generalized Laplacian, the scalar Laplacian, which corresponds to the Laplace-Beltrami operator up to a sign. Considering each component Ik of a nD image as a function over a well-chosen Riemannian manifold, we obtain the Beltrami flow of Sochen et al. in the context of image regularization [74],[77]. The aim of this paper is to show that this Beltrami flow, acting on $C^\infty(X)$, can be extended in a natural way to tangent vector fields and oriented orthonormal frame fields on (X, g) by considering the Clifford bundle of (X, g). The former is devoted to regularization of vector fields on the charts, the latter to regularization of orthonormal frame fields on the charts with respect to the metric g.

Both isotropic and anisotropic regularizations of fields differing from nD images(videos) were widely investigated. Concerning vector fields, we may refer to [25],[83] where the smoothing is made through the smoothing of a corresponding image and where the anisotropy is controlled at each point by the orientation of the vector field. More precisely, an oriented Laplacian is applied on each component of the image. Concerning $\mathrm{SO}(n)$-valued fields, we may refer to [45] in the framework of principal bundles, where the anisotropy is determined by the flow itself too. In this paper, the context is slightly different since the anisotropy of the regularization is entirely determined by the geometry of the manifold where fields are defined. Additionally, let us refer to [81] for S^n-valued fieds regularization and [20] for constrained matrix-valued fields regularization.

Generalizing the Laplace-Beltrami operator acting on functions to tangent vector fields and oriented orthonormal frame fields is not straightforward. This was introduced in [7] for X of dimension $m = 2$. First, considering the Clifford bundle $Cl(X, g)$ of X [55], both functions and tangent vector fields may be viewed as sections of $Cl(X, g)$. This is not the case for oriented orthonormal frame fields but, by the trivializations of the fiber bundle, oriented orthonormal frame fields are locally mappings from X to $\mathrm{SO}(m)$, and sections of $Cl(X, g)$ with values in the bivector part are locally mappings from X to $\mathfrak{so}(m)$. By the canonical isomorphism between the bundle of differential forms of a Riemannian manifold and its Clifford bundle, the Hodge Laplacian Δ [24] may be viewed as a generalized Laplacian on $Cl(X, g)$ and its restriction to functions is minus the Laplace-Beltrami operator. As a consequence, it makes sense to consider the flow generated by the solution of the heat equation $\partial I/\partial t + \Delta I = 0$ on $Cl(X, g)$, that provides anisotropic smoothing of the initial condition. By construction of the Clifford bundle, the anisotropy is determined by the metric of the base manifold. From now on, we call **Clifford-Hodge Laplacian** the Hodge Laplacian on $Cl(X, g)$. In particular, the Clifford-Hodge Laplacian preserves the structures of functions, tangent vector fields and bivector-valued fields. Whereas smoothing of functions and tangent vector fields is done in a natural way, the regularization of oriented orthonormal frame fields needs the use of the exponential map of $\mathrm{SO}(m)$.

Clifford algebras framework [21],[47] finds a wide range of applications in computer science [75]. Application of Clifford bundles to image processing was introduced in [3] where the Di Zenzo's gradient, devoted to nD image segmentation, is generalized using

covariant derivatives instead of usual derivatives. Most properties of Clifford algebras we use in this paper are presented in [3].
This paper is organized as follows. Section 4.2 is devoted to introduce heat equations on vector bundles associated to generalized Laplacians. In particular, we discuss approximations of the solutions. It requires to determine geodesic curves and compute geodesic distances on the base manifold, and to compute the parallel transport map on the vector bundle. We treat the particular case of the scalar Laplacian, and relate it with the Laplace-Beltrami operator. In Section 4.3, we introduce the Clifford bundle $Cl(X,g)$. We determine the connection on $Cl(X,g)$ and the section $F \in \Gamma(\mathrm{End}(Cl(X,g)))$ that make the Clifford-Hodge Laplacian be a generalized Laplacian on $Cl(X,g)$. Then, we detail the method to regularize oriented orthonormal frame fields. In Section 4.4, we treat the case $m = 2$. We first compute explicit formulae of Δ and transport parallel map on $Cl(X,g)$ for X of dimension 2 . Then, we are concerned in the particular case of images. We construct the Riemannian manifold being the base manifold of the Clifford bundle we consider, and a global frame field of the tangent bundle, generating a global frame field of the Clifford bundle. At last, we present applications to regularization of a color image, and regularizations of a vector field and a orientation field related to the image. In Section 4.5, we treat the case $m = 3$. We first compute explicit formulae of Δ and transport parallel map on $Cl(X,g)$, for X of dimension 3. Then, we are concerned in the particular case of videos. We construct the Riemannian manifold being the base manifold of the Clifford bundle we consider. At last, we present an application to regularization of a color video.

4.2 Heat equations on vector bundles

For details on this part, see [13].

4.2.1 Generalized Laplacians on vector bundles

We refer to [54],[78] for an introduction to differential geometry. For a smooth vector bundle E over a manifold X, the symbol $\Gamma(E)$ denotes the space of smooth sections of E. For $x \in X$, E_x denotes the fiber over x.

Definition 4.1 *Let E be a vector bundle over a Riemannian manifold (X,g). A **generalized Laplacian** on E is a second-order differential operator $H\colon \Gamma(E) \longrightarrow \Gamma(E)$, that may be written*

$$H = -\sum_{ij} g^{ij}(x)\partial_i\,\partial_j \;+\; \textit{first-order part}$$

in any local coordinates system, where $(g^{ij}(x))$ is the inverse of the matrix $g(x) = (g_{ij}(x))$.

The heat kernel of a generalized Laplacian on a vector bundle E is related with a connection on E.

Definition 4.2 *Let E be a vector bundle over a Riemannian manifold (X, g), endowed with a connection ∇^E. Since (X, g) is Riemannian, it possesses a canonical connection, the Levi-Cevita connection ∇. To any pair of tangent vector fields V and W on X, we associate an invariant second derivative $\nabla^2_{V,W} : \Gamma(E) \longrightarrow \Gamma(E)$ by setting*

$$\nabla^2_{V,W}\varphi \equiv \nabla^E_V \nabla^E_W \varphi - \nabla^E_{\nabla_V W}\varphi \tag{4.2}$$

*Then, the **connection Laplacian** $\Delta^E : \Gamma(E) \longrightarrow \Gamma(E)$ is defined by*

$$\Delta^E\varphi = -trace(\nabla^2_{\cdot,\cdot}\varphi)$$

where trace denotes the contraction with the metric g.

In particular, if e_i is a local orthonormal frame of TX, the operator Δ^E is given by

$$\Delta^E = -\sum_i \left(\nabla^E_{e_i}\nabla^E_{e_i} - \nabla^E_{\nabla_{e_i}e_i}\right)$$

With respect to the frame $\partial_i := \partial/\partial x_i$ defined by a coordinates system around a point in X, the operator Δ^E equals

$$\Delta^E = -\sum_{ij} g^{ij}\left(\nabla^E_{\partial_i}\nabla^E_{\partial_j} - \sum_k \Gamma^k_{ij}\nabla^E_{\partial_k}\right) \tag{4.3}$$

where Γ^k_{ij}'s are defined by $\nabla_{\partial_i}\partial_j = \sum_k \Gamma^k_{ij}\partial_k$.

We have the following result :
Any generalized Laplacian is of the form $\Delta^E + F$, where Δ^E is the connection Laplacian associated to some connection ∇^E, and F is a section of the bundle End(E). In particular, any connection Laplacian Δ^E is a generalized Laplacian.

4.2.2 The heat kernel of a generalized Laplacian

To any generalized Laplacian H, one may associate an operator $e^{-tH} : \Gamma(E) \longrightarrow \Gamma(E)$, for $t > 0$, with the property that $I(t, x) = e^{-tH}I(x)$ satisfies the heat equation $\partial I/\partial t + HI = 0$.
We shall define e^{-tH} as an integral operator of the form

$$(e^{-tH}I)(x) = \int_X K_t(x, y, H)I(y)dy \tag{4.4}$$

where $K_t(x, y, H) : E_y \longrightarrow E_x$ is a linear map depending smoothly on x, y and t. This kernel K is called the **heat kernel of** H.

In the following theorem, we give some results on approximations of the heat kernel and solutions of the heat equation.

Theorem 4.1 *Let $x \in X$ and a normal coordinates system around x, we denote by $\mathbf{y^i}$ the normal coordinates of a point y in the injectivity radius of X at x, ∂_i the corresponding*

partial derivatives, and by $g_{ij}(\mathbf{y})$ *the scalar product of* ∂_i *and* ∂_j *at* $\mathbf{y}$*. Moreover, we define*

$$J(x,y) = det(g_{ij}(\mathbf{y}))^{1/2} \qquad for\ y = exp_x(\mathbf{y})$$

Let ϵ *chosen smaller than the injectivy radius of* X*. Let* $\Psi\colon \mathbb{R}_+ \longrightarrow [0,1]$ *be a smooth function such that* $\Psi(s) = 1$ *if* $s < \epsilon^2/4$ *and* $\Psi(s) = 0$ *if* $s > \epsilon^2$*.*
Let $\tau(x,y)\colon E_y \longrightarrow E_x$ *be the parallel transport along the unique geodesic curve joining* x *and* y*, and* $d(x,y)$ *its length.*
Let $K_t^N(x,y,H)$ *be the kernel defined by*

$$\Big(\frac{1}{4\pi t}\Big)^{\frac{m}{2}} e^{-d(x,y)^2/4t}\ \Psi(d(x,y)^2) \sum_{i=0}^{N} t^i \Phi_i(x,y,H) J(x,y)^{-\frac{1}{2}}$$

where the sections Φ_i *are given by* $\Phi_0(x,y,H) = \tau(x,y)$ *and*

$$\tau(x,y)^{-1}\Phi_i(x,y,H) = -\int_0^1 s^{i-1}\tau(x_s,y)^{-1}(B_x.\Phi_{i-1})(x_s,y,H)ds$$

B_x *is the operator* $J^{1/2} \circ H_x \circ J^{-1/2}$ *where* H_x *is the operator* H *with respect to the first variable.*

1. For every $N > m/2$*, the kernel* $K_t^N(x,y,H)$ *is asymptotic to* $K_t(x,y,H)$ *:*

$$\Big\| \partial_t^k \big[\, K_t(x,y,H) - K_t^N(x,y,H)\,\big] \Big\|_l = O(t^{N-m/2-l/2-k})$$

where $\|\ \|_l$ *is a norm on* C^l *sections.*

2. Let us denote by k_t^N *the operator defined by*

$$(k_t^N I)(x) = \int_X K_t^N(x,y,H) I(y) dy \tag{4.5}$$

Then for every N*,* $\lim_{t\to 0} \|k_t^N I - I\|_l = 0$*.*

3. We have the following estimate :

$$\Big\| e^{-tH} I - \sum_{i=0}^{k} \frac{(-tH)^i}{i!} I \Big\|_j = O(t^{k+1})$$

which justifies the notation e^{-tH}*.*

In the sequel, we make use the following property :

(P1) $J(x,y) = 1 + O(\|\mathbf{y}\|^2)$.

4.2.3 Discrete approximations of heat equations solutions

As mentionned above, for arbitrary base manifold and vector bundle, it is not possible to compute the solution of the equation (4.1), but for the problem we consider in

this paper, the computation of an approximation of (4.4) appears to be sufficient. A natural choice is to consider the operator k_t^N (4.5), for some N. Additionally, there is a freedom in the choice of the function Ψ of Theorem 4.1, that determines the neighborhoods where the convolutions are computed. For the problem we consider in this paper, we need to compute discretizations of such approximations. As a consequence, the function Ψ determines the size of the masks involved in the discrete convolutions. From (P1), we approximate $J(x,y)$ by 1.

Let us first consider the particular case of the operator k_t^0, defined by

$$\begin{aligned}(k_t^0 I)(x) &= \int_X K_t^0(x,y,H)I(y)dy \\ &= \left(\frac{1}{4\pi t}\right)^{\frac{m}{2}} \int_X e^{-d(x,y)^2/4t}\ \Psi(d(x,y)^2)\,\tau(x,y)I(y)\,J(x,y)^{-\frac{1}{2}}\,dy\end{aligned}$$

We discretize it as the discrete convolution of $\tau(x,y)I(y)$ with a mask whose inputs are geodesic distances from the current point to x (up to the normalization of the mask).

Remark. the kernel K_t^0 entirely depends on the metric of the base manifold and the parallel transport map of the vector bundle. The first one determines geodesics and their lengths on the base manifold, the second one the map τ. As a consequence, any generalized Laplacian on a vector bundle equipped with a connection generates the same operator k_t^0, and the subsequent diffusion process.

As last, let us mention that the Euler scheme may be obtained from this point of view. We have $\tau(x,x) = Id$ and $\Phi_1(x,x,H) = -J^{1/2} \circ H \circ J^{-1/2}(x,x)$. Then, considering the operator k_t^1 of (4.5), defined by

$$\begin{aligned}(k_t^1 I)(x) &= \int_X K_t^1(x,y,H)I(y)dy \\ &= \left(\frac{1}{4\pi t}\right)^{\frac{m}{2}} \int_X e^{-d(x,y)^2/4t}\,\Psi(d(x,y)^2)\,(\tau(x,y) + t\Phi_1(x,y,H))I(y)\,J(x,y)^{-\frac{1}{2}}\,dy\end{aligned}$$

and choosing Ψ generating sufficiently small neighborhoods, we obtain that the discretization of $k_t^1 I$ at a point x results from the convolution of $(\tau(x,y) + t\Phi_1(x,y,H))I(y)$ with a normalized 1x1 mask, i.e. with 1. In other words, we have

$$I(x) - tHI(x) \tag{4.6}$$

This is the Euler scheme of (4.1).

4.2.4 An example : the scalar/Beltrami Laplacian

The scalar Laplacian on a Riemannian manifold (X,g) of dimension m is the connection Laplacian (4.3) on the vector bundle $E = C^\infty(X)$. In other words, it is the connection Laplacian on a smooth vector bundle E of rank 1 with connection ∇^E defined by the symbols

$$\Upsilon_1 = \cdots = \Upsilon_m = 0$$

i.e. $\nabla_X^E(f) = d_X f$. It follows the transport parallel map on $C^\infty(X)$

Proposition 4.1 *Let (X, g), E and ∇^E as defined above, γ be a C^1 curve in X such that $\gamma(0) = y$. Then, the parallel transport Y along γ of the scalar $Y_0 = Y_0^1 1(y)$ is $Y(t) = Y_0^1 1(\gamma(t))$.*

In local coordinates, the scalar Laplacian is defined by

$$\Delta(f) = -\sum_{ij} g^{ij}\Big(\partial_i\partial_j - \sum_k \Gamma_{ij}^k \partial_k\Big) f \tag{4.7}$$

The Laplace-Beltrami operator Δ_g is the differential operator of order 2 on $C^\infty(X)$ defined by

$$\Delta_g(f) = \frac{1}{\sqrt{g}} \sum_{jk} \partial_j(\sqrt{g} g^{jk} \partial_k f)$$

It is well-known that if a Riemannian manifold (X, g) is equipped with the Levi-Cevita connection, then Δ_g is minus the scalar Laplacian (4.7). This makes the PDE's $\partial I/\partial t = \Delta_g I$ and $\partial I/\partial t + \Delta I = 0$ be equivalent.

4.3 The Clifford-Hodge Laplacian : an extension of the scalar Laplacian for multivector fields smoothing

4.3.1 The Clifford-Hodge Laplacian : a generalized Laplacian on the Clifford bundle of a Riemannian manifold

The Hodge Laplacian Δ is a generalized Laplacian acting on differential forms of a Riemannian manifold. It is defined by

$$\Delta = d\delta + \delta d$$

where d is the exterior derivative operator and δ its formal adjoint [24].
In particular, when applied to 0-forms, i.e. functions, Δ corresponds to the scalar Laplacian (4.7).

One of the main ideas of this paper is the following : the Hodge Laplacian can also be applied to tangent vector fields and generators of orthonormal frame fields by considering the Clifford bundle of X.

Definition 4.3 (Clifford bundle) *Let (X, g) be a Riemannian manifold, and let us denote by TX its tangent bundle. The Clifford bundle $Cl(X, g)$ of (X, g) is the quotient bundle*

$$Cl(X, g) = \mathcal{T}(TX) \Big/ I(TX)$$

where $\mathcal{T}(TX)$ is the bundle whose fiber at $x \in X$ is the tensor algebra of T_xX and $I(TX)$ is the bundle whose fiber at $x \in X$ is the two-sided ideal $I(T_xX)$ in $\mathcal{T}(T_xX)$, generated by elements $v \otimes v + \|v\|^2$ for $v \in T_xX$.

We obtain a bundle of Clifford algebras over X, and the fiberwise multiplication in $Cl(X, g)$ gives an algebra structure to the space $\Gamma(Cl(X, g))$ of sections of $Cl(X, g)$.

More precisely, let $(e_1, \cdots, e_m)$ be a local oriented orthonormal frame field on $\Omega \subset X$. Then, any section s of $Cl(X, g)$ takes the form

$$s = s_1\, 1 + s_2\, e_1 + s_{m+1}\, e_m + \cdots + s_{2^m}\, e_1 \cdots e_m$$

on Ω, for some functions $s_{i_1 \cdots i_k}$ defined on Ω where $i_1 < \cdots < i_k$ and $k \in \{1 \cdots m\}$.

Given a finite-dimensional vector space V equipped with a quadratic form Q, there is a vector space isomorphism between the exterior algebra $\bigwedge V$ of V and $Cl(V, Q)$. In particular, if $Q \equiv 0$, they are isomorphic as algebras. Let (X, g) be a Riemannian manifold, we denote by $\bigwedge T^*X$ the bundle of differential forms of (X, g). By the constructions of $\bigwedge T^*X$ and $Cl(X, g)$ as associated bundles to the principal bundle $\mathrm{PSO}(X)$ of oriented orthonormal frame fields of (X, g), it follows a canonical vector bundle isomorphism between $\bigwedge T^*X$ and $Cl(X, g)$. As a consequence, we may identify $\Gamma(\bigwedge T^*X)$ and $\Gamma(Cl(X, g))$, as follows

$$\text{k-form} : \sum_{\substack{i_1 < \cdots < i_k \\ 1 \leqslant i_k \leqslant m}} \omega_{i_1 \cdots i_k} e^{i_1} \wedge \cdots \wedge e^{i_k} \longleftrightarrow \sum_{\substack{i_1 < \cdots < i_k \\ 1 \leqslant i_k \leqslant m}} \omega_{i_1 \cdots i_k}\, e_{i_1} \cdots e_{i_k}$$

$$0\text{-form} : \qquad f \longleftrightarrow f1$$

Under this identification, the Hodge Laplacian may be applied to $\Gamma(Cl(X, g))$ (see [55] for details). In the Clifford algebras context, it is the square of a first order differential operator, namely the **Dirac operator**. Let us first introduce the connection on $Cl(X, g)$ induced by the Levi-Cevita connection on TX.

Proposition 4.2 *The Levi-Cevita connection of a Riemannian manifold (X, g) induces an algebra connection on its Clifford bundle, i.e. a connection ∇^C satisfying*

$$\nabla^C(\varphi\psi) = (\nabla^C\varphi)\psi + \varphi(\nabla^C\psi)$$

for any $\varphi, \psi \in \Gamma(Cl(X, g))$.

Proof. [14] The Levi-Cevita connection may be extended in a unique way to a connection ∇ on $\mathcal{T}(TX)$ by linearity and postulation of the Leibniz rule.
For $U, V \in \Gamma(TX)$ we have

$$\begin{aligned} \nabla_U(V \otimes V - g(V, V)) \;&=\; \frac{1}{2}\Big[(\nabla_U V + V) \otimes (\nabla_U V + V) - g(\nabla_U V + V, \nabla_U V + V)\Big] \\ &\quad -\frac{1}{2}\Big[(\nabla_U V - V) \otimes (\nabla_U V - V) - g(\nabla_U V - V, \nabla_U V - V)\Big] \end{aligned} \tag{4.8}$$

We prove (4.8) by developping both right and left terms of the equality.

For the first one we obtain

$$\nabla_U V \otimes V + V \otimes \nabla_U V - 2g(V, \nabla_U V)$$

Indeed, by property of the Levi-Cevita connection, for any $U, W, Z \in \Gamma(TX)$

$$d_U g(W,Z) = g(\nabla_U W, Z) + g(W, \nabla_U Z)$$

Then, taking $W = Z = V$, it gives

$$d_U g(V,V) = 2g(\nabla_U V, V)$$

Developping the left term we have

$$\nabla_U (V \otimes V - g(V,V)) = \nabla_U V \otimes V + V \otimes \nabla_U V - d_U g(V,V)$$

and the equality (4.8) is proved.

As the right term of (4.8) belongs to $I(TX)$, it proves that ∇ preserves the ideal $I(TX)$.

We deduce that ∇ induces a connection ∇^C on $Cl(X,g)$. Indeed, for $a, b \in \Gamma(\mathcal{T}(TX))$ in the same equivalence class (denoted by $\dot{a} = \dot{b}$), $\nabla(b) = \nabla(a + I_1)$ for some $I_1 \in \Gamma(I(TX))$. Hence $\nabla(b) = \nabla(a) + I_2$ for some $I_2 \in \Gamma(I(TX))$. Therefore $\dot{\overline{\nabla(a)}} = \dot{\overline{\nabla(b)}}$, and ∇^C is well-defined.

The rest of the proof is devoted to show that ∇^C is an algebra connection.
Let $\varphi, \psi \in \Gamma(Cl(X,g))$. By definition, there exist $a, b \in \Gamma(\mathcal{T}(TX))$ such that $\varphi = \dot{a}$ and $\psi = \dot{b}$. Then,

$$\begin{aligned}
\nabla^C(\varphi\,\psi) &= \dot{\overline{\nabla(a \otimes b)}} \\
&= \nabla(a) \otimes \dot{\overline{b + a}} \otimes \nabla(b) \\
&= \dot{\overline{\nabla(a) \otimes}}\, b + a\, \dot{\overline{\otimes \nabla(b)}} \\
&= \dot{\overline{\nabla(a)}}\, \dot{b} + \dot{a}\, \dot{\overline{\nabla(b)}} \\
&= \nabla^C(\varphi)\psi + \varphi \nabla^C(\psi)
\end{aligned}$$

which ends the proof. □

Definition 4.4 *Let $Cl(X,g)$ be the Clifford bundle of a Riemannian manifold (X,g) equipped with the connection ∇^C. Let $(e_1, \cdots, e_m)$ be a local orthormal frame field of TX. The Dirac operator is the first-order differential operator $D\colon \Gamma(Cl(X,g)) \longrightarrow \Gamma(Cl(X,g))$ defined locally by*

$$D\sigma = \sum_{i=1}^{m} e_i \nabla^C_{e_i} \sigma \tag{4.9}$$

It can be shown that this definition is independant of the choice of the local orthonormal frame field.

Proposition 4.3 *Under the isomorphism between $Cl(X,g)$ and $\bigwedge T^*X$, the Clifford-Hodge operator D^2 may be identified with the Hodge Laplacian Δ.*

Proof. [55] From the fact that $d^2 = \delta^2 = 0$, we have

$$\Delta = (d + \delta)^2$$

on $\bigwedge T^*X$. Hence it suffices to prove that D may be identified with $d + \delta$.
Endowing Clifford algebras with the outer $\wedge$ and the inner $\cdot$ products, D may be decomposed as follows

$$D = \sum_{j=1}^{m} e_j \wedge \nabla_{e_j} + \sum_{j=1}^{m} e_j \cdot \nabla_{e_j}$$

Then, it can be shown that the operator $\sum_{j=1}^{m} e_j \wedge \nabla_{e_j}$ satisfies the properties that define in a unique way the exterior derivative d on $\bigwedge T^*X$. Moreover, computing the adjoint of $\sum_{j=1}^{m} e_j \wedge \nabla_{e_j}$, we obtain $\sum_{j=1}^{m} e_j \cdot \nabla_{e_j}$ which ends the proof. □

As Δ preserves the subbundles $\bigwedge^k T^*X$ of $\bigwedge T^*X$ for $k \in \{0 \cdots m\}$, we deduce that D^2 preserves the subbundles $\bigwedge^k TX$ of $Cl(X, g)$.

Proposition 4.4 *Let E be a vector bundle over a manifold X equipped with a connection ∇^E. Let $V, W \in \Gamma(TX)$. The operator*

$$R_{V,W} = \nabla^E_V \nabla^E_W - \nabla^E_W \nabla^E_V - \nabla^E_{[V,W]}$$

*is a zero-order operator on $\Gamma(E)$, i.e. $R_{V,W} \in \Gamma(End(E))$. It is called the **curvature transformation** associated to V and W.*

Proposition 4.5 *Let $Cl(X, g)$ be the Clifford bundle of a Riemannian manifold (X, g) equipped with the connection ∇^C. The Clifford-Hodge operator D^2 is a generalized Laplacian.*

Proof. [55] We first remind that the definition of D does not depend of the choice of local orthonormal frame fields. Let us fix a point $x \in X$ and choose a local orthonormal frame field $(e_1, \cdots, e_m)$ such that $(\nabla e_j)_x = 0$ for each j, where ∇ is the Levi-Cevita connection of TX. Then, for $\varphi \in \Gamma(Cl(X, g))$ we have at x

$$\begin{aligned} D^2\varphi &= \sum_{ij} e_i \nabla^C_{e_i}(e_j \nabla^C_{e_j} \varphi) \\ &= \sum_{ij} e_i e_j \nabla^C_{e_i} \nabla^C_{e_j} \varphi \end{aligned}$$

since $\nabla^C_{e_i}(e_j \nabla^C_{e_j} \varphi) = \nabla^C_{e_i} e_j \, \nabla^C_{e_j} \varphi + e_j \nabla^C_{e_i} \nabla^C_{e_j} \varphi$, and $(\nabla^C_{e_i} e_j)_x = (\nabla_{e_i} e_j)_x = 0$. It may rewritten as

$$\begin{aligned} D^2\varphi &= -\sum_{i} \nabla^C_{e_i} \nabla^C_{e_i} \varphi + \sum_{i<j} e_i e_j (\nabla^C_{e_i} \nabla^C_{e_j} - \nabla^C_{e_i} \nabla^C_{e_j}) \varphi \\ &= -\sum_{i} \nabla^C_{e_i} \nabla^C_{e_i} \varphi + \sum_{i<j} e_i e_j R_{e_i, e_j}(\varphi) \end{aligned}$$

Indeed, as TX is endowed with the Levi-Cevita connection, $[e_i, e_j] = \nabla_{e_i} e_j - \nabla_{e_j} e_i$ and $([e_i, e_j])_x = 0$ by property of $(e_1, \cdots, e_m)$. As a consequence, $(\nabla^C_{[e_i, e_j]})_x = 0$ and we

deduce from the previous proposition that $(\nabla^C_{e_i}\nabla^C_{e_j} - \nabla^C_{e_i}\nabla^C_{e_j})_x = (R_{e_i,e_j})_x$.
Therefore we have

$$D^2 = \Delta^C + F$$

where Δ^C is the connection Laplacian on $Cl(X,g)$ with respect to the connection ∇^C and $F = \sum_{i<j} e_i e_j R_{e_i,e_j}$ is a section of $\mathrm{End}(Cl(X,g))$. □

4.3.2 Application to functions, vector fields and oriented orthonormal frame fields smoothing

As the operator D^2 is a generalized Laplacian, we may consider the corresponding heat equation, whose solution arises from the convolution of the initial condition with the heat kernel $K_t(x,y,D^2)$ associated to D^2.

Definition 4.5 *Let $s_0 \in \Gamma(Cl(X,g))$. The **Clifford-Hodge flow** of s_0 is the solution s_t of the heat equation*

$$\frac{\partial s_t}{\partial t} = D^2 s_t$$

of initial condition s_0.

As D^2 preserves the subbundles $\bigwedge^k TX$ for $k \in \{0,\cdots,m\}$, we deduce that the Clifford-Hodge flow preserves the subbundles $\bigwedge^k TX$ too.

Let $x \in X$. From the embeddings of T_xX and $\mathbb{R}$ into $Cl(T_xX, g(x))$, both tangent vector fields and functions on a Riemannian manifold may be viewed as sections of its Clifford bundle. More precisely, we have the identifications

$$C^\infty(X) \simeq \Gamma(\bigwedge^0 TX) \qquad \Gamma(TX) \simeq \Gamma(\bigwedge^1 TX)$$

Let us denote by $\Gamma(\mathrm{P\,SO}(X))$ the set of smooth oriented orthonormal frame fields of TX. On a local trivialization (U,Φ) of $Cl(X,g)$, we have the identifications

$$\Gamma(P\,\mathrm{SO}(U)) \simeq C^\infty(U,\mathrm{SO}(m)) \qquad \Gamma(\bigwedge^2 TU) \simeq C^\infty(U,\mathfrak{so}(m))$$

the latter arising from the Lie algebra isomorphism $\mathfrak{spin}(m) \simeq \mathfrak{so}(m)$. We call such fields generators of orthonormal frame fields.

As the Clifford-Hodge flow preserves the subbundles $\bigwedge^k TX$, it preserves the structures of functions, tangent vector fields and generators of orthonormal frame fields. As a consequence, it provides a tool to regularize such fields.

Through the regularization of sections of degree 2, the Clifford-Hodge flow provides also a tool to smooth orthonormal frame fields, as follows. Given a mapping f from U to $\mathrm{SO}(m)$, we construct $\tilde{f} \in \Gamma(\bigwedge^2 TU)$ such that $f = \rho \circ exp \circ \tilde{f}$ where ρ is the projection map of the covering $\mathrm{Spin}(m) \longrightarrow \mathrm{SO}(m)$ and exp the exponential map from $\mathfrak{spin}(m)$ to $\mathrm{Spin}(m)$. Then, the Clifford-Hodge flow provides a regularization of $\tilde{f}$ given by sections $\tilde{f}_{t,t\geqslant 0} \in \Gamma(\bigwedge^2 TU)$. Computing $\rho \circ exp \circ \tilde{f}_t$, we obtain mappings $f_{t,t\geqslant 0} \in C^\infty(U,\mathrm{SO}(m))$.

In this sense, we obtain a regularization of f.

Let us give some precisions concerning the construction of $\tilde{f}$ for $m \geqslant 3$.
Two methods may be envisaged to construct $\tilde{f}$. The first one consists in characterizing the rotations $f(x), x \in U$, by their angles and invariant planes from the computation of eigenvalues and eigenvectors. Then $\tilde{f}$ follows in a straightforward way using the fact that bivectors in $\mathbb{R}_{n,0}$ represent oriented planes in $\mathbb{R}^n$. The second one uses the matrix logarithm log: $\mathrm{SO}(m) \longrightarrow \mathfrak{so}(m)$ with values in the matrix representation of the Lie algebra $\mathfrak{so}(m)$, i.e. the antisymmetric matrices. We may write

$$log \circ f(x) = \sum_{i<j} a_{ij}(x) E_{ij}$$

where E_{ij} is the elementary $m \times m$ antisymmetric matrix such that $E_{ij}(i,j) = -1$ and $E_{ij}(j,i) = 1$. The Lie algebra isomorphism $\mathfrak{so}(m) \longrightarrow \mathfrak{spin}(m)$ maps E_{ij} to $\frac{1}{2} e_i e_j$. Hence we obtain

$$\tilde{f}(x) = \sum_{i<j} \frac{1}{2} a_{ij}(x)\, e_i e_j$$

For $m = 3$, the first method is suitable since the spectrum of a rotation is easily computable from geometric calculus methods [47]. Indeed, let us suppose that $f(x)$ is the rotation of angle θ in the oriented plane $\mathcal{P}$ in $\mathbb{R}^3$, given by the matrix

$$A = \begin{pmatrix} a_{11} & a_{12} & a_{13} \\ a_{21} & a_{22} & a_{23} \\ a_{31} & a_{32} & a_{33} \end{pmatrix}$$

in the orthonormal basis (e_1, e_2, e_3).

Then, considering the Clifford algebra $Cl(\mathbb{R}^3, -\| \ \|_2)$, we have

$$\begin{cases} a_{11} + a_{22} + a_{33} & = & 1 + 2cos(\theta) \\ (a_{12} - a_{21}) e_1 e_2 + (a_{13} - a_{31}) e_1 e_3 + (a_{23} - a_{32}) e_1 e_2 & = & -2sin(\theta) \dfrac{B}{\|B\|} \end{cases}$$

where B stands for the bivector representing the oriented plane $\mathcal{P}$ of the rotation. A proof and a generalization for $m > 3$ may be found in [47].

From the two equalities, we may construct $\tilde{f}(x) = \dfrac{\theta}{2} \dfrac{B}{\|B\|}$, $\theta \in [0, 2\pi[$, which satisfies $\rho \circ \exp \circ \tilde{f}(x) = f(x)$.

Note that $\tilde{f}(x)$ is not defined in a unique way since

$$\rho \circ exp \circ \left(\frac{\theta}{2} \frac{B}{\|B\|} \right) = \rho \circ exp \circ \left((\theta/2 + k\pi) \frac{B}{\|B\|} \right) \quad \text{for any } k \in \mathbb{Z}$$

More generally, for $B = \theta_1 B_1 + \cdots + \theta_i B_i$ of the 'orthogonal' form mentionned in Section 1.2.2, we have

$$\rho \circ exp \circ \Big(\theta_1 B_1 + \cdots + \theta_i B_i \Big) = \rho \circ exp \circ \Big((\theta_1 + k\pi) B_1 + \cdots + (\theta_i + k\pi) B_i \Big)$$

The π periodicity raises a problem when convolving $\tilde{f}$ with a kernel $K_t^N(x, y, D^2)$. It may be solved by defining $\tilde{f}$ locally on the normal neighborhoods determined by the function Ψ of Section 4.2.3. Let $x_0 \in U$ and θ_j's defined as above. Let $\Omega_{x_0} \subset U$ be such a neighborhood of x_0. We state $\widetilde{\theta_j}(x) = \theta_j(x) - \pi$ if $\theta_j(x) - \theta_j(x_0) \geqslant \pi/2$, $\widetilde{\theta_j}(x) = \theta_j(x) + \pi$ if $\theta_j(x) - \theta_j(x_0) < -\pi/2$, and $\widetilde{\theta_j}(x) = \theta_j(x)$ otherwise. This makes the functions $\widetilde{\theta_j}$ be valued in $[\theta_j(x_0) - \pi/2, \theta_j(x_0) + \pi/2[$ on Ω_{x_0}. Then we define $\tilde{f} = \widetilde{\theta_1} e_1 e_2 + \cdots \widetilde{\theta_{C_m^2}} e_{m-1} e_m$ on Ω_{x_0}. Extending this construction for each $x_0 \in U$, we construct $\tilde{f}$ for which the convolution with the kernel $K_t^N(x, y, D^2)$ makes sense.

At last, let us treat the particular case $m = 2$ since $\mathrm{Spin}(2) \simeq \mathrm{SO}(2)$.
Given $f \in C^\infty(U, \mathrm{SO}(2))$, we construct $\tilde{f} = \widetilde{\theta} e_1 e_2$ such that $exp(\widetilde{\theta} e_1 e_2) = cos(\theta) + sin(\theta) e_1 e_2$. There is a 2π periodicity in the choice of $\tilde{f}$, that may be solved by defining $\tilde{f}$ locally on the neighborhoods Ω_{x_0}. Indeed, we state $\widetilde{\theta}(x) = \theta(x) - 2\pi$ if $\theta(x) - \theta(x_0) \geqslant \pi$, $\widetilde{\theta}(x) = \theta(x) + 2\pi$ if $\theta(x) - \theta(x_0) < -\pi$ and $\widetilde{\theta}(x) = \theta(x)$ otherwise. Then we extend this construction for each $x_0 \in U$ as mentionned above.

The heat kernel of a generalized Laplacian H on a vector bundle E equipped with a connection ∇^E is determined by geodesic distances on the base manifold, transport parallel map associated to ∇^E along geodesic curves, and H itself. In the rest of the paper we give explicit formulae of the operator D^2 and parallel transport map on $Cl(X, g)$ for X of dimension 2 and 3. We present applications in the contexts of image and video processing.

4.4 The case $m = 2$

4.4.1 The operator D^2 and parallel transport map on $Cl(X, g)$

Let us first determine the connection ∇^C in an orthonormal frame (e_1, e_2). Let $\Gamma_{ij}^{k'}$ be the Levi-Cevita connection's symbols of (X, g) with respect to the frame (e_1, e_2).

$$\nabla^C_{e_1} 1 = 0 \qquad \nabla^C_{e_2} 1 = 0$$

$$\nabla^C_{e_1} e_1 = \Gamma_{11}^{2'} e_2 \qquad \nabla^C_{e_1} e_2 = -\Gamma_{11}^{2'} e_1$$
$$\nabla^C_{e_2} e_1 = \Gamma_{21}^{2'} e_2 \qquad \nabla^C_{e_2} e_2 = -\Gamma_{21}^{2'} e_1$$

$$\nabla^C_{e_1} e_1 e_2 = 0 \qquad \nabla^C_{e_2} e_1 e_2 = 0$$

Proposition 4.6 *Let (X, g) be a Riemannian manifold of dimension 2. Let (e_1, e_2) be an orthonormal frame on X and $\varphi = \varphi_1 1 + \varphi_2 e_1 + \varphi_3 e_2 + \varphi_4 e_1 e_2 \in \Gamma(Cl(X, g))$. Then*

$$D^2(\varphi_1 1) = \Big(- d^2_{e_1, e_1} \varphi_1 - d^2_{e_2, e_2} \varphi_1 - \Gamma_{21}^{2'} d_{e_1} \varphi_1 + \Gamma_{11}^{2'} d_{e_2} \varphi_1 \Big) 1$$

$$= -\Delta_g(\varphi_1)1$$

$$\begin{aligned} D^2(\varphi_2 e_1 + \varphi_3 e_2) &= \Big(- d^2_{e_1,e_1}\varphi_2 - d^2_{e_2,e_2}\varphi_2 - \Gamma^{2'}_{21} d_{e_1}\varphi_2 + \Gamma^{2'}_{11} d_{e_2}\varphi_2 + 2\,\Gamma^{2'}_{11} d_{e_1}\varphi_3 \\ &\quad + 2\,\Gamma^{2'}_{21} d_{e_2}\varphi_3 + \varphi_2(d_{e_2}\Gamma^{2'}_{11} - d_{e_1}\Gamma^{2'}_{21}) + \varphi_3(d_{e_1}\Gamma^{2'}_{11} + d_{e_2}\Gamma^{2'}_{21})\Big) e_1 \\ &\quad + \Big(- d^2_{e_1,e_1}\varphi_3 - d^2_{e_2,e_2}\varphi_3 - \Gamma^{2'}_{21} d_{e_1}\varphi_3 + \Gamma^{2'}_{11} d_{e_2}\varphi_3 - 2\,\Gamma^{2'}_{11} d_{e_1}\varphi_2 \\ &\quad - 2\,\Gamma^{2'}_{21} d_{e_2}\varphi_2 + \varphi_2(-d_{e_2}\Gamma^{2'}_{21} - d_{e_1}\Gamma^{2'}_{11}) + \varphi_3(-d_{e_1}\Gamma^{2'}_{21} + d_{e_2}\Gamma^{2'}_{11})\Big) e_2 \end{aligned}$$

$$\begin{aligned} D^2(\varphi_4 e_1 e_2) &= \Big(- d^2_{e_1,e_1}\varphi_4 - d^2_{e_2,e_2}\varphi_4 - \Gamma^{2'}_{21} d_{e_1}\varphi_4 + \Gamma^{2'}_{11} d_{e_2}\varphi_4\Big) e_1 e_2 \\ &= -\Delta_g(\varphi_4) e_1 e_2 \end{aligned}$$

where Δ_g stands for the Laplace-Beltrami operator on (X, g) (see Section 4.2.4).

Proof. We obtain $D^2(\varphi)$ from (4.9) and the relations above defining ∇^C in the frame (e_1, e_2). Then we simplify the expression using some properties of the Levi-Cevita connection :
(i) In an orthonormal frame, symbols satisfy $\Gamma^{k'}_{ij} = -\Gamma^{j'}_{ik}$.
(ii) $[e_1, e_2] = -\Gamma^{2'}_{11} e_1 - \Gamma^{2'}_{21} e_2$ □

Proposition 4.7 (Parallel transport on $Cl(X, g)$) *Let (X, g) be a Riemannian manifold of dimension 2. Let (e_1, e_2) be an orthonormal frame on X, and $Y_0 = Y^1_0 1(y) + Y^2_0 e_1(y) + Y^3_0 e_2(y) + Y^4_0 e_1 e_2(y) \in Cl(X, g)_y$. Let γ be a C^1 curve in X such that $\gamma(0) = y$. The parallel transport Y of Y_0 along γ is*

$$\begin{aligned} Y(t) &= Y^1_0\, 1(\gamma(t)) + \Big[f_1 \cdot \Big((Y^2_0 f_1 + Y^3_0 f_2) S(t) \Big) \Big] e_1(\gamma(t)) \\ &+ \Big[f_2 \cdot \Big((Y^2_0 f_1 + Y^3_0 f_2) S(t) \Big) \Big] e_2(\gamma(t)) + Y^4_0\, e_1 e_2(\gamma(t)) \end{aligned}$$

where (f_1, f_2) is an orthonormal basis generating $Cl(\mathbb{R}^2, -\| \|_2)$ and $S(t) \in$ Spin(2) $\subset Cl(\mathbb{R}^2, -\| \|_2)$ defined by

$$S(t) = exp\Big(f_1 f_2 \int_0^t \dot\gamma_1(s)\, \Gamma^{2'}_{11}(s) + \dot\gamma_2(s)\, \Gamma^{2'}_{21}(s)\, ds \Big)$$

Proof. The parallel transport of Y_0 along γ is the solution $Y(t) = Y_1(t)\, 1(\gamma(t)) + Y_2(t)\, e_1(\gamma(t)) + Y_3(t)\, e_2(\gamma(t)) + Y_4(t)\, e_1 e_2(\gamma(t))$ of the differential equation

$$\begin{cases} \nabla^C_{\dot\gamma} Y(t) = 0 \\ \\ Y(0) = Y_0 \end{cases} \tag{4.10}$$

$$
\begin{aligned}
\nabla^C_{\dot\gamma} Y(t) &= \nabla^C_{\dot\gamma} Y_1\, 1 + Y_2\, e_1 + Y_3\, e_2 + Y_4\, e_1e_2\,(t) \\
&= \frac{\partial Y_1}{\partial t}(t)\, 1(t) + Y_1(t)(\dot\gamma_1(t)\nabla^C_{e_1} 1\,(t) + \dot\gamma_2(t)\nabla^C_{e_2} 1\,(t)) \\
&\quad + \frac{\partial Y_2}{\partial t}(t)\, e_1(t) + Y_2(t)(\dot\gamma_1(t)\nabla^C_{e_1} e_1\,(t) + \dot\gamma_2(t)\nabla^C_{e_2} e_1\,(t)) \\
&\quad + \frac{\partial Y_3}{\partial t}(t)\, e_2(t) + Y_3(t)(\dot\gamma_1(t)\nabla^C_{e_1} e_2\,(t) + \dot\gamma_2(t)\nabla^C_{e_2} e_2\,(t)) \\
&\quad + \frac{\partial Y_4}{\partial t}(t)\, e_1e_2(t) + Y_4(t)(\dot\gamma_1(t)\nabla^C_{e_1} e_1e_2\,(t) + \dot\gamma_2(t)\nabla^C_{e_2} e_1e_2\,(t)) \\
&= \frac{\partial Y_1}{\partial t}(t)\, 1(t) \\
&\quad + \frac{\partial Y_2}{\partial t}(t)\, e_1(t) + Y_2(t)(\dot\gamma_1(t)\,\Gamma^{2'}_{11}(t)\, e_2(t) + \dot\gamma_2(t)\,\Gamma^{2'}_{21}(t)\, e_2(t)) \\
&\quad + \frac{\partial Y_3}{\partial t}(t)\, e_2(t) + Y_3(t)(-\dot\gamma_1(t)\,\Gamma^{2'}_{11}(t)\, e_1(t) - \dot\gamma_2(t)\,\Gamma^{2'}_{21}(t)\, e_1(t)) \\
&\quad + \frac{\partial Y_4}{\partial t}(t)\, e_1e_2(t)
\end{aligned}
$$

Finally, we obtain a differential equation on $\mathbb{R}^4$.

$$
\begin{pmatrix} dY_1/dt \\ dY_2/dt \\ dY_3/dt \\ dY_4/dt \end{pmatrix} = \begin{pmatrix} 0 & 0 & 0 & 0 \\ 0 & 0 & \dot\gamma_1\,\Gamma^{2'}_{11} + \dot\gamma_2\,\Gamma^{2'}_{21} & 0 \\ 0 & -\dot\gamma_1\,\Gamma^{2'}_{11} - \dot\gamma_2\,\Gamma^{2'}_{21} & 0 & 0 \\ 0 & 0 & 0 & 0 \end{pmatrix} \begin{pmatrix} Y_1 \\ Y_2 \\ Y_3 \\ Y_4 \end{pmatrix}
$$

of initial condition $Y_1(0) = Y^1_0$, $Y_2(0) = Y^2_0$, $Y_3(0) = Y^3_0$ and $Y_4(0) = Y^4_0$.

It leads to $Y_1(t) = Y^1_0$, $Y_4(t) = Y^4_0$ and a differential equation on $\mathbb{R}^2$

$$
\begin{pmatrix} dY_2/dt \\ dY_3/dt \end{pmatrix} = \begin{pmatrix} 0 & \dot\gamma_1\Gamma^{2'}_{11} + \dot\gamma_2\Gamma^{2'}_{21} \\ -\dot\gamma_1\Gamma^{2'}_{11} - \dot\gamma_2\Gamma^{2'}_{21} & 0 \end{pmatrix} \begin{pmatrix} Y_2 \\ Y_3 \end{pmatrix} \tag{4.11}
$$

of initial condition $Y_2(0) = Y^2_0$ and $Y_3(0) = Y^3_0$.

Under the identification between $\mathbb{R}^2$ and $\mathbb{C}$, (4.11) becomes

$$
\begin{cases} \partial(Y_2 + i\,Y_3)/\partial t &= i\,(\dot\gamma_1\,\Gamma^{2'}_{11} + \dot\gamma_2\,\Gamma^{2'}_{21})(Y_2 + i\,Y_3) \\ Y_2(0) + i\,Y_3(0) &= Y^2_0 + i\,Y^3_0 \end{cases} \tag{4.12}
$$

The solution of (4.12) is

$$
Y_2(t) + i\,Y_3(t) = exp\Big(i\int_0^t \dot\gamma_1(s)\,\Gamma^{2'}_{11}(s) + \dot\gamma_2(s)\,\Gamma^{2'}_{21}(s)\; ds\Big)(Y^2_0 + i\,Y^3_0) \tag{4.13}
$$

Under the identification between $\mathbb{R}^2$ and $\mathbb{C}$, the right term of (4.13) is the rotation of angle $\int_0^t \dot{\gamma_1}(s)\,\Gamma_{11}^{2'}(s) + \dot{\gamma_2}(s)\,\Gamma_{21}^{2'}(s)\,ds$ applied to the vector (Y_0^2, Y_0^3).

Embedding $\mathbb{R}^2$ of orthonormal basis (f_1, f_2) into the Clifford algebra $Cl(\mathbb{R}^2, -\|\ \|_2)$ of basis $(1, f_1, f_2, f_1 f_2)$, (4.13) may be written into the Clifford algebras context as

$$Y_2(t)f_1 + Y_3(t)f_2 = exp\Big(f_1 f_2 \int_0^t \dot{\gamma_1}(s)\,\Gamma_{11}^{2'}(s) + \dot{\gamma_2}(s)\,\Gamma_{21}^{2'}(s)\ ds\Big)(Y_0^2 f_1 + Y_0^3 f_2)$$

Then $Y_2(t) = f_1 \cdot (Y_2(t)f_1 + Y_3(t)f_2)$ and $Y_3(t) = f_2 \cdot (Y_2(t)f_1 + Y_3(t)f_2)$, where $\cdot$ is the inner product of $Cl(\mathbb{R}^2, -\|\ \|_2)$. □

4.4.2 The particular context of images

Let us consider a nD image defined by a function $I\colon (x,y) \longmapsto (I_1(x,y), \cdots, I_n(x,y))$ on a domain $\Omega \subset \mathbb{R}^2$. I determines a surface S embedded in $\mathbb{R}^{n+2}$ parametrized by

$$\varphi\colon (x,y) \longmapsto (x, y, I_1(x,y), \cdots, I_n(x,y))$$

Then endow $\mathbb{R}^{n+2}$ of a metric h of the form

$$h(p) = \begin{pmatrix} 1 & 0 \\ 0 & 1 \end{pmatrix} \oplus \begin{pmatrix} h_1(p) & 0 & 0 & \cdots\cdots & 0 \\ 0 & h_2(p) & 0 & \cdots\cdots & 0 \\ 0 & 0 & \ddots & & \vdots \\ \vdots & \vdots & & \ddots & \vdots \\ 0 & 0 & \cdots\cdots & 0 & h_n(p) \end{pmatrix}$$

where $h_1, \cdots, h_n$ are positive functions and denote by g the metric on S induced by h makes the couple (S, g) be a Riemannian manifold of dimension 2 of global chart (Ω, φ).

On the manifold S the natural frame is $(\partial/\partial x, \partial/\partial y)$ induced by the cartesian coordinates system (x, y). However, the Clifford-Hodge operator D^2 is defined with respect to orthonormal frame fields on the base manifold (see Sect.4.3.1). In what follows, we construct an oriented orthonormal frame field (e_1, e_2) on S and compute the transformation of Levi-Cevita connection's symbols with respect to the frame change from $(\partial/\partial x, \partial/\partial y)$ to (e_1, e_2).

Proposition 4.8 (Positively oriented orthonormal basis of T_pS)
Let $\begin{pmatrix} E & F \\ F & G \end{pmatrix}$ *be the matrix representation of* g *at* p *in the basis* $(\partial/\partial x, \partial/\partial y)(p)$. *Let* λ^+ *and* λ^- $(\lambda^+ \geqslant \lambda^-)$ *be the two eigenvalues of the induced endomorphism. Then a positively oriented orthonormal basis* (e_1, e_2) *of* T_pS *may be constructed from eigenvectors, distinguishing four cases :*

(i) if $F \neq 0$, *take* $(e_1, e_2) =$

$$\left(\begin{pmatrix} \dfrac{\lambda^+ - G}{\sqrt{\lambda^+}\sqrt{F^2 + (\lambda^+ - G)^2}} \\ \dfrac{F}{\sqrt{\lambda^+}\sqrt{F^2 + (\lambda^+ - G)^2}} \end{pmatrix}, sign(F) \begin{pmatrix} \dfrac{\lambda^- - G}{\sqrt{\lambda^-}\sqrt{F^2 + (\lambda^- - G)^2}} \\ \dfrac{F}{\sqrt{\lambda^-}\sqrt{F^2 + (\lambda^- - G)^2}} \end{pmatrix} \right)$$

in the basis $(\partial/\partial x, \partial/\partial y)(p)$.

(ii) if $F = 0$ *and* $E > G$, *take*

$$(e_1, e_2) = \Big(\frac{\partial/\partial x(p)}{\sqrt{E}}, \frac{\partial/\partial y(p)}{\sqrt{G}}\Big)$$

(iii) if $F = 0$ *and* $E < G$, *take*

$$(e_1, e_2) = \Big(\frac{\partial/\partial y(p)}{\sqrt{G}}, -\frac{\partial/\partial x(p)}{\sqrt{E}}\Big)$$

(iv) if $F = 0$ *and* $E = G$, *the whole space* T_pS *is eigenspace. Then for any* θ,

$$\left(\begin{pmatrix} \frac{\cos(\theta)}{\sqrt{E}} \\ \\ \frac{\sin(\theta)}{\sqrt{E}} \end{pmatrix}, \begin{pmatrix} \frac{-\sin(\theta)}{\sqrt{E}} \\ \\ \frac{\cos(\theta)}{\sqrt{E}} \end{pmatrix}\right)$$

in the basis $(\partial/\partial x, \partial/\partial y)(p)$ *is a positively oriented orthonormal basis of* T_pS.

Proof. As unit eigenvectors, they form an orthonormal basis of T_pS. The orientation is clearly positive in the cases $(ii), (iii)$ and (iv). For the case (i), one just need to compute the 2-form

$$\omega = \Big[\Big(\frac{\lambda^+ - G}{\sqrt{\lambda^+}\sqrt{F^2 + (\lambda^+ - G)^2}}\Big)dx + \Big(\frac{F}{\sqrt{\lambda^+}\sqrt{F^2 + (\lambda^+ - G)^2}}\Big)dy\Big] \wedge$$

$$\Big[\Big(\frac{\lambda^- - G}{\sqrt{\lambda^-}\sqrt{F^2 + (\lambda^- - G)^2}}\Big)dx + \Big(\frac{F}{\sqrt{\lambda^-}\sqrt{F^2 + (\lambda^- - G)^2}}\Big)dy\Big]$$

Then

$$\omega = \frac{F(\lambda^+ - \lambda^-)}{\sqrt{\lambda^+\lambda^-}\sqrt{F^2 + (\lambda^+ - G)^2}\sqrt{F^2 + (\lambda^- - G)^2}}\, dx \wedge dy$$

and the sign of the scalar term is the sign of F. □

To complete the construction, we state $(e_1, e_2) = \Big(\frac{\partial/\partial x(p)}{\sqrt{E}}, \frac{\partial/\partial y(p)}{\sqrt{E}}\Big)$ when the case *(iv)* holds.

Following this construction for each $p \in S$, we obtain a positively oriented orthonormal frame field (e_1, e_2) on S, where e_1 is the unit vector field of highest variations (eigenvectors associated to the eigenvalues λ^+) and e_2 the unit vector field of lowest variations (eigenvectors associated to the eigenvalues λ^-).

By the antisymmetry property of its symbols $\Gamma_{ij}^{k'}$ in an orthonormal frame, the Levi-Cevita connection is entirely determined by the symbols $\Gamma_{11}^{2'}$ and $\Gamma_{21}^{2'}$ in such frames. In the next proposition, we determine the expressions of these two symbols in a frame (v_1, v_2) in function of the symbols Γ_{ij}^{k} of the connection in the frame $(\partial/\partial x, \partial/\partial y)$.

Proposition 4.9 *Let (v_1, v_2) be a frame such that $v_1 = a\,\partial/\partial x + b\,\partial/\partial y$ and $v_2 = c\,\partial/\partial x + d\,\partial/\partial y$. Then*

$$\Gamma_{11}^{2'} = 1/(ad-bc)\times$$

$$\Big(-ab\frac{\partial a}{\partial x} - a^2 b\,\Gamma_{11}^1 - 2ab^2\,\Gamma_{12}^1 - b^2\frac{\partial a}{\partial y} - b^3\,\Gamma_{22}^1 + a^3\,\Gamma_{11}^2 + a^2\frac{\partial b}{\partial x} + 2a^2 b\,\Gamma_{12}^2 + ab\frac{\partial b}{\partial y} + ab^2\,\Gamma_{22}^2\Big)$$

$$\Gamma_{21}^{2'} = 1/(ad-bc)\times$$

$$\Big(-bc\frac{\partial a}{\partial x} - acb\,\Gamma_{11}^1 - (bc+ad)b\,\Gamma_{12}^1 - bd\frac{\partial a}{\partial y} - b^2 d\,\Gamma_{22}^1 + a^2 c\,\Gamma_{11}^2 + ac\frac{\partial b}{\partial x} + (bc+ad)a\,\Gamma_{12}^2$$

$$+ad\frac{\partial b}{\partial y} + abd\,\Gamma_{22}^2\Big)$$

Proof. By definition, we have

$$\nabla_{v_1} v_1 = \Gamma_{11}^{1'} v_1 + \Gamma_{11}^{2'} v_2 \qquad \nabla_{v_2} v_1 = \Gamma_{21}^{1'} v_1 + \Gamma_{21}^{2'} v_2$$

With respect to the frame $(\partial_x, \partial_y) := (\partial/\partial x, \partial/\partial y)$, we obtain

$$\begin{aligned}
\nabla_{v_1} v_1 &= \nabla_{a\partial_x + b\partial_y} a\,\partial_x + b\,\partial_y \\
&= a\nabla_{\partial_x} a\,\partial_x + a\nabla_{\partial_x} b\,\partial_y + b\nabla_{\partial_y} a\,\partial_x + b\nabla_{\partial_y} b\,\partial_y \\
&= a\Big[\frac{\partial a}{\partial x}\,\partial_x + a\Big(\Gamma_{11}^1\,\partial_x + \Gamma_{11}^2\,\partial_y\Big)\Big] + a\Big[\frac{\partial b}{\partial x}\,\partial_y + b\Big(\Gamma_{12}^1\,\partial_x + \Gamma_{12}^2\,\partial_y\Big)\Big] \\
&\quad + b\Big[\frac{\partial a}{\partial y}\,\partial_x + a\Big(\Gamma_{21}^1\,\partial_x + \Gamma_{21}^2\,\partial_y\Big)\Big] + b\Big[\frac{\partial b}{\partial y}\,\partial_y + b\Big(\Gamma_{22}^1\,\partial_x + \Gamma_{22}^2\,\partial_y\Big)\Big]
\end{aligned}$$

$$= \Big[a\frac{\partial a}{\partial x} + a^2\,\Gamma_{11}^1 + 2ab\,\Gamma_{12}^1 + b\frac{\partial a}{\partial y} + b^2\,\Gamma_{22}^1\Big]\partial_x + \Big[a\frac{\partial b}{\partial x} + a^2\,\Gamma_{11}^2 + 2ab\,\Gamma_{12}^2 + b\frac{\partial b}{\partial y} + b^2\,\Gamma_{22}^2\Big]\partial_y$$

Then, since

$$\partial_x = \frac{1}{ad-bc}(d\,v_1 - b\,v_2) \qquad \partial_y = \frac{1}{ad-bc}(-c\,v_1 + a\,v_2)$$

we obtain

$$\begin{aligned}
\nabla_{v_1} v_1 &= \frac{1}{ad-bc}\Big[ad\frac{\partial a}{\partial x} + a^2 d\,\Gamma_{11}^1 + 2abd\,\Gamma_{12}^1 + bd\frac{\partial a}{\partial y} + b^2 d\,\Gamma_{22}^1 - a^2 c\,\Gamma_{11}^2 - ac\frac{\partial b}{\partial x} \\
&\quad -2abc\,\Gamma_{12}^2 - bd\frac{\partial b}{\partial y} - b^2 c\,\Gamma_{22}^2\Big] v_1 \\
&\quad + \frac{1}{ad-bc}\Big[-ab\frac{\partial a}{\partial x} - a^2 b\,\Gamma_{11}^1 - 2ab^2\,\Gamma_{12}^1 - b^2\frac{\partial a}{\partial y} - b^3\,\Gamma_{22}^1 + a^3\,\Gamma_{11}^2 + a^2\frac{\partial b}{\partial x} \\
&\quad +2a^2 b\,\Gamma_{12}^2 + ab\frac{\partial b}{\partial y} + ab^2\,\Gamma_{22}^2\Big] v_2
\end{aligned}$$

from which we deduce $\Gamma_{11}^{2'}$,

and

$$\begin{aligned}\nabla_{v_2} v_1 &= \frac{1}{ad-bc}\Big[cd\frac{\partial a}{\partial x} + acd\,\Gamma_{11}^1 + (bc+ad)d\,\Gamma_{12}^1 + d^2\frac{\partial a}{\partial y} + bd^2\,\Gamma_{22}^1 - ac^2\,\Gamma_{11}^2 - c^2\frac{\partial b}{\partial x}\\ &\quad -(bc+ad)c\,\Gamma_{12}^2 - cd\frac{\partial b}{\partial y} - cbd\,\Gamma_{22}^2\Big]v_1\\ &\quad +\frac{1}{ad-bc}\Big[-bc\frac{\partial a}{\partial x} - acb\,\Gamma_{11}^1 - (bc+ad)b\,\Gamma_{12}^1 - bd\frac{\partial a}{\partial y} - b^2d\,\Gamma_{22}^1 + a^2c\,\Gamma_{11}^2\\ &\quad +ac\frac{\partial b}{\partial x} + (bc+ad)a\,\Gamma_{12}^2 + ad\frac{\partial b}{\partial y} + abd\,\Gamma_{22}^2\Big]v_2\end{aligned}$$

from which we deduce $\Gamma_{21}^{2'}$. □

4.4.3 Experiments

We show three applications of the Clifford-Hodge flow in dimension 2.

The Clifford-Hodge flow of functions on Riemannian manifolds of dimension 2 may be devoted to anisotropic regularization of nD images. Let us detail the context of the regularization. Let $I = (I_1, \cdots, I_n)$ be a nD image. As mentionned above, it induces a Riemannian manifold (S, g) of dimension 2. Then we consider each component I_i as a section of the Clifford bundle $Cl(S, g)$ of degree 0, and apply the Clifford-Hodge flow on each one of them. Under the identification between sections of $Cl(S, g)$ of degree 0 and functions of S, we get n PDE's

$$\frac{\partial I_i}{\partial t} + \Delta I_i = 0$$

where Δ is the scalar Laplacian on $C^\infty(S, g)$.

The Beltrami framework of Sochen et al. in the context of image regularization (see e.g. [74],[77]) yields to define each component I_i as a function over (S, g), and then to solve the n PDE's $\partial I_i/\partial t = \Delta_g I_i$. From Section 4.2.4, it corresponds to solve heat equations associated to the scalar Laplacian over the Riemannian manifold (S, g). This makes the image regularization process induced by Clifford-Hodge and Beltrami flows be equivalent. In [74], the diffusion process arises from the Euler scheme (4.6). In [77], the diffusion process arises from a convolution of the initial data with a mask corresponding to the discretization of the kernel K_t^0 mentionned in Section 4.2.3.

Fig. 4.1 is an illustration of the anisotropic regularization of a color image ($n = 3$) induced by the Clifford-Hodge flow. It is computed from the convolution with a 5x5 mask discretizing the kernel K_t^0. Fig. 4.1(a) is taken from the Berkeley image segmentation database [58]. Fig. 4.1(b) is the result of the regularization after 5 iterations for $h_1 = h_2 = h_3 = 0.01$ and $t = 0.5$, the metric g being updated at each iteration. We obtain a smoothing of the image on regions of low color variations whereas high edges are preserved.

The Clifford-Hodge flow of tangent vector fields on Riemannian manifolds of dimension 2 may be devoted to anisotropic regularization of vector fields related to nD images, that is illustrated on Fig. 4.2. Fig. 4.2(a) is the unit vector field $v = (v_1, v_2)$ indicating

(a) Original image (b) Anisotropic Clifford-Hodge flow

FIGURE 4.1 – Clifford-Hodge flow of functions

edge orientations in a region around the hat of Fig. 4.1(b). Let (S, g) be the Riemannian manifold associated to the color image of Fig. 4.1(b), and (Ω, φ) be the global chart of S. Using the chart, v may be viewed as the tangent vector field $v = (v_1, v_2)$ in the frame $(\partial/\partial x, \partial/\partial y)$. Then under the frame change from $(\partial/\partial x, \partial/\partial y)$ to (e_1, e_2) (see Section 4.4.2), we may consider the Clifford-Hodge flow of v. Fig. 4.2(b) is the result of the Clifford-Hodge flow of v after 99 iterations for $h_1 = h_2 = h_3 = 0.01$ and $t = 0.3$. It is computed from the convolution with a 5x5 mask discretizing the kernel K_t^0. We see that it tends to preserve the vector field on high edges of the image, conversely to vanish it on low edges.

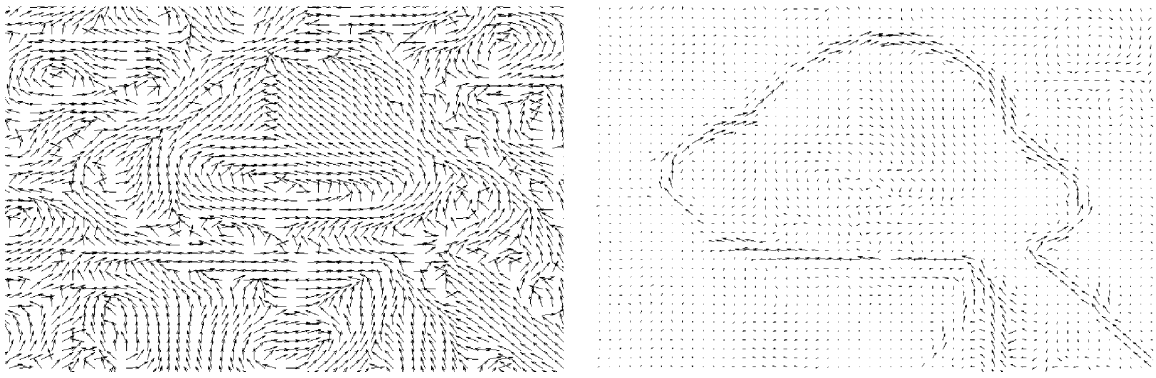

(a) Unit vector field of edge orientations (b) Anisotropic Clifford-Hodge flow

FIGURE 4.2 – Clifford-Hodge flow of tangent vector field

In dimension 2, the Clifford-Hodge flow of oriented orthonormal frame fields on Riemannian manifolds may be devoted to anisotropic regularization of orientation fields related to nD images. Let $v = (v_1, v_2)$ be the unit vector field on $\Omega \subset \mathbb{R}^2$ of Fig. 4.2(a). For each $p \in S$, $v(p)$ may be represented by polar coordinates $(1, \theta(p))$, $\theta(p) \in [0, 2\pi[$. Let us corrupt the function θ by adding to it a random map with values in $[-\pi/2, \pi/2]$. The corresponding unit vector field u is on Fig. 4.3(a). Using the chart (Ω, φ) of S, u is a tangent vector field of S that may be written $u = \lambda(\cos(\psi)e_1 + \sin(\psi)e_2)$, for some functions λ, ψ. Then it may be viewed (up to a normalization) as the result of a rotation field of angle ψ applied to e_1. Following Section 4.3.2, we construct $\widetilde{\psi}e_1e_2 \in \Gamma(\bigwedge^2 TX)$ such that the rotation field of angle ψ equals $exp \circ \widetilde{\psi}e_1e_2$, and we regularize it through the Clifford-

Hodge flow of $\widetilde{\psi}e_1e_2$. From Section 4.4.1, it produces the scalar Laplacian/Beltrami flow of the function $\widetilde{\psi}$. Hence we obtain a unit vector field u_t in the frame (e_1, e_2). By the inverse frame change from (e_1, e_2) to $(\partial/\partial x, \partial/\partial y)$, we obtain (up to normalization) a unit vector field in the frame $(\partial/\partial x, \partial/\partial y)$, and consequently on the chart. Fig. 4.3(b) is the result of this process after 1000 iterations for $h_1 = h_2 = h_3 = 0.1$ and $t = 0.3$. It is computed from the convolution with a 5x5 mask discretizing the kernel K_0^t. Up to details, we refind the original unit vector field of Fig. 4.2(a).

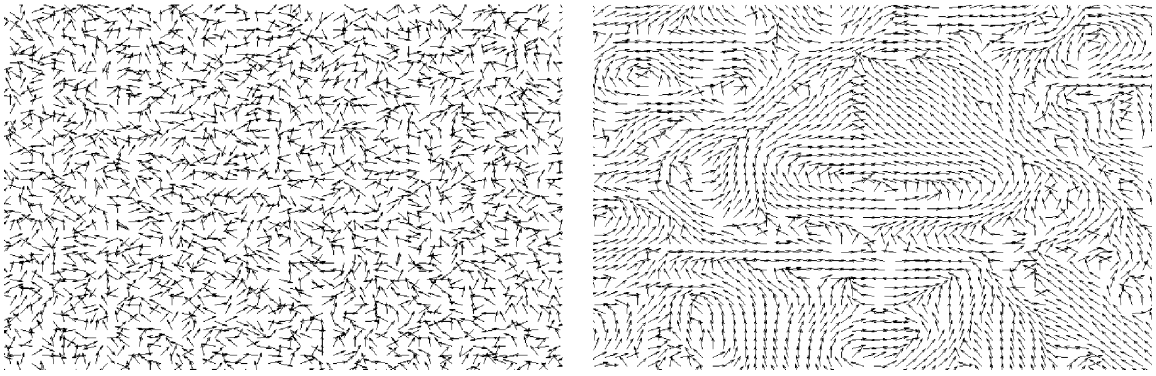

(a) Noisy unit vector field of edge orientations (b) Anisotropic Clifford-Hodge flow

FIGURE 4.3 – Clifford-Hodge flow of oriented orthonormal frame field

The results concerning regularization of images and orientation fields should have been foreseen. Indeed, it is a well-known fact that the Beltrami flow tends to diffuse in the direction of edges on regions located on high edges, and behaves as a gaussian diffusion on homogeneous regions. By the result of Fig. 4.2 where the unit vector field of edge orientations is preserved on high edges and where its components are averaged on regions of low color variations, we may deduce more generally that the Clifford-Hodge flow acts in this way.

4.5 The case $m = 3$

4.5.1 The operator D^2 and parallel transport map on $Cl(X, g)$

Let us first determine the connection ∇^C in an orthonormal frame (e_1, e_2, e_3). Let $\Gamma_{ij}^{k'}$ be the Levi-Cevita connection's symbols of (X, g) with respect to the frame (e_1, e_2, e_3).

$$\nabla^C_{e_1} 1 = 0 \qquad \nabla^C_{e_2} 1 = 0 \qquad \nabla^C_{e_3} 1 = 0$$

$$\begin{array}{lll}
\nabla^C_{e_1} e_1 = \Gamma_{11}^{2'} e_2 + \Gamma_{11}^{3'} e_3 & \nabla^C_{e_2} e_1 = \Gamma_{21}^{2'} e_2 + \Gamma_{21}^{3'} e_3 & \nabla^C_{e_3} e_1 = \Gamma_{31}^{2'} e_2 + \Gamma_{31}^{3'} e_3 \\
\nabla^C_{e_1} e_2 = \Gamma_{12}^{1'} e_1 + \Gamma_{12}^{3'} e_3 & \nabla^C_{e_2} e_2 = \Gamma_{22}^{1'} e_1 + \Gamma_{22}^{3'} e_3 & \nabla^C_{e_3} e_2 = \Gamma_{32}^{1'} e_1 + \Gamma_{32}^{3'} e_3 \\
\nabla^C_{e_1} e_3 = \Gamma_{13}^{1'} e_1 + \Gamma_{13}^{2'} e_2 & \nabla^C_{e_2} e_3 = \Gamma_{23}^{1'} e_1 + \Gamma_{23}^{2'} e_2 & \nabla^C_{e_3} e_3 = \Gamma_{33}^{1'} e_1 + \Gamma_{33}^{2'} e_2
\end{array}$$

$$\begin{array}{lll}
\nabla^C_{e_1} e_1e_2 = \Gamma_{12}^{3'} e_1e_3 - \Gamma_{11}^{3'} e_2e_3 & \nabla^C_{e_2} e_1e_2 = \Gamma_{22}^{3'} e_1e_3 - \Gamma_{21}^{3'} e_2e_3 & \nabla^C_{e_3} e_1e_2 = \Gamma_{32}^{3'} e_1e_3 - \Gamma_{31}^{3'} e_2e_3 \\
\nabla^C_{e_1} e_1e_3 = \Gamma_{13}^{2'} e_1e_2 + \Gamma_{11}^{2'} e_2e_3 & \nabla^C_{e_2} e_1e_3 = \Gamma_{23}^{2'} e_1e_2 + \Gamma_{21}^{2'} e_2e_3 & \nabla^C_{e_3} e_1e_3 = \Gamma_{33}^{2'} e_1e_2 + \Gamma_{31}^{2'} e_2e_3 \\
\nabla^C_{e_1} e_2e_3 = \Gamma_{12}^{1'} e_1e_3 - \Gamma_{13}^{1'} e_1e_2 & \nabla^C_{e_2} e_2e_3 = \Gamma_{22}^{1'} e_1e_3 - \Gamma_{23}^{1'} e_1e_2 & \nabla^C_{e_3} e_2e_3 = \Gamma_{32}^{1'} e_1e_3 - \Gamma_{33}^{1'} e_1e_2
\end{array}$$

$$\nabla^C_{e_1} e_1e_2e_3 = 0 \qquad \nabla^C_{e_2} e_1e_2e_3 = 0 \qquad \nabla^C_{e_3} e_1e_2e_3 = 0$$

Proposition 4.10 *Let (X, g) be a Riemannian manifold of dimension 3. Let (e_1, e_2, e_3) be an orthonormal frame on X and $\varphi = \varphi_1\, 1 + \varphi_2\, e_1 + \varphi_3\, e_2 + \varphi_4\, e_3 + \varphi_5\, e_1e_2 + \varphi_6\, e_1e_3 + \varphi_7\, e_2e_3 + \varphi_8\, e_1e_2e_3 \in \Gamma(Cl(X, g))$. Then*

$$\begin{aligned} D^2(\varphi_1\, 1) &= \Big(- d^2_{e_1,e_1}\varphi_1 - d^2_{e_2,e_2}\varphi_1 - d^2_{e_3,e_3}\varphi_1 + \Gamma^{2'}_{11} d_{e_2}\varphi_1 + \Gamma^{3'}_{11} d_{e_3}\varphi_1 - \Gamma^{2'}_{21} d_{e_1}\varphi_1 \\ &\quad + \Gamma^{3'}_{22} d_{e_3}\varphi_1 - \Gamma^{3'}_{31} d_{e_1}\varphi_1 - \Gamma^{3'}_{32} d_{e_2}\varphi_1 \Big) 1 \\ &= -\Delta_g(\varphi_1) 1 \end{aligned}$$

$$D^2(\varphi_2\, e_1 + \varphi_3\, e_2 + \varphi_4\, e_3) =$$

$$\begin{aligned} &\Big(- d^2_{e_1,e_1}\varphi_2 - d^2_{e_2,e_2}\varphi_2 - d^2_{e_3,e_3}\varphi_2 + d_{e_1}\varphi_2(-\Gamma^{2'}_{21} - \Gamma^{3'}_{31}) + d_{e_2}\varphi_2(\Gamma^{2'}_{11} - \Gamma^{3'}_{32}) + d_{e_3}\varphi_2(\Gamma^{3'}_{22} + \Gamma^{3'}_{11}) \\ &\quad + 2\Gamma^{2'}_{11}\, d_{e_1}\varphi_3 + 2\Gamma^{2'}_{21}\, d_{e_2}\varphi_3 + 2\Gamma^{2'}_{31}\, d_{e_3}\varphi_3 + 2\Gamma^{3'}_{11}\, d_{e_1}\varphi_4 + 2\Gamma^{3'}_{21}\, d_{e_2}\varphi_4 + 2\Gamma^{3'}_{31}\, d_{e_3}\varphi_4 \\ &\quad + \varphi_2(-d_{e_1}\Gamma^{2'}_{21} - d_{e_1}\Gamma^{3'}_{31} + d_{e_2}\Gamma^{2'}_{11} + d_{e_3}\Gamma^{3'}_{11} + (\Gamma^{3'}_{21})^2 + (\Gamma^{2'}_{31})^2 - 2\Gamma^{3'}_{21}\Gamma^{2'}_{31} - \Gamma^{3'}_{11}\Gamma^{3'}_{22} + \Gamma^{3'}_{32}\Gamma^{2'}_{11}) \\ &\quad + \varphi_3(d_{e_1}\Gamma^{2'}_{11} - d_{e_1}\Gamma^{3'}_{32} + d_{e_2}\Gamma^{2'}_{21} + d_{e_3}\Gamma^{3'}_{12} + d_{e_3}\Gamma^{2'}_{31} - 2\Gamma^{3'}_{22}\Gamma^{2'}_{31} - \Gamma^{3'}_{12}\Gamma^{3'}_{22} + \Gamma^{3'}_{21}\Gamma^{3'}_{22} + \Gamma^{3'}_{32}\Gamma^{2'}_{21}) \\ &\quad + \varphi_4(d_{e_1}\Gamma^{3'}_{11} + d_{e_1}\Gamma^{3'}_{22} - d_{e_2}\Gamma^{3'}_{12} + d_{e_2}\Gamma^{3'}_{21} + d_{e_3}\Gamma^{3'}_{31} + 2\Gamma^{3'}_{21}\Gamma^{3'}_{32} - \Gamma^{3'}_{22}\Gamma^{3'}_{31} - \Gamma^{3'}_{32}\Gamma^{3'}_{12} - \Gamma^{2'}_{31}\Gamma^{3'}_{32}) \Big) e_1 \end{aligned}$$

$$\begin{aligned} &+ \Big(- d^2_{e_1,e_1}\varphi_3 - d^2_{e_2,e_2}\varphi_3 - d^2_{e_3,e_3}\varphi_3 + d_{e_1}\varphi_3(-\Gamma^{2'}_{21} - \Gamma^{3'}_{31}) + d_{e_2}\varphi_3(\Gamma^{2'}_{11} - \Gamma^{3'}_{32}) + d_{e_3}\varphi_3(\Gamma^{3'}_{22} + \Gamma^{3'}_{11}) \\ &\quad - 2\Gamma^{2'}_{11}\, d_{e_1}\varphi_2 - 2\Gamma^{2'}_{21}\, d_{e_2}\varphi_2 - 2\Gamma^{2'}_{31}\, d_{e_3}\varphi_2 + 2\Gamma^{3'}_{12}\, d_{e_1}\varphi_4 + 2\Gamma^{3'}_{22}\, d_{e_2}\varphi_4 + 2\Gamma^{3'}_{32}\, d_{e_3}\varphi_4 \\ &\quad + \varphi_2(-d_{e_1}\Gamma^{2'}_{11} - d_{e_2}\Gamma^{2'}_{21} - d_{e_2}\Gamma^{3'}_{31} + d_{e_3}\Gamma^{3'}_{21} - d_{e_3}\Gamma^{2'}_{31} + 2\Gamma^{3'}_{11}\Gamma^{2'}_{31} + \Gamma^{3'}_{12}\Gamma^{3'}_{11} - \Gamma^{3'}_{11}\Gamma^{3'}_{21} - \Gamma^{3'}_{31}\Gamma^{2'}_{11}) \\ &\quad + \varphi_3(-d_{e_1}\Gamma^{2'}_{21} + d_{e_2}\Gamma^{2'}_{11} - d_{e_2}\Gamma^{3'}_{32} + d_{e_3}\Gamma^{3'}_{22} + (\Gamma^{3'}_{12})^2 + (\Gamma^{2'}_{31})^2 + 2\Gamma^{3'}_{12}\Gamma^{2'}_{31} - \Gamma^{3'}_{11}\Gamma^{3'}_{22} - \Gamma^{3'}_{31}\Gamma^{2'}_{21}) \\ &\quad + \varphi_4(d_{e_1}\Gamma^{3'}_{12} - d_{e_1}\Gamma^{3'}_{21} + d_{e_2}\Gamma^{3'}_{11} + d_{e_2}\Gamma^{3'}_{22} + d_{e_3}\Gamma^{3'}_{32} + 2\Gamma^{3'}_{12}\Gamma^{3'}_{31} - \Gamma^{3'}_{11}\Gamma^{3'}_{32} - \Gamma^{3'}_{31}\Gamma^{3'}_{21} + \Gamma^{2'}_{31}\Gamma^{3'}_{31}) \Big) e_2 \end{aligned}$$

$$\begin{aligned} &+ \Big(- d^2_{e_1,e_1}\varphi_4 - d^2_{e_2,e_2}\varphi_4 - d^2_{e_3,e_3}\varphi_4 + d_{e_1}\varphi_4(-\Gamma^{2'}_{21} - \Gamma^{3'}_{31}) + d_{e_2}\varphi_4(\Gamma^{2'}_{11} - \Gamma^{3'}_{32}) + d_{e_3}\varphi_4(\Gamma^{3'}_{22} + \Gamma^{3'}_{11}) \\ &\quad - 2\Gamma^{3'}_{11}\, d_{e_1}\varphi_2 - 2\Gamma^{3'}_{21}\, d_{e_2}\varphi_2 - 2\Gamma^{3'}_{31}\, d_{e_3}\varphi_2 - 2\Gamma^{3'}_{12}\, d_{e_1}\varphi_3 - 2\Gamma^{3'}_{22}\, d_{e_2}\varphi_3 - 2\Gamma^{3'}_{32}\, d_{e_3}\varphi_3 \\ &\quad + \varphi_2(-d_{e_1}\Gamma^{3'}_{11} - d_{e_2}\Gamma^{3'}_{21} + d_{e_2}\Gamma^{2'}_{31} - d_{e_3}\Gamma^{2'}_{21} - d_{e_3}\Gamma^{3'}_{31} + 2\Gamma^{2'}_{11}\Gamma^{3'}_{21} - \Gamma^{3'}_{12}\Gamma^{2'}_{11} - \Gamma^{2'}_{11}\Gamma^{2'}_{31} - \Gamma^{2'}_{21}\Gamma^{3'}_{11}) \\ &\quad + \varphi_3(-d_{e_1}\Gamma^{3'}_{12} - d_{e_1}\Gamma^{2'}_{31} - d_{e_2}\Gamma^{3'}_{22} + d_{e_3}\Gamma^{2'}_{11} - d_{e_3}\Gamma^{3'}_{32} - 2\Gamma^{3'}_{12}\Gamma^{2'}_{21} + \Gamma^{2'}_{11}\Gamma^{3'}_{22} + \Gamma^{3'}_{21}\Gamma^{2'}_{21} - \Gamma^{2'}_{21}\Gamma^{2'}_{31}) \\ &\quad + \varphi_4(-d_{e_1}\Gamma^{3'}_{31} - d_{e_2}\Gamma^{3'}_{32} + d_{e_3}\Gamma^{3'}_{11} + d_{e_3}\Gamma^{3'}_{22} + (\Gamma^{3'}_{12})^2 + (\Gamma^{3'}_{21})^2 - 2\Gamma^{3'}_{12}\Gamma^{3'}_{21} + \Gamma^{2'}_{11}\Gamma^{3'}_{32} - \Gamma^{2'}_{21}\Gamma^{3'}_{31}) \Big) e_3 \end{aligned}$$

$$D^2(\varphi_5\, e_1e_2 + \varphi_6\, e_1e_3 + \varphi_7\, e_2e_3) =$$

$$\Big(- d^2_{e_1,e_1}\varphi_5 - d^2_{e_2,e_2}\varphi_5 - d^2_{e_3,e_3}\varphi_5 + d_{e_1}\varphi_5(-\Gamma^{2'}_{21} - \Gamma^{3'}_{31}) + d_{e_2}\varphi_5(\Gamma^{2'}_{11} - \Gamma^{3'}_{32}) + d_{e_3}\varphi_5(\Gamma^{3'}_{22} + \Gamma^{3'}_{11})$$

$$+2\Gamma_{12}^{3'}\,d_{e_1}\varphi_6+2\Gamma_{22}^{3'}\,d_{e_2}\varphi_6+2\Gamma_{32}^{3'}\,d_{e_3}\varphi_6-2\Gamma_{11}^{3'}\,d_{e_1}\varphi_7-2\Gamma_{21}^{3'}\,d_{e_2}\varphi_7-2\Gamma_{31}^{3'}\,d_{e_3}\varphi_7$$
$$+\varphi_5(-d_{e_1}\Gamma_{31}^{3'}-d_{e_2}\Gamma_{32}^{3'}+d_{e_3}\Gamma_{11}^{3'}+d_{e_3}\Gamma_{22}^{3'}+(\Gamma_{21}^{3'})^2+(\Gamma_{12}^{3'})^2-2\Gamma_{21}^{3'}\Gamma_{12}^{3'}+\Gamma_{11}^{2'}\Gamma_{32}^{3'}-\Gamma_{21}^{2'}\Gamma_{31}^{3'})$$
$$+\varphi_6(d_{e_1}\Gamma_{12}^{3'}+d_{e_1}\Gamma_{31}^{2'}+d_{e_2}\Gamma_{22}^{3'}-d_{e_3}\Gamma_{11}^{2'}+d_{e_3}\Gamma_{32}^{3'}+2\Gamma_{21}^{2'}\Gamma_{12}^{3'}-\Gamma_{11}^{2'}\Gamma_{22}^{3'}+\Gamma_{21}^{2'}\Gamma_{31}^{2'}-\Gamma_{21}^{3'}\Gamma_{21}^{2'})$$
$$+\varphi_7(-d_{e_1}\Gamma_{11}^{3'}-d_{e_2}\Gamma_{21}^{3'}+d_{e_2}\Gamma_{31}^{2'}-d_{e_3}\Gamma_{21}^{2'}-d_{e_3}\Gamma_{31}^{3'}+2\Gamma_{11}^{2'}\Gamma_{21}^{3'}-\Gamma_{11}^{2'}\Gamma_{31}^{2'}-\Gamma_{12}^{3'}\Gamma_{11}^{2'}-\Gamma_{21}^{2'}\Gamma_{11}^{3'})\Big)e_1e_2$$

$$+\Big(-d^2_{e_1,e_1}\varphi_6-d^2_{e_2,e_2}\varphi_6-d^2_{e_3,e_3}\varphi_6+d_{e_1}\varphi_6(-\Gamma_{21}^{2'}-\Gamma_{31}^{3'})+d_{e_2}\varphi_6(\Gamma_{11}^{2'}-\Gamma_{32}^{3'})+d_{e_3}\varphi_6(\Gamma_{22}^{3'}+\Gamma_{11}^{3'})$$
$$-2\Gamma_{12}^{3'}\,d_{e_1}\varphi_5-2\Gamma_{22}^{3'}\,d_{e_2}\varphi_5-2\Gamma_{32}^{3'}\,d_{e_3}\varphi_5+2\Gamma_{11}^{2'}\,d_{e_1}\varphi_7+2\Gamma_{21}^{2'}\,d_{e_2}\varphi_7+2\Gamma_{31}^{2'}\,d_{e_3}\varphi_7$$
$$+\varphi_5(-d_{e_1}\Gamma_{12}^{3'}+d_{e_1}\Gamma_{21}^{3'}-d_{e_2}\Gamma_{11}^{3'}-d_{e_2}\Gamma_{22}^{3'}-d_{e_3}\Gamma_{32}^{3'}-2\Gamma_{12}^{3'}\Gamma_{31}^{3'}+\Gamma_{32}^{3'}\Gamma_{11}^{3'}-\Gamma_{31}^{2'}\Gamma_{31}^{3'}+\Gamma_{31}^{3'}\Gamma_{21}^{3'})$$
$$+\varphi_6(-d_{e_1}\Gamma_{21}^{2'}+d_{e_2}\Gamma_{11}^{2'}-d_{e_2}\Gamma_{32}^{3'}+d_{e_3}\Gamma_{22}^{3'}+(\Gamma_{12}^{3'})^2+(\Gamma_{31}^{2'})^2+2\Gamma_{12}^{3'}\Gamma_{31}^{2'}-\Gamma_{11}^{3'}\Gamma_{22}^{3'}-\Gamma_{31}^{3'}\Gamma_{21}^{2'})$$
$$+\varphi_7(d_{e_1}\Gamma_{11}^{2'}+d_{e_2}\Gamma_{21}^{2'}+d_{e_2}\Gamma_{31}^{3'}-d_{e_3}\Gamma_{21}^{3'}+d_{e_3}\Gamma_{31}^{2'}-2\Gamma_{11}^{3'}\Gamma_{31}^{2'}+\Gamma_{11}^{3'}\Gamma_{21}^{3'}-\Gamma_{12}^{3'}\Gamma_{11}^{3'}+\Gamma_{31}^{3'}\Gamma_{11}^{2'})\Big)e_1e_3$$

$$+\Big(-d^2_{e_1,e_1}\varphi_7-d^2_{e_2,e_2}\varphi_7-d^2_{e_3,e_3}\varphi_7+d_{e_1}\varphi_7(-\Gamma_{21}^{2'}-\Gamma_{31}^{3'})+d_{e_2}\varphi_7(\Gamma_{11}^{2'}-\Gamma_{32}^{3'})+d_{e_3}\varphi_7(\Gamma_{22}^{3'}+\Gamma_{11}^{3'})$$
$$+2\Gamma_{11}^{3'}\,d_{e_1}\varphi_5+2\Gamma_{21}^{3'}\,d_{e_2}\varphi_5+2\Gamma_{31}^{3'}\,d_{e_3}\varphi_5-2\Gamma_{11}^{2'}\,d_{e_1}\varphi_6-2\Gamma_{21}^{2'}\,d_{e_2}\varphi_6-2\Gamma_{31}^{2'}\,d_{e_3}\varphi_6$$
$$+\varphi_5(d_{e_1}\Gamma_{11}^{3'}+d_{e_1}\Gamma_{22}^{3'}-d_{e_2}\Gamma_{12}^{3'}+d_{e_2}\Gamma_{21}^{3'}+d_{e_3}\Gamma_{31}^{3'}+2\Gamma_{21}^{3'}\Gamma_{32}^{3'}-\Gamma_{22}^{3'}\Gamma_{31}^{3'}-\Gamma_{31}^{2'}\Gamma_{32}^{3'}-\Gamma_{32}^{3'}\Gamma_{12}^{3'})$$
$$+\varphi_6(-d_{e_1}\Gamma_{11}^{2'}+d_{e_1}\Gamma_{32}^{3'}-d_{e_2}\Gamma_{21}^{2'}-d_{e_3}\Gamma_{12}^{3'}-d_{e_3}\Gamma_{31}^{2'}+2\Gamma_{22}^{3'}\Gamma_{31}^{2'}-\Gamma_{21}^{3'}\Gamma_{22}^{3'}+\Gamma_{22}^{3'}\Gamma_{12}^{3'}-\Gamma_{32}^{3'}\Gamma_{21}^{2'})$$
$$+\varphi_7(-d_{e_1}\Gamma_{21}^{2'}-d_{e_1}\Gamma_{31}^{3'}+d_{e_2}\Gamma_{11}^{2'}+d_{e_3}\Gamma_{11}^{3'}+(\Gamma_{21}^{3'})^2+(\Gamma_{31}^{2'})^2-2\Gamma_{21}^{3'}\Gamma_{31}^{2'}-\Gamma_{22}^{3'}\Gamma_{11}^{3'}+\Gamma_{32}^{3'}\Gamma_{11}^{2'})\Big)e_2e_3$$

$$\begin{aligned}D^2(\varphi_8\,e_1e_2e_3) &= \Big(-d^2_{e_1,e_1}\varphi_8-d^2_{e_2,e_2}\varphi_8-d^2_{e_3,e_3}\varphi_8+\Gamma_{11}^{2'}d_{e_2}\varphi_8+\Gamma_{11}^{3'}d_{e_3}\varphi_8-\Gamma_{21}^{2'}d_{e_1}\varphi_8\\ &\quad +\Gamma_{22}^{3'}d_{e_3}\varphi_8-\Gamma_{31}^{3'}d_{e_1}\varphi_8-\Gamma_{32}^{3'}d_{e_2}\varphi_8\Big)e_1e_2e_3\\ &= -\Delta_g(\varphi_8)e_1e_2e_3\end{aligned}$$

Proof. We obtain $D^2(\varphi)$ from (4.9) and the relations above defining ∇^C in the frame (e_1,e_2,e_3). Then we simplify the expression using some properties of the Levi-Cevita connection :
(i) In an orthonormal frame, symbols satisfy $\Gamma_{ij}^{k'}=-\Gamma_{ik}^{j'}$.
(ii) $[e_1,e_2]=-\Gamma_{11}^{2'}e_1-\Gamma_{21}^{2'}e_2+\Gamma_{12}^{3'}e_3-\Gamma_{21}^{3'}e_3$

$$[e_3,e_1]=\Gamma_{11}^{3'}e_1+\Gamma_{31}^{2'}e_2+\Gamma_{12}^{3'}e_2+\Gamma_{31}^{3'}e_3$$

$$[e_2,e_3]=-\Gamma_{21}^{3'}e_1+\Gamma_{31}^{2'}e_1-\Gamma_{22}^{3'}e_2-\Gamma_{32}^{3'}e_3$$

□

Proposition 4.11 (Parallel transport on $Cl(X,g)$) *Let (X,g) be a Riemannian manifold of dimension 3. Let (e_1,e_2,e_3) be an orthonormal frame on X, and $Y_0 = Y_0^1 1(y)+Y_0^2 e_1(y)+Y_0^3 e_2(y)+Y_0^4 e_3(y)+Y_0^5 e_1e_2(y)+Y_0^6 e_1e_3(y)+Y_0^7 e_2e_3(y)+Y_0^8 e_1e_2e_3(y) \in Cl(X,g)_y$. Let γ be a C^1 curve in X such that $\gamma(0)=y$. The parallel transport Y of Y_0 along γ is obtained from the solution of the following differential equation on $\mathbb{R}^8$.*

$$dY_1/dt = 0, \begin{pmatrix} dY_2/dt \\ dY_3/dt \\ dY_4/dt \end{pmatrix} = A \begin{pmatrix} Y_2 \\ Y_3 \\ Y_4 \end{pmatrix}, \begin{pmatrix} dY_5/dt \\ dY_6/dt \\ dY_7/dt \end{pmatrix} = B \begin{pmatrix} Y_5 \\ Y_6 \\ Y_7 \end{pmatrix}, dY_8/dt = 0 \quad (4.14)$$

where $A=$

$$\begin{pmatrix} 0 & \dot\gamma_1\Gamma_{11}^{2'} + \dot\gamma_2\Gamma_{21}^{2'} + \dot\gamma_3\Gamma_{31}^{2'} & \dot\gamma_1\Gamma_{11}^{3'} + \dot\gamma_2\Gamma_{21}^{3'} + \dot\gamma_3\Gamma_{31}^{2'} \\ -\dot\gamma_1\Gamma_{11}^{2'} - \dot\gamma_2\Gamma_{21}^{2'} - \dot\gamma_3\Gamma_{31}^{2'} & 0 & \dot\gamma_1\Gamma_{12}^{3'} + \dot\gamma_2\Gamma_{22}^{3'} + \dot\gamma_3\Gamma_{32}^{3'} \\ -\dot\gamma_1\Gamma_{11}^{3'} - \dot\gamma_2\Gamma_{21}^{3'} - \dot\gamma_3\Gamma_{31}^{2'} & -\dot\gamma_1\Gamma_{12}^{3'} - \dot\gamma_2\Gamma_{22}^{3'} - \dot\gamma_3\Gamma_{32}^{3'} & 0 \end{pmatrix}$$

and $B =$

$$\begin{pmatrix} 0 & \dot\gamma_1\Gamma_{12}^{3'} + \dot\gamma_2\Gamma_{22}^{3'} + \dot\gamma_3\Gamma_{32}^{3'} & -\dot\gamma_1\Gamma_{11}^{3'} - \dot\gamma_2\Gamma_{21}^{3'} - \dot\gamma_3\Gamma_{31}^{2'} \\ -\dot\gamma_1\Gamma_{12}^{3'} - \dot\gamma_2\Gamma_{22}^{3'} - \dot\gamma_3\Gamma_{32}^{3'} & 0 & \dot\gamma_1\Gamma_{11}^{2'} + \dot\gamma_2\Gamma_{21}^{2'} + \dot\gamma_3\Gamma_{31}^{2'} \\ \dot\gamma_1\Gamma_{11}^{3'} + \dot\gamma_2\Gamma_{21}^{3'} + \dot\gamma_3\Gamma_{31}^{2'} & -\dot\gamma_1\Gamma_{11}^{2'} - \dot\gamma_2\Gamma_{21}^{2'} - \dot\gamma_3\Gamma_{31}^{2'} & 0 \end{pmatrix}$$

of initial condition $Y_i(0) = Y_0^i$, for $i \in \{1,\cdots,8\}$.

The solutions $Y_1(t)$ and $Y_8(t)$ are given by $Y_1(t) = Y_0^1$ and $Y_8(t) = Y_0^8$. To the best of knowledge of the author, there exist no explicit formulae for $(Y_2(t),Y_3(t),Y_4(t))$ and $(Y_5(t),Y_6(t),Y_7(t))$. In practice, we suppose the matrices A and B to be locally constant. This gives explicit solutions of (4.14).

Corollary 4.1 *Let us suppose that Christoffel's symbols $\Gamma_{ij}^{k'}$ and coordinates $\dot\gamma_i$ of $\dot\gamma$ are constant on some open set $\Omega_y \supset y$. Let (f_1,f_2,f_3) be an orthonormal basis of $\mathbb{R}^3$ generating the Clifford algebra $Cl(\mathbb{R}^3,-\|\ \|_2)$ and $S_1(t), S_2(t) \in Spin(3) \subset Cl(\mathbb{R}^3,-\|\ \|_2)$ defined by*

$$S_1(t) = exp\left[\frac{t\sqrt{\alpha^2+\beta^2+\delta^2}}{2}\left(\frac{\alpha f_1f_2+\beta f_1f_3+\delta f_2f_3}{\sqrt{\alpha^2+\beta^2+\delta^2}}\right)\right]$$

and

$$S_2(t) = exp\left[\frac{t\sqrt{\alpha^2+\beta^2+\delta^2}}{2}\left(\frac{\delta f_1f_2-\beta f_1f_3+\alpha f_2f_3}{\sqrt{\alpha^2+\beta^2+\delta^2}}\right)\right]$$

where $\alpha = \dot\gamma_1\Gamma_{11}^{2'} + \dot\gamma_2\Gamma_{21}^{2'} + \dot\gamma_3\Gamma_{31}^{2'}$, $\beta = \dot\gamma_1\Gamma_{11}^{3'} + \dot\gamma_2\Gamma_{21}^{3'} + \dot\gamma_3\Gamma_{31}^{2'}$ and $\delta = \dot\gamma_1\Gamma_{12}^{3'} + \dot\gamma_2\Gamma_{22}^{3'} + \dot\gamma_3\Gamma_{32}^{3'}$.

The solution $Y(t)$ of (4.14) is given on Ω_y by Y(t)=

$$
\begin{aligned}
&Y_0^1 1(\gamma(t)) + \Big[f_1 \cdot \Big(S_1(t)^\dagger (Y_0^2 f_1 + Y_0^3 f_2 + Y_0^4 f_3) S_1(t)\Big)\Big] e_1(\gamma(t)) \\
&+ \Big[f_2 \cdot \Big(S_1(t)^\dagger (Y_0^2 f_1 + Y_0^3 f_2 + Y_0^4 f_3) S_1(t)\Big)\Big] e_2(\gamma(t)) \\
&+ \Big[f_3 \cdot \Big(S_1(t)^\dagger (Y_0^2 f_1 + Y_0^3 f_2 + Y_0^4 f_3) S_1(t)\Big)\Big] e_3(\gamma(t)) \\
&+ \Big[f_1 \cdot \Big(S_2(t)^\dagger (Y_0^5 f_1 + Y_0^6 f_2 + Y_0^7 f_3) S_2(t)\Big)\Big] e_1 e_2(\gamma(t)) \\
&+ \Big[f_2 \cdot \Big(S_2(t)^\dagger (Y_0^5 f_1 + Y_0^6 f_2 + Y_0^7 f_3) S_2(t)\Big)\Big] e_1 e_3(\gamma(t)) \\
&+ \Big[f_3 \cdot \Big(S_2(t)^\dagger (Y_0^5 f_1 + Y_0^6 f_2 + Y_0^7 f_3) S_2(t)\Big)\Big] e_2 e_3(\gamma(t)) + Y_0^8 e_1 e_2 e_3(\gamma(t))
\end{aligned}
$$

Proof. We aim at solving the differential equations

$$
\begin{pmatrix} dY_2/dt \\ dY_3/dt \\ dY_4/dt \end{pmatrix} = A \begin{pmatrix} Y_2 \\ Y_3 \\ Y_4 \end{pmatrix} \text{ and } \begin{pmatrix} dY_5/dt \\ dY_6/dt \\ dY_7/dt \end{pmatrix} = B \begin{pmatrix} Y_5 \\ Y_6 \\ Y_7 \end{pmatrix} \tag{4.15}
$$

where A and B are antisymmetric of the form

$$
A = \begin{pmatrix} 0 & \alpha & \beta \\ -\alpha & 0 & \delta \\ -\beta & -\delta & 0 \end{pmatrix} \qquad B = \begin{pmatrix} 0 & \delta & -\beta \\ -\delta & 0 & \alpha \\ \beta & -\alpha & 0 \end{pmatrix}
$$

They got the same eigenvalues, i.e. 0, $i\sqrt{\alpha^2+\beta^2+\delta^2}$ and its conjugate. The eigenspaces associated to 0 are $\mathbb{R}(\delta, -\beta, \alpha)$ for A, and $\mathbb{R}(\alpha, \beta, \delta)$ for B. The two-dimensional eigenspaces of the complex eigenvalue $i\sqrt{\alpha^2+\beta^2+\delta^2}$ are their orthogonal supplementary in $\mathbb{R}^3$. Let u_1 resp. v_1 be an eigenvector of A resp. B relative to the eigenvalue 0, let (u_2, u_3) resp. (v_2, v_3) be a basis of the eigenspace relative to the eigenvalue $i\sqrt{\alpha^2+\beta^2+\delta^2}$, and P_1 resp. P_2 be the basis change matrix from (f_1, f_2, f_3) to (u_1, u_2, u_3) resp. (v_1, v_2, v_3).

In the basis (u_1, u_2, u_3) of coordinates (Z_2, Z_3, Z_4), the first differential equation of (4.15) is

$$
\begin{pmatrix} dZ_2/dt \\ d(Z_3 + i\, Z_4)/dt \end{pmatrix} = \begin{pmatrix} 0 & 0 \\ 0 & i\sqrt{\alpha^2+\beta^2+\delta^2} \end{pmatrix} \begin{pmatrix} Z_2 \\ Z_3 + i\, Z_4 \end{pmatrix} \tag{4.16}
$$

of initial condition

$$
\begin{pmatrix} Z_2(0) \\ Z_3(0) \\ Z_4(0) \end{pmatrix} = P_1^{-1} \begin{pmatrix} Y_0^2 \\ Y_0^3 \\ Y_0^4 \end{pmatrix}
$$

In the basis (v_1, v_2, v_3) of coordinates (Z_5, Z_6, Z_7), the second differential equation of (4.15) is

$$
\begin{pmatrix} dZ_5/dt \\ d(Z_6 + i\, Z_7)/dt \end{pmatrix} = \begin{pmatrix} 0 & 0 \\ 0 & i\sqrt{\alpha^2+\beta^2+\delta^2} \end{pmatrix} \begin{pmatrix} Z_5 \\ Z_6 + i\, Z_7 \end{pmatrix} \tag{4.17}
$$

of initial condition

$$\begin{pmatrix} Z_5(0) \\ Z_6(0) \\ Z_7(0) \end{pmatrix} = P_2^{-1} \begin{pmatrix} Y_0^5 \\ Y_0^6 \\ Y_0^7 \end{pmatrix}$$

Solutions of (4.16) and (4.17) are

$$\begin{cases} Z_2(t) &= Z_2(0) \\ Z_3(t) + iZ_4(t) &= exp(i\,t\,\sqrt{\alpha^2+\beta^2+\delta^2})(Z_3(0) + iZ_4(0)) \end{cases}$$

$$\begin{cases} Z_5(t) &= Z_5(0) \\ Z_6(t) + iZ_7(t) &= exp(i\,t\,\sqrt{\alpha^2+\beta^2+\delta^2})(Z_6(0) + iZ_7(0)) \end{cases}$$

and general solutions of (4.15) are

$$\begin{pmatrix} Y_2(t) \\ Y_3(t) \\ Y_4(t) \end{pmatrix} = P_1 \begin{pmatrix} Z_2(t) \\ Z_3(t) \\ Z_4(t) \end{pmatrix} \quad \text{and} \quad \begin{pmatrix} Y_5(t) \\ Y_6(t) \\ Y_7(t) \end{pmatrix} = P_2 \begin{pmatrix} Z_5(t) \\ Z_6(t) \\ Z_7(t) \end{pmatrix}$$

We see that solutions of (4.15) are given by rotations of angle $t\sqrt{\alpha^2+\beta^2+\delta^2}$ in $\mathbb{R}^3$ with respect to the planes that are eigenspaces for the eigenvalue $i\sqrt{\alpha^2+\beta^2+\delta^2}$ applied to the initial condition vectors. As in the case $m = 2$, using the Clifford algebras context, such operations take a straightforward form. For this, we embed $\mathbb{R}^3$ of basis (f_1, f_2, f_3) into $Cl(\mathbb{R}^3, -\| \|_2)$.

Indeed, oriented planes in $\mathbb{R}^3$ are represented by bivectors in $Cl(\mathbb{R}^3, -\| \|_2)$. In particular, the bivector representing the orthogonal of the vector $a_1f_1 + a_2f_2 + a_3f_3$ results from the product $(a_1f_1 + a_2f_2 + a_3f_3)f_1f_2f_3$. Hence the rotation of angle $t\sqrt{\alpha^2+\beta^2+\delta^2}$ in the oriented plane orthogonal to $\delta f_1 - \beta f_2 + \alpha f_3$ resp. $\alpha f_1 + \beta f_2 + \delta f_3$ is given by the spinor

$$S_1(t) = exp\left[\frac{t\sqrt{\alpha^2+\beta^2+\delta^2}}{2}\left(\frac{\alpha f_1f_2 + \beta f_1f_3 + \delta f_2f_3}{\sqrt{\alpha^2+\beta^2+\delta^2}}\right)\right]$$

resp.

$$S_2(t) = exp\left[\frac{t\sqrt{\alpha^2+\beta^2+\delta^2}}{2}\left(\frac{\delta f_1f_2 - \beta f_1f_3 + \alpha f_2f_3}{\sqrt{\alpha^2+\beta^2+\delta^2}}\right)\right]$$

Then we have

$$Y_2(t)f_1 + Y_3(t)f_2 + Y_4(t)f_3 = S_1(t)^\dagger(Y_0^2f_1 + Y_0^3f_2 + Y_0^4f_3)S_1(t)$$

and

$$Y_5(t)f_1 + Y_6(t)f_2 + Y_7(t)f_3 = S_2(t)^\dagger(Y_0^5f_1 + Y_0^6f_2 + Y_0^7f_3)S_2(t)$$

This gives the parallel transport $Y(t)$ of Y_0. □

4.5.2 The particular context of videos

Let us consider a nD video defined by a function $I\colon (x,y,z) \longmapsto (I_1(x,y,z),\cdots,I_n(x,y,z))$ on a domain $\Omega \subset \mathbb{R}^3$. I determines a submanifold S of $\mathbb{R}^{n+3}$ of dimension 3 parametrized by

$$\varphi\colon (x,y,z) \longmapsto (x,y,z,I_1(x,y,z),\cdots,I_n(x,y,z))$$

Then endow $\mathbb{R}^{n+3}$ of a metric h of the form

$$h(p) = \begin{pmatrix} \lambda & 0 & 0 \\ 0 & \lambda & 0 \\ 0 & 0 & \beta \end{pmatrix} \oplus \begin{pmatrix} h_1(p) & 0 & 0 & \cdots\cdots & 0 \\ 0 & h_2(p) & 0 & \cdots\cdots & 0 \\ 0 & 0 & \ddots & & \vdots \\ \vdots & \vdots & & \ddots & \vdots \\ 0 & 0 & \cdots\cdots & 0 & h_n(p) \end{pmatrix} \tag{4.18}$$

where $h_1,\cdots,h_n$ are positive functions, $\lambda,\beta > 0$ and denote by g the metric on S induced by h makes the couple (S,g) be a Riemannian manifold of dimension 3 of global chart (Ω,φ).

As for the case $m = 2$, an oriented orthonormal frame field (e_1,e_2,e_3) may be constructed on (S,g) from the matrix representation of g in the frame $(\partial/\partial x, \partial/\partial y, \partial/\partial z)$. Indeed, for each $p \in S$, a positively oriented orthonormal basis of T_pS may be constructed from its eigenvectors.

Then we need to compute the transformation of Levi-Cevita connection's symbols with respect to the frame change from $(\partial/\partial x, \partial/\partial y, \partial/\partial z)$ to (e_1,e_2,e_3). Remind that by the antisymmetry property of its symbols $\Gamma_{ij}^{k'}$ in an orthonormal frame, the Levi-Cevita connection is determined by the 9 symbols $\Gamma_{11}^{2'},\Gamma_{11}^{3'},\Gamma_{21}^{2'},\Gamma_{21}^{3'},\Gamma_{31}^{2'},\Gamma_{31}^{3'},\Gamma_{12}^{3'},\Gamma_{22}^{3'}$ and $\Gamma_{32}^{3'}$ in such frames. In the next proposition, we determine the expressions of these 9 symbols in a frame (v_1,v_2,v_3) in function of the symbols Γ_{ij}^{k} of the connection in the frame $(\partial/\partial x, \partial/\partial y, \partial/\partial z)$.

Proposition 4.12 *Let (v_1,v_2,v_3) be a frame on (S,g) and*

$$A = \begin{pmatrix} a_{11} & a_{12} & a_{13} \\ a_{21} & a_{22} & a_{23} \\ a_{31} & a_{32} & a_{33} \end{pmatrix}$$

be the change frame field from $(\partial/\partial x, \partial/\partial y, \partial/\partial z)$ to (v_1,v_2,v_3). Then

$\Gamma_{11}^{2'} =$

$$\frac{1}{\det A}(a_{31}a_{23} - a_{21}a_{33})\Big(a_{11}\frac{\partial a_{11}}{\partial x} + (a_{11})^2\Gamma_{11}^1 + 2a_{11}a_{21}\Gamma_{12}^1 + 2a_{11}a_{31}\Gamma_{13}^1 + a_{21}\frac{\partial a_{11}}{\partial y}$$
$$+(a_{21})^2\Gamma_{22}^1 + 2a_{21}a_{31}\Gamma_{23}^1 + a_{31}\frac{\partial a_{11}}{\partial z} + (a_{31})^2\Gamma_{33}^1\Big) + \frac{1}{\det A}(a_{11}a_{33} - a_{13}a_{31})\Big((a_{11})^2\Gamma_{11}^2$$
$$+a_{11}\frac{\partial a_{21}}{\partial x} + 2a_{11}a_{21}\Gamma_{12}^2 + 2a_{11}a_{31}\Gamma_{31}^2 + a_{21}\frac{\partial a_{21}}{\partial y} + (a_{21})^2\Gamma_{22}^2 + 2a_{21}a_{31}\Gamma_{23}^2 + a_{31}\frac{\partial a_{21}}{\partial z}$$
$$+(a_{31})^2\Gamma_{33}^2\Big) + \frac{1}{\det A}(a_{11}a_{23} - a_{13}a_{21})\Big((a_{11})^2\Gamma_{11}^3 + a_{11}\frac{\partial a_{31}}{\partial x} + 2a_{11}a_{21}\Gamma_{12}^3 + 2a_{11}a_{31}\Gamma_{13}^3$$

$$+a_{21}\frac{\partial a_{31}}{\partial y}+(a_{21})^2\Gamma^2_{32}+2a_{21}a_{31}\Gamma^3_{23}+a_{31}\frac{\partial a_{31}}{\partial z}+(a_{31})^2\Gamma^3_{33}\Big)$$

$$\Gamma^{3'}_{11}=$$

$$\frac{1}{\det A}(a_{21}a_{32}-a_{22}a_{31})\Big(a_{11}\frac{\partial a_{11}}{\partial x}+(a_{11})^2\Gamma^1_{11}+2a_{11}a_{21}\Gamma^1_{12}+2a_{11}a_{31}\Gamma^1_{13}+a_{21}\frac{\partial a_{11}}{\partial y}$$
$$+(a_{21})^2\Gamma^1_{22}+2a_{21}a_{31}\Gamma^1_{23}+a_{31}\frac{\partial a_{11}}{\partial z}+(a_{31})^2\Gamma^1_{33}\Big)+\frac{1}{\det A}(a_{31}a_{12}-a_{11}a_{32})\Big((a_{11})^2\Gamma^2_{11}$$
$$+a_{11}\frac{\partial a_{21}}{\partial x}+2a_{11}a_{21}\Gamma^2_{12}+2a_{11}a_{31}\Gamma^2_{31}+a_{21}\frac{\partial a_{21}}{\partial y}+(a_{21})^2\Gamma^2_{22}+2a_{21}a_{31}\Gamma^2_{23}+a_{31}\frac{\partial a_{21}}{\partial z}$$
$$+(a_{31})^2\Gamma^2_{33}\Big)+\frac{1}{\det A}(a_{11}a_{22}-a_{12}a_{21})\Big((a_{11})^2\Gamma^3_{11}+a_{11}\frac{\partial a_{31}}{\partial x}+2a_{11}a_{21}\Gamma^3_{12}+2a_{11}a_{31}\Gamma^3_{13}$$
$$+a_{21}\frac{\partial a_{31}}{\partial y}+(a_{21})^2\Gamma^2_{32}+2a_{21}a_{31}\Gamma^3_{23}+a_{31}\frac{\partial a_{31}}{\partial z}+(a_{31})^2\Gamma^3_{33}\Big)$$

$$\Gamma^{2'}_{21}=$$

$$\frac{1}{\det A}(a_{31}a_{23}-a_{21}a_{33})\Big(a_{12}\frac{\partial a_{11}}{\partial x}+a_{12}a_{11}\Gamma^1_{11}+(a_{12}a_{21}+a_{22}a_{11})\Gamma^1_{12}+(a_{12}a_{31}+a_{32}a_{11})\Gamma^1_{13}$$
$$+a_{22}\frac{\partial a_{11}}{\partial y}+a_{22}a_{21}\Gamma^1_{22}+(a_{22}a_{31}+a_{32}a_{21})\Gamma^1_{23}+a_{32}\frac{\partial a_{11}}{\partial z}+a_{32}a_{31}\Gamma^1_{33}\Big)+\frac{1}{\det A}(a_{11}a_{33}$$
$$-a_{13}a_{31})\Big(a_{12}\frac{\partial a_{21}}{\partial x}+a_{12}a_{11}\Gamma^2_{11}+(a_{12}a_{21}+a_{22}a_{11})\Gamma^2_{12}+(a_{12}a_{31}+a_{32}a_{11})\Gamma^2_{13}+a_{22}\frac{\partial a_{21}}{\partial y}$$
$$+a_{22}a_{21}\Gamma^2_{22}+(a_{22}a_{31}+a_{32}a_{21})\Gamma^2_{23}+a_{32}\frac{\partial a_{21}}{\partial z}+a_{32}a_{31}\Gamma^2_{33}\Big)+\frac{1}{\det A}(a_{11}a_{23}-a_{13}a_{21})$$
$$\Big(a_{12}\frac{\partial a_{31}}{\partial x}+a_{12}a_{11}\Gamma^3_{11}+(a_{12}a_{21}+a_{22}a_{11})\Gamma^3_{12}+(a_{12}a_{31}+a_{32}a_{11})\Gamma^3_{13}+a_{22}\frac{\partial a_{31}}{\partial y}+a_{22}a_{21}\Gamma^3_{22}$$
$$+(a_{22}a_{31}+a_{32}a_{21})\Gamma^3_{23}+a_{32}\frac{\partial a_{31}}{\partial z}+a_{32}a_{31}\Gamma^3_{33}\Big)$$

$$\Gamma^{3'}_{21}=$$

$$\frac{1}{\det A}(a_{21}a_{32}-a_{22}a_{31})\Big(a_{12}\frac{\partial a_{11}}{\partial x}+a_{12}a_{11}\Gamma^1_{11}+(a_{12}a_{21}+a_{22}a_{11})\Gamma^1_{12}+(a_{12}a_{31}+a_{32}a_{11})\Gamma^1_{13}$$
$$+a_{22}\frac{\partial a_{11}}{\partial y}+a_{22}a_{21}\Gamma^1_{22}+(a_{22}a_{31}+a_{32}a_{21})\Gamma^1_{23}+a_{32}\frac{\partial a_{11}}{\partial z}+a_{32}a_{31}\Gamma^1_{33}\Big)+\frac{1}{\det A}(a_{31}a_{12}$$
$$-a_{11}a_{32})\Big(a_{12}\frac{\partial a_{21}}{\partial x}+a_{12}a_{11}\Gamma^2_{11}+(a_{12}a_{21}+a_{22}a_{11})\Gamma^2_{12}+(a_{12}a_{31}+a_{32}a_{11})\Gamma^2_{13}+a_{22}\frac{\partial a_{21}}{\partial y}$$
$$+a_{22}a_{21}\Gamma^2_{22}+(a_{22}a_{31}+a_{32}a_{21})\Gamma^2_{23}+a_{32}\frac{\partial a_{21}}{\partial z}+a_{32}a_{31}\Gamma^2_{33}\Big)+\frac{1}{\det A}(a_{11}a_{22}-a_{12}a_{21})$$
$$\Big(a_{12}\frac{\partial a_{31}}{\partial x}+a_{12}a_{11}\Gamma^3_{11}+(a_{12}a_{21}+a_{22}a_{11})\Gamma^3_{12}+(a_{12}a_{31}+a_{32}a_{11})\Gamma^3_{13}+a_{22}\frac{\partial a_{31}}{\partial y}+a_{22}a_{21}\Gamma^3_{22}$$
$$+(a_{22}a_{31}+a_{32}a_{21})\Gamma^3_{23}+a_{32}\frac{\partial a_{31}}{\partial z}+a_{32}a_{31}\Gamma^3_{33}\Big)$$

$$\Gamma^{2'}_{31}=$$

$$\frac{1}{\det A}(a_{31}a_{23}-a_{21}a_{33})\Big(a_{13}\frac{\partial a_{11}}{\partial x}+a_{13}a_{11}\Gamma^1_{11}+(a_{13}a_{21}+a_{23}a_{11})\Gamma^1_{12}+(a_{13}a_{31}+a_{33}a_{11})\Gamma^1_{13}$$

$$+a_{23}\frac{\partial a_{11}}{\partial y}+a_{23}a_{21}\Gamma^1_{22}+(a_{23}a_{31}+a_{33}a_{21})\Gamma^1_{23}+a_{33}\frac{\partial a_{11}}{\partial z}+a_{33}a_{31}\Gamma^1_{33}\Big)+\frac{1}{\det A}(a_{11}a_{33}$$
$$-a_{13}a_{31})\Big(a_{13}\frac{\partial a_{21}}{\partial x}+a_{13}a_{11}\Gamma^2_{11}+(a_{13}a_{21}+a_{23}a_{11})\Gamma^2_{12}+(a_{13}a_{31}+a_{33}a_{11})\Gamma^2_{13}+a_{23}\frac{\partial a_{21}}{\partial y}$$
$$+a_{23}a_{21}\Gamma^2_{22}+(a_{23}a_{31}+a_{33}a_{21})\Gamma^2_{23}+a_{33}\frac{\partial a_{21}}{\partial z}+a_{33}a_{31}\Gamma^2_{33}\Big)+\frac{1}{\det A}(a_{11}a_{23}-a_{13}a_{21})$$
$$\Big(a_{13}\frac{\partial a_{31}}{\partial x}+a_{13}a_{11}\Gamma^3_{11}+(a_{13}a_{21}+a_{23}a_{11})\Gamma^3_{12}+(a_{13}a_{31}+a_{33}a_{11})\Gamma^3_{13}+a_{23}\frac{\partial a_{31}}{\partial y}+a_{23}a_{21}\Gamma^3_{22}$$
$$+(a_{23}a_{31}+a_{33}a_{21})\Gamma^3_{23}+a_{33}\frac{\partial a_{31}}{\partial z}+a_{33}a_{31}\Gamma^3_{33}\Big)$$

$\Gamma^{3'}_{31}=$

$$\frac{1}{\det A}(a_{21}a_{32}-a_{22}a_{31})\Big(a_{13}\frac{\partial a_{11}}{\partial x}+a_{13}a_{11}\Gamma^1_{11}+(a_{13}a_{21}+a_{23}a_{11})\Gamma^1_{12}+(a_{13}a_{31}+a_{33}a_{11})\Gamma^1_{13}$$
$$+a_{23}\frac{\partial a_{11}}{\partial y}+a_{23}a_{21}\Gamma^1_{22}+(a_{23}a_{31}+a_{33}a_{21})\Gamma^1_{23}+a_{33}\frac{\partial a_{11}}{\partial z}+a_{33}a_{31}\Gamma^1_{33}\Big)+\frac{1}{\det A}(a_{31}a_{12}$$
$$-a_{11}a_{32})\Big(a_{13}\frac{\partial a_{21}}{\partial x}+a_{13}a_{11}\Gamma^2_{11}+(a_{13}a_{21}+a_{23}a_{11})\Gamma^2_{12}+(a_{13}a_{31}+a_{33}a_{11})\Gamma^2_{13}+a_{23}\frac{\partial a_{21}}{\partial y}$$
$$+a_{23}a_{21}\Gamma^2_{22}+(a_{23}a_{31}+a_{33}a_{21})\Gamma^2_{23}+a_{33}\frac{\partial a_{21}}{\partial z}+a_{33}a_{31}\Gamma^2_{33}\Big)+\frac{1}{\det A}(a_{11}a_{22}-a_{12}a_{21})$$
$$\Big(a_{13}\frac{\partial a_{31}}{\partial x}+a_{13}a_{11}\Gamma^3_{11}+(a_{13}a_{21}+a_{23}a_{11})\Gamma^3_{12}+(a_{13}a_{31}+a_{33}a_{11})\Gamma^3_{13}+a_{23}\frac{\partial a_{31}}{\partial y}+a_{23}a_{21}\Gamma^3_{22}$$
$$+(a_{23}a_{31}+a_{33}a_{21})\Gamma^3_{23}+a_{33}\frac{\partial a_{31}}{\partial z}+a_{33}a_{31}\Gamma^3_{33}\Big)$$

$\Gamma^{3'}_{12}=$

$$\frac{1}{\det A}(a_{21}a_{32}-a_{22}a_{31})\Big(a_{11}\frac{\partial a_{12}}{\partial x}+a_{11}a_{12}\Gamma^1_{11}+(a_{11}a_{22}+a_{21}a_{12})\Gamma^1_{12}+(a_{11}a_{32}+a_{31}a_{12})\Gamma^1_{13}$$
$$+a_{21}\frac{\partial a_{12}}{\partial y}+a_{21}a_{22}\Gamma^1_{22}+(a_{21}a_{32}+a_{31}a_{22})\Gamma^1_{23}+a_{31}\frac{\partial a_{12}}{\partial z}+a_{31}a_{32}\Gamma^1_{33}\Big)+\frac{1}{\det A}(a_{31}a_{12}$$
$$-a_{11}a_{32})\Big(a_{11}\frac{\partial a_{22}}{\partial x}+a_{11}a_{12}\Gamma^2_{11}+(a_{31}a_{12}+a_{11}a_{32})\Gamma^2_{13}+(a_{11}a_{22}+a_{21}a_{12})\Gamma^2_{12}+a_{21}\frac{\partial a_{22}}{\partial y}$$
$$+a_{21}a_{22}\Gamma^2_{22}+(a_{21}a_{32}+a_{31}a_{22})\Gamma^2_{23}+a_{31}\frac{\partial a_{22}}{\partial z}+a_{31}a_{32}\Gamma^2_{33}\Big)+\frac{1}{\det A}(a_{11}a_{22}-a_{12}a_{21})$$
$$\Big(a_{11}\frac{\partial a_{32}}{\partial x}+a_{11}a_{12}\Gamma^3_{11}+(a_{11}a_{22}+a_{21}a_{12})\Gamma^3_{12}+(a_{11}a_{32}+a_{31}a_{12})\Gamma^3_{13}+a_{21}\frac{\partial a_{32}}{\partial y}+a_{21}a_{22}\Gamma^3_{22}$$
$$+(a_{21}a_{32}+a_{31}a_{22})\Gamma^3_{23}+a_{31}\frac{\partial a_{32}}{\partial z}+a_{31}a_{32}\Gamma^3_{33}\Big)$$

$\Gamma^{3'}_{22}=$

$$\frac{1}{\det A}(a_{21}a_{32}-a_{22}a_{31})\Big(a_{12}\frac{\partial a_{12}}{\partial x}+(a_{12})^2\Gamma^1_{11}+2a_{12}a_{22}\Gamma^1_{12}+2a_{12}a_{32}\Gamma^1_{13}+a_{22}\frac{\partial a_{12}}{\partial y}$$
$$+(a_{22})^2\Gamma^1_{22}+2a_{22}a_{32}\Gamma^1_{23}+a_{32}\frac{\partial a_{12}}{\partial z}+(a_{32})^2\Gamma^1_{33}\Big)+\frac{1}{\det A}(a_{31}a_{12}-a_{11}a_{32})\Big((a_{12})^2\Gamma^2_{11}$$
$$+a_{12}\frac{\partial a_{22}}{\partial x}+2a_{12}a_{22}\Gamma^2_{12}+2a_{12}a_{32}\Gamma^2_{31}+a_{22}\frac{\partial a_{22}}{\partial y}+(a_{22})^2\Gamma^2_{22}+2a_{22}a_{32}\Gamma^2_{23}+a_{32}\frac{\partial a_{22}}{\partial z}$$
$$+(a_{32})^2\Gamma^2_{33}\Big)+\frac{1}{\det A}(a_{11}a_{22}-a_{12}a_{21})\Big((a_{12})^2\Gamma^3_{11}+a_{12}\frac{\partial a_{32}}{\partial x}+2a_{12}a_{22}\Gamma^3_{12}+2a_{12}a_{32}\Gamma^3_{13}$$

$$+a_{22}\frac{\partial a_{32}}{\partial y} + (a_{22})^2\Gamma^3_{22} + 2a_{22}a_{32}\Gamma^3_{23} + a_{32}\frac{\partial a_{32}}{\partial z} + (a_{32})^2\Gamma^3_{33}\Big)$$

$$\Gamma^{3'}_{32} =$$

$$\frac{1}{\det A}(a_{21}a_{32} - a_{22}a_{31})\Big(a_{13}\frac{\partial a_{12}}{\partial x} + a_{13}a_{12}\Gamma^1_{11} + (a_{13}a_{22} + a_{23}a_{12})\Gamma^1_{12} + (a_{13}a_{32} + a_{33}a_{12})\Gamma^1_{13}$$
$$+a_{23}\frac{\partial a_{12}}{\partial y} + a_{23}a_{22}\Gamma^1_{22} + (a_{23}a_{32} + a_{33}a_{22})\Gamma^1_{23} + a_{33}\frac{\partial a_{12}}{\partial z} + a_{33}a_{32}\Gamma^1_{33}\Big) + \frac{1}{\det A}(a_{31}a_{12}$$
$$-a_{11}a_{32})\Big(a_{13}\frac{\partial a_{22}}{\partial x} + a_{13}a_{12}\Gamma^2_{11} + (a_{13}a_{22} + a_{23}a_{12})\Gamma^2_{12} + (a_{13}a_{32} + a_{33}a_{12})\Gamma^2_{13} + a_{23}\frac{\partial a_{22}}{\partial y}$$
$$+a_{23}a_{22}\Gamma^2_{22} + (a_{23}a_{32} + a_{33}a_{22})\Gamma^2_{23} + a_{33}\frac{\partial a_{22}}{\partial z} + a_{33}a_{32}\Gamma^2_{33}\Big) + \frac{1}{\det A}(a_{11}a_{22} - a_{12}a_{21})$$
$$\Big(a_{13}\frac{\partial a_{32}}{\partial x} + a_{13}a_{12}\Gamma^3_{11} + (a_{13}a_{22} + a_{23}a_{12})\Gamma^3_{12} + (a_{13}a_{32} + a_{33}a_{12})\Gamma^3_{31} + a_{23}\frac{\partial a_{32}}{\partial y} + a_{23}a_{22}\Gamma^3_{22}$$
$$+(a_{23}a_{32} + a_{33}a_{22})\Gamma^3_{23} + a_{33}\frac{\partial a_{32}}{\partial z} + a_{33}a_{32}\Gamma^3_{33}\Big)$$

4.5.3 Experiments

(a) Original video (left) / Anisotropic Clifford-Hodge flow (right) for $\beta = 1$

(b) Original video (left) / Anisotropic Clifford-Hodge flow (right) for $\beta = 10$

FIGURE 4.4 – Clifford-Hodge flow of functions

In dimension 3, the Clifford-Hodge flow on functions may be devoted to anisotropic regularization of nD videos. The process is the 3D counterpart of the 2D process devoted to anisotropic regularization of nD images mentionned above . Let $I = (I_1, \cdots, I_n)$ be a nD video. It induces a Riemannian manifold (S, g) of dimension 3. Then we consider each component I_i as a section of the Clifford bundle $Cl(S, g)$ of degree 0, and apply

the Clifford-Hodge flow on each one of them. Under the identification between sections of $Cl(S,g)$ of degree 0 and functions on S, we get n PDE's

$$\frac{\partial I_i}{\partial t} + \Delta I_i = 0$$

where Δ is the scalar Laplacian on $C^\infty(S,g)$.

In this application, we aim at showing the role of the parameter β of (4.18) in the regularization process. By construction of the Riemannian manifold (S,g) , β controls the norms of tangent vector fields in the direction $\partial/\partial z$. More precisely, it controls the measure of video's variations in the temporal direction.

Fig. 4.4. is an illustration of anisotropic regularizations of a color video (n=3) induced by the Clifford-Hodge flow. Fig. 4.4(a) (left) and Fig. 4.4(b) (left) is a capture of a video taken in the DynTex database [64]. Fig. 4.4(a) (right) and Fig. 4.4(b) (right) are corresponding captures of anisotropic regularizations of the original video. They are computed from a convolution with a 3x3x3 mask discretizing the kernel K_t^1 (see Section. 4.2.3). They result from 3 iterations for $h_1 = h_2 = h_3 = 0.01$, $t = 0.3$ and $\lambda = 1$, where the metric g is updated at each iteration. They differ from the parameter β, where $\beta = 1$ on Fig. 4.4(a) (right) and $\beta = 10$ on Fig. 4.4(b) (right).

As mentionned above, the more β is taken high, the more variations of the video in the temporal direction are considered as high. From the property of the Beltrami flow of diffusing in the direction of edges, we conclude that the more β is taken high, the more the diffusion process behaves as a frame by frame diffusion. This is illustrated on Fig. 4.4 where some details of the original video have been removed (see inside the red ellipses) by the diffusion process for $\beta = 1$, conversely only smoothed for $\beta = 10$.

Troisième partie

Transformée de Fourier-Clifford pour le traitement d'image

Sommaire

5 Clifford-Fourier Transform for Color Image Processing 138
5.1 Introduction . . . 138
5.2 Fourier transform and group actions . . . 138
5.3 Clifford Fourier transform in $L^2(\mathbb{R}^2, (\mathbb{R}^n, Q))$ . . . 140
5.3.1 The cases n=3,4 : Group morphisms from $\mathbb{R}^2$ to Spin(4) . . . 141
5.3.2 The cases n=3,4 : The Clifford Fourier transform . . . 144
5.4 Application to color image filtering . . . 146
5.4.1 Clifford Fourier transform of color images . . . 146
5.4.2 Color image filtering . . . 148
5.5 Related works . . . 153
5.5.1 The hypercomplex Fourier transform of Sangwine et al. . . . 153
5.5.2 The quaternionic Fourier transform of Bülow . . . 154
Appendix . . . 156
A. Lie groups representations and Fourier transforms . . . 156
B. Bivectors orthogonalization in $\mathbb{R}_{4,0}$ . . . 158

5 Clifford-Fourier Transform for Color Image Processing

Cette Section a fait l'objet d'une publication en collaboration avec Michel Berthier et Christophe Saint-Jean [5].

5.1 Introduction

During the last years several attempts have been made to generalize the classical approach of scalar signal processing with the Fourier transform to higher dimensional signals. The reader will find a detailed overview of the related works at the beginning of [12]. We only mention in this introduction some of the approaches investigated by several authors.
Motivated by the spectral analysis of color images, S. Sangwine and T. Ell have proposed in [32] and [69] a generalization based on the use of quaternions : a color corresponds to an imaginary quaternion and the imaginary complex i is replaced by the unit quaternion μ coding the grey axis. A quaternionic definition is also given by T. Bülow and G. Sommer in the context of analytic signals, for signals defined on the plane and with values in the algebra $\mathbb{H}$ of quaternions [15]. Concerning analytic signals, M. Felsberg makes use of the Clifford algebras $\mathbb{R}_{2,0}$ and $\mathbb{R}_{3,0}$ to define an appropriate Clifford Fourier transform [35].
A generalization in the Clifford algebras context appears also in J. Ebling and G. Scheuermann [31]. The authors mainly use their transformation to analyze frequencies of vector fields. Using the same Fourier kernel, B. Mawardi and E. Hitzer obtain an uncertainty principle for $\mathbb{R}_{3,0}$ multivector functions [59]. The reader may find in [12] definitions of Clifford Fourier transform and Clifford Gabor filters based on the Dirac operator and Clifford analysis.
One could ask the reason why to propose a new generalization. An important thing when dealing with Fourier transform is its link with group representations. We then recall in Section 5.2 the usual definition of the Fourier transform of a function defined on an abelian Lie group by means of the characters of the group. The definition we propose in Section 5.3 relies mainly on the generalization of the notion of characters, that is why we study the group morphisms from $\mathbb{R}^2$ to Spin(3) and Spin(4). These morphisms help to understand the behavior of the Fourier transform with respect to well chosen spinors. We treat in Section 5.4 three applications corresponding to specific bivectors of $\mathbb{R}_{4,0}$. They consist in filtering frequencies according to color, hue and chrominance part of a given color. In Section 5.5, we show that for particular choices of group morphisms and under well chosen identification with quaternions, the Clifford Fourier transform we propose coincides with the definitions of S. Sangwine [69] and T. Bülow [16].

5.2 Fourier transform and group actions

Let us recall briefly some basic ideas related to the group approach of the definition of the Fourier transform. Details can be found in the Appendix A, see also [39] for examples of applications to Fourier descriptors.
Let G be a Lie group. The Pontryagin dual of G, denoted $\widehat{G}$, is the set of equivalence

classes of unitary irreducible representations of G. It appears that if G is abelian, every irreducible unitary representation of G is of dimension 1, i.e. is a continuous group morphism from G to S^1. This is precisely the definition of a character. It is well known that the characters of $\mathbb{R}^m$ are given by

$$(x_1, \cdots, x_m) \longmapsto e^{i(u_1x_1+\cdots+u_mx_m)}$$

with u_1,$u_2, \cdots, u_m$ real. This shows that $\widehat{\mathbb{R}^m} = \mathbb{R}^m$. The characters of SO(2) are the group morphisms

$$\theta \longmapsto e^{in\theta}$$

for $n \in \mathbb{Z}$ and the corresponding Pontryagin dual is $\mathbb{Z}$. The characters of $\mathbb{Z}/n\mathbb{Z}$ are the groups morphisms

$$u \longmapsto e^{i\frac{2\pi ku}{n}}$$

for $k \in \mathbb{Z}/n\mathbb{Z}$, from which we deduce that $\mathbb{Z}/n\mathbb{Z}$ is its own Pontryagin dual.

In the general case (provided that G is unimodular), the Fourier transform of a function $f \in L^2(G;\mathbb{C})$ is defined on $\widehat{G}$ by

$$\widehat{f}(\varphi) = \int_G f(x)\varphi(x^{-1})d\nu(x)$$

(for ν a well chosen invariant measure on G). Applying this formula to the case $G = \mathbb{R}^m$, resp. G =SO(2), resp. $G = \mathbb{Z}/n\mathbb{Z}$ leads to the usual definition of the Fourier transform, resp. Fourier coefficients, resp. discrete Fourier transform.

Traditionally, the Fourier transform in $L^2(\mathbb{R}^m, (\mathbb{R}^n, \| \|_2))$ is defined by n standard Fourier transforms in $L^2(\mathbb{R}^m, \mathbb{R})$ on each one of the components, embedding $\mathbb{R}$ into $\mathbb{C}$. Using group representations theory, we are able to define Fourier transforms that treat jointly the different components.

From now on, we deal with the abelian group $G = (\mathbb{R}^2, +)$ since this paper is devoted to image processing applications.

Let us make some crucial remarks about the case $n = 2$.
Let f be a real or complex valued function defined on $\mathbb{R}^2$. Its Fourier transform is given by

$$\widehat{f}(a, b) = \int_{\mathbb{R}^2} f(x, y)e^{-i(ax+by)}\, dx\, dy$$

Identifying $\mathbb{C}$ with $(\mathbb{R}^2, \| \|_2)$, we have S^1=SO(2) and the action of S^1 on $\mathbb{C}$, given by the complex multiplication, corresponds to the action of the group SO(2) on $(\mathbb{R}^2, \| \|_2)$. Hence, we can define a Fourier transform in $L^2(\mathbb{R}^2, (\mathbb{R}^2, \| \|_2))$ using the action of group morphisms from $\mathbb{R}^2$ to SO(2) on $(\mathbb{R}^2, \| \|_2)$. These ones are real unitary representations of the group $\mathbb{R}^2$ of dimension 2.

The Fourier transform of $f \in L^2(\mathbb{R}^2, (\mathbb{R}^2, \| \|_2))$ defined above can be written in the Clifford algebra language. Indeed, from the embedding of $(\mathbb{R}^2, \| \|_2)$ into $\mathbb{R}_{2,0}$, f may be viewed as a $\mathbb{R}^1_{2,0}$-valued function

$$f(x, y) = f_1(x, y)e_1 + f_2(x, y)e_2$$

where $e_1^2 = e_2^2 = 1$ and $e_1 e_2 = -e_2 e_1$. From this point of view, the Fourier transform of f is given by

$$\widehat{f}(a,b) = \int_{\mathbb{R}^2} [\cos((ax+by)/2)1 + \sin((ax+by)/2)e_1e_2](f_1(x,y)e_1 + f_2(x,y)e_2)$$

$$[\cos(-(ax+by)/2)1 + \sin(-(ax+by)/2)e_1e_2]\, dx\, dy$$

using the fact that the action of Spin(2) on $\mathbb{R}^1_{2,0}$ corresponds to the action of SO(2) on $(\mathbb{R}^2, \| \|_2)$. We can write this last formula in the following form :

$$\widehat{f}(a,b) = \int_{\mathbb{R}^2} (f_1(x,y)e_1 + f_2(x,y)e_2) \perp \varphi_{a,b}(-x,-y) dx\, dy$$

where $\varphi_{a,b}$ is the morphism from $\mathbb{R}^2$ to Spin(2) that sends (x,y) to $\exp[((ax+by)/2)(e_1e_2)]$ and $\perp$ denotes the action $v \perp s = s^{-1}vs$ of Spin(2) on $\mathbb{R}^1_{2,0}$, and more generally the action of Spin(n) on $\mathbb{R}^1_{n,0}$.

Note that group morphisms from $\mathbb{R}^2$ to Spin(2) followed by the action on $\mathbb{R}^1_{2,0}$ correspond to the action of group morphisms from $\mathbb{R}^2$ to SO(2) on $(\mathbb{R}^2, \| \|_2)$. In other words, they are real unitary representations of $\mathbb{R}^2$ of dimension 2 too.

Remark. As in the standard case, where the Fourier transform of a real valued function is defined by embedding $\mathbb{R}$ into $\mathbb{C}$, we define here the Fourier transform of a real valued function by embedding $\mathbb{R}$ into $\mathbb{R}^2$.

Starting from these elementary observations, we now proceed to generalize this construction for $\mathbb{R}^n$-valued functions defined in $\mathbb{R}^2$. In other words, we are looking for a generalization of the action of group morphisms to SO(2) on the values of a $(\mathbb{R}^2, \| \|_2)$-valued function.

5.3 Clifford Fourier transform in $L^2(\mathbb{R}^2, (\mathbb{R}^n, Q))$

Let $f \in L^2(\mathbb{R}^2, (\mathbb{R}^n, Q))$ where Q is a positive definite quadratic form. We propose to associate the Fourier transform of f with the action of the following group morphisms on the values of f, depending on the parity of n.

If n is even, then we consider the morphisms

$$\varphi : \mathbb{R}^2 \longrightarrow \mathrm{SO}(Q)$$

If n is odd, then we embed $(\mathbb{R}^n, Q)$ into $(\mathbb{R}^{n+1}, Q \oplus 1)$ and consider the morphisms

$$\varphi : \mathbb{R}^2 \longrightarrow \mathrm{SO}(Q \oplus 1)$$

Thus the generalization we propose is based on the computation of real unitary representations of dimension n or $n+1$ of the abelian group $\mathbb{R}^2$. The main fact is that we no more consider equivalent classes of representations. This means in particular that the Fourier transform we define depends on the positive definite quadratic form of $\mathbb{R}^n$.

Remark. Recall that up to a change of the basis, a positive definite quadratic form is given by the identity matrix. Thus, f may always be viewed as a $(\mathbb{R}^p,\|\ \|_2)$-valued function(p denotes n if n is even and $n+1$ if n is odd). As a consequence of the change of the basis, $\mathrm{SO}(Q)$ become $\mathrm{SO}(p)$ and group morphisms from $\mathbb{R}^2$ to $\mathrm{SO}(Q)$ become group morphisms from $\mathbb{R}^2$ to $\mathrm{SO}(p)$.

As for the case of $\mathbb{R}^2$-valued functions, we can rewrite the Fourier transform in the Clifford algebra language, using the fact that the action of $\mathrm{Spin}(p)$ on $\mathbb{R}^1_{p,0}$ corresponds to the action of $\mathrm{SO}(p)$ on $\mathbb{R}^p$. Moreover, it appears to be much more easier to compute group morphisms to $\mathrm{Spin}(p)$ rather than group morphisms to the matrix group $\mathrm{SO}(p)$.

If n is even, then from the embedding of $\mathbb{R}^n$ into $\mathbb{R}_{n,0}$, f may be viewed as a $\mathbb{R}^1_{n,0}$-valued function :

$$f(x,y)=f_1(x,y)e_1+f_2(x,y)e_2+\cdots+f_n(x,y)e_n,$$

where $e_i^2=1$ and $e_ie_j=-e_je_i$. Denoting by φ a group morphism from $\mathbb{R}^2$ to $\mathrm{Spin}(n)$, we define the Clifford-Fourier transform of f by

$$\widehat{f}(\varphi)=\int_{\mathbb{R}^2}\varphi(x,y)f(x,y)\varphi(-x,-y)dx\,dy=\int_{\mathbb{R}^2}f(x,y)\perp\varphi(-x,-y)dx\,dy.$$

If n is odd, we first embed $\mathbb{R}^n$ into $\mathbb{R}^{n+1}$. Then, from the embedding of $\mathbb{R}^{n+1}$ into $\mathbb{R}_{n+1,0}$, f may be viewed as a $\mathbb{R}^1_{n+1,0}$-valued function :

$$f(x,y)=f_1(x,y)e_1+f_2(x,y)e_2+\cdots+f_n(x,y)e_n+0e_{n+1},$$

where $e_i^2=1$ and $e_ie_j=-e_je_i$. Denoting by φ a group morphism from $\mathbb{R}^2$ to $\mathrm{Spin}(n+1)$, we define the Clifford-Fourier transform of f by

$$\widehat{f}(\varphi)=\int_{\mathbb{R}^2}\varphi(x,y)f(x,y)\varphi(-x,-y)dx\,dy=\int_{\mathbb{R}^2}f(x,y)\perp\varphi(-x,-y)dx\,dy.$$

Remark. If n is even, the Clifford Fourier transform of f is a $\mathbb{R}^1_{n,0}$-valued function. If n is odd, the Clifford Fourier transform of f is a $\mathbb{R}^1_{n+1,0}$-valued function.

Remark. For Q=1 on $\mathbb{R}$, the Fourier transforms we define correspond to the standard Fourier transforms of $\mathbb{R}$-valued functions.

From now on, we deal with the case $n=3$ since this paper is devoted to color image processing. However, we have seen above that we treat the cases $n=3$ and $n=4$ in the same manner, by computing group morphisms from $\mathbb{R}^2$ to Spin(4).

5.3.1 The cases n=3,4 : Group morphisms from $\mathbb{R}^2$ to Spin(4)

This part is devoted to the computation of group morphisms from $\mathbb{R}^2$ to Spin(4).

Using the fact that the group Spin(4) is isomorphic to the group Spin(3) $\times$ Spin(3), we first compute group morphisms from $\mathbb{R}^2$ to Spin(3).

One can verify that Spin(3) is the group

$$\text{Spin}(3) = \{a1 + be_1e_2 + ce_2e_3 + de_3e_1,\ a^2 + b^2 + c^2 + d^2 = 1\}$$

and is isomorphic to the group of unit quaternions.

Proposition 5.1 *The group morphisms from $\mathbb{R}^2$ to Spin(3) are given by*

$$(x, y) \longmapsto e^{\frac{1}{2}(ux+vy)B}$$

where B belongs to $\mathbb{S}^2_{3,0}$, the set of unit bivectors in $\mathbb{R}_{3,0}$, and u and v are real.

Proof. We have to determine the abelian subalgebras of the Lie algebra $\mathfrak{spin}(3) = \mathbb{R}^2_{3,0}$ of the Lie group Spin(3). More precisely, as the exponential map of $\mathbb{R}^2$ is onto, group morphisms from $\mathbb{R}^2$ to Spin(3) are given by Lie algebra morphisms from the abelian Lie algebra $\mathfrak{R}^2$ of $\mathbb{R}^2$ to $\mathfrak{spin}(3)$. Taking two generators (f_1, f_2) of $\mathfrak{R}^2$, any morphism φ from $\mathfrak{R}^2$ to $\mathfrak{spin}(3)$ satisfies :

$$\varphi(f_1) \times \varphi(f_2) = 0.$$

We deduce that $Im(\varphi)$ is an abelian subalgebra of $\mathbb{R}^2_{3,0}$ whose dimension is inferior or equal to 2. If $a = a_1e_1e_2 + a_2e_3e_1 + a_3e_2e_3$ and $b = b_1e_1e_2 + b_2e_3e_1 + b_3e_2e_3$ satisfy $a \times b = 0$, then the structure relations of $\mathbb{R}^2_{3,0}$, i. e.

$$e_1e_2 \times e_3e_1 = e_2e_3, \quad e_3e_1 \times e_2e_3 = e_1e_2, \quad e_2e_3 \times e_1e_2 = e_3e_1,$$

imply

$$(a_1b_2 - a_2b_1)e_2e_3 - (a_1b_3 - a_3b_1)e_3e_1 + (a_2b_3 - a_3b_2)e_1e_2 = 0.$$

This shows that two commuting elements of $\mathbb{R}^2_{3,0}$ are colinear and that the abelian subalgebras of $\mathbb{R}^2_{3,0}$ are of dimension 1. If we write $\varphi(f_1) = \frac{1}{2}uB$ and $\varphi(f_2) = \frac{1}{2}vB$ for some $u, v \in \mathbb{R}$ and $B \in \mathbb{S}^2_{3,0}$, we see that the morphisms from $\mathfrak{R}^2$ to $\mathbb{R}^2_{3,0}$ are parameterized by two real numbers and one unit bivector, and are given by

$$\varphi_{u,v,B} \colon (x, y) \longmapsto \frac{1}{2}(ux + vy)B.$$

Consequently, the group morphisms from $\mathbb{R}^2$ to Spin(3) are the morphisms $\widetilde{\varphi}_{u,v,B}$ with

$$\widetilde{\varphi}_{u,v,B} \colon (x, y) \longmapsto e^{\frac{1}{2}(ux+vy)B}.$$

□

Let us recall what group is Spin(4). Every τ in Spin(4) is of the form $\tau = u + Iv$

$$= (a1 + be_1e_2 + ce_2e_3 + de_3e_1) + I(a'1 + b'e_1e_2 + c'e_2e_3 + d'e_3e_1)$$

where I denotes the pseudoscalar of $\mathbb{R}_{4,0}$ and the following relations hold :

$$u\overline{u} + v\overline{v} = 1 \qquad u\overline{v} + v\overline{u} = 0.$$

The morphism $\chi : \mathrm{Spin}(4) \longrightarrow \mathrm{Spin}(3) \times \mathrm{Spin}(3)$ with

$$\chi(u+Iv) = (u+v, u-v)$$

is an isomorphism. An alternative description of Spin(4) relies on the following fact : the morphism $\psi : \mathbb{H}_1 \times \mathbb{H}_1 \longrightarrow \mathrm{SO}(4)$ defined by

$$(\tau,\rho) \longmapsto (v \longmapsto \tau v \overline{\rho})$$

(where v is a vector of $\mathbb{R}^4$ considered as a quaternion) is a universal covering of SO(4) (see [67]). This means that Spin(4) is isomorphic to $\mathbb{H}_1 \times \mathbb{H}_1$. We will use this remark later on to compare our transform to Sangwine's and Bülow's ones.

Proposition 5.2 *The group morphisms from* $\mathbb{R}^2$ *to Spin(4) are the morphisms* $\widetilde{\phi}_{u,v,B,w,z,C}$ *that send* (x,y) *to*

$$e^{\frac{1}{8}[x(u+w)+y(v+z)][B+C+I(B-C)]}\, e^{\frac{1}{8}[x(u-w)+y(v-z)][B-C+I(B+C)]}$$

with u, v, w, z *real and* B, C *two elements of* $\mathbb{S}^2_{3,0}$.

Proof. The group law of Spin(3) $\times$ Spin(3) being

$$\Big((a,b),(c,d)\Big) \longmapsto (ac,bd),$$

the group morphisms from $\mathbb{R}^2$ to Spin(3) $\times$ Spin(3) are the morphisms $\widetilde{\varphi}_{u,v,B,w,z,C}$ defined by

$$\widetilde{\varphi}_{u,v,B,w,z,C} : (x,y) \longmapsto \Big(e^{\frac{1}{2}(ux+vy)B}, e^{\frac{1}{2}(wx+zy)C}\Big)$$

with u, v, w, z real and B, C two elements of $\mathbb{S}^2_{3,0}$.

By χ^{-1}, the group morphisms from $\mathbb{R}^2$ to Spin(4) are the $\widetilde{\phi}_{u,v,B,w,z,C}$ that send (x,y) to

$$\frac{e^{\frac{1}{2}(ux+vy)B} + e^{\frac{1}{2}(wx+zy)C}}{2} + I\,\frac{e^{\frac{1}{2}(ux+vy)B} - e^{\frac{1}{2}(wx+zy)C}}{2}$$

However, this writing is not convenient to determine group morphisms to SO(4) since it doesn't provide explicitly the rotations in $\mathbb{R}^4$ that $\widetilde{\phi}_{u,v,B,w,z,C}$ generates by its action on $\mathbb{R}^1_{4,0}$. The solution comes from an "orthogonalization" of the corresponding Lie algebras morphism from $\mathfrak{R}^2$ to $\mathbb{R}^2_{4,0}$, namely the linear map

$$\phi_{u,v,B,w,z,C}(X,Y) = T_{(0,0)}\,\widetilde{\phi}_{u,v,B,w,z,C}(X,Y)$$

where T denotes the linear tangent map. By definition :

$$\phi_{u,v,B,w,z,C}(X,Y) = \frac{d}{dt}\Big(\widetilde{\phi}_{u,v,B,w,z,C}(exp(t(X,Y)))\Big)\Big|_{t=0}$$

The exponential map of $\mathbb{R}^2$ being the identity map, we get

$$\begin{aligned}\phi_{u,v,B,w,z,C}(X,Y) &= \frac{d}{dt}\Big(\widetilde{\phi}_{u,v,B,w,z,C}(t(X,Y))\Big)\Big|_{t=0}\\ &= \frac{d}{dt}\Big(\frac{e^{\frac{1}{2}t(uX+vY)B} + e^{\frac{1}{2}t(wX+zY)C}}{2} + I\,\frac{e^{\frac{1}{2}t(uX+vY)B} - e^{\frac{1}{2}t(wX+zY)C}}{2}\Big)\Big|_{t=0}\end{aligned}$$

$$= \frac{(uX+vY)B+(wX+zY)C}{4} + I\,\frac{(uX+vY)B-(wX+zY)C}{4}$$

The orthogonalization of the morphism $\phi_{u,v,B,w,z,C}$ consists in decomposing the bivector $\phi_{u,v,B,w,z,C}(X,Y)$ for each X,Y into commuting bivectors whose squares are real. The corresponding spinor is written as a product of commuting spinors of the form e^{F_i} with $F_i^2 < 0$. These ones represent rotations of angle $-F_i^2$ in the oriented planes given by the F_i's. In our case, the bivector $\phi_{u,v,B,w,z,C}(X,Y)$ is decomposed into $F_1 + F_2$ where

$$F_1 = \frac{1}{8}\Big[(X(u+w)+Y(v+z))(B+C+I(B-C))\Big]$$

$$F_2 = \frac{1}{8}\Big[(X(u-w)+Y(v-z))(B-C+I(B+C))\Big]$$

(see the Appendix B for details). The group morphisms $\widetilde{\phi}_{u,v,B,w,z,C}$ from $\mathbb{R}^2$ to Spin(4) can then be written as

$$\widetilde{\phi}_{u,v,B,w,z,C}(x,y) = e^{[\frac{(ux+vy)B+(wx+zy)C}{4} + I\,\frac{(ux+vy)B-(wx+zy)C}{4}]}$$

$$= e^{\frac{1}{8}[(x(u+w)+y(v+z))(B+C+I(B-C))]}\; e^{\frac{1}{8}[(x(u-w)+y(v-z))(B-C+I(B+C))]}$$

□

This is the convenient form to describe group morphisms from $\mathbb{R}^2$ to SO(4).

To conclude this part, let us remark that the expression of the morphisms $\widetilde{\phi}_{u,v,B,w,z,C}$ may be simplified. Indeed, when B and C describe $\mathbb{S}^2_{3,0} \subset \mathbb{R}_{4,0}$, the unit bivectors

$$D = \frac{1}{4}(B+C+I(B-C)) \qquad ID = \frac{1}{4}(B-C+I(B+C))$$

describe $\mathbb{S}^2_{4,0}$, the set of unit bivectors in $\mathbb{R}_{4,0}$.

Therefore, the morphisms $\widetilde{\phi}_{u,v,B,w,z,C}$ are parametrized by four real numbers and one unit bivector $D \in \mathbb{S}^2_{4,0}$, and may be written

$$\widetilde{\Phi}_{u,v,w,z,D}(x,y) = e^{\frac{1}{2}[(x(u+w)+y(v+z))D]}\; e^{\frac{1}{2}[(x(u-w)+y(v-z))ID]}.$$

5.3.2 The cases n=3,4 : The Clifford Fourier transform

From the computation of group morphisms from $\mathbb{R}^2$ to Spin(4), we give an explicit formula of the Clifford Fourier transform $\widehat{f}$ of $f \in L^2(\mathbb{R}^2,(\mathbb{R}^3,Q))$ or $L^2(\mathbb{R}^2,(\mathbb{R}^4,Q))$.

Definition 5.1 *Let $f \in L^2(\mathbb{R}^2,(\mathbb{R}^3,Q))$, resp. $L^2(\mathbb{R}^2,(\mathbb{R}^4,Q))$ and denote by f the embedding of f into the Clifford algebra $Cl(\mathbb{R}^4, Q\oplus 1)$, resp. $Cl(\mathbb{R}^4,Q)$. The Clifford Fourier transform of f is given by*

$$\widehat{f}(u,v,w,z,D) = \int_{\mathbb{R}^2} f(x,y)\perp\widetilde{\Phi}_{u,v,w,z,D}(-x,-y)dx\,dy$$

$$= \int_{\mathbb{R}^2} e^{\frac{1}{2}[(x(u+w)+y(v+z))D]} e^{\frac{1}{2}[(x(u-w)+y(v-z))ID]} f(x,y)$$

$$e^{-\frac{1}{2}[(x(u+w)+y(v+z))D]} e^{-\frac{1}{2}[(x(u-w)+y(v-z))ID]} dx\,dy.$$

Decomposing f as $f_{||}+f_{\perp}$ with respect to the plane generated by the bivector D, we get $\widehat{f}(u,v,w,z,D)=$

$$\int_{\mathbb{R}^2} f_{||}(x,y)e^{[-(x(u+w)+y(v+z))D]}dx\,dy+\int_{\mathbb{R}^2} f_{\perp}(x,y)e^{[-(x(u-w)+y(v-z))ID]}dx\,dy$$

Indeed, the plane generated by ID represents the orthogonal of the plane generated by D in $\mathbb{R}^4$.

Proposition 5.3 *The Clifford Fourier transform is left-invertible. Its inverse is the map* $\check{}$ *given by*

$$\check{g}(a,b)=\int_{\mathbb{R}^4\times\mathbb{S}^2_{4,0}} g(u,v,w,z,D)\perp\widetilde{\Phi}_{u,v,w,z,D}(a,b)\,du\,dv\,dw\,dz\,d\nu$$

where ν *is a unit measure on* $\mathbb{S}^2_{4,0}$.

Proof. We have to verify that $\check{}\circ\widehat{}\,(f)(\lambda,\mu)=f(\lambda,\mu)$ for all $(\lambda,\mu)\in\mathbb{R}^2$.

$$\check{}\circ\widehat{}\,(f)(\lambda,\mu)=$$

$$\int_{\mathbb{R}^4\times\mathbb{S}^2_{4,0}}\left[\int_{\mathbb{R}^2} f_{||}(x,y)e^{[-(x(u+w)+y(v+z))D]}dx\,dy\right]e^{[(\lambda(u+w)+\mu(v+z))D]}du\,dv\,dw\,dz\,d\nu \tag{5.1}$$

$$+\int_{\mathbb{R}^4\times\mathbb{S}^2_{4,0}}\left[\int_{\mathbb{R}^2} f_{\perp}(x,y)e^{[-(x(u-w)+y(v-z))ID]}dx\,dy\right]e^{[(\lambda(u-w)+\mu(v-z))ID]}du\,dv\,dw\,dz\,d\nu \tag{5.2}$$

It is sufficient to prove that $(5.1)=f_{||}(\lambda,\mu)$.

$$\begin{aligned}
(5.1)&=\int_{\mathbb{R}^4\times\mathbb{S}^2_{4,0}}\int_{\mathbb{R}^2} f_{||}(x,y)e^{[(\lambda-x)(u+w)+(\mu-y)(v+z)]D}dx\,dy\,du\,dv\,dw\,dz\,d\nu\\
&=\int_{\mathbb{R}^4\times\mathbb{S}^2_{4,0}}\int_{\mathbb{R}^2} f_{||}(x,y)e^{u(\lambda-x)D}e^{w(\lambda-x)D}e^{v(\mu-y)D}e^{z(\mu-y)D}dx\,dy\,du\,dv\,dw\,dz\,d\nu\\
&=\int_{\mathbb{R}^2}\int_{\mathbb{R}^3\times\mathbb{S}^2_{4,0}} f_{||}(x,y)\Big(\int_{\mathbb{R}} e^{u(\lambda-x)D}du\Big)e^{w(\lambda-x)D}e^{v(\mu-y)D}e^{z(\mu-y)D}dw\,dv\,dz\,d\nu\,dx\,dy\\
&=\int_{\mathbb{R}^2}\int_{\mathbb{R}^2\times\mathbb{S}^2_{4,0}} f_{||}(x,y)\delta_{\lambda,x}\Big(\int_{\mathbb{R}} e^{w(\lambda-x)D}dw\Big)e^{v(\mu-y)D}e^{z(\mu-y)D}dv\,dz\,d\nu\,dx\,dy\\
&=\int_{\mathbb{R}^2}\int_{\mathbb{R}\times\mathbb{S}^2_{4,0}} f_{||}(x,y)\delta_{\lambda,x}\delta_{\lambda,x}\Big(\int_{\mathbb{R}} e^{v(\mu-y)D}dv\Big)dz\,d\nu\,dx\,dy\\
&=\int_{\mathbb{R}^2}\int_{\mathbb{S}^2_{4,0}} f_{||}(x,y)\delta_{\lambda,x}\delta_{\lambda,x}\delta_{\mu,y}\Big(\int_{\mathbb{R}} e^{z(\mu-y)D}dz\Big)d\nu\,dx\,dy\\
&=\int_{\mathbb{R}^2}\int_{\mathbb{S}^2_{4,0}} f_{||}(x,y)\delta_{\lambda,x}\delta_{\lambda,x}\delta_{\mu,y}\delta_{\mu,y}\,d\nu\,dx\,dy\\
&=\int_{\mathbb{R}^2} f_{||}(x,y)\delta_{\lambda,x}\delta_{\lambda,x}\delta_{\mu,y}\delta_{\mu,y}\,dx\,dy\\
&=f_{||}(\lambda,\mu)
\end{aligned}$$

□

5.4 Application to color image filtering

5.4.1 Clifford Fourier transform of color images

For the applications we have in mind to color image filtering, we define a partial Clifford Fourier transform, i.e. we deal with a subset of the set of unitary group representations of $\mathbb{R}^2$ of dimension 4. The subset we consider will depend of the colors we aim at filtering.
More precisely, we restrict the Definition 5.1 to the set of group morphisms $\widetilde{\Phi}_{u,v,0,0,D}$ where the bivector D is fixed.

Definition 5.2 *Clifford Fourier transform with respect to a bivector.*
Let $f \in L^2(\mathbb{R}^2,(\mathbb{R}^3,Q))$, resp. $L^2(\mathbb{R}^2,(\mathbb{R}^4,Q))$ and denote by f the embedding of f into the Clifford algebra $Cl(\mathbb{R}^4,Q\oplus 1)$, resp. $Cl(\mathbb{R}^4,Q)$. The Clifford Fourier transform of f with respect to the bivector D is defined by

$$\widehat{f}_D(u,v) = \int_{\mathbb{R}^2} f(x,y) \perp \widetilde{\Phi}_{u,v,0,0,D}(-x,-y)dxdy$$

$$= \int_{\mathbb{R}^2} e^{\frac{1}{2}(xu+yv)ID} e^{\frac{1}{2}(xu+yv)D} f(x,y) e^{-\frac{1}{2}(xu+yv)D} e^{-\frac{1}{2}(xu+yv)ID} dxdy.$$

It follows the definition of the Clifford Fourier transform of a color image.

Definition 5.3 *Clifford Fourier transform of a color image.*
Let I be a color image. We associate to I a function $f \in L^2(\mathbb{R}^2,(\mathbb{R}^3,Q))$ defined by

$$f(x,y) = r(x,y)e_1 + g(x,y)e_2 + b(x,y)e_3 + 0e_4$$

where r, g and b correspond to the red, green and blue levels.
The Clifford Fourier transform of I with respect to Q and D is the $Cl(\mathbb{R}^4,Q\oplus 1)$-valued function $\widehat{I}_{Q,D}$ defined by

$$\widehat{I}_{Q,D}(u,v) = \widehat{f}_D(u,v) = \int_{\mathbb{R}^2} f(x,y) \perp \widetilde{\Phi}_{u,v,0,0,D}(-x,-y)dxdy.$$

Thus, given a color image, we define a set of associated Clifford Fourier transforms parametrized by the set of positive definite quadratic forms on $\mathbb{R}^3$ and unit bivectors in $\mathbb{R}_{4,0}$.

As the Clifford Fourier transform in $L^2(\mathbb{R}^3,Q)$ and $L^2(\mathbb{R}^4,Q)$, we can show that the Clifford Fourier transform of a color image is invertible.

Proposition 5.4 *Let $f \in L^2(\mathbb{R}^2,(\mathbb{R}^3,Q))$ and D be a unit bivector in $Cl(\mathbb{R}^4,Q\oplus 1)$. Then, the Clifford Fourier transform of f with respect to D is invertible. Its inverse is the map $\breve{}$ defined by*

$$\breve{g}(x,y)=\int_{\mathbb{R}^2} g(u,v)\perp \widetilde{\Phi}_{u,v,0,0,D}(x,y)dudv.$$

Proof. Decomposing f with respect to the plane generated by D as $f=f_\parallel+f_\perp$ we have

$$\widehat{f}_D(u,v)=\int_{\mathbb{R}^2}(f_\parallel(x,y)+f_\perp(x,y))\perp \widetilde{\Phi}_{u,v,0,0,D}(-x,-y)dxdy$$

This can be written

$$\widehat{f}_D(u,v)=\widehat{f}_{D_\parallel}(u,v)+\widehat{f}_{D_\perp}(u,v)$$

where

$$\begin{aligned}\widehat{f}_{D_\parallel}(u,v)&=\int_{\mathbb{R}^2} f_\parallel(x,y)\perp \widetilde{\Phi}_{u,v,0,0,D}(-x,-y)dxdy\\&=\int_{\mathbb{R}^2} f_\parallel(x,y)e^{-(ux+vy)D}dxdy\end{aligned}$$

and

$$\begin{aligned}\widehat{f}_{D_\perp}(u,v)&=\int_{\mathbb{R}^2} f_\perp(x,y)\perp \widetilde{\Phi}_{u,v,0,0,D}(-x,-y)dxdy\\&=\int_{\mathbb{R}^2} f_\perp(x,y)e^{-(ux+vy)ID}dxdy.\end{aligned}$$

Let us remark that each one of the two integrals may be identified with the Fourier transform of a function from $\mathbb{R}^2$ to $\mathbb{C}$. Then, we deduce that there exists an inversion formula (left and right) for the Clifford Fourier transform $\widehat{f}_D$ given by

$$f(x,y)=\int_{\mathbb{R}^2}\widehat{f}_D(u,v)\perp \widetilde{\Phi}_{u,v,0,0,D}(x,y)dudv$$

Indeed, the right term equals

$$\int_{\mathbb{R}^2}(\widehat{f}_{D_\parallel}(u,v)+\widehat{f}_{D_\perp}(u,v))\perp \widetilde{\Phi}_{u,v,0,0,D}(x,y)dudv$$

$$=\int_{\mathbb{R}^2}\widehat{f}_{D_\parallel}(u,v)e^{(ux+vy)D}dudv+\int_{\mathbb{R}^2}\widehat{f}_{D_\perp}(u,v)e^{(ux+vy)ID}dudv \tag{5.3}$$

Each one of these integrals may be identified with the inversion formula of the Fourier transform of a function from $\mathbb{R}^2$ to $\mathbb{C}$, hence

$$(5.3)=f_\parallel(x,y)+f_\perp(x,y)=f(x,y).$$

□

The following proposition is useful for applications and in particular for applications to the frequencies filtering developed in the next section. It gives an integral representation of any 3D-valued signal defined on the plane by 3D-valued cosinusoidal signals. This representation is obtained from the Clifford Fourier transform with respect to some bivector. In this proposition we show that the representation is invariant with respect to the choice of the bivector. In the discrete case, we obtain a decomposition of the signal as a sum of cosinusoidal signals.

Proposition 5.5 *Using the previous notations, if B and D are elements of $\mathbb{S}^2_{4,0}$, we have*

$$\begin{aligned}&\widehat{f}_B(u,v)\perp\widetilde{\Phi}_{u,v,0,0,B}(x,y)+\widehat{f}_B(-u,-v)\perp\widetilde{\Phi}_{-u,-v,0,0,B}(x,y)\\&=\widehat{f}_D(u,v)\perp\widetilde{\Phi}_{u,v,0,0,D}(x,y)+\widehat{f}_D(-u,-v)\perp\widetilde{\Phi}_{-u,-v,0,0,D}(x,y)\end{aligned}$$

Moreover, the e_4 component of this expression is null.

Proof. Simple computations show that

$$\begin{aligned}&\widehat{f}_B(u,v)\perp\widetilde{\Phi}_{u,v,0,0,B}(x,y)+\widehat{f}_B(-u,-v)\perp\widetilde{\Phi}_{-u,-v,0,0,B}(x,y)\\&=\int_{\mathbb{R}^2}e^{-\frac{xu+yv}{2}(B+IB)}e^{\frac{\lambda u+\mu v}{2}(B+IB)}f(\lambda,\mu)\,e^{-\frac{\lambda u+\mu v}{2}(B+IB)}e^{\frac{xu+yv}{2}(B+IB)}d\lambda d\mu\\&\quad+\int_{\mathbb{R}^2}e^{\frac{xu+yv}{2}(B+IB)}e^{-\frac{\lambda u+\mu v}{2}(B+IB)}f(\lambda,\mu)\,e^{\frac{\lambda u+\mu v}{2}(B+IB)}e^{-\frac{xu+yv}{2}(B+IB)}d\lambda d\mu\\&=\int_{\mathbb{R}^2}2cos(u(x-\lambda)+v(y-\mu))f_{\parallel}(\lambda,\mu)d\lambda d\mu\\&\quad+\int_{\mathbb{R}^2}2cos(u(x-\lambda)+v(y-\mu))f_{\perp}(\lambda,\mu)d\lambda d\mu.\end{aligned}\tag{5.4}$$

Hence

$$(5.4)=\int_{\mathbb{R}^2}2cos(u(x-\lambda)+v(y-\mu))f(\lambda,\mu)d\lambda d\mu.$$

□

This proposition justifies the fact that these filters are symmetric with respect to the transformation $(u,v)\mapsto(-u,-v)$.

5.4.2 Color image filtering

We now present applications to color image filtering. The use of the Fourier transform is motivated by the well known fact that non trivial filters in the spatial domain may be implemented efficiently with masks in the Fourier domain. Although it seems natural to believe that the results on grey level images may be generalized, there are not so many works dedicated to the specific case of color images. Let us mention the reference [69] where an attempt is made through the use of an *ad hoc* quaternionic transform. The mathematical construction we propose appears to be well founded since it explains the fundamental role of bivectors and scalar products in terms of group actions. As explained before, the possibility to choose the bivector D and the quadratic form Q is an asset allowing a wider range of applications. Indeed, Sangwine et al. proposal can be written in our formalism by considering appropriate D and Q.

The applications proposed in this paper are based on the following fact :

$$(\widehat{f_D})_{||}=\widehat{(f_{||})_D}\qquad\text{and}\qquad(\widehat{f_D})_{\perp}=\widehat{(f_{\perp})_D}.$$

In other words, the part of the Clifford Fourier transform of f that is parallel to D corresponds to the standard Fourier transform of the part of f that is parallel to D. The

same principle holds for the orthogonal part.

We use low pass, high pass and directional filters on the D-parallel part, resp. D-orthogonal part, leaving the D-parallel part, resp. D-orthogonal unmodified. The choice of the bivector D and the quadratic form Q (that determines the D-orthogonal part) will depend on the colors we aim at filtering. Then, we show the action of such filters using the inversion formula of the Clifford Fourier transform.

There is an other way to decompose a color $\alpha = (r, g, b)$, that is with respect to its luminance and chrominance parts, respectively denoted by l_α and v_α. Embedding the color space RGB into the Clifford algebra $\mathbb{R}_{4,0}$ by

$$i_\alpha = r\, e_1 + g\, e_2 + b\, e_3 + 0\, e_4,$$

the former corresponds to the projection of i_α on the axis generated by the unit vector $(e_1 + e_2 + e_3)/\sqrt{3}$, the latter its projection on the orthogonal plane in $e_1e_2e_3$, called the chrominance plane, represented by the unit bivector $(e_1e_2 - e_1e_3 + e_2e_3)/3$. In what follows we make use of the following fact too : every hue can be represented as an equivalence class of bivectors of $\mathbb{R}_{4,0}$. More precisely, we have the following result.

Proposition 5.6 *Let T be the set of bivectors*

$$T = \{(e_1 + e_2 + e_3) \wedge i_\alpha,\ \alpha \in RGB\}$$

with the following equivalence relation :

$$B \simeq C \iff B = \lambda C \quad \textit{for } \lambda > 0$$

Then, there is a bijection between $T/\simeq$ and the set of hues.

Proof. (See Section 2.2.2) □

Fig. 5.1 shows the original images used for these experiments. Fig. 5.1(a) H is a modified color version of the Fourier house containing red, desatured red, green, cyan stripes in various directions, a uniform red circle and a red square with lower luminance. Fig. 5.1(b) F is a natural image taken from the Berkeley image segmentation database [58].

Fig. 5.2(a) is the centered log-modulus of the D-parallel part of $\widehat{H}_{Q_1,D}$ where Q_1 is the quadratic form such that $Q_1 \oplus 1$ is given by the identity matrix I_4 in the basis (e_1, e_2, e_3, e_4), and D the bivector e_1e_4. Fig. 5.2(b) is the result of a directional cut filter around $\pi/2$ which removes of vertical frequencies. Let us point out that horizontal green stripes are not altered since green color 255 e_2 belongs to $ID = e_2e_3$.

Fig. 5.3 shows the difference between a low pass filter in the D-parallel part of $\widehat{H}_{Q_1,e_1e_4}$ (Fig. 5.3(a)) and the D-parallel part $\widehat{H}_{Q_1,\frac{1}{\sqrt{2}}(e_2+e_3)e_1}$ (Fig. 5.3(b)). The first one consists in removing high frequencies of the red components of the image, whereas the second one consists in removing high frequencies of the red hue part of the image.

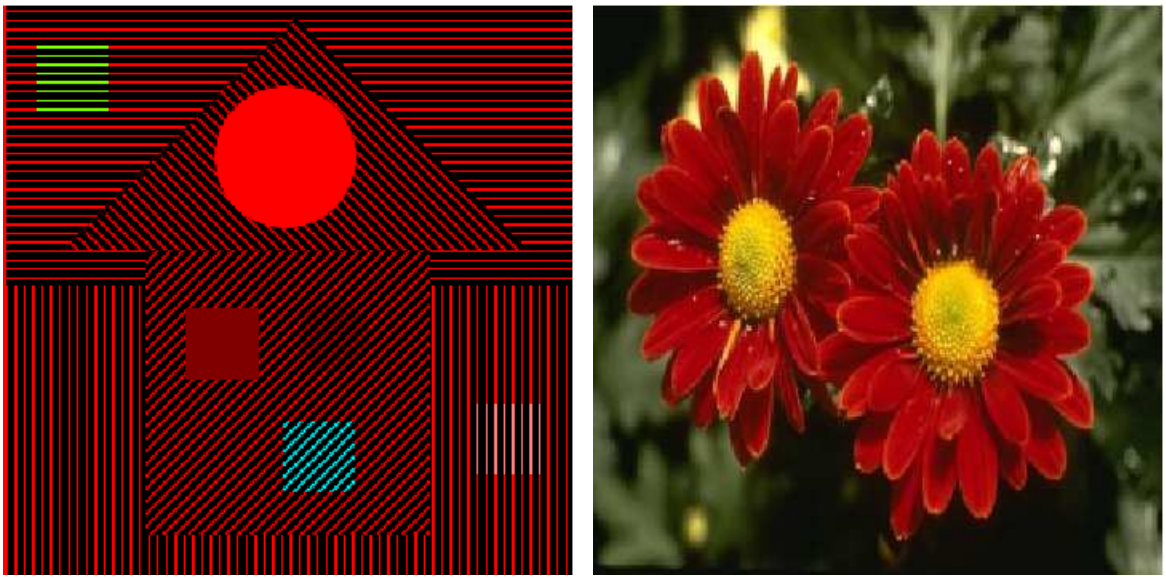

(a) Fourier house (b) Flowers

FIGURE 5.1 – Original images

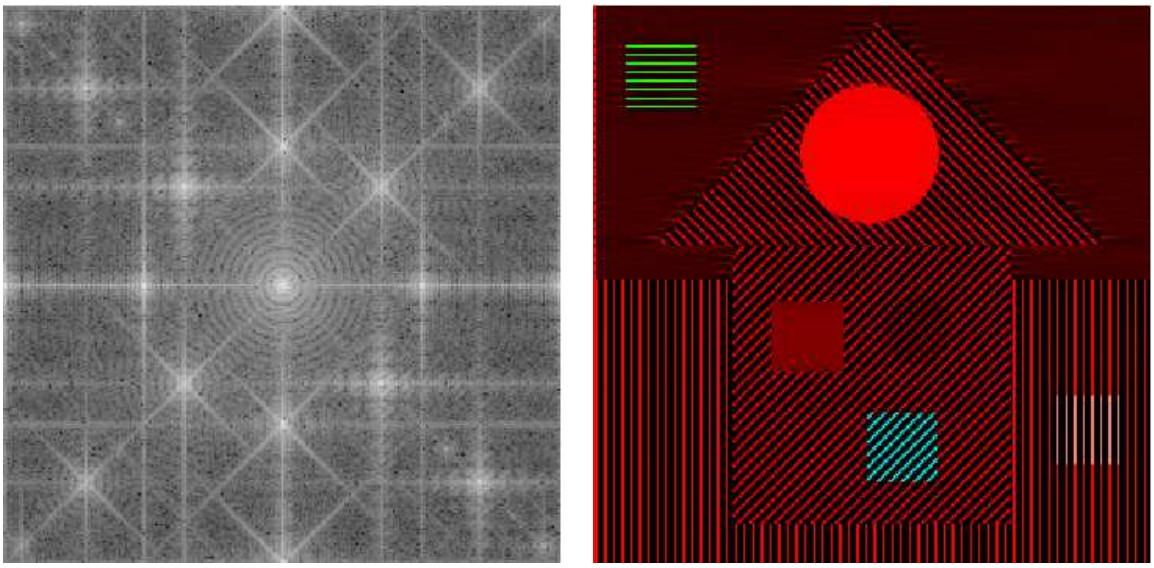

(a) Log-modulus of the parallel part (b) Directional cut filtering for the red color

FIGURE 5.2 – The Clifford-Fourier transform $\widehat{H}_{Q_1,e_1e_4}$

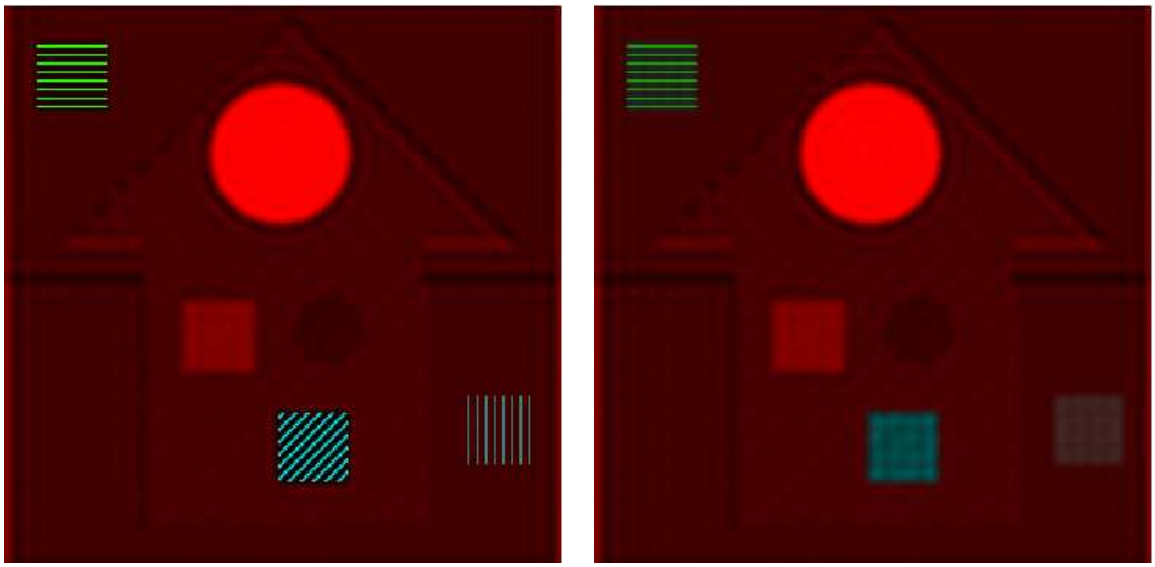

(a) red color (b) red hue

FIGURE 5.3 – Low pass filtering

In Fig. 5.3(a), we can see that both green and cyan stripes are not modified. As in the previous case, this comes from the fact that both green color and cyan color 255 e_2 + 255 e_3 belong to ID. The result is different in Fig. 5.3(b). The unit bivector $\frac{1}{\sqrt{2}}(e_2 + e_3)e_1 = \frac{1}{\sqrt{2}}(e_1 + e_2 + e_3) \wedge e_1$ represents the red hue, involving that the cyan stripes are blurred. Indeed, unit bivectors representing cyan and red hues are opposite, therefore they generate the same plane. Green stripes are no more invariant to the low pass filter since the green axis e_2 is not orthogonal to the bivector $\frac{1}{\sqrt{2}}(e_2 + e_3)e_1$.

In Fig. 5.4, the color α has been chosen to match with the color of the background green leaves. As the low pass filter (Fig. 5.4(a)) removes green high frequencies, the center of flowers containing yellow high frequencies turns red. In Fig. 5.4(b), background pixels corresponding to green low frequencies appear almost grey.

To conclude this part, we propose to compare the results of two low pass filters on the D-orthogonal part with respect to the same bivector $D = e_1e_4$ but changing the quadratic form. As a consequence, the bivector ID differs in the two cases. For the first one (Fig. 5.5(a)), we take Q_1, whereas for the second one (Fig. 5.5(b)), we construct the quadratic form Q_2 such that Q_2 is given by I_4 in the basis $(e_1, \frac{1}{\sqrt{2}}(e_1 + e_2), \frac{i_\alpha}{\|i_\alpha\|}, e_4)$. In other words, we orthogonalize the red, the yellow and the color of leaves which are the main colors in the image.

In Fig. 5.5(a), the unit bivector ID is e_2e_3. Hence, the low pass filter removes green and blue high frequencies but preserves red high frequencies. This explains why the image turns red. In Fig. 5.5(b), the unit bivector ID is $\frac{(e_1+e_2)}{\sqrt{2}}\frac{i_\alpha}{\|i_\alpha\|}$, then it contains the colors of the background and inside the flowers. Therefore, the low pass filter removes all the high frequencies in the image except the ones of the red petals.

For some specific applications, a fine tuning of the quadratic form Q should give better results.

(a) Low pass filter in the parallel part

(b) High pass filter in the parallel part

FIGURE 5.4 – The Clifford-Fourier transform $\widehat{F}_{Q_1,\frac{v_\alpha \wedge e_4}{\|v_\alpha \wedge e_4\|}}$, with $\alpha = (96, 109, 65)$

(a) The Clifford-Fourier transform $\widehat{F}_{Q_1,e_1e_4}$

(b) The Clifford-Fourier transform $\widehat{F}_{Q_2,e_1e_4}$

FIGURE 5.5 – Low pass filters in the ID part

5.5 Related works

To conclude this paper, we show how to recover the hypercomplex Fourier transform of S. Sangwine and the quaternionic Fourier transform of T. Bülow in the Clifford algebras context, using the appropriate morphism from $\mathbb{R}^2$ to Spin(4). First of all, let us recall the definitions of these Fourier transforms.

5.5.1 The hypercomplex Fourier transform of Sangwine et al.

In [32], the authors define the discrete hypercomplex Fourier transform. It can be extended to $\mathbb{R}^2$ as follows. Let $f : \mathbb{R}^2 \to \mathbb{H}$, then its hypercomplex Fourier transform is given by

$$F(u,v) = \int_{\mathbb{R}^2} e^{-\mu(xu+yv)} f(x,y) dx\, dy$$

where $\mu \in \mathbb{H}_0 \cap \mathbb{H}_1$.
There is a freedom in the choice of μ in the hypercomplex Fourier transform as we have a freedom in the choice of the bivector D in the Clifford Fourier transform for color images. In fact, they have the same role, i.e. they decompose the four-dimensional space $\mathbb{R}^4$ into two orthogonal two-dimensional subspaces and decompose the Fourier transform into two standard Fourier transforms.
This is shown in the following proposition.

Proposition 5.7 *Let $\mu = \mu_1 i + \mu_2 j + \mu_3 k$ be a unit quaternion. Let $f \in L^2(\mathbb{R}^2, (\mathbb{R}^4, Q))$ where Q is the quadratic form represented by I_4 in the basis (e_1, e_2, e_3, e_4), and let C be the unit bivector $e_4 \wedge (\mu_1 e_1 + \mu_2 e_2 + \mu_3 e_3)$. Then, $\widehat{f}_C$ given by*

$$\begin{aligned}\widehat{f}_C(u,v) &= \int_{\mathbb{R}^2} f(x,y) \perp \widetilde{\Phi}_{u,v,0,0,C}(-x,-y) dxdy \\ &= \int_{\mathbb{R}^2} e^{\frac{1}{2}(xu+yv)IC} e^{\frac{1}{2}(xu+yv)C} f(x,y) e^{-\frac{1}{2}(xu+yv)C} e^{-\frac{1}{2}(xu+yv)IC} dxdy\end{aligned}$$

corresponds to the hypercomplex Fourier transform of f seen as a $\mathbb{H}$-valued function under the identification[4]

$$e_1 \leftrightarrow i \quad e_2 \leftrightarrow j \quad e_3 \leftrightarrow k \quad e_4 \leftrightarrow 1.$$

Proof. We have to determine the four-dimensional rotation that is generated by the action of the unit quaternion $e^{\mu\phi}$ on $\mathbb{H}$ given by

$$q \longmapsto e^{\mu\phi} q.$$

It is explained in [32] that this rotation may be decomposed as the sum of two two-dimensional rotations of angle $-\phi$ in the planes generated by $(1, \mu)$ and its orthogonal (with respect to the euclidean quadratic form).
Therefore, we can identify this rotation with the action of the spinor

$$e^{-\frac{\phi}{2}(C+IC)}$$

4. The product law needs not to be respected since we just use an isomorphism of vector spaces.

on the four-dimensional space $\mathbb{R}^1_{4,0}$. As a consequence, the action of group morphisms $(x,y) \longmapsto e^{\mu(xu+yv)}$ from $\mathbb{R}^2$ to $\mathbb{H}_1$ on $\mathbb{H}$ corresponds to the action of group morphisms $(x,y) \longmapsto e^{-\frac{1}{2}(xu+yv)(C+IC)}$ from $\mathbb{R}^2$ to Spin(4) on $\mathbb{R}^1_{4,0}$. □

Remark. To the best of our knowledge, the authors restrict for their applications to μ taken as the grey axis, i.e.

$$\mu = \frac{1}{\sqrt{3}}(i+j+k).$$

In other words, the Fourier transform they propose is decomposed as a standard Fourier transform of the luminance part and a standard Fourier transform of the chrominance part.

5.5.2 The quaternionic Fourier transform of Bülow

The quaternionic Fourier transform [16] of a function $f : \mathbb{R}^2 \to \mathbb{R}$ is the quaternion valued function $\mathcal{F}(f)$ defined by

$$\mathcal{F}(f)(y_1,y_2) = \int_{\mathbb{R}^2} exp(-2\pi i y_1 x_1) f(x_1,x_2) exp(-2\pi j y_2 x_2)\, dx_1 dx_2.$$

The link between this Fourier transform and the one proposed here is given by the next result.

Proposition 5.8 *Let $f \in L^2(\mathbb{R}^2;\mathbb{R}e_4)$ where (e_1,e_2,e_3,e_4) is the basis of $\mathbb{R}^4$ that generates $\mathbb{R}_{4,0}$. The Clifford Fourier transform of f defined by*

$$\widehat{f}_C(2\pi y_1,0,0,2\pi y_2) = \int_{\mathbb{R}^2} f(x_1,x_2) \perp \widetilde{\Phi}_{2\pi y_1,0,0,2\pi y_2,C}(-x_1,-x_2)\, dx_1 dx_2$$

where C is the bivector $-\frac{1}{4}(e_1+e_2)(e_3-e_4)$ corresponds to the quaternionic Fourier transform of f seen as a $\mathbb{H}$-valued function under the following identification[5]

$$e_1 \leftrightarrow i \quad e_2 \leftrightarrow j \quad e_3 \leftrightarrow k \quad e_4 \leftrightarrow 1.$$

Proof. We have to determine one of the two elements of Spin(3) × Spin(3) that generate the following rotation in $\mathbb{H}$:

$$f(x_1,x_2) \longmapsto exp(-2\pi i y_1 x_1) f(x_1,x_2) exp(-2\pi j y_2 x_2).$$

Simple computations show that the rotation

$$f(x_1,x_2) \longmapsto exp(-2\pi i y_1 x_1) f(x_1,x_2)$$

can be written in $\mathbb{R}^1_{4,0}$ as

$$f(x_1,x_2) \longmapsto e^{-\pi x_1 y_1 (e_4 e_1 + e_2 e_3)} f(x_1,x_2) e^{\pi x_1 y_1 (e_4 e_1 + e_2 e_3)}.$$

5. The product law needs not to be respected since we just use an isomorphism of vector spaces.

In the same way,

$$f(x_1, x_2) \longmapsto f(x_1, x_2) exp(-2\pi j y_2 x_2)$$

corresponds to

$$f(x_1, x_2) \longmapsto e^{-\pi x_2 y_2 (e_4 e_2 + e_1 e_3)} f(x_1, x_2)\, e^{\pi x_2 y_2 (e_4 e_2 + e_1 e_3)}$$

By associativity, this shows that

$$exp(-2\pi i y_1 x_1)\, f(x_1, x_2)\, exp(-2\pi j y_2 x_2) = e^{-\tau} e^{-\rho} f(x_1, x_2) e^{\rho} e^{\tau}$$

where

$$\tau = \pi x_2 y_2 (e_4 e_2 + e_1 e_3)$$

and

$$\rho = \pi x_1 y_1 (e_4 e_1 + e_2 e_3).$$

By definition,

$$\chi(e^{\rho} e^{\tau}) = \chi(e^{\pi x_1 y_1\, e_4 e_1}) \chi(e^{\pi x_1 y_1\, e_2 e_3}) \chi(e^{\pi x_2 y_2\, e_4 e_2}) \chi(e^{\pi x_2 y_2\, e_1 e_3}).$$

From simple computations, we get

$$\chi(e^{\rho} e^{\tau}) = (e^{2\pi x_1 y_1\, e_2 e_3}, e^{2\pi x_2 y_2\, e_1 e_3})$$

and conclude therefore that

$$(x_1, x_2) \mapsto (e^{2\pi x_1 y_1\, e_2 e_3}, e^{2\pi x_2 y_2\, e_1 e_3})$$

is the morphism $\widetilde{\phi}_{2\pi y_1, 0, e_2 e_3, 0, 2\pi y_2, e_1 e_3}$.

From Section 5.3.1, this latter may be rewritten $\widetilde{\Phi}_{2\pi y_1, 0, 0, 2\pi y_2, \frac{1}{4}(e_1 + e_2)(e_3 - e_4))}$. Indeed, we have

$$\begin{aligned}
\frac{1}{4}\Big(e_2 e_3 + e_1 e_3 + I(e_2 e_3 - e_1 e_3)\Big) &= \frac{1}{4}\Big(e_2 e_3 + e_1 e_3 - e_1 e_4 - e_2 e_4\Big) \\
&= \frac{1}{4}\Big(e_1(e_3 - e_4) + e_2(e_3 - e_4)\Big) \\
&= \frac{1}{4}\Big((e_1 + e_2)(e_3 - e_4)\Big)
\end{aligned}$$

□

Appendix

A. Lie groups representations and Fourier transforms

From the groups theory approach, the basic structure we need to define Fourier transforms is locally compact unimodular groups. Let us start by the definition of the dual of a topological group G, that is the set of the equivalence classes of its unitary irreducible representations, denoted by $\widehat{G}$. We refer to [85] for details.

Definition 5.4 *Group representation.*
Let G be a topological group and V be a topological vector space over $\mathbb{R}$ or $\mathbb{C}$.
A continuous linear representation (φ, V) from G to V is a group morphism

$$\varphi \colon g \longmapsto \varphi(g)$$

from G to $GL(V)$ such that the map

$$(a, g) \longmapsto \varphi(g)(a)$$

from $V \times G$ to V is continuous.

In general, V is an Hilbert space. If V is finite-dimensional, then the representation is said to be finite, and the dimension of V is called the degree of the representation.

Definition 5.5 *Irreducible representation.*
A subspace W of V is said to be invariant by φ if $\varphi(g)(W) \subset W, \forall g \in G$.
Then, the representation φ is said to be irreducible if W and $\{0\}$ are the only subspaces of V that are invariant by φ.

Definition 5.6 *Equivalent representations.*
Let (φ_1, V_1) and (φ_2, V_2) be two linear representations of the same group G. We say that they are equivalent if there exists an isomorphism $\gamma : V_1 \longrightarrow V_2$ such that

$$\gamma \circ \varphi_1(g) = \varphi_2(g) \circ \gamma, \quad \forall g \in G.$$

From now on, V is a $\mathbb{C}$-vector space equipped with a hermitian form $<,>$.

Definition 5.7 *Unitary representation.*
The representation φ is unitary with respect to $<,>$ if

$$< \varphi(g)(a), \varphi(g)(b) > = < a, b > \quad \forall a, b \in V \ \ \forall g \in G.$$

We now restrict to locally compact unimodular groups. On such groups, we can construct a measure that is invariant with respect to both left and right translations. It a called a Haar measure. From a Haar measure is defined a Haar integral of the group.

Proposition 5.9 *Let G be a locally compact unimodular group, and ν denotes a Haar measure. Then, for $f \in L^2(G;\mathbb{C})$ and $h \in G$, we have*

$$\int_G f(g)\,d\nu(g) = \int_G f(gh)\,d\nu(g) = \int_G f(hg)\,d\nu(g).$$

Remark. Locally compact abelian groups and compact groups are unimodular.

Definition 5.8 *Fourier transform on locally compact unimodular groups.*
Let G be a locally compact unimodular group with Haar measure ν. The Fourier transform of $f \in L^2(G;\mathbb{C})$ is the map $\hat{f}$ defined on $\widehat{G}$ by

$$\hat{f}(\varphi) = \int_G f(g)\varphi(g^{-1})\,d\nu(g).$$

Theorem 5.1 *Inversion formula of the Fourier transform.*
$\hat{f}(\varphi)$ is a Hilbert-Schmidt operator over the space of the representation φ. There is a measure over $\widehat{G}$ denoted by $\widehat{\nu}$ such that $\hat{f} \in L^2(\widehat{G};\mathbb{C})$ and $f \longmapsto \hat{f}$ is an isometry. Moreover, the following inverse formula holds :

$$f(g) = \int_{\widehat{G}} Trace(\hat{f}(\varphi)\varphi(g))\,d\widehat{\nu}(\varphi).$$

Let us now have a closer look on Lie groups. We refer to [46] for an introduction to differential geometry.

Definition 5.9 *Lie group and Lie algebra.*
A real C^∞ Lie group is a topological group endowed with a structure of real C^∞-manifold. The Lie algebra of G is (isomorphic to) the tangent space of G at the neutral element e : T_eG. It is usually denoted by $\mathfrak{g}$. It can be made into an algebra over $\mathbb{R}$ by considering the Lie bracket $[\,,\,]$ that satifies : $(X,Y) \longmapsto [X,Y]$ from $\mathfrak{g}\times\mathfrak{g}$ to $\mathfrak{g}$ is $\mathbb{R}$-bilinear. Moreover it satisfies

$$[X,X] = 0 \quad \forall\, X \in \mathfrak{g}$$

and

$$[X,[Y,Z]] + [Y,[Z,X]] + [Z,[X,Y]] = 0 \quad \forall\, X,Y,Z \in \mathfrak{g}.$$

Definition 5.10 *Exponential map.*
Let G be a C^∞ Lie group. The exponential map of G is the map from $\mathfrak{g}$ to G

$$exp : X \longmapsto f(1)$$

where $f : \mathbb{R} \longrightarrow G$ satisfies

$$f(t+s) = f(t)f(s) \quad \forall t,s \in \mathbb{R}$$

and

$$f'(0) = X.$$

f is called a one-parameter subgroup.

To compute group morphisms from $\mathbb{R}^2$ to Spin(3) and Spin(4), we use the following result on Lie groups morphisms.

Proposition 5.10 *Let G and H be two C^∞ Lie groups, and exp_G, exp_H be the corresponding exponential maps. Let $\phi\colon G \longrightarrow H$ be a Lie group morphism. The linear tangent map of ϕ at g, denoted by $T_g\phi$, is the linear map from T_gG to $T_{\phi(g)}H$ given by*

$$T_g\phi(X) = \frac{d}{dt}\phi(g\, exp_G(tX))_{|_{t=0}}$$

Then, if we note e the neutral element of G we have

$$\phi(exp_G(X)) = exp_H(T_e\phi(X)). \tag{5.5}$$

The map $T_e\phi$ is a Lie algebra morphism, i.e. it satisfies

$$T_e\phi([X,Y]) = [T_e\phi(X), T_e\phi(Y)] \quad \forall X, Y \in \mathfrak{g}$$

From (5.5), we deduce that if the group G is connected and the exponential map of G is onto, then the Lie group morphisms from G to H are determined by Lie algebras morphisms from $\mathfrak{g}$ to $\mathfrak{h}$.

B. Bivectors orthogonalization in $\mathbb{R}_{4,0}$

In this Appendix, we detail the calculation leading to the decomposition of the bivector $F =$

$$\frac{(uX+vY)B + (wX+zY)C}{4} + I\,\frac{(uX+vY)B - (wX+zY)C}{4}$$

of Section 5.3.1 into

$$\frac{1}{8}\Big[(X(u+w)+Y(v+z))(B+C+I(B-C))\Big] + \frac{1}{8}\Big[(X(u-w)+Y(v-z))(B-C+I(B+C))\Big]$$

This decomposition follows of the general decomposition of Hestenes et al. [47] mentionned in the Introduction. On $\mathbb{R}_{4,0}$, the result is the following. Let $P \in \mathbb{R}^2_{4,0}$, and consider

$$\lambda_1 = \frac{1}{2}\Big(-|P|^2 + (|P|^4 - |P\wedge P|^2)^{1/2}\Big) \qquad \lambda_2 = \frac{1}{2}\Big(-|P|^2 - (|P|^4 - |P\wedge P|^2)^{1/2}\Big)$$

If $\lambda_1 \neq \lambda_2$, then $P = P_1 + P_2$ where

$$P_1 = \frac{P}{1 + \frac{1}{2}\lambda_1^{-1}\, P\wedge P} \qquad P_2 = \frac{P}{1 + \frac{1}{2}\lambda_2^{-1}\, P\wedge P}$$

P_1 and P_2 satisfy the following relations : $P_1P_2 = P_2P_1 = P_1 \wedge P_2$ and $P_1^2, P_2^2 < 0$

Let us first determine λ_1 and λ_2. Remind that $-|P|^2 = \langle P^2\rangle_0$.

We have $F^2 =$

$$\frac{1}{16}\Big[-(uX+vY)^2+(uX+vY)(wX+zY)(BC+CB)-(wX+zY)^2\Big]$$
$$+\frac{1}{16}I\Big[-(uX+vY)^2+(uX+vY)(wX+zY)(CB-BC)+(wX+zY)^2\Big]$$
$$+\frac{1}{16}I\Big[-(uX+vY)^2+(uX+vY)(wX+zY)(BC-CB)+(wX+zY)^2\Big]$$
$$+\frac{1}{16}\Big[-(uX+vY)^2-(uX+vY)(wX+zY)(BC+CB)-(wX+zY)^2\Big]$$

Hence
$$-|F|^2=\langle F^2\rangle_0=\frac{1}{16}\Big(-(uX+vY)^2-(wX+zY)^2-(uX+vY)^2-(wX+zY)^2\Big)$$
$$=-\frac{1}{8}\Big((uX+vY)^2+(wX+zY)^2\Big)$$
and $|F|^4=\frac{1}{64}\Big((uX+vY)^2+(wX+zY)^2\Big)^2$

Moreover, $F\wedge F=\langle F^2\rangle_4=\frac{1}{8}I\Big[(wX+zY)^2-(uX+vY)^2\Big]$. Hence, we have
$|F\wedge F|^2=\langle (F\wedge F)^\dagger(F\wedge F)\rangle_0=\frac{1}{64}\Big[(wX+zY)^2-(uX+vY)^2\Big]^2$.

After simplifications, we obtain $|F|^4-|F\wedge F|^2=\frac{1}{16}\Big[(uX+vY)^2(wX+zY)^2\Big]$.

Consequently, $\lambda_1=\frac{1}{2}\Big[-\frac{1}{8}\Big((uX+vY)^2+(wX+zY)^2\Big)+\frac{1}{4}(uX+vY)(wX+zY)\Big]$
$$=\frac{1}{2}\Big[-\frac{1}{8}\Big((uX+vY)^2+(wX+zY)^2+2(uX+vY)(wX+zY)\Big)\Big]$$
$$=\frac{1}{2}\Big[-\frac{1}{8}\Big(X(u+w)+Y(v+z)\Big)^2\Big]$$
$$=-\frac{1}{16}\Big(X(u+w)+Y(v+z)\Big)^2$$

In the same way, we obtain $\lambda_2=-\frac{1}{16}\Big(X(u-w)+Y(v-z)\Big)^2$.

The next step is to compute $1+\frac{1}{2}\lambda_1^{-1}\,F\wedge F$. It equals
$$1+\frac{1}{2}\left(\frac{-16}{[X(u-w)+Y(v-z)]^2}\right)\frac{1}{8}I\Big((wX+zY)^2-(uX+vY)^2\Big)$$
$$=1-I\left(\frac{(wX+zY)^2-(ux+vY)^2}{[X(u-w)+Y(v-z)]^2}\right)$$
The term in parenthesis is of the form $\frac{a^2-b^2}{(a+b)^2}$. Thus it may be simplified and we obtain

$$1+\frac{1}{2}\lambda_1^{-1}\,F\wedge F=1+I\left(\frac{X(u-w)+Y(v-z)}{X(u+w)+Y(v+z)}\right) \tag{5.6}$$

Expression (5.6) is of the form $1+\alpha I$. It follows that its inverse is $\dfrac{1-\alpha I}{1-\alpha^2}$, and we have

$$\frac{1}{1+I\left(\dfrac{X(u-w)+Y(v-z)}{X(u+w)+Y(v+z)}\right)}=\frac{1-I\left(\dfrac{X(u-w)+Y(v-z)}{X(u+w)+Y(v+z)}\right)}{1-\left(\dfrac{X(u-w)+Y(v-z)}{X(u+w)+Y(v+z)}\right)^2}$$

The denominator is of the form $1+\dfrac{(a-b)^2}{(a+b)^2}=\dfrac{4ab}{(a+b)^2}$, then from $F_1=\dfrac{F}{1+\frac{1}{2}\lambda_1^{-1}F\wedge F}$ we have

$$F_1=F\left[1-I\left(\frac{X(u-w)+Y(v-z)}{X(u+w)+Y(v+z)}\right)\right]\times\frac{[X(u+w)+Y(v+z)]^2}{4\,(uX+vY)(wX+zY)}$$

Hence,

$$\begin{aligned}
F_1=&\frac{[X(u+w)+Y(v+z)]^2}{4\,(uX+vY)(wX+zY)}\times\\
&\left[\frac{1}{4}[(uX+vY)B+(wX+zY)C]+\frac{1}{4}I[(uX+vY)B-(wX+zY)C]\right.\\
&-\frac{1}{4}\left(\frac{X(u-w)+Y(v-z)}{X(u+w)+Y(v+z)}\right)(uX+vY)IB-\frac{1}{4}\left(\frac{X(u-w)+Y(v-z)}{X(u+w)+Y(v+z)}\right)(wX+zY)IC\\
&\left.-\frac{1}{4}\left(\frac{X(u-w)+Y(v-z)}{X(u+w)+Y(v+z)}\right)(uX+vY)B+\frac{1}{4}\left(\frac{X(u-w)+Y(v-z)}{X(u+w)+Y(v+z)}\right)(wX+zY)C\right]
\end{aligned}$$

$$\begin{aligned}
F_1=&\frac{[X(u+w)+Y(v+z)]^2}{4\,(uX+vY)(wX+zY)}\times\\
&\left[\frac{1}{4}(uX+vY)B\left(\frac{2(wX+zY)}{X(u+w)+Y(v+z)}\right)+\frac{1}{4}(uX+vY)IB\left(\frac{2(wX+zY)}{X(u+w)+Y(v+z)}\right)\right.\\
&\left.+\left[\frac{1}{4}(wX+zY)C\left(\frac{2(uX+vY)}{X(u+w)+Y(v+z)}\right)-\frac{1}{4}(wX+zY)IC\left(\frac{2(uX+vY)}{X(u+w)+Y(v+z)}\right)\right]\right.
\end{aligned}$$

$$F_1=\frac{[X(u+w)+Y(v+z)]}{8}\Big(B+IB+C-IC\Big)$$

In the same way, we obtain $F_2=\dfrac{[X(u-w)+Y(v-z)]}{8}\Big(B+IB-C+IC\Big)$.

This ends the calculation.

Références

[1] M. F. Atiyah and G. I. MacDonald, *Introduction to Commutative Algebra*, The Advanced Book Program, Perseus Books Reading, Massachusetts (1969).

[2] G. Aubert and P. Kornprobst, *Mathematical Problems in Image Processing : Partial Differential Equations of Variations*, Springer (second edition 2006).

[3] T. Batard, C. Saint-Jean and M. Berthier, *A Metric Approach to nD Images Edge Detection with Clifford Algebras*, J. Mathematical Imaging and Vision, 33(3) (2009), pp. 296–312.

[4] T. Batard and M. Berthier, *Clifford Algebras Bundles to Multidimensional Image Segmentation*, To appear in Advances in Applied Clifford Algebras. Special Issue of the Proc. of the 8th International Conference on Clifford Algebras and their Applications in Mathematical Physics ICCA8 (2008).

[5] T. Batard, C. Saint-Jean and M. Berthier, *Clifford-Fourier Transform for Color Image Processing*, To appear in Lecture Notes in Computer Science. Proc. of 3rd Int. Conf. Applications of Geometric Algebras in Computer Science and Engineering AGACSE 2008.

[6] T. Batard and M. Berthier, *Heat kernels of generalized Laplacians-Application to Color Image Smoothing*, To appear in Proc. 2009 IEEE Int. Conf. Image Processing ICIP 2009.

[7] T. Batard and M. Berthier, *The Clifford-Hodge Flow : an Extension of the Beltrami Flow*, Lecture Notes in Computer Science, 5702 (2009), pp. 394–401.

[8] T. Batard, *Clifford Bundles : a unifying Framework for Images(Videos), Vector Fields and Orthonormal Frame Fields Regularization*, submitted (2009).

[9] W. E. Baylis, *Clifford (Geometric) Algebras with Applications to Physics, Mathematics, and Engineering*, Birkhäuser, Basel (1999).

[10] E. Bayro Corrochano, *Geometric Algebra with Applications in Science and Engineering*, Springer (2001).

[11] N. Bourbaki, *Eléments de mathématiques. Algèbre. Chapitres 1 à 3*, Diffusion C.C.L.S, Paris (1970).

[12] F. Brackx, N. De Schepper and F. Sommen, *The Two-Dimensional Clifford-Fourier Transform*, J. Mathematical Imaging and Vision, 26(1-2) (2006), pp. 5–18.

[13] N. Berline, E. Getzler and M. Vergne, *Heat Kernels and Dirac Operators*, Springer-Verlag, Heidelberg, (2004).

[14] M. Blau, *Connections on Clifford bundles and the Dirac operator*, Letters in Mathematical Physics, 13 (1987), pp. 83–92.

[15] T. Bülow and G. Sommer, *The Hypercomplex Signal - a novel Approach to the Multidimensional Analytic Signal*, IEEE Trans. Signal Processing, 49(11) (2001), pp. 2844–2852.

[16] T. Bülow, *Hypercomplex Spectral Signal Representations for the Processing and Analysis of Images*, PhD Thesis, Kiel (1999).

[17] T. Carron and P. Lambert, *Color Edge Detector using jointly Hue, Saturation and Intensity*, in Proc. 1994 IEEE Int. Conf. Image Processing ICIP, 3 (1994), pp. 977–981.

[18] T. Carron, *Segmentation d'Images Couleur dans la base Teinte-Luminance-Saturation : approche numérique et symbolique*, Thèse de doctorat, Université de Savoie (1995).

[19] T. Chan and J. Shen, *Image Processing and Analysis : Variational, Pde, Wavelet, and Stochastic Methods*, Society for Industrial and Applied Mathematic (2005).

[20] C. Chefd'hotel, D. Tschumperlé, R. Deriche and O. Faugeras, *Regularizing flows for Constrained Matrix-Valued Images*, J. Mathematical Imaging and Vision, 20 (2004), pp. 147–162.

[21] C. Chevalley, *The Algebraic Theory of Spinors and Clifford Algebras*, new edn. Springer, 1995.

[22] W. K. Clifford, *Applications of Grassmann's Extensive Algebra*, American Journal of Mathematics, I (1878), pp. 350–358.

[23] A. Cumani, *Edge Detection in Multispectral Images*, Computer Vision, Graphics, and Image Processing : Graphical Models and Image Processing, 53(1) (1991), pp. 40–51.

[24] G. De Rham, *Variétés différentiables : Formes, Courants, Formes harmoniques*, Hermann, Paris, (1973).

[25] U. Diewald, T. Preusser and M. Rumpf, *Anisotropic Diffusion in Vector Field Visualization on Euclidean Domains and Surfaces*, IEEE Trans. Visualization on Computer Graphics, 6(2) (2000), pp. 139–149.

[26] S. Di Zenzo, *A note on the Gradient of a Multi-Image*, Computer Vision, Graphics, and Image Processing, 33(1) (1986), pp. 116–125.

[27] C. Doran and A. Lasenby, *Geometric Algebra for Physicists*, Cambridge University Press, (2007).

[28] L. Dorst, D. Fontijne and S. Mann, *Geometric Algebra for Computer Science : An Object-Oriented Approach to Geometry*, Morgan Kaufmann, (2009).

[29] B. Doubrovine, S. Novikov and A. Fomenko, *Modern Geometry- Methods and Applications. Part I : The Geometry of Surfaces, Transformations Groups, and Fields*, second edn. Springer, (1991).

[30] R. Duits, M. Felsberg, G. Granlund and B. ter Haar Romeny, *Image Analysis and Reconstruction using a Wavelet Transform Constructed from a Reducible Representation of the Euclidean Motion Group*, Int. J. Computer Vision, 72(1) (2007), pp. 79–102.

[31] J. Ebling and G. Scheuermann, *Clifford Fourier Transform on Vector Fields*, IEEE Trans. Visualization and Computer Graphics, 11(4) (2005), pp. 2844–2852.

[32] T. A. Ell and S. Sangwine, *Hypercomplex Fourier Transforms of Color Images*, IEEE. Trans. Image Processing, 16(1) (2007), pp. 5–18.

[33] C. Evans, T. A. Ell and S. Sangwine, *Colour-sensitive edge detection using hypercomplex filters*, In Proc. 10th European Signal Processing Conference EUSIPCO 2000, pp. 107–110.

[34] M. Fairchild, *Color Appearance Models*, John Wiley and Sons, New York (2005).

[35] M. Felsberg, *Low-level Image Processing with the Structure Multivector*, PhD Thesis, Kiel (2002).

[36] T. Frankel, *The Geometry of Physics : an Introduction*, revised edn. Cambridge University Press, (2001).

[37] E. M. Franken, R. Duits, B. ter Haar Romeny, *Nonlinear Diffusion on the 2D Euclidean Motion Group*, Lecture notes in Computer Science, 4485 (2007), pp. 461–472.

[38] A. Fuster, L. Astola and L. Florack, *A Riemannian Scalar Measure for Diffusion Tensor Images*, Lecture notes in Computer Science, 5702 (2009), pp. 419–426.

[39] J. P. Gauthier, G. Bornard and M. Silbermann, *Harmonic Analysis on Motion Groups and their Homogeneous Spaces.*, IEEE Trans. Systems, Man, and Cybernetics, 21 (1991).

[40] T. Gevers and H.M.G. Stokman, *Classifying Color Transitions into Shadow-Geometry, Illumination, Highlight or Material Edges.* In Proc. 2000 IEEE Int. Conf. Image Processing ICIP 2000, I, pp. 521–524.

[41] T. Gevers and A.W.M. Smeulders, *Color based image segmentation*, Pattern Recognition 32 (1999), pp. 453–464.

[42] F. Gourd, J. P. Gauthier and H. Younes, *Une méthode d'Invariants de l'Analyse Harmonique en Reconnaissance de Formes*, Traitement du Signal 6(3) (1989), pp. 161–178.

[43] W. Graf, *Differentials Forms as Spinors*, Annales de l'Institut Henri Poincaré, 29 (1) (1978), pp. 85–109.

[44] W. Greub, S. Halperin and R. Vanstone, *Connections, Curvature and Cohomology. vol. I-III*, Academic Press, New York (1972, 1973 and 1976).

[45] Y. Gur and N. Sochen, *Regularizing Flows over Lie Groups*, J. Mathematical Imaging and Vision, 33(2) (2009), pp. 195–208.

[46] S. Helgason, *Differential geometry, Lie groups and symmetric spaces*, Academic Press, London (1978).

[47] D. Hestenes and G. Sobczyk, *Clifford Algebra to Geometric Calculus*, D. Reidel, Dordrecht, (1984).

[48] D. Hestenes, *New Foundations for Classical Mechanics*, second edn. Fundamental Theories of Physics, Kluwer Academic Publishers (1999).

[49] D. Hestenes, *Space Time Algebra*, Gordon and Breach (1966).

[50] E. Hewitt and K.A. Ross, *Abstract Harmonic Analysis*, Springer, Berlin (1963).

[51] D. Husemoller, *Fibre Bundles*, 3rd edn. Springer (1993).

[52] R. Kimmel and N. Sochen, *Orientation Diffusion or How to Comb a Porcupine ?*, J. Visual Communication and Image Representation, 13 (2001), pp. 238–248.

[53] R. Kimmel, *Numerical Geometry of Images : Theory, Algorithms, and Applications*, Springer-Verlag, New York (2003).

[54] S. Kobayashi and K. Nomizu, *Foundations of differential geometry. vol. I*, John Wiley and Sons, New York (1963).

[55] H. B. Lawson and M.-L. Michelson, *Spin Geometry*, Princeton University Press, Princeton (1989).

[56] R. Lenz, *Color Edge Detectors for Conical Color Spaces*, In Proceedings of CGIP 2000. First International Conference on Color in Graphics and Image Processing, (2000), pp. 284–289.

[57] P. Lounesto, *Clifford Algebras and Spinors*, London Mathematical Society Lecture Notes Series, Cambridge University Press, Cambridge (1997).

[58] D. Martin, C. Fowlkes, D. Tal and J. Malik, *A Database of Human Segmented Natural Images and its Application to Evaluating Segmentation Algorithms and Measuring Ecological Statistics*, In Proc. 8th IEEE Int. Conf. Computer Vision ICCV 2001, pp. 416–423.

[59] B. Mawardi and E. Hitzer, *Clifford Fourier Transformation and uncertainty principle for the Clifford Algebra* $Cl_{3,0}$, Advances in Applied Clifford Algebras, 16(1) (2006), pp. 41–61.

[60] M.A. Naimark and A.I. Stern, *Theory of Group Representations*, Springer, Berlin (1982).

[61] N. Paragios, Y. Chen and O. Faugeras, *Handbook of Mathematical Models in Computer Vision*, Springer (2005).

[62] X. Pennec, P. Fillard and N. Ayache, *A Riemannian Framework for Tensor Computing*, Int. J. Computer Vision, 66(1) (2006), pp. 41–66.

[63] P. Perona, *Orientation diffusions*, IEEE Trans. Image Processing, 7 (1999), pp. 457–467.

[64] R. Péteri, M. Huiskes and S. Fazekas, *DynTex a comprehensive database of Dynamic Textures,* `http://old-www.cwi.nl/projects/dyntex`.

[65] J. Petitot, *Neurogéométrie de la Vision - Modèles Mathématiques et Physiques des Architectures Fonctionnelles*, Ecole Polytechnique (2008).

[66] A. M. Polyakov, *Quantum geometry of bosonic strings*, Physics Letters B, 103B(3) (1981), pp. 207–210.

[67] M. Postnikov, *Lectures in Geometry. Lie groups and Lie algebras*, Mir, Moscow (1986).

[68] S. Sangwine and T. A. Ell, *Colour Image Filters based on Hypercomplex Convolution*, IEEE Proceedings-Vision, Image and Signal Processing 147(2) (2000), pp. 89–93.

[69] S. Sangwine and T. A. Ell, *Hypercomplex Fourier Transforms of Color Images*, In Proc. 2001 IEEE Int. Conf. Image Processing ICIP 2001, 1, pp. 137–140.

[70] S. Sangwine, T. A. Ell and B. N. Gatsheni, *Colour-Dependent Linear Vector Image Filtering*, In Proc. 12th European Signal Processing Conference, EUSIPCO 2004, pp. 585–588.

[71] G. Sapiro, *Color Snakes*, Computer Vision and Image understanding, 68(2) (1997), pp. 407–416.

[72] G. Sapiro, *Geometric Partial Differential Equations and Image Analysis*, Cambridge University Press (2006).

[73] F. Smach, C. Lemaître, J. P. Gauthier, J. Miteran and M. Atri, *Generalized Fourier Descriptors with Applications to Objects Recognition in SVM Context*, J. Mathematical Imaging and Vision, 30(1) (2008), pp. 43–71.

[74] N. Sochen, R. Kimmel and R. Malladi, *A General Framework for Low Level Vision*, IEEE Trans. Image Processing, 7 (1998), pp. 310–318.

[75] G. Sommer, *Geometric Computing with Clifford Algebras. Theorical Foundations and Applications in Computer Vision and Robotics*, Springer-Verlag, Berlin (2001).

[76] A. Spira and R. Kimmel, *An efficient solution to the Eikonal equation on parametric manifolds*, Interfaces and Free Boundaries, 6(3) (2004), pp. 315–327.

[77] A. Spira, R. Kimmel and N. Sochen, *A Short-time Beltrami Kernel for Smoothing Images and Manifolds*, IEEE Trans. Image Processing, 16 (2007), pp. 1628–1636.

[78] M. Spivak, *A Comprehensive Introduction to Differential Geometry*, Publish or Perish, Inc., Houston (1979).

[79] N. Steenrod, *The Topology of Fibre Bundles*, Princeton University Press (1999).

[80] B. Tang, G. Sapiro, and V. Casselles, *Direction diffusion*, In Proc. 1999 IEEE Int. Conf. Computer Vision ICCV 1999, pp. 1245–1252.

[81] B. Tang, G. Sapiro, and V. Casselles, *Diffusion of General Data on Non-Flat Manifolds via Harmonic Maps Theory : The Direction Diffusion Case*, Int. J. Computer Vision, 36(2) (2000), pp. 149–161.

[82] D. Tschumperlé and R. Deriche, *Orthonormal vector sets regularization with PDE's and applications*, Int. J. Computer Vision, 50(3) (2002), pp. 237–252.

[83] D. Tschumperlé and R. Deriche, *Vector-valued Image Regularization with PDE's : A Common Framework for Different Applications*, IEEE Trans. Pattern Analysis and Machine Intelligence, 27 (2005), pp. 506–517.

[84] D. Tschumperlé, *Fast Anisotropic Smoothing of Multivalued Images using Curvature-preserving PDE's*, Int. J. Computer Vision, 68(1) (2006), pp. 65–82.

[85] N. J. Vilenkin, *Special Functions and the Theory of Group Representations*, Translations of Mathematical Monograph, vol.22, American Mathematical Society, Providence, Rhode Island (1968).

[86] A. Yezzi jr, *Modified Curvature Motion for Image Smoothing and Enhancement*, IEEE Trans. Image Processing, 7(3) (1998), pp. 345–352.